SCACR 2023

Short Course/Conference on Applied Coastal Research

4 - 6 SEPTEMBER 2023 • ISTANBUL / TURKEY

Book of ABSTRACTS

www.scacr2023.org

Content

CONTENT

CONTENT

CONTENT

CONTENT

CONTENT

CONTENT

CONTENT

CONTENT

CONTENT

CONTENT

CONTENT

PREFACE

The 10th Short Course/Conference on Applied Coastal Research (SCACR 2023) was held on September 4-6, 2023 in Istanbul, Turkey.

SCACR aims to bring together graduate students, field and laboratory experimentalists, theoreticians and numerical modelers in coastal and port engineering. The purpose of SCACR events is to inform all participants about the latest scientific and engineering developments in coastal, port and offshore engineering and to exchange views with users and stakeholders of coastal areas.

SCACR also aims to organize short courses for young researchers that address some of the "important" topics in current coastal and offshore engineering design research.

We would like to express our deepest gratitude to our keynote speakers, Nobuhisa Kobayashi, Han Ligteringen, Marcel R.A. van Gent, Giuseppe Roberto Tomasicchio, Waleed Hamza and Piero Lionello.

Chair of SCACR 2023

Prof. Dr. Yalcin Yuksel

ADVISORY COMMITTEE

J. Alsina
Universitat Politècnica de Catalunya, Spain

C. Altomare
Universitat Politècnica de Catalunya, Spain

A. Antonini
Delft University of Technology, Holland

A. S. Arcilla
Universitat Politècnica de Catalunya, Spain

F. Aristodemo
University of Calabria, Italy

G. Barbaro
University of Reggio Calabria, Italy

G. Bellotti
Roma Tre University, Italy

R. Briganti
University of Nottingham, UK

M. Brocchini
Marche Polytechnic University, Italy

M. Calabrese
University of Napoli, Italy

L. Cappietti
University of Firenze, Italy

J.-L. Chen
National Cheng Kung University, Taiwan

E. Ciralli
Progetti & Opere, Italy

F. D'Alessandro
University of Milan, Italy

F. Dentale
University of Salerno, Italy

M. Di Risio
University of L'Aquila, Italy

A. Farhadzadeh
Stony Brook University, USA

J. Figlus
Texas A&M University, Texas

J. Fortes
National Laboratory of Civil Engineering (LNEC), Lisbon

E. Foti
University of Catania, Italy

L. Franco
Univ. of Roma, Italy

A. Francone
University of Salento, Italy

R. Guanche Garcia
University of Cantabria, Spain

W. Hamza
United Arab Emirates University, UAE

B. Hofland
Delft TU, Holland

A. C. Henderson
United Arab Emirates University, UAE

G. Iglesias
University College Cork, Ireland

S. Ilic
Lancaster University, UK

J. Jimenez
Universitat Politècnica de Catalunya, Spain

B. Kamranzad
University of Strathclyde, UK

T. Karambas
Aristotle University of Thessaloniki, Greece

Akira Kawamori
Alpha Hydraulic Engineering Consultants CO. Ltd.

K.-H. Kim
Catholic Kwandong University, South Korea

N. Kobayashi
University of Delaware, USA

J.P. Latham
Imperial College London, UK

H. Ligteringen
Delft TU, Holland

P. Lionello
University of Salento, Italy

S. Longo
University of Parma, Italy

J. Lopez Lara
University of Cantabria, Spain

M. Losada
University of Granada, Spain

M. A. Maraqa
UAE University, UAE

L. Martinelli
University of Padova, Italy

R. Mayerle
Univ. of Kiel, Germany

J. Medina
University of Valencia, Spain

J. Melby
US Army Corps of Engineers, USA

I. Nistor
University of Ottawa, Canada

A. Payo Garcia
British Geological Survey, UK

V. Penchev
BDCA, CORES, Bulgaria

P. Ruol
University of Padova, Italy

F. Sancho
National Laboratory of Civil Engineering (LNEC), Portugal

A. Saponieri
University of Salento, Italy

S. Schimmels
University of Hannover, Germany

H. Schuttrumpf
RWTH Aachen University, Germany

D. Simmonds
University of Plymouth, UK

A. Stocchino
The Hong Kong Polytechnic University, Hong Kong

F. T. Pinto
University of Porto, Portugal

G. Tomasicchio
University of Salento, Italy

A. Torres-Freyermuth
Universidad Nacional Autonoma de Mexico, Mexico

P. Troch
Ghent University, Belgium

J. W. van der Meer
IHE Delft, Holland

M. van Gent
Deltares, Holland

D. Vicinanza
University of Campania, Italy

Y. Yuksel
Yıldız Technical University, Turkey

Z. T. Yuksel
Consultant, Turke

LOCAL ORGANIZING COMMITTEE

Yalçın Yüksel *(Chair)*

Cihan Şahin *(Vice Chair)*

Ayşen Ergin

Ahmet Cevdet Yalçıner

Z. Tuğçe Yüksel

Işıkhan Güler

Esin Çevik

Adem Akpınar

Cüneyt Baykal

Serdar Beji

G. Güney Doğan Bingöl

Kubilay Cihan

Yeşim Çelikoğlu

Tunç Gökçe

Hasan Gökhan Güler

Anıl Arı Güner

Selçuk İz

Sedat Kabdaşlı

Özgür Kırca

Doğan Kısacık

Bergüzar Özbahçeci

Merih Özcan
Mehmet Öztürk

Ilgar Şafak

Gülizar Özyurt Tarakçıoğlu

Oral Yağcı

Oral
PRESENTATIONS

POTENTIAL CHANGES IN FUTURE WIND AND WAVE CLIMATE OVER THE BLACK SEA

Fulya Islek, Yildiz Technical University, islek.fulya@gmail.com
Yalcin Yuksel, Yildiz Technical University, yalcinyksl@gmail.com
Cihan Sahin, Yildiz Technical University, cihansahin81@gmail.com

INTRODUCTION

Global climate change will be expected to induce long-term changes in both wind and wave climate, e.g., intensity, frequency, direction duration, and extreme events (Hdidouan and Staffell, 2017; Lemos et al. 2019). Previous studies have recently reported the effects of climate change on wind climate (Rusu, 2018; Islek et al. 2022a) and wave climate (Rusu, 2019; Islek et al. 2022b) in enclosed basins, such as the Mediterranean Sea, Baltic Sea, Black Sea. Changing wind and wave conditions will affect navigation safety, harbor operations, coastal processes (e.g., shoreline evolution, longshore sediment transport rates), and even ecology in the Black Sea.

The present study aims to (i) reveal possible impacts of climate change on wind and wave climate, (ii) detect region(s) where future changes are most likely (iii) determine the location(s) where future changes are less likely in the Black Sea until the end of the 21st century.

MATERIALS AND METHODS

In the present study, high-resolution EUR-11 wind fields (with a spatial resolution of 0.11° and a temporal resolution of 6 hours) provided by the Rossby Centre regional atmospheric model, version RCA4, are considered. The wind fields developed by SMHI (Swedish Meteorological and Hydrologic Institute) are forced with boundary conditions provided by EC-EARTH (Strandberg et al., 2014). The regional climate model is available via the EURO-CORDEX database. The wave characteristics are generated using MIKE 21 SW (spectral wave) for historical and future periods. Model results are validated against buoy measurements. Future assessments are based on the two-time slices corresponding to the near future 2021–2060 and the middle future 2061–2100 under two climate scenarios (Representative Concentration Pathway, RCP4.5, and RCP8.5).

Projected changes are calculated using future change (*FC*) and their statistical significance levels based on the Student's t-test are evaluated (Scheer, 1986). The *FC* is the subtraction of the considered parameters obtained for the historical period from those obtained for future periods ($FC = X_{RCP} - X_{Hist}$).

RESULTS AND DISCUSSION

In the near future (NF) under two climate scenarios, the following results are mainly found for extreme wind and wave characteristics (V_{99th}, H_{max}):

- In the NF under the RCP4.5 scenario, the entire Black Sea will be characterized by significant increases, except for the small region in the eastern Black Sea (Figure 1).
- In the NF, the RCP8.5 scenario continues to suggest increases in extremes over the Black Sea. The increases in V_{99th} are more significant over the entire basin, while increases in H_{max} are more markedly only in the eastern basin, compared with the RCP4.5 scenario.
- The results in the NF indicate that the Black Sea exhibits more drastic increases under the RCP8.5 scenario than the RCP4.5 scenario.

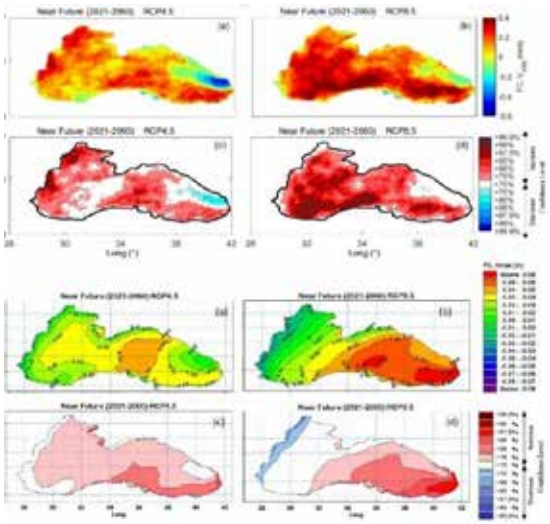

Figure 1. FC in the V_{99th} and H_{max} for NF under RCP4.5 and RCP8.5 scenarios. Significance of differences based on the Student's t-test for different confidence levels.

REFERENCES

Scheer, T.B. (1986). The significance of differences between means. An empirical study. Comparative Biochemistry and Physiology Part A: Physiology, vol. 83 (3), pp. 405–408.

Strandberg, G., Barring, L., Hansson, U., Jansson, C., Jones, C., Kjellström, E., Kolax, M., Kupiainen, M., Nikulin, G., Samuelsson, P., Ullestig, A. and Wang, S. (2014): CORDEX scenarios for Europe from the Rossby Centre regional climate model RCA4. Reports Meteorology and Climatology, vol. 116, pp. 1–84.

Rusu, E. (2018): An analysis of the storm dynamics in the Black Sea. Romanian Journal of Technical Sciences-Applied Mechanics, vol. 63(2), pp. 127–142.

Rusu L (2019): Evaluation of the near future wave energy resources in the Black Sea under two climate scenarios. Renewable Energy, vol. 142, pp. 137–146.

Islek. F., Yuksel, Y., and Sahin C. (2022a): Evaluation of regional climate models and future wind characteristics in the Black Sea, International Journal of Climatology, vol. 47, pp. 1877–1901.

Islek. F., Yuksel, Y., and Sahin C. (2022b): Evaluation of regional climate models and future wave characteristics in an enclosed sea: A case study of the Black Sea, Ocean Engineering, vol. 262, 112220.

USING STILLING WAVE BASIN TO WITHSTAND SEA LEVEL RISE IN COASTAL AREAS

Nisa Bahadiroglu, İzmir Institute of Technology, nisabahadiroglu@iyte.edu.tr
Dogan Kisacik, İzmir Institute of Technology, dogankisacik@iyte.edu.tr
Lorenzo Cappietti, University of Florence, lorenzo.cappietti@unifi.it

INTRODUCTION

Izmir, Turkey, is a significant coastal city that has experienced rapid economic growth and urbanization. This process has taken place mainly around Izmir Bay, which is a vital part of the city supporting its development. However, unplanned development and inadequate infrastructure have made the region vulnerable to natural disasters, especially because of the increasing threats caused by sea level rise due to global warming. This scenario may end with coastal flooding, erosion, and damage to infrastructure and property. The inner bay of Izmir consists of vertical and armoured rubble mound sloping structures, and they would be insufficient for avoiding coastal flooding in the climate change scenario. Therefore, it is of pivotal importance to implement robust adaptation measures in low-elevation coastal zones (The EU Floods, 2020 and, The United Nations Office for Disaster Risk Reduction, UNDRR). Increasing the crest height of existing flood defense structures is a common method for reducing wave overtopping, but this can be limited in urbanized coastal areas. Alternative methods, namely: small storm walls, parapets, and stilling wave basins, can be utilized to limit wave overtopping to tolerable values. This study focuses on developing the stilling wave basin (SWB) approach. This work has been conducted by experimental modeling.

EXPERIMENTAL SETUP

Experiments are conducted in the medium-size Wave-Current Flume (one of the three LABIMA's wave flumes) of the Maritime Engineering Laboratory (LABIMA) at the University of Florence in Italy. The flume is an entire steel and glass structure measuring 37.27 m in length, 0.80 m in width, and 0.8 m in height. It is possible to generate regular and random waves with a maximum wave height of up to 35 cm, a period of approximately 2 s, and a water depth of 60 cm. Hydrodynamic conditions and geometric properties of the coastal protection structures are Froude scaled 1/16 based on the case of Izmir Bay. The scale model is made up of three primary components: the simple caisson, the rubble-mound armour protection, and the superstructure components (see Figure 1). The rubble-mound armour is comprised of stones that weigh 0.490 kg each for the inner core and stones that weigh 0.654 kg each for the outer armour, with a total length of 0.71 m. The caisson is a wooden box that has a height of 0.25 m. The armour crest height is 0.25 m from the bottom with three stones width (0.22m), and its seaward slope is ½.

The superstructure includes a continuous Landward Storm Wall (LSW), a Seaward Storm Wall (SSW) with gaps, and a promenade slope. This component ensemble creates the Stilling Wave Basin (SWB). Here, h_b and h_r are the seaward and landward storm wall heights, respectively. The crest of the h_b and h_r are located at the same level above the still water level. X_r is the horizontal length of the sloping promenade, where C_b is the blocking coefficient that determines the gap ratio of the seaward storm wall part.

Stilling wave basin geometry combines h_b, h_r, X_r, and C_b parameters. In total, sixty-three different geometric configurations are tested under four different hydrodynamic conditions, including two wave climates in two water depths. In addition, to identify the SWB effect on the overtopping discharge, reference tests without SWB but having the same crest freeboard are conducted under the same hydrodynamic conditions. Overtopping discharge is recorded after each test.

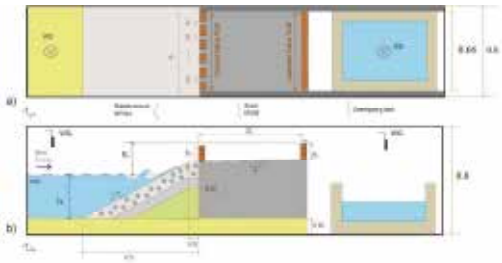

Figure 1 - Experimental set a) plan view, b) middle line cross-section (all dimensions are in meters)

RESULT

The results show a reduction effect of the SWB on overtopping discharge compared to tests done without it. Also, since it was aimed to examine the effect of each design parameter that characterizes each tested configuration, the results are examined accordingly. It is concluded that the overtopping discharge has an inverse relation with the basin volume. Based on this fact, a reduction coefficient is obtained for rubble mound armored sloping structures in the presence of the SWB. The reduction coefficient is expressed as a function of the basin volume and proposed as an addition to the existing overtopping discharge formula in EurOtop Manual 2018.

REFERENCES

EurOtop 2018 (2018) : Manual on wave overtopping of sea defenses and related structures, pp. 174-187.

The EU Floods Directive (2020).

The United Nations Office for Disaster Risk Reduction (2020).

LONG-TERM CHANGE IN GLOBAL SWELL DOMINANCE BASED ON 6 DECADES OF RE-ANALYSIS DATA

Bahareh Kamranzad, University of Strathclyde, bahareh.kamranzad@strath.ac.uk
Khalid Amarouche, Bursa Uludağ University, khalidamarouche@uludag.edu.tr
Adem Akpinar, Bursa Uludağ University, ademakpinar@uludag.edu.tr

ABSTRACT
We discuss the impact of changing climate on swell domination, globally using 6 decades of wave simulation and show how the share of swells in significant wave height varies spatially during various decades. Such outcomes will help us develop a learning pattern to detect future changes in swell-dominated areas.

INTRODUCTION
Surface ocean waves are in general a combination of seas (locally generated waves) and swells. Understanding swell domination in the ocean is crucial for safety during recreational activities, coastal erosion control, and marine operations. Swell can create hazardous conditions for boats, surfers, and swimmers, and can contribute to shoreline erosion. Hence, it is important to develop an understanding of swell climate in a specific region for any future planning. Moreover, the changing climate and climatic fluctuations can affect the swell-dominated areas. In this study, we discuss the change in swell-dominated areas on a global scale. To detect the long-term changes in swell patterns, we used 6 decades of modelled wave climate using JRA-55 re-analysis wind field to discuss the decadal and multi-decadal variations.

METHODOLOGY
We used the JRA-55 re-analysis wind dataset (KOBAYASHI et al., 2015), with a spatial resolution of 60 km and a temporal resolution of 6 hours, to force the SWAN (Simulating WAves Nearshore) Cycle III version 41.31 (The SWAN Team, 2019) numerical wave model for the entire globe between 1958 and 2019. The bottom conditions were provided from the General Bathymetric Chart of the Oceans (GEBCO: https://www.gebco.net/) (spatial resolution: 30 arc-seconds). The computational grid covering the entire globe (0° E-360° E in longitude and 90° S-90° N in latitude) was employed with a spatial resolution of 1° and computational time steps of 30 minutes. The output grid was also considered with the spatial and temporal resolutions of 1° and 6 hours, respectively. The wave model was calibrated by tuning the whitecapping coefficient to minimize errors in comparison with the measurement, i.e., in-situ and satellite data. The validated model was then used to generate the wave climate including significant wave height (combined sea and swell waves) (H_s) and swell wave height (H_{swell}), for six decades (1958-2019), and the results were used in inter and intra-annual assessment of variation in wave climate.

RESULTS & DISCUSSION
Based on the simulated wave climate for the period of 6 decades, the ratio of H_{swell} to H_s was calculated for each time step and the average values of the ratio were calculated for various multi-decadal scales. Figure 1 shows the ratio of H_{swell} to H_s for three 20-yearly periods, i.e., 1960-1979, 1980-1999 and 2000-2019. According to this figure, the regions with higher swell dominance ratios have varied across different time scales, with the most recent period displaying higher dominance in certain areas. The study also conducted a decadal-scale analysis to quantify these changes and identify regions that are more vulnerable to fluctuations in wave climate in terms of swell dominance. Further details of these findings will be discussed in the full paper.

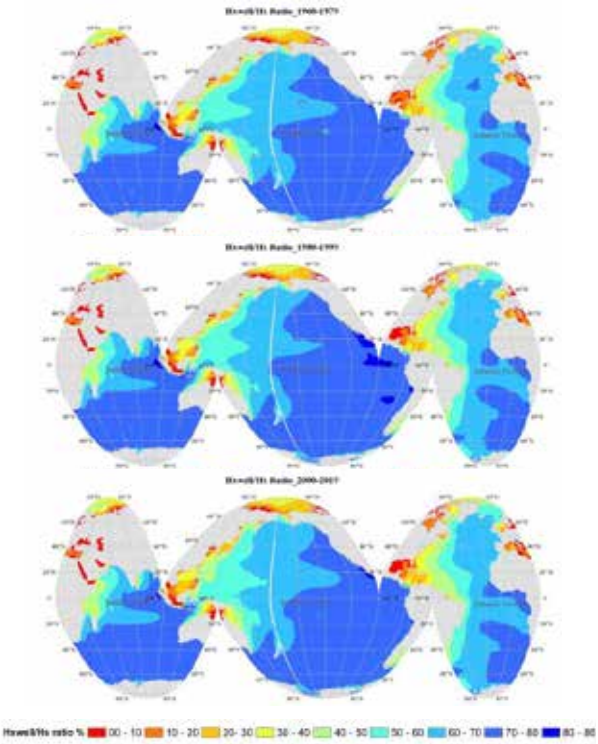

Figure 1 Spatial distribution of swell-dominated areas in multi-decadal scales

REFERENCES
Kobayashi, Ota, Harada, Ebita, Moriya, Onoda, Onogi, Kamahori, Kobayashi, Endo, Miyaoka, Takahashi (2015): The JRA-55 Reanalysis: General Specifications and Basic Characteristics. Journal of the Meteorological Society of Japan. Ser. II, vol. 93(1), pp. 5-48.

The SWAN Team, (2019). SWAN Cycle III version 41.31.

FUTURE CHANGES IN MAGNITUDE AND FREQUENCY OF EXTREME WAVES IN THE MEDITERRANEAN SEA

Andrea Lira Loarca, Dept. of Civil, Chemical and Environmental Eng., University of Genoa, andrea.lira.loarca@unige.it
Giovanni Besio, Dept. of Civil, Chemical and Environmental Engineering, University of Genoa, giovanni.besio@unige.it

INTRODUCTION

The impacts of climate change on coastal areas worldwide are posing a threat due to the increasing occurrence of extreme sea levels. Rising sea surface and air temperatures, in combination with continued sea-level rise, make the roughly 20 million people living in low-lying coastal areas highly vulnerable. The Mediterranean Sea is particularly vulnerable to climate change impacts, with a higher susceptibility to extreme events than the global average. As a result, it has been identified as a vulnerability hotspot (Ali, 2022).The projected changes in waves and their regional and local variability are critical in determining future coastal water levels and impacts. While past studies have relied on Global Climate Models (GCM) with low spatial resolution to analyze the future wave climate changes, high-resolution Regional Climate Models (RCMs) projections can improve the characterization of wave climate at a local scale. This is especially important for conducting coastal impact assessments and adaptation studies.

Therefore, this study focuses on analyzing the frequency and magnitude of extreme wave events in the Mediterranean Sea. We employ a regional ensemble of wave climate projections developed with the numerical wave model Wavewatch III, forced by surface wind field data from 17 EURO-CORDEX GCM-RCMs. By examining the seasonality of extreme wave events, we hope to provide valuable insights into the potential impacts of climate change on the Mediterranean coastal region.

DATA AND METHODS

Wave climate projections in the Mediterranean Sea were generated on a 10km grid providing, for each GCM-RCM combination, 3-hourly data for 1970-2005 for the reference period and 2006-2100 for projections under the high-emission scenario RCP8.5 of H_s, T_p and θ (De Leo, 2020; Lira-Loarca, 2021). To remove any inherent biases in the GCM-RCM simulations, we used a monthly-EQM method to bias-adjust the wave projections. Future changes were assessed against a validated hindcast generated using the same setup for the period of 1979 until 2020, which was utilized as a reference for the bias correction (Mentaschi, 2015).

To analyze the magnitude and frequency of extreme waves for different thresholds, we employed different extreme indices for rough and high wave days as well as the frequency of rough and high sea states. Additionally, we analyzed the indices seasonally to examine the future temporal variability in wave extremes. To ensure the robustness of our results, we followed the AR6 methodology to identify areas with robust, conflicting, or no robust change while accounting for internal variability.

RESULTS

Figures 1 and 2 present the changes for Mid-century (2030-2050) with respect to Hindcast for rough wave days and frequency of events for Hs>1.25 m. Different indices will be presented as well as the seasonality of the results.

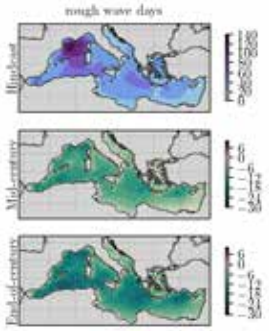

Figure 1 - Number of rough wave days for hindcast and projected changes for mid- and end-of-century.

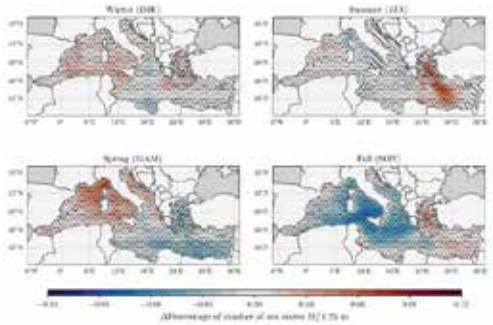

Figure 2 - Seasonal changes in number of sea states between the for Mid-Century and Hindcast for H_s >1.25 m

REFERENCES

Ali, Cramer, Carnicer, Georgopoulou, Hilmi, Le Cozannet, Lionello. (2022). Mediterranean Region. Climate Change 2022: Impacts, Adaptation, and Vulnerability. WGII AR6.
De Leo, Besio, Mentaschi (2021): Trends and variability of ocean waves under RCP8. 5 emission scenario in the Mediterranean Sea. Ocean Dynamics, 71(1), pp.97-117.
Lira-Loarca, Ferrari, Mazzino, Besio (2021): Future wind and wave energy resources and exploitability in the Mediterranean Sea by 2100. Applied Energy, 302, p.117492.
Mentaschi, Besio, Cassola, Mazzino (2015): Performance evaluation of Wavewatch III in the Mediterranean Sea. Ocean Modelling, 90, pp.82-94

BEYOND LIMITS: EXAMINING BEACH CARRYING CAPACITY UNDER CLIMATE CHANGE

Rut Romero-Martín, Universitat Politècnica de Catalunya· BarcelonaTech, rut.romero@upc.edu
Herminia I. Valdemoro, Universitat Politècnica de Catalunya· BarcelonaTech, herminia.valdemoro@upc.edu
José A. Jiménez, Universitat Politècnica de Catalunya· BarcelonaTech, jose.jimenez@upc.edu

Tourism is one of the most important economic activities in Spain, which is one of the world's leading destinations. On the Spanish Mediterranean coast, Catalonia is a region that also has tourism as a major economic driver, contributing around 12% of its GDP (2019) and employing more than 300,000 people. Most of this tourism is concentrated in coastal areas and can be categorized as sun-and-beach tourism, so its contribution to highly touristic coastal municipalities can exceed 20% of their GDP (Garola et al. 2022).

This makes these areas highly economically vulnerable to any disturbance affecting demand, as occurred in recent years under the COVID-19 pandemic (e.g. Moreno-Luna et al., 2021) or the resource to be exploited (Garola et al., 2022). In this context, the main exploited natural resources are beaches and their capacity to provide a recreational function. In this sense, climate change becomes one of the most important threats potentially affecting the survival of the region's beaches and, consequently, the current tourism industry.

Here, we analyze the evolution and management of the beach carrying capacity (BCC) in a territory under the effects of sea level rise (SLR). To do so, we adapt the methodology presented by López-Doriga et al. (2019) to include the implementation of adaptation measures to manage the BCC. To this end, several adaptation tipping points are defined according to the expected consequences on the provision of recreational services: critical point (PC), collapse point (PCL), and no-return point (PNR). The analysis is performed at different spatial scales reflecting the structure of the management system, i.e. municipality, county, and region. These are the spatial units where the BCC of individual beaches, the demand (beach users), and the resources needed for adaptation are integrated.

In this context, this work aims to analyze different adaptation strategies for the long-term management of the BCC in Catalonia (Spain, NW Mediterranean) to cope with the effects of sea level rise during this century.

To this end, four different scenarios have been analyzed.

- *Baseline scenario*. The evolution of the BCC along Catalonia until the end of the century. To this end, we consider current evolution rates plus the projected impact of sea level rise on beaches. This will be done for two IPCC AR6 scenarios (SSP2-4.5 and SSP5-8.5). This scenario does not consider the implementation of any adaptation measure.
- *Max. intervention scenario*. It is built by estimating the resources needed to locally maintain the current BCC. This involves compensating for beach erosion to maintain a given width to accommodate users according to a target user density by the site. This scenario considers beach nourishment as the adaptation measure to be adopted and estimates the quantity (volume) and quality (characteristics) of sediment to be used. It serves to define the characteristics of the strategic sediment reservoir required to maintain the current BCC throughout this century.
- *Min. intervention scenario*. It is built by estimating the resources needed to locally maintain the BCC within a tolerable range, which is given by the *critical point* fixed at each location. It also considers beach nourishment as an adaptation measure, but the volume of the intervention is lower and it is not homogeneously applied throughout the territory.
- *Spatial planning scenario*. It is built by redistributing the demand (beach users) along the territory to maintain the BCC within a tolerable range in a given spatial unit. Here we estimate from where and to where users should move to optimize the integrated (within the spatial unit) BCC. To build this scenario, in addition to the evolution of the BCC we consider the existing demand throughout the territory. Since this scenario will have serious consequences for the local economy, we use two different spatial scales: *county* (which integrates several neighboring municipalities) and *regional* (the entire territory).

In the final work, we shall present the following methodology in detail and the obtained results for all scenarios. In this sense, we identify which are the hotspots in terms of the most vulnerable municipalities, and the expected timing of the collapse of their BCC without adaptation and, the implications of each of the analyzed adaptation strategies.

ACKNOWLEDGEMENTS
This work was done in the *CoastSpace* project (TED2021-130001B-C21 MCIN/AEI/10.13039/ 501100011033).

REFERENCES
Garola, López-Dóriga, Jiménez (2022): The economic impact of sea level rise-induced decrease in the carrying capacity of Catalan beaches (NW Mediterranean, Spain). *Ocean & Coastal Management*, 218, 106034.
López-Dóriga, Jiménez, Valdemoro, Nicholls (2019). Impact of sea-level rise on the tourist-carrying capacity of Catalan beaches. *Ocean & Coastal Management*, 170, 40-50.
Moreno-Luna, Robina-Ramírez, Sánchez, Castro-Serrano (2021): Tourism and sustainability in times of COVID-19: The case of Spain. *Int. J. Environmental Research and Public Health*, 18(4), 1859.

COASTAL ARCHAEOLOGICAL AND NATURAL SITES OF TURKIYE THREATENED BY SEA LEVEL RISE

İremnaz Kösem, Middle East Technical University, e216226@metu.edu.tr
A. Çağatay Uysal, Middle East Technical University, cauysal@metu.edu.tr
Akdeniz İnce, Middle East Technical University, akdeniz.ince@metu.edu.tr
Gülizar Özyurt Tarakcıoğlu, Middle East Technical University, gulizar@metu.edu.tr
Ayşen Ergin, Middle East Technical University, ergin@metu.edu.tr
M. Lütfi Süzen, Middle East Technical University, suzen@metu.edu.tr
Deniz Burcu Erciyas, Middle East Technical University, berciyas@metu.edu.tr
Uğur Çalışkan, Mugla Sıtkı Kocman University, ugurcaliskan@mu.edu.tr
Ahmet Cevdet Yalçıner, Middle East Technical University, yalciner@metu.edu.tr
Güzden Varinlioglu, İzmir University of Economics, guzden.varinlioglu@ieu.edu.tr

INTRODUCTION

Throughout history, humanity preferred to live near the water. Therefore, the coasts have become the centers of trade and cultural exchange. Turkiye has numerous cultural heritage sites on the coast under the threat of sea level rise due to climate change. The Scientific and Technological Research Council of Turkiye (TUBITAK) funded project "Vulnerability of Coastal Cultural Heritage Areas to Sea Level Rise and Its Impacts" (No: 122M613) focuses on Turkish coastal cultural heritage sites protected by law. The project aims to quantify coastal vulnerability by using the Fuzzy Coastal Vulnerability Assessment Model (Ozyurt, 2010) and integrating this information into a specific module that will be developed for the cultural heritage context.

METHODOLOGY

Firstly, the heritage sites that will be analyzed are determined based on their proximity to the coast. In this project, the coastal area is defined as a zone below 10-m elevation and within 1 km distance from the shoreline using the DEM data of the Copernicus database. The archaeological and natural heritage sites of the 1st - 3rd degree of protection are considered among various cultural heritage sites with different protection levels classified by law. Most of the cultural heritage site information (location, area, and protection level) are obtained from mesoscale Environmental Order Plans of the coastal provinces accessed via WMS servers of the Ministry of Environment, Urbanization, and Climate Change. The missing information was retrieved as GIS layers from the Ministry's open-source ATLAS database (www.atlas.gov.tr) by manually drawing the polygons on the map. The coastal area layer and the cultural heritage information overlapped in the GIS environment to determine the sites to be analyzed by the project.

INITIAL RESULTS

Within the coastal area defined by the project, Turkiye has 1221 heritage sites (742 archeological and 479 natural heritage sites) located at the coast under possible risks of sea level rise. 22% of these heritage sites are located in the Mediterranean, 40% in the Aegean, 32% in the Marmara, and 6% in the Black Sea Region. First-degree heritage sites with the highest protection level constitute 33% of natural and 55% of the archeological sites at the coast. Table 1 shows more sites close to the shoreline but probably have low vulnerability due to higher elevations. Still, %75 of the sites satisfy both the elevation and distance criteria indicating that these sites have higher risks considering the impacts of sea level rise.

Table 1: Classification of the collected heritage sites. (N: Natural, A: Archeological)

Site Type / Satisfied Criteria	N	A	Total
Below 10 m Elevation	416	527	943
Within 1 km Distance from the Shoreline	470	714	1184
Both	407	499	906
Total	479	742	1221

It should be noted that these numbers are expected to increase significantly when the other areas protected by special laws and wildlife sanctuaries are included in the assessment within the project's scope at later stages.

The project's next steps include assessing various natural and social factors affecting the vulnerability of these sites. The most vulnerable sites will be determined based on vulnerability assessments to coastal erosion and flooding, which are the direct impacts of sea-level rise. Then, FCVAM model integrated with a separate module, which will be generated to assess the vulnerability of cultural heritage sites specifically, will be applied to each vulnerable site. The separate module will assess each heritage site's physical and social characteristics, enhancing the vulnerability. Ongoing research results of the vulnerability factors for these sites will also be presented during the conference.

REFERENCES

European Union, Copernicus Land Monitoring Service, (2016) European Environment Agency (EEA)
Ozyurt. Ergin. (2010): Improving coastal vulnerability assessments to sea-level rise: a new indicator-based methodology for decision-makers. Journal of Coastal Research, vol. 2. pp. 265-273.

COASTAL FLOODING ANALYSIS OF COASTAL SETTLEMENTS AS A PREREQUISITE TO ADAPTATION MEASURES

Andrea Tadić, University of Rijeka, Faculty of Civil Engineering, andrea.tadic@uniri.hr
Igor Ružić, University of Rijeka, Faculty of Civil Engineering, iruzic@uniri.hr
Nino Krvavica, University of Rijeka, Faculty of Civil Engineering, nkrvavica@uniri.hr

INTRODUCTION

The Adriatic Coast is of great cultural and economic importance for the Republic of Croatia, and sea level rise (SLR) could be one of the costliest impacts of climate change in the long-term. Estimates of average SLR along the Croatian coast range from 0.32 m to 0.65 m by 2100, with extreme estimates reaching values as high as 1.1 m. Adding the effects of storm surges (0.84 – 1.15 m) results in extreme occasional SL of 1.4 – 2.2 m above current mean SL by the end of the century (Republic of Croatia, 2020). Common coastal vulnerability assessments (e.g., Gornitz, 1990) include coastal flooding as one of the parameters. However, flood risk depends on the intensity of flooding and the site itself. Therefore, an individual approach is needed to propose adaptation measures and activities. In this paper, inundation areas, water depths, and wave heights were analyzed for different SLR scenarios in four Croatian coastal settlements previously classified with very high or high coastal vulnerability (Ružić et al., 2020): Cres, Krk, Punat, and Volosko. These settlements also represent a valuable cultural heritage.

METHODOLOGY

The analyses were based on the high-resolution products of the photogrammetric survey conducted with a drone (DJI Phantom 4 Advanced): digital orthophoto maps and 3D point clouds. The extreme sea levels during storm surges were analysed, ranging from already measured 1.15 m above sea level to predicted extremes. Flooded areas were determined in QGIS v.3.16 for six scenarios based on terrain elevations. From these, the floodplain areas were determined, as well as the inundated areas of protected cultural properties and the number of flooded buildings. The spatial distribution of the calculated water depths is also presented. Numerical simulations of wave propagation to the inundated areas were performed in SWAN for different sea levels and the relevant winds with a 50-year return period.

RESULTS

The results of performed analyses show that Cres and Punat are the most affected by flooding, with a similar size of flooded area per meter of coastline (over 30 m²/m'). The buildings in Cres and Rab are closer to the coastline, which results in greater damage. In contrast, the flooded areas in Punat are non-built-up public spaces, with only a few buildings affected. With SLR, the main problem in all studied locations will be a greater water depth of up to 0.5 m, which poses a threat to human lives. The risk level will be higher due to wave heights exceeding 20 cm with the SLR of 30 cm. An example of the resulting maps of Punat is shown in Figure 1. Most of the flooded areas in Volosko are located on coastal structures and in the southern part of the town. The biggest problem here will be increased overtopping, which can lead to other damaging effects.

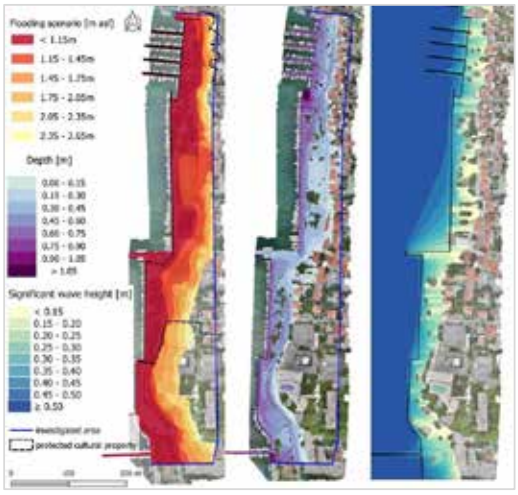

Figure 1. Coastal flooding maps for Punat (flooded area, water depths, and waves for SL 1.75 m asl)

CONCLUSIONS

In the analysed areas there is a risk of more frequent flooding from storm surges, which is further expressed. A methodology was developed to perform a quality analysis of coastal flooding to support future risk analyses and flood mapping, based on 3D point clouds.

The results of this study confirm that there is no *one-size-fits-all* solution and that an individualised approach is required when proposing measures to adapt to SLR and reduce the negative impacts of flooding. The concept of protecting old urban centers must be based on a multidisciplinary analysis of the entire, larger area, not just specific (problematic) sections of the coast. As part of regular maintenance, coastal infrastructure must also be adapted to expected sea levels. Given the complexity of the coastal flooding problem, it is necessary to define the guidelines and protection concepts for each settlement as soon as possible so that they can be implemented through the preparation of future spatial planning documents.

Numerical simulations were based on bathymetries generated from 3D point clouds, which enables the application for more complex simulations.

REFERENCES

Gornitz (1990): Vulnerability of the East Coast, U.S.A. to future sea level rise, Journal of Coastal Research, Special Issue no. 9, pp. 201-237.

Republic of Croatia (2020): Strategy for adaptation to climate change of the Republic of Croatia (in Croatian)

Ružić, Benac, Tadić, Krvavica, Petrović, Ljubičić, Jakupović (2020): Vulnerability analysis of the coastal zone of the Primorje-Gorski Kotar County due to sea level rise (in Croatian)

FUZZY-BASED COASTAL VULNERABILITY MODEL APPLICATION ON TURKISH COASTS WITH HERITAGE SITES

Akdeniz Ince, Middle East Technical University, akdenizince@gmail.com
Gulizar Ozyurt Tarakcioglu, Middle East Technical University, gulizar@metu.edu.tr
Aysen Ergin, Middle East Technical University, ergin@metu.edu.tr
Iremnaz Kosem, Middle East Technical University, e216226@metu.edu.tr
A. Cagatay Uysal, Middle East Technical University, cauysal@metu.edu.tr

INTRODUCTION

Global sea level rise severely threatens the "Coastal Cultural Heritage Areas" and "Natural Conservation Zones". Considering the long shorelines and Anatolia's history, Turkey has many of these areas at its shores. The importance of these areas to Turkey's economic and social development goals cannot be disregarded. Thus, as a part of the TUBITAK-funded project (No: 122M613), the shorelines where nature conservation and coastal cultural heritage areas exist are to be studied for their vulnerability to the impacts of sea level rise. Although impact analysis of sea level rise, such as coastal erosion rate and flooded areas due to extreme water levels, indicate the vulnerability of shoreline, a holistic approach considering human activities and physical characteristics of the coastline presents a much more accurate representation of coastal vulnerability. Therefore, two shorelines with cultural and natural heritage characteristics (Elaia Ancient City, Izmir, and Sile, Istanbul) are analyzed in this study to show the advantages of the holistic approach, as the consequences of impacts could be irreversible for shorelines with heritage properties. Based on satellite imagery data, the selected sites have high coastal erosion rates (EMODnet coastal behavior dataset, https://emodnet.ec.europa.eu/). Sile is an urban environment, whereas Elaia Ancient City is part of a wetland.

FUZZY COASTAL VULNERABILITY ASSESSMENT

The coastal vulnerability is assessed by "Coastal Vulnerability Index (CVI)" which is determined by "Fuzzy Coastal Vulnerability Assessment Model (FCVAM)" (Ozyurt, 2010). The setup of the FCVAM model is moved from MATLAB to Python environment for open-source distribution of the model by modifying the simpful library (Spolaor et al., 2020) to define the fuzzy logic rulesets. Additionally, a Python-QGIS link is being developed to accelerate the assessment process by taking the inputs from the GIS environment directly for pre-processing and automatically getting the inputs of the model. While FCVAM model assesses sea level rise impacts on land, groundwater, and rivers along the coast, this study only focuses on coastal erosion, flooding due to storm surges, and inundation. Therefore, 12 input parameters out of 20 of the original parameter group of FCVAM model are used in the assessment (Table 1). The output of FCVAM model application provides CVI scores of individual impacts and a cumulative impact score. To ensure to reflect the local site conditions in the assessment, an extensive database is being collected and processed within GIS environment for each model input parameter.

Table 1 - Input Parameters of FCVAM model

Physical Parameters	Human Impact Parameters
Rate of Sea Level Rise (RSLR)	Reduction of Sediment Supply
Geomorphology	River Flow Regulation
Beach Slope	Engineered Frontage
Significant Wave Height	Natural Protection Degradation
Sediment Budget	Coastal Protection Structures
Tidal Amplitude	
Extreme Water Level	

RESULTS

The initial results show that although erosion rates via the EMODnet database indicate coastal erosion is a significant problem for these sites, Sile has higher vulnerability (4.00 vs. 3.11 out of 5.00) in terms of coastal erosion vulnerability, including the influence of sea level rise. In contrast, the wetland geomorphology improves the resilience of Elaia. On the other hand, flooding due to extreme water levels and inundation for both sites are similar, with higher vulnerability scores than coastal erosion. Overall CVI scores indicate moderate vulnerability (3.36) for Elaia shoreline and high vulnerability (3.79) for Sile considering the impacts of sea level rise on land. The results highlight the importance of a holistic approach rather than focusing on a single or narrow set of indicators.

This study also showed the importance of validating global/regional datasets at local levels. The coastal erosion rates by EMODnet database only sometimes reflect the local conditions. Similarly, datasets used as inputs have their advantages and drawbacks in the context of Turkey and for the project. This study will also present such examples in addition to the utilization of FCVAM model in the context of vulnerability of heritage sites to sea level rise. Additionally, alternative scenarios within the datasets (such as sea level rise scenarios) will be shown to provide an overview of the future vulnerability, which is valuable for decision-makers and stakeholders for adaptation measures.

REFERENCES

Ozyurt. (2010). Fuzzy Vulnerability Assessment of Coastal Areas to Sea Level Rise. Ph.D. Thesis. Dept. of Civil Eng. Middle East Technical University, Ankara, Turkey

Spolaor, Fuchs, Cazzaniga, Kaymak, Besozzi, & Nobile (2020). Simpful: A user-friendly Python library for Fuzzy Logic. International Journal of Computational Intelligence Systems, 13(1), 1687.

ASSESSMENT OF THE COASTAL VULNERABILITY INDEX FOR THE COMPLEX COASTLINE OF PRIMORJE-GORSKI KOTAR COUNTY, ADRIATIC SEA, CROATIA

Igor Ružić, University of Rijeka, Faculty of Civil Engineering, iruzic@uniri.hr
Andrea Tadić, University of Rijeka, Faculty of Civil Engineering, andrea.tadic@uniri.hr
Čedomir Benac, University of Rijeka, cbenac@uniri.hr

INTRODUCTION

Coastal vulnerability assessment is a complex process, usually simplified due to a great number of parameters (Pantusa et al., 2018). This task becomes even more complex when analyzing the coastal vulnerability of Primorje-Gorski Kotar County (PGZ), with extremely indented coasts, complex coastal geomorphology, and a total coastline length of 1.235 km. Carbonate rocky coasts prevail and less resistant siliciclastic rocks are reduced. Gravel and sandy beaches extend in places on the coasts

METHODOLOGY

Index-based approaches express coastal vulnerability through a one-dimensional Coastal Vulnerability Index (CVI).
The CVI for PGZ is calculated for 25 m wide segments, each represented by a single point. Using a simpler method did not produce realistic results due to the variability of CVI variables along the study area. The CVI was therefore calculated in every point using a modified formulation of Gornitz (1990):

$$CVI_{total} = \sqrt{\frac{a^2+b^2+c^2+d^2-e^2}{5}} \quad (1)$$

a - geological fabric
b - coastal slope
c - significant wave height
d - coastal flooding
e - beach

Coastal slope (b) implies the propensity for rockfalls and landslides, which occur frequently on steep coasts but are not normally the subject of vulnerability assessments. Significant wave height, H_S (c), was simulated using the numerical model SWAN under representative wind conditions. The variable H_S was used to account for the influence of high-impact, low-probability events on coastal vulnerability. Coastal flooding (d) was analyzed for current and predicted extreme sea levels.

RESULTS

The classes for each variable and the total CVI values were divided into five categories: very low (1), low (2), moderate (3), high (4), and very high (5) vulnerability. Defining them was a challenging task.
Each vulnerability variable was analyzed and mapped individually, considering their individual negative impacts. Figure 1 shows the results of the total CVI for the PGZ analysis.
The average value of total CVI is 2.02, indicating low vulnerability, but 13% (160 km) of the analyzed coastline has high and very high vulnerability, which is quite worrying. 24% of the coastline is at risk of coastal flooding during current extreme events, which will increase to 30% and 35% if sea levels rise by 60 and 120 cm, respectively.

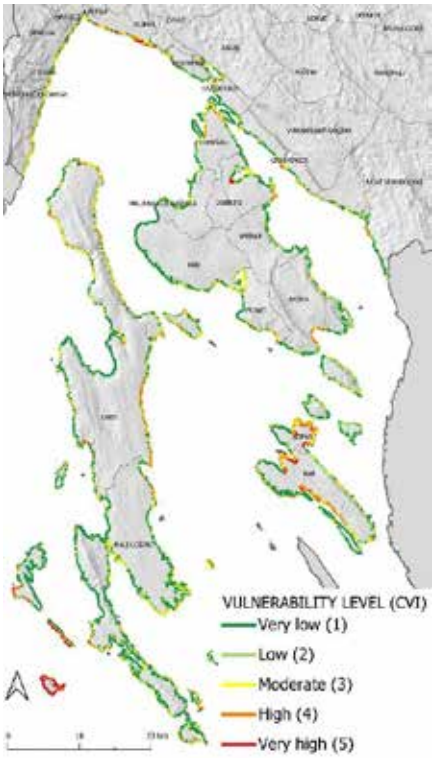

Figure 1 - Total CVI of PGZ

CONCLUSIONS

The complex geological fabric and coastal morphology of the investigated area required adaptation of existing approaches to determine the degree of coastal vulnerability. The presented CVI analysis takes into account the geological fabric and its combination with terrain slopes. Such an approach proved its worth in February of this year, when localised rockfalls and landslides occurred after an strong earthquake.
Due to the characteristics of the coastal area, it was necessary to perform CVI analyses for every 25 m of coastline. This was a challenging task that required an original approach. The conducted analyses showed that the most vulnerable areas are the existing settlements.

REFERENCES

Gornitz (1990): Vulnerability of the East Coast, U.S.A. to future sea level rise, Journal of Coastal Research, Special Issue no. 9, pp. 201-237.
Pantusa, D'Alessandro, Riefolo, Principato, Tomasicchio (2018): Application of a coastal vulnerability index. A case study along the Apulian Coastline, Italy, Water (Switzerland), vol. 10(9), pp. 1-16.

SCARC 2023.
Conference on Applied Coastal Research
4 – 6 September. Istanbul, Turkey

Development of a low cost, self-configuring ADCP and integrated deployment and recovery system

David W. Velasco[1], Cristobal Molina[2]

[1] *Nortek Group. San Diego. USA*
[2] *Nortek Group. Oslo. Norway*

***Abstract* – Here we present the development of a short range (0.5 to 20 m), low cost (< USD 5,000), three-beam, 1 MHz acoustic Doppler current profiler called the Nortek ECO. The system employs a robust wideband velocity measurement technique where the only required user inputs are: 1) when deployment should start, 2) how often to sample, and 3) what is the water type. The hardware is highly portable, measuring only 130 mm tall by 85 mm in diameter and weighing 1.0 kg in air. It communicates externally with Bluetooth Low Energy technology and is powered by an embedded smart Li-Ion battery that is charged by induction. Three independent activation methods are implemented, including Near-Field Communication, and all communication controlled via a platform-independent Progressive Web App. Coupled with the ADCP is a deployment and recovery system allowing for single person operation at depths up to 50 m. Discussion of the system concept and design are presented, including sample data. This is an example for preparing the full paper that is identical with the extended summaries format. It must be written in Times New Roman.**

Keywords - Portable ADCP, Shallow Water, Low Cost.

I. INTRODUCTION

Since its commercial inception in the early 1980s, theAcoustic Doppler Current Profiler (ADCP) has been expanding our knowledge of the world's water bodies, from small streams to the open ocean. For the oceanographic community, having a single instrument capable of collecting three-dimensional current profiles that were accurate, precise and with no drift was revolutionary. Here we present a newly developed ADCP, called the Nortek ECO (Fig. 1) that will continue this tradition, being designed to be highly portable, low cost, and yet require no prior experience to successfully collect high quality current profile data.Body paragraphs (like this one) should be set in Times New Roman 10pt, full justification, in two column format. Line spacing is single-spacing [1].

Fig. 1. ECO ADCP shown next to a standard size soda can for scale.

Additionally, it has been recognized that one of the job functions of any Oceanographic Instrumentation Technician (OIT) is the actual deployment of instruments in various ocean environments [1]. For many technicians, designing, deploying, recovering and maintaining an ADCP deployment apparatus is almost as complex as (and as costly as) the instrument itself. With this in mind, we also report on the ECO's integrated deployment and recovery system, which is made up of a ready-to-deploy subsurface buoy and a timed release.

SCARC 2023.
Conference on Applied Coastal Research
4 – 6 September. Istanbul, Turkey

II. DESIGN CONCEPT AND IMPLEMENTATION

The system's design concept was purposely constrained by seven factors as presented, all the while maintaining a target Manufacturer Suggested Retail Price of under USD 5,000 for the ADCP itself (under USD 7,000 inclusive of deployment/recovery system).

A. Small size

The first objective was to make the ADCP about the size of a soda can (Fig. 1), which had direct implications to most subsequent requirements. This process focused primarily on the design of a new electronics platform. We started by implementing a transducer multiplexing (sequential pinging) architecture that significantly reduced the transmit/receive circuitry size. The electronics platform also uses a single wireless communication method (Bluetooth Low Energy) that eliminated the need for multiple interface circuitry such as Serial and Ethernet, as well as external connectors (see section II.E. for details). We then established an internal battery as the single power source, which eliminated the need for input power line protection and filtering, further reducing the electronics size. Moreover, the system's Digital Signal Processor (DSP) was optimized to minimize standby current consumption, reducing the required battery size. Finally, the minimal transducer set required for three-dimensional currents (3) was used, minimizing the head's diameter. The resulting electronics platform allowed for a highly portable system only 130 mm tall by 85 mm in diameter, with in air weight of 1.0 kg and in water weight of 280 kg and total volume of 693 cm2.

B. Self-configuring

The second objective was to reduce the required user input to the absolute minimal for complete system configuration:

1)when deployment should start

2) How often to sample, and

3) Approximate water salinity.

In contrast, to configure a traditional ADCP for current profiling in an up-looking, autonomous deployment, users must also provide additional information on 1) available power and memory, 2) required deployment duration, 3) estimated depth range, and 4) desired spatial resolution. Next, we describe how each of these were addressed so the ECO can self-configure.

We start by discussing available power, which has historically been a difficult parameter to determine automatically. This is primarily due to ADCPs having traditionally used alkaline batteries as power source, whose voltage seldom is representative of available capacity, especially when not measured under a load or when a fresh

battery is not used or both. Furthermore, user-supplied batteries rarely meet the same specifications of their manufacturer-supplied counterparts. However, with recent advancements in smart Lithium-Ion batteries, accurate power

capacity can be easily determined. In the ECO implementation, a 7.2 VDC, 10.5 Ah smart Li-Ion battery was chosen, with embedded electronics capable of accurately reporting its capacity level and charge state. Lithium-Ion technology was chosen mostly due to it being long lasting and efficient at charging and energy transfer.

Available memory capacity has expanded significantly in recent years, and the ECO employs a micro-SD 16 GB card for data storage. At maximum number of cells (30) and shortest measurement interval (2 minutes), the ECO uses less than 1 MB/day. If a lunar cycle deployment is considered—a typical coastal oceanography deployment duration—at this acquisition rate the ECO has enough memory for almost 50 years of back-to-back monthly deployments, making storage a non-limiting factor. Directly connected to available power and memory is the required deployment duration.

TABLE I. SAMPLE ECO DEPLOYMENT DURATION (DAYS)

		Deployment Depth			
		4 m	8 m	12 m	20 m
Meas. Interval	2 min.	12	27	25	33
	5 min.	11	55	63	78
	10 min.	20	108	122	151
	30 min.	41	208	232	285

SCARC 2023.
Conference on Applied Coastal Research
4 – 6 September. Istanbul, Turkey

This has traditionally been an important input so that ADCP configuration software can compute whether the available power and memory are sufficient to meet the user requested duration. In the ECO implementation, rather than requesting a deployment duration from the user, the user is given the maximum duration based on a dynamic calculation of the available battery capacity and the instrument's configuration. This calculation is conservatively weighted to account for factors such as temperature and large depth range fluctuations (which impact transmit pulse power). An internal model is then consulted, and the maximum number of days automatically displayed. As an example, Table 1 shows a small subset of the model's output relating the user requested measurement interval (in minutes) and deployment depth, returning the duration, in days, of the deployment.

Depth range and spatial resolution are connected parameters that together define where in the water column velocity measurements will take place. In practice these define the cell size and their quantity. The choice of cell size is always a tradeoff between the user's desired spatial resolution and the acceptable velocity precision, which is generally given by:

$$\sigma = \frac{C}{F\,D\,\sqrt{N}}$$

where C is a configuration specific constant, F is the carrier frequency, D is the cell size, and N is number of pings within the measurement interval. The ECO self-configures the number of cells and their size to cover the entire water column, adjusting the number of pings aiming to return a horizontal velocity precision of 1 cm/s or better within the user requested measurement interval. The choice of depth range and spatial resolution traditionally required advance knowledge of the site's depth, including tidal variations and is traditionally set beyond the maximum expected value for uplooking systems as a safety margin. In the ECO implementation, the height of the water column is regularly determined using pressure sensor data. These data are then used for continual range and resolution configuration adjustments Further processing is done with acoustic ranging during the automated quality control step (see section II.C.).

C. Three-dimensional currents from 0.5 to 20 m

Given that Doppler shift can only be detected along an ADCP beam's radial axis, linear algebra dictates that it must have at the very least three beams if three-dimensional current measurement is intended. Therefore, the ECO employs three wideband capable transducers of 1 MHz carrier frequency. The choice of frequency was based on: 1) Nortek's extensive experience with this frequency, and 2) this frequency's improved transducer construction through optimizing the tradeoff between ceramic diameter (25 mm), profiling range and bandwidth.

Secondly, the low end of the profiling range requirement (0.5 m), coupled with the self-configuring requirement and minimal user input, presents the most challenging of the ECO's development processes. For short ranges (< 2 m), profiling techniques such as pulse-to-pulse coherent have been successfully used [2-4]. However, even with advanced implementations such as Nortek's Multi Correlation Pulse Coherent (MCPC) method [5,6], the inherent range-velocity tradeoff still exists. This demands significant user intervention at both system configuration and data analysis stages in order to obtain consistently robust results. And, even then, conditions such as high turbulent flows still exist that prevent successful data collection with a pulse-to-pulse coherent method. With these limitations in mind and the desire for minimal user input, we have opted for an implementation of the wideband processing technique used in Nortek's AD2CP platform (U.S. Patent 7,911,880), with modifications for a wider bandwidth and pulse lag settings optimized for short range performance.

D. Automated Data Quality Control

As data are collected, the ECO's firmware automatically performs data quality control of both acoustic and ancillary sensor data. Below we list the filters applied, which are done in a sequential order as listed below.

1) Fish Detection Filter – Following the algorithm first described in [5], data is flagged where an improbably high echo intensity for the local (profile) statistics exists, as opposed to a fixed, pre-defined value as is commonly implemented.

2) Low Correlation Filter – Masks data where the complex correlation score between the two pulse echoes in the wideband processing is below 50%.

3) Bin Mapping – Maps depth cells to the vertical orientation based on tilt data.

4) Data Transformation – Applies mask to all beams forrespective cells where at least one beam has already been masked.

5) Percent Good: Filter – Divides number of cells that have passed previous filters by total number of available cells, and masks those < 50%.

6) Sidelobe Filter – Masks cells contaminated by surface sidelobe by comparing the minimum absolute pressure during averaging interval to a conservative cutoff value of 1050 hPa for the corresponding surface pressure.

7) Out of Water Filter – Masks cells above surface in similar fashion as sidelobe filter, but using along-beam projected distances.

8) High Tilt Filter – Masks entire profile where either pitch or roll is > 40°.

9) High Acceleration Filter – Computes standard deviation of pitch and roll over ensemble interval and masks entire profile where this exceeds 5°.

Once all filters are performed, the data remaining are ensemble-averaged over the measurement interval and are stored to memory.

E. No External Connectors

Lack of physical connections demands, explicitly, wireless communication and, implicitly, both an induction charged power source as well as an activation (wake-up) mechanism. As a consequence, the implementation also fully removed the need for the user to open up the instrument at all, for the life of the device.
Bluetooth Low Energy (BLE) was chosen as the communication technology as it offers flexibility and capability in a low energy framework that is widely used in most devices today. Additionally, BLE allows for significantly faster scan and connection sequence when compared to classic Bluetooth and Wi-Fi.
As far as an activation mechanism, although magnetic switches and other similar hardware have been used in underwater systems lacking outside connectors, we have opted for three independent activation means: 1) induction charging, 2) Near-Field Communication (NFC), and 3) vertical acceleration (termed “Shake & Wake”). For the first, once placed on the induction charging plate, battery charging is initiated, the main processor is awaken and the BLE processor starts broadcasting the ECO’s identification continuously while on the charging plate. The second alternate activation method, NFC, uses a chipset inside the ECO as a target device. Once the initiator device (normally a smartphone) scans the NFC tag it creates an interrupt to the BLE processor, which then wakes up the ECO’s main processor. The last activation alternative, Shake & Wake, uses a dedicated accelerometer to wake up the instrument upon sensing a vertical acceleration in excess of 1 g above background, at which point an interrupt to the BLE processor is created in the same fashion as the NFC. Although false triggering (e.g. during transport) may occur under some conditions, broadcasting has minimal impact on battery capacity. But to minimize false triggering, three limitations are placed: 1) only vertical accelerations are considered, 2) accelerations must be both positive and negative, and 3) single-cycle accelerations are not considered. Finally, the ECO shuts off the battery at a minimally safe capacity such that it will always store enough energy to wake up the main processor. Long term drawdown is only a few mW, allowing for multi-year storage.

F. Complete Package

By “complete package” we mean that the user, upon instrument delivery, has everything needed for a successful deployment in water depths up to 50 m. Exempt from this requirement is the vessel to arrive at the desired site (if one is needed), anchor weights and a device for configuration, such as a smartphone. To meet this requirement and address common challenges related to deploying and retrieving an ADCP, including manufacturing a deployment frame, the ECO implementation provides an integrated deployment and recovery system comprised of two sub-surface buoys and a time-release device, (Fig. 2 and Fig. 3). With this system, both deployment and recovery of the ECO can be easily performed by a single-person with minimal vessel support (e.g. only a kayak).

The main components of the deployment and recovery system are shown in Fig. 2. The top buoy houses the ECO ADCP itself, which is secured to the buoy via a locking ring. A timed-release device is housed in the bottom buoy. Both buoys are connected by a supplied rope loop, about 30 cm long. Inside the bottom buoy is a supplied coil of 60 m, 4 mm

SCARC 2023.
Conference on Applied Coastal Research
4 – 6 September. Istanbul, Turkey

diameter, Polyester rope. The rope is kept in place by a lid. The Release has holes for shackles at both its top and bottom. One end of the rope is attached to the top shackle while the other end to the bottom shackle. The top buoy is also attached to the top shackle and the anchor weight is attached to the bottom shackle. Once the release is activated, the top cap of the release (with shackle attached) is freed, floating to the surface pulled by the buoyancy of the top buoy, and at the same time bringing up with it the rope coiled inside the bottom buoy. As all components are attached together, the entire mooring inclusive of anchor can be retrieved. The ECO ADCP and Release are both rated to 50 m.

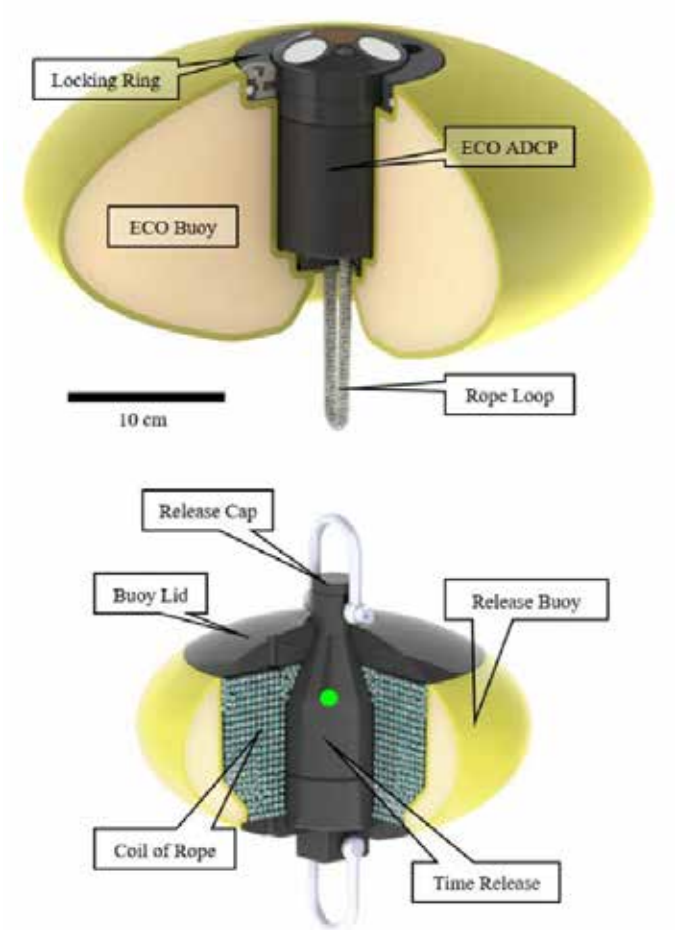

Fig 2. ECO buoy (top) and Release buoy (bottom) cutaway view showing main components. With the ECO ADCP installed, the top buoy has 11 kg of buoyancy and with the Release installed, the bottom buoy has 3 kg of buoyancy. Drawings are to scale and a 10 cm marker is shown for reference. All exposed materials are non-corrosive.

SCARC 2023.
Conference on Applied Coastal Research
4 – 6 September. Istanbul, Turkey

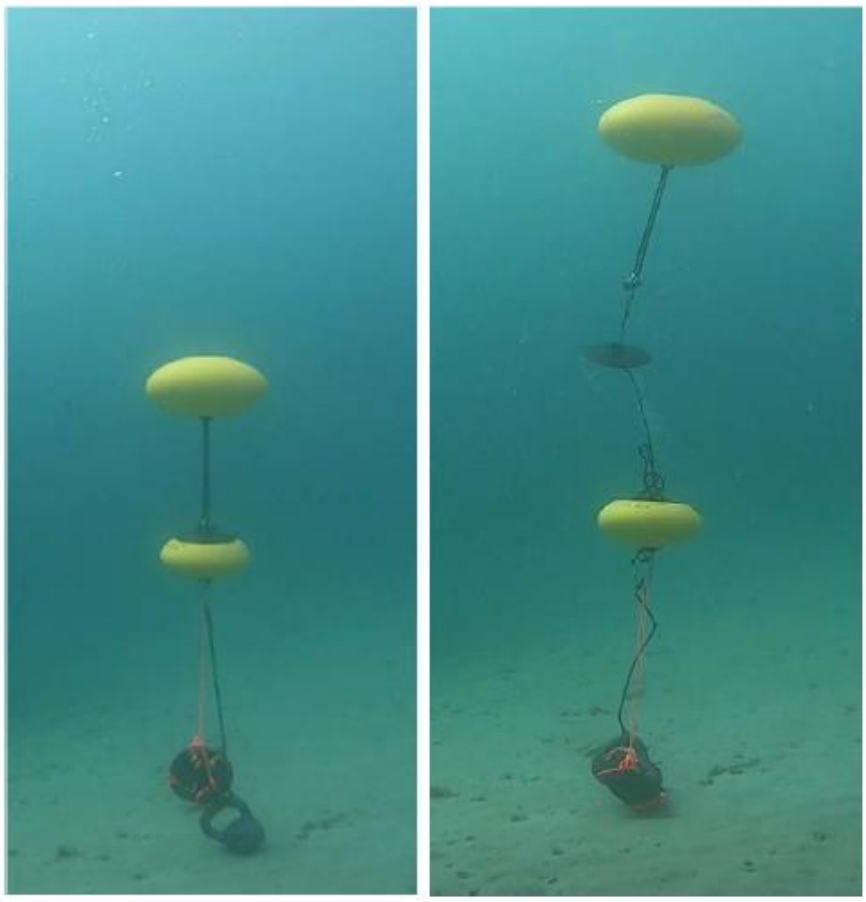

Fig 3. Complete mooring line as deployed (left). Once released (right), the ECO buoy (top buoy) floats toward the surface pulling the Release buoy lid along with the coil of rope housed inside it, allowing for retrieval of entire mooring, inclusive of anchor weight.

The ECO Release is a time-release mechanism comprised of a high-torque motor powered by four user-replaceable AA batteries (Fig. 4). The device is programed to activate at a user-defined date and time. Once activated, the release's motor drives a low-friction titanium screw which holds the release's top cap. The ECO Release has a Safe Working Load of 200 kg, which is a factor of 8 greater than the typical load with the ECO buoy. The motor also provides > 25 kg of lifting force thus capable of dislodging potential biofouling between the cap and its female socket.

SCARC 2023.
Conference on Applied Coastal Research
4 – 6 September. Istanbul, Turkey

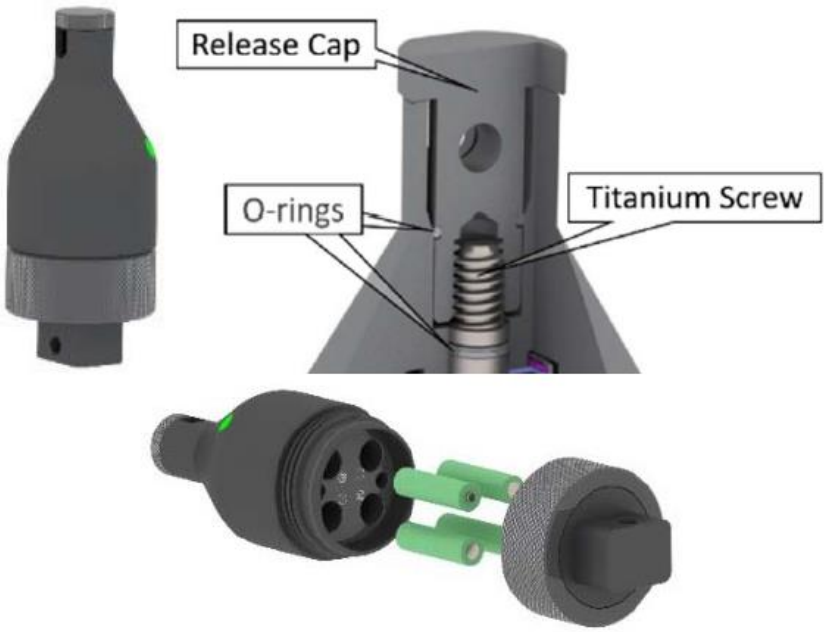

Fig. 4. ECO timed-release device (top-left). Cutaway of release's top showing titanium screw and removable top cap with hole for shackle (top right). O-ring seals help minimize sediment intrusion and biofouling around the titanium screw. Bottom image shows AA-size battery compartment with screw-on lid.

A mooring analysis was performed with Dynamic Systems Analysis' (DSA) *ProteusDS* software, which is an ocean engineering program used to simulate the dynamic mooring response in wind, waves, and currents. The mooring was resolved with a finite element model and the top buoy with a rigid body model. The hydrodynamic drag, buoyancy, and added mass effects were accounted for and the result shows that tilts remain under 8° under steady-current cases up to 1 m/s (Fig. 5). Although the ECO's tilt data are averaged over the ensemble and not stored for every ping, visual observations of tilt during test deployments compare well with the modelled results. With respect to waves, dynamic loads were also modelled at 10 m mean depth (no mean currents) and showed that mean tension on the anchor remains consistently around 140 N under various conditions (Fig. 6), matching the static floatation of the combined ECO buoy (11kg) and Release buoy (3 kg).

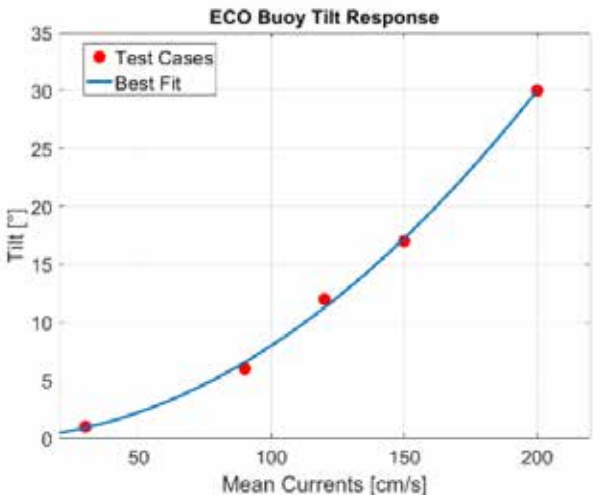

Fig. 5. Modelled ECO buoy tilt response to mean currents. Tilt remains under 8° for currents up to 1 m/s.

SCARC 2023.
Conference on Applied Coastal Research
4 – 6 September. Istanbul, Turkey

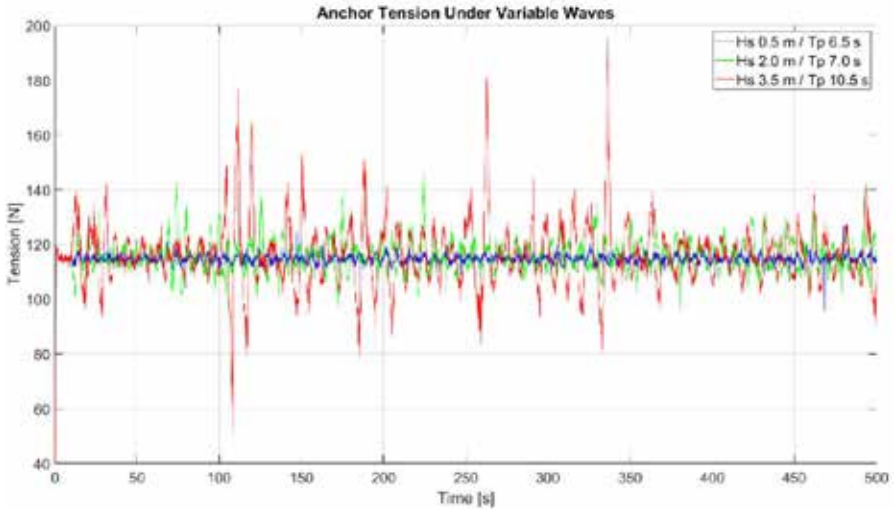

Fig. 6. Modelled anchor tension for three separate cases. Water depth used was 10 m and no mean currents were assumed.

Finally, for deployments in shallow water where the height of the mooring line may limit the useable profiling range, a bottom mount is also available as an option for the ECO. It is easily carried by one person, foldable for easy packing and transport, made of non-corrosive material, and low profile for operation in shallow water.

G. Multi-platform, cloud-based operation with geolocation

The seventh and last requirement envisioned: 1) maximizing usability across multiple devices (from mobile phones to desktop computers) and operating system; and 2) delivering a ready-to-use data report with minimal user interaction required. Furthermore, cloud-based data storage also opens up data sharing capability, allowing greater interdisciplinary collaboration among users as well as faster system enhancements.

Unlike platform-specific software, which must be developed independently and installed by the user on individual machines, the ECO software is implemented as a Progressive Web Application (WebApp) accessed online at eco.nortekgroup.com (Fig. 7) and utilizing the browser's Web Bluetooth interface for communication. WebApps offer a consistent user interface through a web browser, without needto install in a local machine. Although ECO data files inside the instrument's memory are stored in a proprietary binary format, once transferred to the WebApp data are converted to the human-readable JavaScript Object Notation (JSON) format, which is both open-source and self-describing. Additionally, data sharing has been implemented both internally and externally in both JSON and ASCII formats, allowing users to quickly share ECO deployments with anyone with an ECO account, thus facility interdisciplinary collaboration,

SCARC 2023.
Conference on Applied Coastal Research
4 – 6 September. Istanbul, Turkey

Fig. 7. Screenshot of ECO WebApp main page showing the main setup steps (top) and sample data display (bottom). Note the easy-to-read approach with three layers shown.

As data download and display is performed on a WebApp, it is also inherently cloud-based. We have opted for Microsoft's Azure cloud computing platform for this service. User access is controlled with password-protected credentials to an individual ECO account. The built-in GNSS receiver allows ECO deployment data location to be easily mapped within the WebApp. Geolocation also provides automatic magnetic declination compensation through a NOAA/NCEI API.

Finally, although data from all depth cells are recorded by the ECO, in the interest of user accessibility, especially having in mind the before mentioned requirement of no prior experience needed, data display on the WebApp is limited to three layers at a time, and their position within the water column may be user defined, or automatically set.

III. SAMPLE DATA

Extensive field tests have been conducted with the ECO ADCP, both in shallow water (< 2 m) as well as deeper water (> 10 m). As of submission deadline for this paper, more than 45 in-water deployments have been performed in six countries with more than 12 separate instruments, and more than 2500 hours of data have been collected. In this section we highlight one such deployment showing performance of the ECO ADCP in comparison with a reference system.

A five day deployment east of Toulon, France, was conducted between 03/JUN/2020 and 08/JUN/2020. The site location is shown on Fig. 8, at a mean depth of 13 m and about 400 m from shore. The ECO was deployed by divers on a fixed bottom frame (Fig. 9). About 60 m to the west of the ECO was a Signature1000 reference ADCP, which was deployed along the same isobath. Oceanographic engineering firm Nortek Méditerranée operates a MetOcean buoy at this site, and wind speed and direction data were also collected.

The ECO was configured for a measurement interval of 10 minutes and it self-configured for 16 depth cells of 1 m each, a 0.1 m blanking distance (default) and 35 pings evenly spread over 105 s (0.33 Hz effective sampling rate), bringing the predicted horizontal precision to 0.99 cm/s. The Signature1000 was set for two concurrent measurements: Average and Burst/Waves, both using wideband pulses. In the Average Mode, it was configured for a measurement interval of 5 minutes sampled over 20 depth cells of 1 m each, a 0.1 m blanking distance and 105 pings over 105 s (1 Hz effective sampling rate). This had a predicted horizontal precision of 0.34 cm/s, a factor of almost 3 improvement over the ECO. Data from the Signature was further averaged to 10 minutes to match the ECO's interval. In the Burst/Wave Mode, the Signature1000 was configured for a continuous internal sampling rate of 8 Hz, internally averaging every two pings, for an effective sampling rate of 4 Hz throughout the five day deployment. A total of 20 depth cells of 1 m each were used, and blanking was 0.1 m, all set to match the ECO. The sampling rate used allowed for directional waves computation with the Signature1000 and these data are shown on the bottom of Fig. 11.

Fig. 8. Location of ECO/Signature1000 comparison deployment within the Golfe de Giens east of Toulon, France. ECO Location: 43.0838 N, 6.0879 E. Signature1000 was about 60 m to the west of the ECO along the same isobath. Mean water depth approximately 13 m. Nortek Med MetOcean buoy was about 70 m to the east of the ECO.

Fig. 9. ECO as installed in a bottom frame in the northern Golfe de Giens east of Toulon, France.

In evaluating the comparison deployment data quality, we start with the ancillary sensor data. As shown in Fig. 10 (a. and b.), both systems captured the small tidal and temperature variations at the site, showing nearly identical data. Compass heading (not shown) for both systems was steady at 264° for the Signature1000 and 117° for the ECO. Tilt data not shown), showed the ECO had less than 2° total tilt (with 0.4° standard deviation) while the Signature1000 showed larger tilt of approximately 9° (with 0.4° standard deviation). Although this tilt is higher than normally recommended (±5°), the shallow depth at the site meant negligible impact due to tilt.

Two acoustic parameters must be checked: correlation score and Signal-to-Noise Ratio (SNR) data. For wideband ADCPs, correlation describes how similar a returned echo is to itself at a delayed time, and its magnitude is a key quality measure of the velocity data. Acceptable correlation values vary between system hardware design and firmware implementation. A commonly used threshold is 50% [7]; data below this value is considered suspect. It is important to note that the impact of lower correlation values is a worsening of velocity precision and not of velocity accuracy

Signal-to-Noise Ratio (SNR) refers to the energy of the acoustic signal in relation to the energy of the system's noise. Data where the SNR is less than 3 dB above the noise floor are considered invalid. Both the ECO and Signature1000 systems used in this deployment had a noise level of approximately 26 dB and minimal SNR of 40 dB, even at the top of the water column (i.e. farthest range from instrument) as shown in Fig. 10.

Signal-to-Noise data (Fig. 10, e. and f.) show very similar patterns between the two instruments and a typical decay with range is observed. SNR values for both the ECO and the Signature1000 tend to be slightly lower for the second half of the deployment indicating water with fewer particles moved into the site. This also matches the noticeable drop in water temperature observed during this time. Review of correlation data (Fig. 10, c. and d.) shows both systems had values well in excess of 90% for the entire deployment and most of the water column, giving further assurance of data quality.

SCARC 2023.
Conference on Applied Coastal Research
4 – 6 September. Istanbul, Turkey

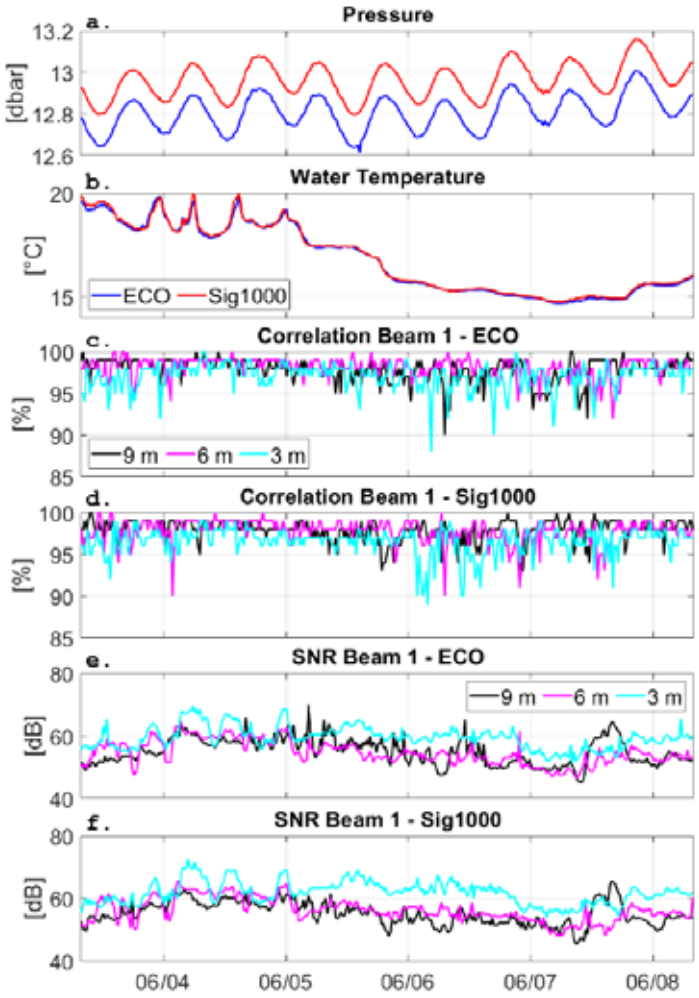

Fig. 10. ECO and Signature1000 environmental sensor and acoustic data. Panel a. shows pressure, b. water temperature, c. and d. are acoustic correlation score, and e. and f. are Signal-to-Noise Ratio (SNR) for the ECO and Signature1000, respectively. Panels c.-f. are for the three range layers normally used in the ECO's WebApp display and represent the top/middle/bottom of the water column. Distances are ranges above the top of the instrument. All times UTC.

Once satisfied with the overall data quality, we can proceed to review the current data (Fig. 11, a.) for the three range layers used. For the most part, the data compares very well, with the ECO data generally being slightly noisier when compared to the reference Signature1000 ADCP due to the coarser precision owed to the lesser number of pings accumulated over the 10 minute averaged interval (210 pings for the Signature1000 versus 35 pings for the ECO).

SCARC 2023.
Conference on Applied Coastal Research
4 – 6 September. Istanbul, Turkey

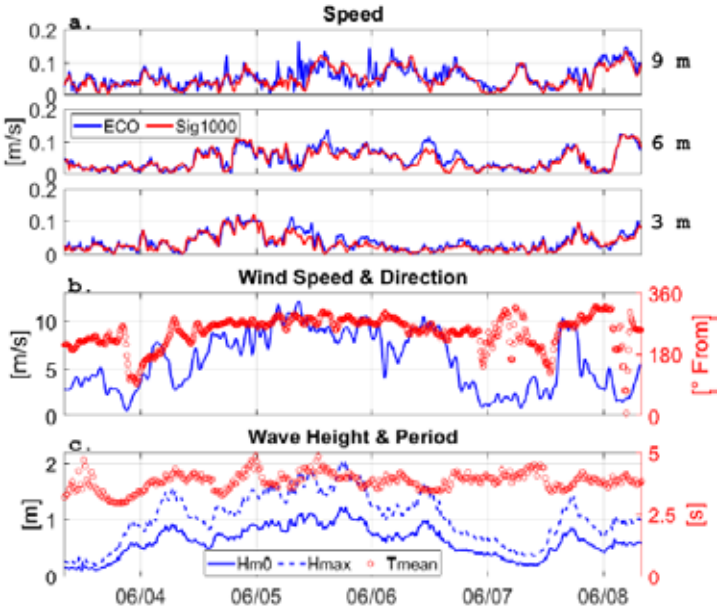

Fig. 11. ECO and Signature1000 horizontal current speed and direction, wind speed and direction, and basic wave statistics. Wind data are from a surface MetOcean buoy about 70 m away from the site. Wave data computed from Signature1000. All times UTC.

A linear regression of the horizontal current speed, $\sqrt{U^2 + V^2}$., between the two instruments for the three layers is shown in Fig. 12. A regression score (R2) of 0.73 was obtained which is significant given the number of points used (1080) and the inherent lower noise of the reference system in relation to the ECO, as evidenced by the scatter in the plot. Most of the outliers, especially those above the 1:1 line, are from the topmost range layer. The potential wind-induced shear within the top of the water column, in addition to undoubtedly higher near surface turbulence due to the wave conditions, poses a challenge for Doppler systems unless they provide both the spatial and temporal resolution to resolve these velocities. This is further complicated the farther away an up-looking ADCP is from the surface due to sidelobe interference, and the slanted beam separation distance as they intersect the surface. These effects contribute to the scatter observed in the regression, so in an effort to validate the regression model and better quantify any potential bias in the ECO velocities, we also produced a histogram of the difference in horizontal current speed between the two instruments (taking the Signature1000 as the independent variable) and fitted a Gaussian distribution function centered on the mean of the data (Fig. 13). From this we observe a bias of only +0.0049 m/s, which is less than the constant of the regression model (0.0089 m/s). Considering the test site produced very low mean currents of less than 10 cm/s, the resulting bias falls well within the 1% ± 0.5 cm/s accuracy specification for the ECO.

SCARC 2023.
Conference on Applied Coastal Research
4 – 6 September. Istanbul, Turkey

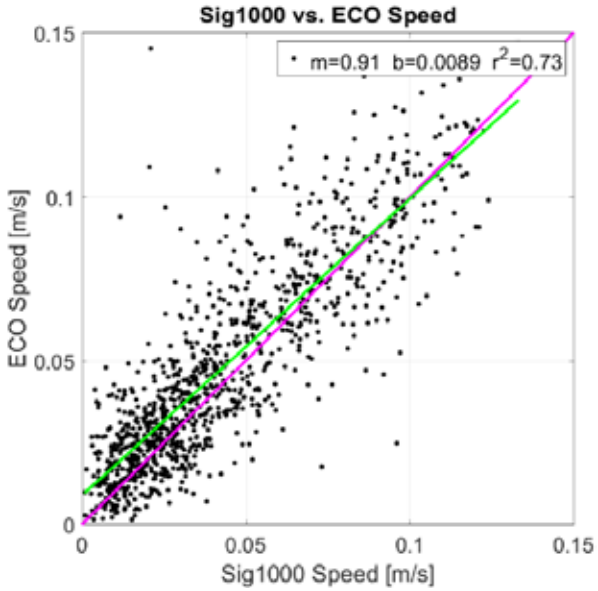

Fig. 12. Linear regression model of horizontal speed data from both instruments for the three layers used (3 m, 6 m, 9 m above instrument). R2 value of least-squares fit line (green) given on graph as well as y-interceptand slope. The 1:1 line (magenta) is also shown.

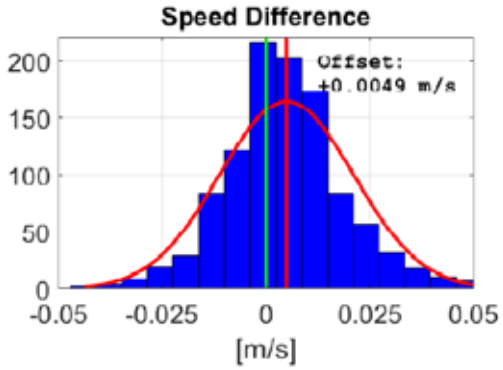

Fig. 13. Histogram of velocity residuals (ECO minus Signature1000) for the horizontal speed for the three layers used. A Gaussian distribution function was fitted to the data. Green vertical line represents 0 m/s difference while red vertical line is center of distribution. Offset from 0 m/s given.

IV. CONCLUSIONS

We have presented the design concept and development of a short range, low cost ADCP called the Nortek ECO. The system is based on a completely new electronics platform and designed to be self-configuring such that only three user inputs are needed: 1) when deployment should start, 2) how often to sample, and 3) what is the water type it will measure. It uses an implementation of Nortek's AD2CP technology to profile currents over a maximum range of 20 m and in water depths as shallow as 0.5 m. The hardware is complemented by an integrated deployment and retrieval system comprised of a subsurface buoy and time-release mechanism. The instrument contains no moving parts and no external connectors. Power is supplied by an inductively charged battery and all communications performed via a Bluetooth Low Energy link.

Data is visualized in a cloud-based Progressive WebApplication (WebApp), thus not requiring native software installation and being able to run on most smart devices. Datafrom a test deployment were presented where a bias of only +0.0049 m/s was observed against a reference system.

V. ACKNOWLEDGEMENTS

The authors would like to thank Antoine Bezile at Nortek Méditerranée for assistance with the ECO deployment, as well as Ryan Nicoll at DSA for assistance with the mooring analysis.

REFERENCES

[1] MATE Center, "Oceanographic Instrumentation Technician", Knowledge and Skill Guidelines for Marine Science and Technology report. Vol. 4, Monterrey, CA, USA, 2010.
[2] R. Lhermitte, R. Serafin, "Pulse-to-Pulse Coherent Doppler Sonar Signal Processing Techniques," J. Atmos. Oceanic Tehcnol., 1(4), 293- 308, 1984.
[3] F. Rowe, K. Deines and R. Gordon, "High resolution current profiler," Proceedings of the 1986 IEEE Third Working Conference on Current Measurement, St. Petersburg, FL, USA, 1986, pp. 184-189.
[4] A. Lohrmann and S. Nylund, "Pure coherent Doppler systems – how far can we push it?," 2008 IEEE/OES 9th Working Conference on Current Measurement Technology, Charlston, SC, 2008, pp. 19-24.
[5] A. E. Hay, L. Zedel, S. Nylund, R. Craig and J. Culina, "The Vectron – A pulse coherent acoustic Doppler system for remote turbulence resolving velocity measurements," 2015 IEEE/OES Eleventh Current, Waves and Turbulence Measurement (CWTM). 2-6 March 2015, St.Petersburg, FL, USA.
[6] A. Y. Shcherbina, E. A. D'Asaro, and S. Nylund, 2018, "Observing finescale oceanic velocity structure with an autonomous Nortek acoustic Doppler current profiler," J. Atmos. Oceanic Technol., 35(2), 411–427, 2018.
[7] A. Lohrmann and S. Nylund, "A new long range current profiler," 2013 OCEANS – San Diego, San Diego, CA, 2013, pp. 1-7.

MECHANICALLY GENERATED LINEAR WATER WAVES PROPAGATING OVER TOPOGRAPHY

Maciej Paprota, Institute of Hydro-Engineering, Polish Academy of Sciences, mapap@ibwpan.gda.pl

INTRODUCTION

Spectral methods are considered efficient and robust approach to solve nonlinear equations of free-surface flows (Canuto et al. 1988). Their first application to water waves was derived independently by Dommermuth and Yue (1987) and West et al. (1987) for waves propagating over horizontal bottom. The problem of waves propagating over bottom topography was then solved within the framework of a pseudo-spectral method formalism by Liu and Yue (1998) and Smith (1998). However, none of the previous derivations covers mechanically generated waves over an arbitrary shape flume bottom. In the present study, a spectral method approach is used to derive a wavemaker model with arbitrary wave flume bottom topography. We use fully spectral Fourier Galerkin approach, in which the nonlinear corrugated bottom boundary condition is expanded in a Taylor series up to an arbitrary order and the problem is solved entirely in a spectral domain upon replacing nonlinear terms with convolution sums.

SOLUTION

A potential flow problem of mechanically generated linear waves propagating over closed flume bottom topography under a restoring force of gravity (represented by an acceleration g) is considered. An initial boundary-value problem is formulated in a rectangular fluid domain of size l x d (length x depth) and time t. The Cartesian coordinate system is used to define fluid elements along the horizontal x-axis, which coincides with still water level, and upward-pointing z-axis. The upper boundary is free and is described by means of the elevation function $\eta(x, t)$, while the flume bottom topography is defined through fluctuation function $\beta(x)$ around $z = -d$. The waves are generated by a rigid and impermeable moving paddle (piston-type) displaced from its mean position ($x = 0$) according to $\chi(t)$, while, eventually, they are fully reflected at a vertical wall located at the far end of the flume ($x = l$). The problem is schematically presented in figure 1.

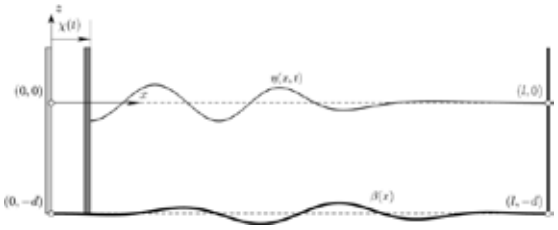

Figure 1 - A scheme of mechanically generated waves propagating over topography in a closed flume.

In order to find the solution, we introduce potential function $\varphi(x,z,t)$ of velocity $\boldsymbol{v}$, such that $\boldsymbol{v} = \nabla\varphi$. Laplace equation, $\Delta\varphi = 0$, linear free-surface boundary conditions ($z = 0$), $\partial_t\eta = \partial_z\varphi$, $\partial_t\varphi = -g\eta$, linear wavemaker boundary ($x = 0$), $\partial_t\chi = \partial_x\varphi$, and no-flow condition at the vertical wall ($x = l$), $\partial_x\varphi = 0$, define the most of the wavemaker problem. The remaining part is the nonlinear bottom boundary condition

$$\partial_x\beta\partial_x\varphi - \partial_z\varphi = 0,\ z = -d + \beta, \quad (1)$$

and is expanded (around $z = -d$) in a Taylor series to preserve a simple rectangular fluid domain. We also employ an additional potential approach, in which $\varphi = \sum\varphi_i$. Component potentials satisfy homogeneous wave problem, wavemaker problem, and topography condition. By applying the method of weighted residuals and truncated Fourier expansions of η, φ, and β, free-surface and bottom boundary conditions are redefined in a spectral space with respect to component amplitudes and wave numbers. The problem is solved in a spectral space with a convolution treatment of nonlinear terms appearing in the bottom boundary condition (1).

RESULTS

In figure 2, outcome of the model is presented for waves propagating from left to right changing their length as they are climbing up the submerged slope.

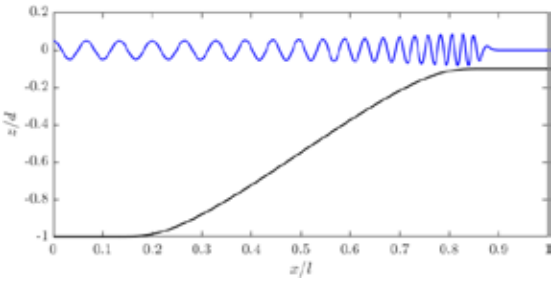

Figure 2 - Linear waves propagating up the slope.

REFERENCES

Canuto, Hussaini, Quarteroni, Zang (1988): Spectral Methods in Fluid Dynamics. Springer-Verlag, Berlin.
Dommermuth, Yue (1987): High-order spectral method for the study of nonlinear gravity waves. Journal of Fluid Mechanics, vol. 184, pp. 267-288.
West, Brueckner, Janda (1987): A new numerical method for surface hydrodynamics. Journal of Geophysical Research, vol. 92, pp. 11803-11824.
Liu, Yue (1998): On generalized Bragg scattering of surface waves by bottom ripples. Journal of Fluid Mechanics, vol. 356, pp. 297-326.
Smith (1998): An operator expansion formalism for nonlinear surface waves over variable depth. Journal of Fluid Mechanics, vol. 363, pp. 333-347.

CONSTRUCTION AND NOURISHMENT OF ARTIFICIAL GRAVEL BEACHES IN CROATIA

Dalibor Carević, Faculty of Civil Engineering, University of Zagreb, dalibor.carevic@grad.unizg.hr
Hanna Miličević, Faculty of Civil Engineering, University of Zagreb, hanna.milicevic@grad.unizg.hr

The mainstay of Croatian tourism is the offer that develops on the beaches, which are the destination for tourists, whether they come from the sea (sailors) or from the land. The Croatian coast is characterized by steep rocky coasts, mainly composed of karstified limestone (90%). The sediment on the beaches gradually wears down by the influence of storm waves and disappears, while at the same time the beach is nourished by new material brought in by natural or artificial means. The natural supply of material to Croatian beaches is mainly by paleocurrents and recent currents. In the case of artificial beaches, the supply of sediment is possible only by human influence using machinery (nourishment).
The Adriatic Sea is small (in the oceanographic sense) and, in combination with an indented coastline, has a relatively mild wave climate. In such a defined environment, a specific Croatian rocky coast has developed, where the proportion of pebble and sandy beaches does not exceed 5% of the total coast length. Given this low percentage of "suitable" beach areas, and under the pressure of the growing number of tourists, coastal municipalities and towns are forced to nourish existing beaches, thus saving valuable beach space, and are even forced to build new beaches. Additional problem was the complete lack of data on the extent of beach nourishment and construction in Croatia, which led to a general problem in managing these processes. This was an obvious failure of local municipalities and even the central government in Croatia. As a technical support for this complex social problem, the scientific project BEACHEX was funded by the Croatian Science Foundation under the title “Sustainable construction of artificial gravel beaches-Construction of new beaches and increase of existing capacity”. Among the different goals of the project one of the most important was to establish a database of nourished beaches and newly constructed beaches. To create such a database, a scientific approach was used combining two different methodologies: utilization of the global coastline aerial photographs and implementation of the digital survey of local municipalities.

	CR	FR	IT	DE	NL	ES	DK
AA $\cdot 10^3$ [m^3/y]	56	364	405	1042	6020	8462	1292
LN [km]	108	35	73	128	152	200	80
LS [km]	619	1960	3620	602	292	1760	500
AVN [m^3/m']	0.36	10.4	5.6	10	39.6	42.3	16

Table 1 - Comparison of nourishment in Croatia with other EU countries. AA-average annual nourishment amount; LN-total length of nourished beaches; LS- total length of beaches (gravel, sand, mud); AVN- average annual nourishment amount per meter of beach

By comparing aerial photographs from 1968 and 2020, it was possible to estimate the total number of new beaches built during this period. And, implementing a digital survey of municipalities, it was possible to determine the total number and location of nourished beaches, the total amount of gravel and sand used for nourishment and the total cost of nourishment. All these newly defined data were used to place the Croatian practices in the EU context (Tab.1, Hanson, 2002) and to define the national strategy and legislation for beach nourishment and construction of new beaches.
The second very important goal of the project was to study the morphological behavior of the gravel beaches under the specific Croatian sea conditions (small waves and tidal oscillations) in order to shed light on the processes of material loss on the artificial beaches. For this purpose, an extensive field survey was conducted on Ploče beach in 2020/21, including video monitoring of the beach (Bujak 2023) and geodetic monitoring (Tadić, 2022). Based on these data, the calibration of the X-Beach-G numerical model was conducted, which is specifically applicable for Croatian sea conditions (Fig. 1).

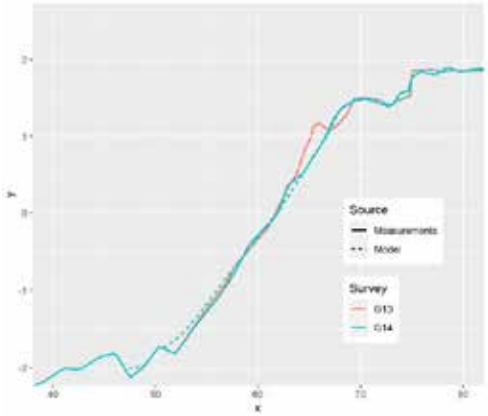

Figure 1 - X-Beach-G numerical model simulation of wave event (October 27, 2020) with a maximum H_s=1.25m and T_p=4.4s

REFERENCES

Tadić, Ružić, Krvavica, Ilić (2022): Post-nourishment changes of an artificial gravel pocket beach using UAV imagery, J. Mar.Sci.Eng., MDPI, vol. 10, pp. 358
Bujak, Ilic, Miličević, Carević (2023). Wave Runup Prediction and Alongshore Variability on a Pocket Gravel Beach under Fetch-Limited Wave Conditions, J. Mar.Sci.Eng, MDPI, vol. 3 (11), pp. 614
Hanson, Brampton, Capobianco, Dette, Hamm, Laustrup, Lechuga, Spangoff (2002). Beach nourishment projects, practices, and objectives-a European overview, Coastal Engineering, 47 2, pp. 81-111

STRATIFICATION AND INTERNAL TIDES ON THE AL-BATINAH SHELF

Gerd Bruss, Sultan Qaboos University, gerd@squ.edu.om
Bastien Queste, University of Gothenburg, bastien.queste@gu.se
Estel Font, University of Gothenburg, estel.font.felez@gu.se
Rob Hall, University of East Anglia, robert.hall@uea.ac.uk

INTRODUCTION AND METHODS

The Al-Batinah shelf in northern Oman extends between Sohar and Muscat at around 24° latitude and experiences high solar radiation and extreme temperatures in summer. This leads to the development of an intense summer thermocline (Claereboudt, 2018) over the shelf. While the influence of thermal stratification on shelf dynamics has been described for other regions, the involved processes along the Oman coasts remain unclear (Bruss et al., 2018). Here we study the influence of stratification on tidal currents and the significance of internal tides. We collected in-situ data with a vertical thermistor chain, several bottom mount ADCPs across the shelf and a glider extending the transect offshore. We perform harmonic analysis in a moving window to assess the interaction between barotropic tides and stratification and apply methods summarized in (Hall et al., 2019) to analyze internal (baroclinic) tides.

RESULTS AND DISCUSSION

In our data, summer stratification on the Al Batinah shelf develops in March and lasts until October with 2-3 week variation between years. This matches with the findings of Font et al. (2022) based on surface heat flux budgets from glider observations. The stratification reaches its peak of N^2 ~10^{-3} s^{-2} around June. The effect of the Arabian Sea monsoon in July/August is variable between years but generally leads to a reduction of the local SST from around 33° to 30°. The intensity of the stratification can also be modulated by a strong monsoon. Harmonic analysis in a moving window reveals that while the constituent properties of the surface tide (sea level) are stable over the seasons, tidal currents are modulated by stratification. When harmonic analysis is restricted to well mixed winter periods, tidal constituent properties for the flow were similar for two different years.

By combining the time series of the vertical profiles of temperature and baroclinic flow we observe for the first time large-amplitude diurnal internal waves in the coastal ocean near Suwayq. Figure 1 shows the collected data exemplary for three days in September 2022 when stratification was intermediate. In fall, maximum isotherm displacement reaches 10 m (~45 % of the local water depth) with a baroclinic flow of up to 25 cms^{-1}. During peak stratification in June-August the thermocline is shallower and vertical displacement smaller. Frequency analysis confirms that the internal waves are generated by the astronomic tide predominantly in the diurnal band. While the tidal variation of the sea surface is dominated by M_2, both the barotropic tidal currents and the internal tide (vertical isotherm displacement and baroclinic horizontal currents) are dominated by K_1. This is likely linked to different spatial patterns between the diurnal and semidiurnal amphidromes in the region. The depth averaged and low pass filtered energy flux of the internal tides is directed towards the shore. It follows a modulated spring-neap cycle but also depends on the strength of the stratification. In our data the internal wave energy flux was strongest in fall when the thermocline is deeper, N^2 is intermediate and vertical isotherm displacement is largest. Internal tides in turn drive mixing through breaking and shear instabilities and thus reduce downstream (inshore) stratification temporarily.

While internal solitary waves have been observed in the Sea of Oman and mesoscale dynamics are well studied, to date there is no description of internal tides or the interactions between stratification and barotropic tidal currents for the regional shelf sea. The Al-Batinah coast is densely populated with developing infrastructure, a diverse ecosystem and expanding marine uses like sea water desalination, aquaculture, fishing and tourism. Our findings have direct implications for studies of the local marine environment underlining the importance to consider stratification.

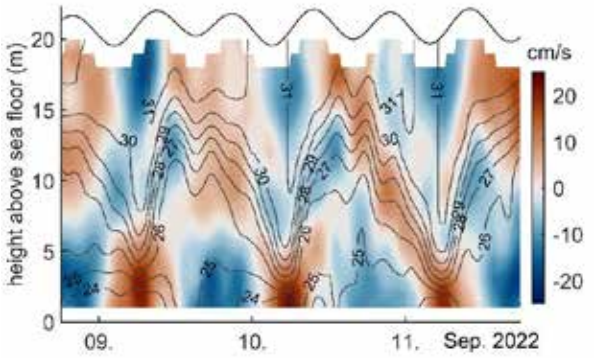

Figure 1: Isotherms and baroclinic cross-shore flow of internal tides near Suwayq.

ACKNOWLEDGMENTS

This study was funded by US Office of Naval Research Global grant N62909-21-1-2008 and SQU grant RC/RG-AGR-FISH-20-01. The authors thank Sultan Qaboos University technical staff for their help with logistics and field deployments.

REFERENCES

Bruss, G., Kwarteng, A., Baawain, M., & Sana, A. (2018). Coastal Currents On The Northern Omani Shelf. International Conference on Coasts, Ports and Marine Structures, Tehran.

Claereboudt, M. R. (2018). Monitoring The Vertical Thermal Structure of the Water Column in Coral Reef Environments Using Divers of Opportunity. Current Trends in Oceanography and Marine Sciences, 107.

Font, E., Queste, B. Y., & Swart, S. (2022). Seasonal to Intraseasonal Variability of the Upper Ocean Mixed Layer in the Gulf of Oman. Journal of Geophysical Research: Oceans, 127(3).

Hall, R. A., Berx, B., & Damerell, G. M. (2019). Internal tide energy flux over a ridge measured by a co-located ocean glider and moored acoustic Doppler current profiler. Ocean Science, 15(6), 1439-1453.

PHYSICAL CHARACTERIZATION OF NON-BUOYANT PLASTIC PARTICLE TRANSPORT IN THE COASTAL ZONE: EXPERIMENTAL METHOD

Giovanni Passalacqua, University of Messina, giovanni.passalacqua@studenti.unime.it
Claudio Iuppa, University of Messina, claudio.iuppa@unime.it
Annamaria Visco, University of Messina, avisco@unime.it
Carla Faraci, University of Messina, carla.faraci@unime.it

INTRODUCTION

Plastic is one of the most used and disposable materials worldwide. It is expected by 2050 that there will be about 12 billion tons of debris dispersed into the environment. Combined with marine littering, pollution and climate change this will threaten our ability to sustainably use oceans, seas and coasts. In this regard, it is important to understand the dynamics and predict the hot spots of plastic pollution. However, few studies have been done so far on the dynamics of plastics in the marine environment and on the parameters that influence most the movement of debris (Van Sebille (2020)). In our research, an experimental method for the identification and tracking of non-buoyant plastic particles (micro and macro) based on 2D image analysis was developed. The proposed method, based on the blob analysis, was implemented and calibrated within the wave flume of the Hydraulics Laboratory at the University of Messina. In this study, preliminary results in terms of cinematic physical parameters, obtained from 4 different samples, will be compared and discussed.

MATERIALS AND METHOD

The transport of plastic particle samples under different hydrodynamic condition was studied by processing video frames using blob analysis, a computer vision technique for detection and analysis of connected pixel. Each sample, composed of 80 elements, was tested under 18 hydrodynamic conditions, varying water depth between 0.15 and 0.23 m, wave period between 1 and 1.66 s, wavelength in the range 1.14 - 2.442 m and wave height from 0.022 to 0.12 m. A camera positioned on the top of a highly inclined (20%) smooth profile recorded the movement of the particles during the tests. Table 1 shows the main characteristics of the 4 analyzed samples. Note that the samples differ in density and size, specifically in thickness *c*, which results in a variation of the Corey shape factor (Corey (1949)).

Table 1: Characterization of the used samples: *id* indicates the sample name, *a*, *b* and *c* are the major, mean and minor axis respectively and *csf* the Corey shape factor.

id	density [g/cm^3]	*a* [mm]	*b* [mm]	*c* [mm]	*csf*
PET_02	1.373	10	5	0.11	0.015
PET_03	1.373	5	5	0.11	0.022
fn_02	1.146	10	5	1.09	0.154
fn_03	1.146	5	5	1.09	0.217

RESULTS AND DISCUSSION

The result of the blob analysis is the spatial coordinates of each particle identified for each frame of the video. This means that it is possible to calculate the displacement performed by the generic element. To minimize errors from blob analysis identification, three centroid displacements were identified: the one of the whole set of particles (global-centroid) and the two sub-centroids which for each frame had x-coordinates (cross-shore) greater (up-centroid) and lesser (down-centroid) than the global-centroid co-ordinate. Such operation was made because during the tests the plastic sample tended to split into two sub-groups, one more prone to movement and one less. Figure 1 shows the global-centroid velocity made dimensionless by means of the second-order velocity of the single water particle at the bottom for the progressive waves u_{global}/v_x, varying the product of wave number *k* and amplitude *a*.

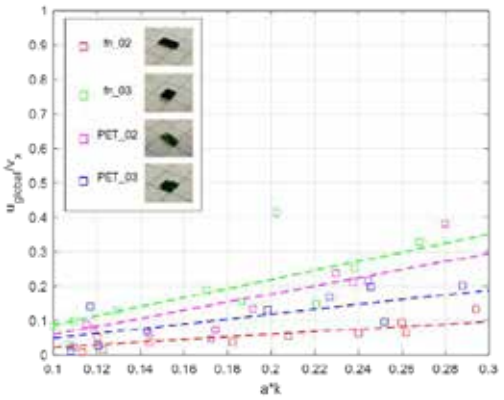

Figure 1 - Dimensionless graphs comparing the product of wave amplitude and wavenumber and the ratio of the velocity measured in the cross-shore direction to the theoretical velocity in the case of global-centroid.

It can be observed from Figure 1 that sample fn_03 has higher velocities than sample fn_02 having the same density but larger size. In contrast, sample PET_03 has lower velocity values than sample PET_02. This result shows that shape is a crucial characteristic for studying the hydrodynamics of plastic particles in the coastal zone.

REFERENCES

A. T. Corey, et al. (1949): Influence of shape on the fall velocity of sand grains, Ph.D. thesis, Colorado A & M College.
E. Van Sebille et al. (2020): The physical oceanography of the transport of floating marine debris, Environmental Research Letters 15 023003.

EXPERIMENTAL RESEARCH ON BEHAVIOR OF PLASTIC DEBRIS OF NEGATIVE BUOYANCY IN OSCILLATING WATER FLOW

Barbara Stachurska, Institute of Hydro-Engineering, Polish Academy of Sciences, b.stachurska@ibwpan.gda.pl

INTRODUCTION

Marine plastic debris, widespread in various environmental compartments across the globe, has become a cutting-edge and pressing environmental issue. Due to the widespread use of plastic, which started around six decades ago (Thompson et al. 2004), plastic debris represents one of the main wastes in seas and oceans. Plastic litters delivered from various sources to the marine environment is subjected to different transport mechanisms (Su et al., 2022). Due to the complexity and diversity in plastic properties, spatio-temporal limits on the field observation and a lack of standardized sampling and analysis of plastic debris, its distribution is poorly mapped and the mechanism associated with its transportation remains unclear. Studying the effects of hydrodynamic processes on plastic transport is an important issue from the physics point of view. By treating plastic as a collection of migrating particle, it is possible to estimate how the hydrodynamic processes occurring in the marine environment interact (Brunner et al.. 2015). For better understanding of the plastic debris paths in sea water, it is necessary to better recognize the interactions of physical processes.

METHODOLOGY

The surface waves effects on plastic debris dynamics dragged on the rippled bottom are investigated by the PIV experiments performed in the wave flume belonging to the Institute of Hydro-Engineering of the Polish Academy of Sciences in Gdańsk, Poland. The horizontal velocities of plastic debris in different profiles over the rippled bottom and for different wave and bottom conditions are analyzed in regard to wave skewness and asymmetry.

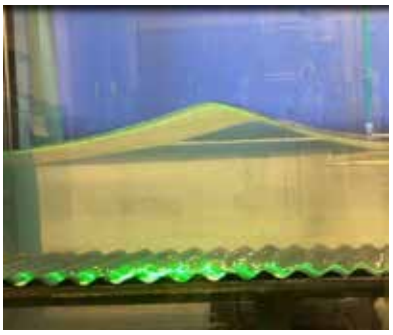

Figure 1 - PIV measurements of plastic debris velocity in the wave flume

From the PIV experimental data, settling velocity of used plastic balls as well as magnitude of instantaneous horizontal velocity over rippled bed were determined. The laboratory tests were carried out with two plastic ball densities: $\rho_s = 1.77 \frac{g}{cm^3}$ and $\rho_s = 2.03 \frac{g}{cm^3}$.

EXPERIMENTAL RESULTS

Experiments indicated that offshore plastic debris transport is mainly associated with acceleration skewness, whereas the velocity skewness characterizes the onshore transport. Application of skewed asymmetric irregular waves over the rippled bed presents the important interaction between wave nonlinearities driving the plastic debris. It was observed that transport paths and fate of negatively buoyant plastic particles in the oscillatory water flow depend on their settling velocity. Moreover, observation of the microplastic grains movement in laboratory environment for given hydrodynamic conditions allowed for the identification of three fundamental types of microplastic grain movement above the sea bed. The results of laboratory tests determine the velocity of plastic debris, characterizing a given type of the movement.

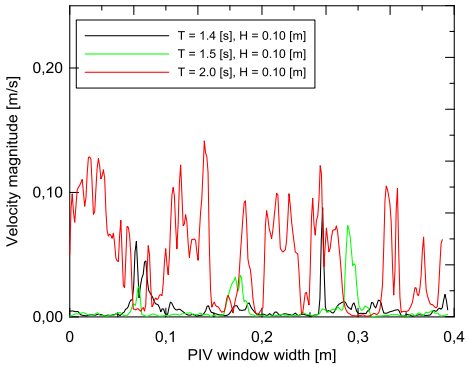

Figure 2 - Measured instantaneous velocity magnitude of plastic debris over higher ripples, $\rho_s = 1.77 \frac{g}{cm^3}$

The obtained results contributed to the recognition of hydrodynamic factors responsible for the transport of plastic along the bottom covered with ripples in oscillating nonlinear water flows.

REFERENCES

Thompson R., Olsen Y., Mitchell R., Davis A., Rowland S., John A., McGonigle D. and Russell A., (2004): Lost at Sea: Where Is All the Plastic?, Science vol. 304, pp: 838.

Su L., Xiong X., Zhang Y., Wu Ch., Xu X., Sun Ch., Shi H., (2022): Global transportation of plastics and microplastics: A critical review of pathways and influences, Science of The Total Environment, vol. 831, pp: 154-168.

Brunner, K., Kukulka T., Proskurowski G., and Law K., (2015): Passive buoyant tracers in the ocean surface boundary layer, J. Geophys. Res. Oceans, vol. 120. pp: 7559-7573.

HYDRODYNAMIC CHARACTERIZATION OF NARTA LAGOON, ALBANIA

Mattia Scovenna, University Of Genova, mattia.scovenna@edu.unige.it
Francesco Deleo, University Of Genova, Francesco.Deleo@unige.it
Giovanni Besio, University Of Genova, giovanni.besio@unige.it

INTRODUCTION

The Narta lagoon places in the central coast of Albania, north of the Bay of Vlorë, and it communicates with the Mediterranean Sea through three narrow channels, often closed because of the sediment transport. The lagoon is characterized by a rich diversity of habitats, which give home to many specialists plants and animal species. In the present, the area under study is modeled both as a closed and open basin, to see how the tide affects the internal circulation, and then a dispersion analysis is performed to understand the faith of particles released in a specific area.

HYDRODYNAMIC AND DISPERSION MODELS

For both the open and closed configurations, the wind used as forcing comes from a clustering procedure that reduces hourly wind data covering the last 40 years in 6 weekly scenarios representative of the whole variability of the initial data-set. The tide used in the open configuration, instead, is predicted with TPXO3.0 software, developed by the Oregon State University. Once the bathymetry, obtained through interpolation of a Deeper Smart sonar measures, and a 20 meters regular grid are coupled, the model is ready to run. The software used is Delft3D, which solves Navier-Stokes equations in each cell of the grid to transform the energy transported by the wind and the tide in the water current.
In Figure 1 it is reported the time averaged surface velocity field related to scenario 4, according to the open configuration. It is evident how the tidal contribution is confined to an area bordering the outlets of the channels and has no effect on the internal circulation of the lagoon.

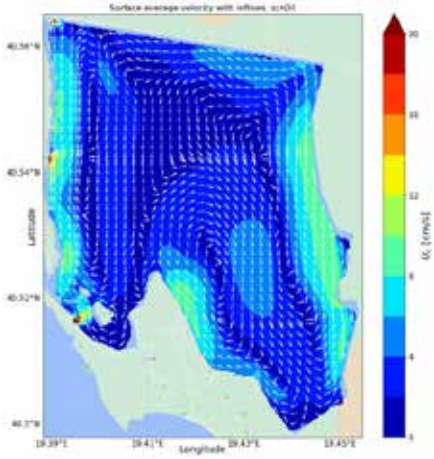

Figure 1 - Velocity field of scenario 4, open configuration.

The second graph shows the trajectories of 11 of the 2526 virtual particles released in the southeast of the domain, in correspondence of the sewage system outlet of Narta municipality. The Lagrangian dispersion analysis is performed using OceanParcels, a set of Python functions that allow to solve the time integral of the velocity field to obtain the particle positions in time. It catches the eye that all particles remain inside the lagoon for the duration of the simulation and tend to follow preferential routes of transport.

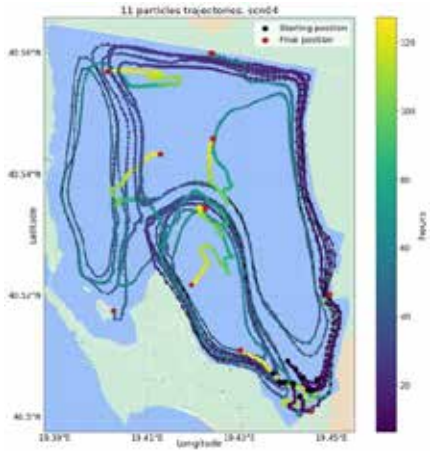

Figure 2 - Particles trajectories.

CONCLUSIONS

The velocity fields show no significant difference between the open and close configuration, suggesting that the tide has no contribution to the hydrodynamic of the lagoon. From the dispersion analysis too, it is possible to conclude that the lagoon acts as a closed basin, experiencing a very limited exchange of water with the sea. For all scenarios, in fact, most of the particles released (80-90%) never leave the lagoon. The hydrodynamic behavior can lead to critical issues in case of release of pollutant substances coming from livelihood activities, such as salinity plants, illegal fishing using pesticides, or sewage discharge. The dilution of any kind of substance is completely inhibited in case of closed channels, but still very low in case of open channels, thus negatively impacting the local biodiversity.

REFERENCES

Topi, (2013): Preliminary report for key biodiversity area of Narta lagoon. ResearchGate.
Iskandar, (2021): Pathways of floating marine debris in Jakarta Bay, Indonesia, ELSEVIER.

ASSESSING IMPACT OF PETROCHEMICAL EFFLUENT ON HEAVY METAL POLLUTION IN MUSA ESTUARY: A NUMERICAL MODELING APPROACH

Mohammad Javad Jourtani, University of Isfahan, jourtani@trn.ui.ac.ir
Ahmad Shanehsazzadeh, University of Isfahan, a.shsnehsazzadeh@eng.ui.ac.ir
Hossein Ardalan, Water Research Institute, Tehran, h.ardalan@wri.ac.ir
Ziaaldin Almasi, Department of Environment, Iran, zialmassi@gmail.com

Estuaries are important ecosystems that provide feeding and breeding grounds for various species and have been crucial to human societies for food, transportation, and agriculture (Savenije, 2005). However, high population densities in estuarine regions have led to pollution from various sources, including sewage, urban and industrial outfalls, and agricultural activities. This study assesses the impact of petrochemical effluent on heavy metal pollution in the Musa Eestuary at the North of Persian Gulf using a numerical modeling approach. The outfall of 22 petrochemical plants have the potential to contaminate seawater and sediment in the estuary.
In order to predict the main dispersion agent in the estuary namely the tidal current, 2D propagation of the tidal wave in the Musa Estuary is simulated by adopting MIKE 21 Flow Model (FM) CFD software. The hydrodynamic model is calibrated and validated through surface elevation and current speed data obtained from field measurement, Fig. 1.

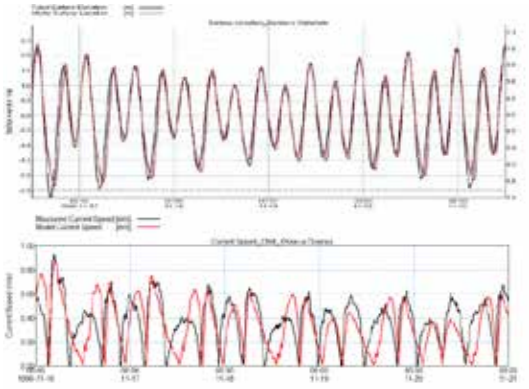

Figure 1 - Comparison of measured and simulated surface elevation in Mahshahr port (up) and measured and simulated current speed at Khowr-e Dowraq station (down).

The MIKE ECO Lab Module was employed to simulate the spatial distribution of Biochemical Oxygen Demand (BOD) and hazardous heavy metal in the Musa Estuary. The Heavy Metal Template, a predefined MIKE ECO Lab template, was used to predict BOD and the total concentration of metal in the water and bed sediment and the potential concentration of metal in biota (Water & Environment, 2007). The results are compared with the data from measuring stations distributed in the estuary.
The results of the ecologic model exhibit good agreement with measured data. As an example, predicted and measured spatial distribution of lead (Pb) concentration in Musa Estuary are compared in Fig. 2. The maximum predicted concentration is 0.78 micrograms, compared to the measured concentration of 0.8 micrograms, indicating the acceptable accuracy of the model.
Understanding the impact of industrial activities on the ambient environment and public health is crucial for sustainable management of estuaries and their water resources. This study has implications for assessing the distribution of other hazardous metals in water bodies and can be used as the prerequisite for the Total Pollution Loads Control System (TPLCS).

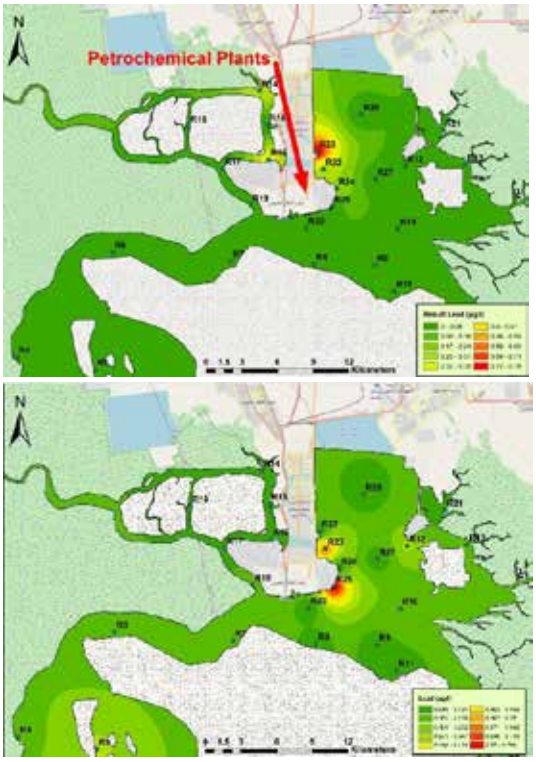

Figure 2 - Predicted (up) and measured (down) spatial distribution of lead (Pb) concentration in Musa Estuary. The sampling point locations are shown in the Figure.

REFERENCES

Savenije, H.H.G. (2005) Salinity and tides in alluvial estuaries. Gulf Professional Publishing.
Water&Environment, D.H.I. (2007) 'MIKE ECO Lab Short Scientific Description', DHI Water and Environment [Preprint].

PLASTIC DEBRIS DISTRIBUTION FROM VIGO WASTEWATER TREATMENT PLANTS

Magda Sousa, Centre for Environmental and Marine Studies, Physics Department, Aveiro University, Portugal, mcsousa@ua.pt
Américo Ribeiro, Centre for Environmental and Marine Studies, Physics Department, Aveiro University, Portugal, americosribeiro@ua.pt
Maite deCastro, Environmental Physics Laboratory, Vigo University, Spain, mdecastro@uvigo.es
Marisela Des, Environmental Physics Laboratory, Vigo University, Spain, mdes@uvigo.es
Moncho Gomez-Gesteira, Environmental Physics Laboratory, Vigo University, Spain, mggesteira@uvigo.es
João Miguel Dias, Centre for Environmental and Marine Studies, Physics Department, Aveiro University, Portugal, joao.dias@ua.pt

INTRODUCTION

The accumulation and dispersion of marine plastic debris is a growing problem on a global scale. The accumulation of plastic waste in estuaries is increasing due to the widespread use of plastics and their inadequate treatment in wastewater plants (WWTPs), which means that they end up being moved to the oceans and affecting marine environments. The Ria de Vigo is the southernmost coastal embayment of the Rias Baixas located on the northwest coast of the Iberian Peninsula. The Ria de Vigo is one of the most densely populated and industrialized areas in the region, being therefore a hotspot for plastic contamination. Reguera et al. (2019) showed a high correlation between WWTPs and the local concentration of microplastic fibers in the marine environment using field data. The assessment of plastic sources, pathways and accumulation areas is a key priority to mitigate this threat. In the aforementioned context, the main objective of this work is to reproduce the fate of marine plastic in the Ria de Vigo and investigate the paths of the plastics discharged by WWTP in Ria de Vigo under different tidal and wind regime conditions, using hydrodynamic and particle-tracking modules from Delft3D model suite.

NUMERICAL MODEL

An implementation of the Delft3D model suite using the Flow and particle-tracking modules was used to improve the knowledge about the fate and distribution of microplastics released by the main WWTPs in the Ria de Vigo. The computed flow patterns from the hydrodynamic modelling results (Des et al., 2019) are used as input for the transport modelling of plastic litter (Delft3D-PART module) by means of offline coupling (Figure 1).

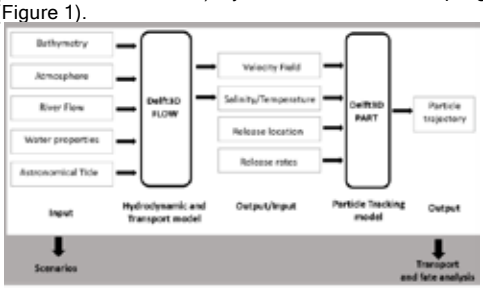

Figure 1 - Overview of the model framework.

Several scenarios were implemented and compared to assess tidal and upwelling/downwelling conditions' effects on the floating plastic transport and fate in Ria de Vigo.

RESULTS

The results show that the forcing conditions significantly affect the speed and direction of the floating plastics. During downwelling conditions, drift trajectories move towards the coast, depositing in this region or being transported into the northern Rias. Over 5 days of release, about 20% of particles from the WWTP are exported to the Rias de Pontevedra and Arousa. In contrast, particles are transported offshore in a southwestern direction under southward winds favorable to upwelling conditions. Regarding the tidal effects, a negligible percentage of floating plastics reaches the upper Ria de Vigo when the emission occurs under ebb spring tide conditions. Under flood conditions, the particles remain close to their release location. The particles released under ebb conditions show a wider dispersion across the Ria de Vigo, with lower concentrations near the release point compared to flood conditions. During these conditions, the particles are transported to the open sea after 5 days, indicating a floating plastics exchange between the Ria de Vigo and the adjacent coast. Under neap tides, a small percentage of particles ross the mouth of the Ria de Vigo.

CONCLUSIONS

The three-dimensional model based on the Delft3D suite, with the hydrodynamic and particle-tracking models, was valuable and accurate in detecting critical zones of floating plastics accumulation in Ria de Vigo and its neighbouring coastal ocean, highlighting this type of application as a useful tool for marine scientists and entrepreneurs. Also, the strong effects of wind and tidal regimes on particle dispersal determine their paths under extreme events in this coastal area.

ACKNOWLEDGEMENTS

The Portugal Space funded this work under the project "SMART".

REFERENCES

Des, deCastro, Sousa, Dias, Goméz-Gesteira (2019): Hydrodynamics of river plume intrusion into an adjacent estuary: The Minho River and Ria de Vigo. JOURNAL OF MARINE SYSTEMS, vol. 189, pp. 87-97.

Reguera, Viñas, Gago (2019): Microplastics in wild mussels (Mytilus spp.) from the north coast of Spain. SCIENTIA MARINA, vol. 83 (4).

DISPERSION MONITORING SERVICIES IN THE MEDITERRANEAN SEA: A MULTI MODEL STATISTICAL APPROACH

Beatrice Maddalena Scotto, University of Genoa, beatrice.scotto@edu.unige.it
Andrea Lira Loarca, University of Genoa, andrea.lira.loarca@unige.it
Giovanni Besio, University of Genoa, giovanni.besio@unige.it

The Mediterranean Sea is a vast and complex ecosystem that is significantly impacted by the increasing traffic of naval routes and the consequent marine pollution. Therefore, the need for accurate and dependable monitoring service is becoming progressively important, particularly for predicting and minimizing the environmental impact of pollutant spills.

This research focuses on the evolution of oil spills in the Mediterranean basin, with a particular emphasis on the Tyrrhenian and Ligurian Seas. The primary objective of this study is to develop a robust framework for a user-friendly application that can provide valuable insights into both past and future oil spill incidents. To validate the methodology presented, a real case scenario of a spillage incident that occurred off Cape Corso is used.

The investigation relies on data from three different ocean models provided by Copernicus Marine (CMEMS), Shom France, and Ifremer. The use of various ocean models aims to create a comparison to observe the differences in output results. The collected open access data are appropriately modified to create a system that could simulate the dispersion of particles and evaluate the experimental distribution of particles in the area of interest. Additionally, a study on the extent of the oil slick is conducted for each model to observe the spatial evolution over time.

Furthermore, barycentres are calculated every instant of each oil spill characterized by a particle cluster. With this information, it was possible to estimate the absolute and relative distance of the particles from the point of release, thereby determining the trajectory travelled by the oil slicks.

Finally, the dispersions created are compared with satellite images obtained from Synthetic Aperture Radar for a more accurate analysis and to evaluate which model fit the real scenario most accurately, thus improving the accuracy of future assessments.

The study shows that the three models used present quite different scenarios (Figure 1), leading to a lack of consistency with reality. This finding provides valuable insights for policymakers and stakeholders involved in marine conservation, essential for the development of effective strategies to prevent and mitigate their effects.

Despite the progress made, uncertainties associated with climate services remain a significant challenge for predicting and mitigating the impact of oil spills on the environment. Therefore, continued investment in research and development of climate monitoring services is critical to address these uncertainties and ensure the long-term sustainability of our planet's fragile ecosystems.

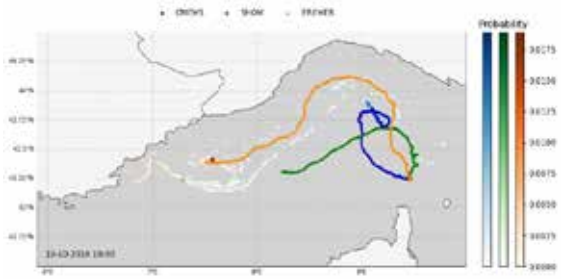

Figure 1 - Trajectory covered by the three models: CMEMS, Ifremer and Shom. On the right the color bar showing the values of the particles' experimental distribution for the three ocean models.

REFERENCES

Escudier, Clementi, Omar, Cipollone, Pistoia, Aydogdu, Drudi, Grandi, Lyubartsev, Lecci, Cretí, Masina, Coppini, Pinardi, (2020). Mediterranean Sea Physical Reanalysis (CMEMS MED-Currents) (Version 1) Data set. Copernicus Monitoring Environment Marine Service (CMEMS). DOI:https://doi.org/10.25423/CMCC/MEDSEA_MULTIYEAR_PHY_006_004_E3R1

Data from MARS3D model simulations, « Modelling and Analysis for Coastal Research » (MARC) project https://marc.ifremer.fr, Ifremer, University of Brest, CNRS, IRD, Laboratoire d'Océanographie Physique et Spatiale (LOPS), IUEM, Brest, France

SEASONAL TO SHORT-TERM DYNAMICS OF NEARSHORE SAND BAR DUE TO WAVE CLIMATE

Nataliya Andreeva, Institute of Oceanology-BAS, n.andreeva@io-bas.bg
Yana Saprykina, Shirshov Institute of Oceanology-RAS, saprykina@ocean.ru
Nikolay Valchev, Institute of Oceanology-BAS, valchev@io-bas.bg
Petya Eftimova, Institute of Oceanology-BAS, eftimova@io-bas.bg
Sergey Kuznetsov, Shirshov Institute of Oceanology-RAS, kuznetsov@ocean.ru

INTRODUCTION

The coastal environments of gently sloping beaches often feature presence of sand bars of various geometry and location. Seasonal variability of wind and wave climate causes sandy beaches to exhibit strong seasonal morphodynamic cycles reflected in the submerged beach profile with the building and offshore migration of sand bars during storms, and their deflating and onshore migration in times of low-energy swell conditions (Ruggiero et al., 2009). Such sand bar migration is associated with imbalance between the cross-shore sediment transport caused by wave non-linearities, undertow and the gravitational downslope effects (Dubarbier et al., 2017). Despite the relevant available studies based on numerical modelling and in-situ measurements, seasonal to short-term (1-2 years) nearshore morphological evolution is still not well understood. The aim of the present study is to examine cross-shore outer bar dynamics on an annual to seasonal timescale due to wave climate at an open-coast non-tidal sandy beach at the Bulgarian Black Sea coast.

STUDY SITE, DATA AND METHODS

Study site is located at Kamchia-Shkorpilovtsi sandy beach. The morphological conditions of the coastal zone include a rectilinear coastline with nearly parallel isobaths and nearshore crescent bars. The coastal area is open to winds and waves from the East, and the regional wind and wave climate exhibits strong seasonal variability. The study site is equipped with a 230 m long perpendicular coastal pier, reaching up to 4.5-5 m of water depth. The morphodynamics of the outer bar were analyzed using discrete measurements of beach profile depths collected in 2008-2010. A total of 33 cross-shore profiles were measured on a monthly basis every 2 m along the pier (Trifonova et al., 2011). Outer bar characteristics used for analysis are bar profile & height, bar crest offshore distance and bar crest depth. Regional wave climate data (1949-2010) were simulated by the SWAN wave model. Set up and validated in Valchev et al. (2012), it provided the necessary for analysis and temporally relevant (2009-2010) monthly Q99 values and hourly time series of significant wave height, peak period, mean wave direction and wave steepness.

RESULTS AND CONCLUSIONS

Analysis of outer bar characteristics dependent on wave forcing, wave non-linearity, storms and direction of wave incidence revealed that in 2009-2010, on an intra-annual timescale, the cross-shore bar (crest) migration followed a certain repetitive seasonal pattern mainly determined by non-linear transformation of waves (Saprykina et al., 2013). During the summers, the bar retained its stability farthermost from the shore due to weakly non-linear and low-energy wave regimes. At the same time, the crest displacements were rather active in autumn-winter and winter-spring periods of both years, as the outer bar was closest to shore in winter. It has been established that highly non-linear wave regimes are responsible for cross-shore bar migration, having wave steepness >0.03, significant heights over 1 m and peak periods more than 6 s. Furthermore, the influence of storms on the bar migration showed that the direction of crest displacement primarily depends on the wave period, the duration of wave conditions with steepness >0.04, angle of wave incidence and total storms duration. Thus, among the studied storms with similar average significant heights, those moving the outer bar seaward had longer periods, twice as long duration of retained over 0.04 steepness, lasted by approx. 20% longer, and were predominantly approaching from E-ENE, as opposed to storms with more oblique angle of incidence NE-ENE displacing the bar shoreward. On annual basis, the bar evolution was found to be mainly governed by wave height and storms angle of approach and duration.

ACKNOWLEDGEMENTS

The study was developed and supported by the Republic of Bulgaria research project with contract № ДО1-404/18.12.2020 and the Russian Foundation for Basic Research project № 20-55-46005.

REFERENCES

Dubarbier, Castelle, Ruessink, Marieu (2017): Mechanisms controlling the complete accretionary beach state se-quence, Journal of Geophysical Research, vol. 44, pp. 5645-5654.
Ruggiero, Walstra, Gelfenbaum, van Ormondt (2009): Seasonal-scale nearshore morphological evolution: Field observations and numerical modeling, Coastal Engineering, vol. 56, pp. 1153-1172.
Saprykina, Kuznetsov, Andreeva, Shtremel (2013): Scenarios of non-linear wave transformation in the coastal zone, Oceanology, vol. 53, pp. 422-431.
Trifonova, Valchev, Andreeva, Eftimova, Kotsev (2011): Measurements and analysis of storm induced short-term morphological changes in the western Black Sea. Journal of Coastal Research, SI 64, vol. 1, pp. 149-154.
Valchev, Trifonova, Andreeva (2012): Past and recent trends in the western Black Sea storminess, Natural Hazards and Earth System Sciences, vol. 12, pp. 961-977.

A SPATIOTEMPORAL MODEL APPROACH FOR ASSESSING THE PLASTIC DEBRIS FATE

Américo Ribeiro, Centre for Environmental and Marine Studies, Physics Department, Aveiro University, Portugal, americosribeiro@ua.pt
Renato Mendes, Underwater Systems and Technology Laboratory, Faculty of Engineering of the University of Porto, Portugal, rpsm@lsts.pt
Leonardo Azevedo, Instituto Superior Técnico, Lisbon University, Lisbon, Portugal, leonardo.azevedo@tecnico.ulisboa.pt
Luisa Lamas, Instituto Hidrográfico, Lisbon, Portugal, Luisa.Lamas@hidrografico.pt
João Miguel Dias, Centre for Environmental and Marine Studies, Physics Department, Aveiro University, Portugal, joao.dias@ua.pt
Magda Sousa, Centre for Environmental and Marine Studies, Physics Department, Aveiro University, Portugal, mcsousa@ua.pt

INTRODUCTION

Plastic debris in the marine environment has become a serious problem and transversal to all countries because of the slowly degrading large plastic debris that generates microplastics (Barboza et al., 2019). Marine plastic pollution is a substantial threat to wildlife and human health. The ability to detect floating plastic debris in short periods after they enter the ocean is a mitigating factor, which avoids the degradation of the macroplastics into smaller pieces and the consequential threat to the food chain. Despite academic and public awareness, there is little information on the transport, source, fate, accumulation and impacts of plastic debris in the oceans. In this perspective, high-resolution numerical ocean modelling allows low-cost marine predictions, which can be combined with the automatic identification and classification of floating plastic debris from remote sensing or *in situ* campaigns predicted by the model.
Here we present a model implementation comprising a high-resolution numerical ocean modelling that can spatiotemporally predict the plastic debris accumulations in the NW Iberian Peninsula.

METHODOLOGY

The 3D high-resolution numerical ocean model for coastal areas (i.e., Delft3D), able to mimic the behaviour of the particles similar to floating plastic debris, was implemented for the NW Iberian Peninsula, from regional oceanic influences into local estuarine dynamics. Afterwards, a Lagrangian modelling approach (based on Delft3D-WAQ Part) coupled with the hydrodynamic model will be used to produce the main pathways and hotspots for plastic debris. The numerical model was designed using a curvilinear grid with higher resolution in the estuaries and increases towards the ocean, and 26 sigma layers with higher discretization at the surface layers. The model inputs comprised tidal, transport conditions, atmospheric, and river data from the highest spatial and temporal resolution available for the study region for 2019. A time-step of 30 seconds was applied, with horizontal and vertical eddy viscosities of 5 $m^2 s^{-1}$ and 0.00001 $m^2 s^{-1}$, respectively,

RESULTS

The tidal wave propagation and salt and heat transport processes were validated by comparing the predicted results with *in-situ* data to 24 tide gauges, 121 Acoustic Doppler Current Profilers and satellite data (Figure 1) for 2019. In general, it was found a good fit between model predictions and observations, where small differences can be found near the shore due to a lack of freshwater temperature data, nevertheless revealing the ability of the model to reproduce the *in-situ* conditions accurately.

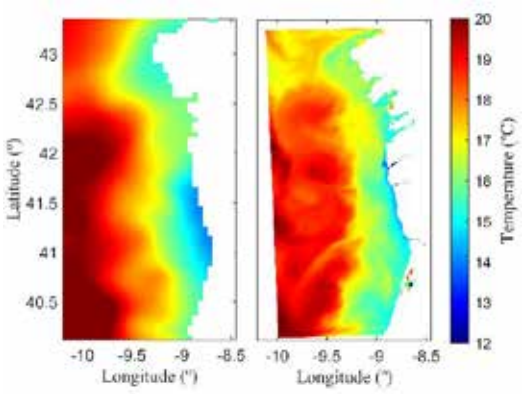

Figure 1 - Sea surface temperature obtained from satellite imagery (left) and model predictions (right) on 13 October 2019.

CONCLUSIONS

The model can spatiotemporally predict the ocean's floating plastic occurrence, considering both hindcasting and forecasting. The modelling results are a central step in the deep-learning methods to predict the evolution of floating plastic debris. This methodology can create impact and environmental engagement through the end-users, stakeholders, and the community, building the necessary influence on the authorities to act on the right strategies for ocean clean-up while making decisions under uncertainty deployed by key decision-makers at local and global levels.

ACKNOWLEDGEMENTS

The Portugal Space funded this work under the project "SMART".

REFERENCES

Barboza, Cózar, Gimenez, Barros, Kershaw, Guilhermino (2019). Macroplastics pollution in the marine environment. In World Seas: an Environmental Evaluation, pp 305-328.

WAVE SPECTRA RECONSTRUCTION BEHIND A SUBMERGED OBSTACLE

Rocchi Stefania, Università Politecnica delle Marche, s.rocchi@staff.univpm.it
Marini Francesco, Università Politecnica delle Marche, f.marini@staff.univpm.it
Corvaro Sara, Università Politecnica delle Marche, s.corvaro@staff.univpm.it
Lorenzoni Carlo, Università Politecnica delle Marche, c.lorenzoni@staff.univpm.it
Mancinelli Alessandro, Università Politecnica delle Marche, a.mancinelli@staff.univpm.it

INTRODUCTION AND AIMS

The presence of a submerged obstacle (sand bar or breakwater) induces a reduction of the transmitted wave energy mainly due to wave breaking dissipation. Moreover, the spectral shape behind such obstacles changes from the incoming one. An energy transfer towards higher frequencies, with respect to the peak frequency f_p, is observed due to the non-linear interactions that occur during the passage over the bar for both random (Beji & Battjes, 1993) and regular waves (Losada et al., 1997).

Van der Meer et al. (2000) studied the spectral change behind a low-crested structure. They found that 40% of the energy in the transmitted wave spectra was in the range $1.5f_p$-$3.5f_p$. This energy transfer was assumed to be independent of the incident wave parameters and the breakwater geometry.

In the present work, an experimental campaign was carried out in order to study the influence of the main wave/geometry parameters in the spectral energy distribution behind a submerged obstacle and to reconstruct more accurate transmitted wave spectra.

EXPERIMENTAL SET-UP

The experiments were carried out in the wave-flume of Laboratorio di Idraulica e Costruzioni Marittime of Università Politecnica delle Marche (Ancona, IT). The experimental set-up is shown in Figure 1.

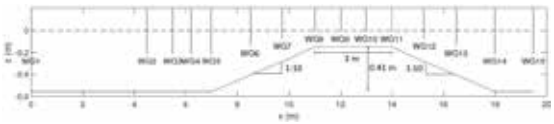

Figure 1 - Experimental set-up of the tested bar.

A smooth submerged trapezoidal bar was constructed, with an upslope and a downslope of 1:10 and a 3m horizontal crest. The height of the horizontal plane section was 0.41m above the flume bottom. The free surface was measured at fifteen stations along the flume (WG1-WG15). The incoming and the transmitted wave spectra are evaluated at WG2 and WG15, respectively. JONSWAP spectra were generated with different peak periods T_p, wave heights H_s and structure freeboards R_c.

RESULTS

The effect of the obstacle in the energy transfer towards higher frequencies is studied. The ratio between the energy of the spectrum at frequencies higher than $1.1f_p$ $m_0(f>1.1f_p)$ and the total energy of the spectrum m_0 is used to reconstruct the spectral shape. The transmitted spectra depend on the offshore wave nonlinearity H_s/h_0 and on the relative water depth $|R_c|/L'$, where h_0 and L' are the offshore water depth and the wavelength above the bar, respectively. From experimental data, Equation 1 was found to accurately describe the transmitted spectrum:

$$\frac{m_0(f>1.1f_p)}{m_0} = \mathrm{B} + \mathrm{C}\left[\tanh\left(D\left|\frac{L'}{R_c}\right|^{2.1}\left(\frac{H_s}{h_0}\right)^{A} - E\right)\right] \qquad (1)$$

where the coefficients depend on f/f_p. In Figure 2 the present method and the method of van der Meer et al. (2000) are applied to two wave conditions. Both methods give appreciable results for shorter waves (panel *a*). When the wavelength further increases (panel *b*), the new approach is able to more adequately represent the transmitted wave spectrum.

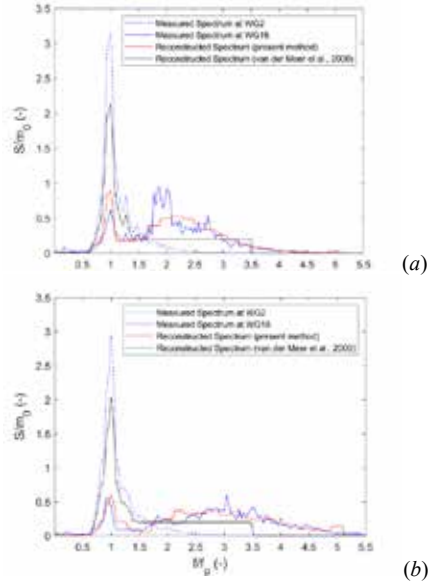

(*a*) (*b*)

Figure 2 - Comparison between the measured normalized spectrum S/m_0 (blue line) and the spectra obtained by the present method (red line) and by the van der Meer et al. (2000)'s method (black line). R_c=-0.10m, H_s=5cm, T_p=2.0s (panel *a*) and T_p=2.5s (panel *b*).

REFERENCES

Beji, Battjes (1993): Experimental investigation of wave propagation over a bar, Coast. Eng., vol 19, pp. 151-162.

Losada, Patterson, Losada (1997): Harmonic generation past a submerged porous step, Coast. Eng., vol. 31, pp. 281-304

van der Meer, Regeling, de Waal (2000): Wave transmission: spectral changes and its effects on run-up and overtopping, In Coast. Eng. 2000, pp. 2156-2168

WATER CIRCULATION MODELING IN THE GULF OF FETHIYE FOR DREDGING OPERATIONS AND POLLUTION CONTROL

Bilge Karakutuk, Middle East Technical University, karakutuk.bilge@metu.edu.tr
G. Guney Dogan, Middle East Technical University, gguneydogan@gmail.com
Ahmet Cevdet Yalciner, Middle East Technical University, yalciner@metu.edu.tr
Aysen Ergin, Middle East Technical University, ergin@metu.edu.tr

ABSTRACT
This study focuses on circulation patterns in Fethiye Bay located in southwestern Turkey under dredging operations for pollution control. Due to its geographic location, enclosed by mountains on three sides, Fethiye Bay and Çalış Beach serve as the only possible paths for the water flowing from the upper basin of the bay (Figure 1). As a semi-enclosed area, the gulf experiences low circulation. Insufficient waste management infrastructure, as well as wastewater, sewage, chemical waste, and solid waste storage facilities in shipyards, contributes to the direct or indirect discharge of liquid and solid waste into the sea. Fethiye Bay faces challenges such as water and consequent material accumulation in areas where sufficient inflow and outflow are not observed during seasonal structuring (METU OERC, 2011). Moreover, the absence of freshwater inflow from external sources leads to decreased dissolved oxygen levels, and increases in seawater temperatures, resulting in eutrophication with nitrogen and phosphorus but low oxygen content in Fethiye Bay.

Figure 1 – Fethiye Bay and current water flow paths into the gulf, shown in blue. (The base map is taken from Google Earth, 2023)

Limited studies by the Muğla Metropolitan Municipality and the Ministry of Environment and Urban Planning, and previous numerical simulations using models like FVCOM and MIKE-3D have been conducted in this area (Akbasoglu, 2011; Akdeniz, 2018). The models have estimated the overall amount and proportion of water flow and the general circulation behavior in Fethiye and Göcek Bays by considering three factors: Coriolis force, tidal wave, and wind forcing with the outdated data. Through the studies, it has been specified that, although wind-induced circulation and water exchange are significant in the bay, they are not as influential as the tidal effect, and the impact of waves on circulation and water exchange in the bay is minimal. During winter, the flows from the streams to the bay are powerful enough to expel water from the bay towards the offshore area. However, the models have not taken into account the water entering Fethiye Bay from the main streams of the Murt River and T2-Discharge Channel. The results of this comprehensive study address the existing literature gap to assess the current condition of Fethiye Bay by using the most recent data. Recently available data includes bathymetric measurements from 2012 and 2022, which provide a comparison of the bathymetry in ten years, in-situ current measurements at two different locations (Figure 1, shown in red arrows), sediment sampling and analysis, sediment layer profiles in the sea bed, and sea level measurements (starting in May 2023).

An extensive evaluation of the water circulation inside Fethiye Bay under different dredging conditions has been performed to determine the optimum dredging area for the improvement of the circulation behavior inside the bay. First, the analysis of the bathymetry changes and shoaling areas where the accumulated sediment amounts have been determined. Second, the hydrodynamic modeling as well as potential pollution analysis have been performed using the Delft3D model, an open-source modeling system developed by Deltares in collaboration with Delft University of Technology (Deltares, 2010a). It enables hydrodynamic computations in coastal areas and consists of various modules dedicated to specific processes such as hydrodynamic flow, sediment transport, morphodynamics, water quality, ecology, and waves. The model has been calibrated using the current data for a sufficient period under storm and flow conditions. Through the study FLOW and WAVE modules have been coupled to observe the effect of the waves and the flow regimes of the rivers over the Fethiye basin together. In conclusion, the water circulation inside Fethiye Bay has been evaluated for before and after behaviors of different dredging scenarios which will provide insightful information before the costly dredging processes.

KEYWORDS
Fethiye Bay, circulation modeling, pollution control, dredging operations, Delft3D model

REFERENCES
Akbasoglu (2011). Wind-induced circulation and sediment transport in semi-enclosed basins; a case study for Fethiye Bay, Ph.D. thesis, METU
Akdeniz (2018). 3-dimensional numerical circulation modeling: a case study on the coastal processes in Göcek and Fethiye bays, Turkey, MS. thesis, METU
Deltares (2010a). Deltares Software Suite 2011, Delft, The Netherlands.
METU OERC (2011). The Yacht Carrying Capacity of Fethiye Gulf Project with Fethiye Municipality, Final Report.

1-DV RANS MODELLING OF UNSTEADY BOUNDARY LAYERS

Furkan Sencer Kaçar, Turkish-German University, furkan.kacar@tau.edu.tr
V. S. Ozgur Kirca, Istanbul Technical University; and also BM SUMER Consultancy & Research, kircave@itu.edu.tr
Mehrnoush Kohandel Gargari, Cyprus International University, mkohandel@ciu.edu.tr
Selahattin Utku Yilmaz, Istanbul Technical University, yilmazselaha@itu.edu.tr

INTRODUCTION

Boundary layers developing under gradually varied unsteady flows such as tsunamis, tidal flows, and flood waves propagating in estuaries have particular importance for application in coastal and hydraulic engineering, such as scour, bank/scour protection, structural design, flood inundation, and sediment transport. Many studies have been conducted involving both physical modelling (Sumer et al., 2010; Kohandel Gargari et al., 2021) and numerical modelling (Williams and Fuhrman, 2016) to study the flow dynamics and turbulence in such boundary layers. Boundary layers associated with gradually-varied involve rising and falling stages, and therefore exhibit a distinct unsteady character. This paper presents the early results of a 1DV numerical modeling study, with which the boundary layers developing under different unsteady flows were investigated.

NUMERICAL MODEL

A Matlab-based 1DV numerical model, MatRANS (Fuhrman et al., 2013), which solves the horizontal component of incompressible Reynolds-Averaged Navier-Stokes (RANS) equations, was utilized in the present study. Two equation turbulence closure model (k-ω) was implemented to the flow solver to handle turbulence closure problem. The derivatives of RANS equations in vertical dimension were solved by adopting finite difference discretization approach. MatRANS has been used successfully in various applications since its initiation, and has been developing since then (Sumer and Fuhrman, 2020).

IMPLEMENTATION OF THE MODEL AND RESULTS

In the present study, first the model is applied to solve the boundary layer developing under solitary waves. Comparison of the model results with the theoretical solution of Liu et al. (2007) for the laminar case, and with the smooth wall results of Sumer et al. (2010) showed a good agreement. Then, the numerical model was set to simulate the gradually-varied flow experiments of Kohandel Gargari et al. (2021). The pressure gradient time series recorded in the aforementioned experiments were used to drive the flow. A 30 cm constant water depth was input to the model together with a Nikuradse's equivalent sand roughness of 0.5 mm. The time variation of cross-sectional average velocity and bed shear stress, as well as the profiles of Reynolds-averaged velocity, turbulent kinetic energy and shear stress were obtained as the output. Comparison of the early results of the model with those from the experiments of Kohandel Gargari et al. (2021) generally exhibits a good agreement although there are some differences, which shows that MatRANS is capable of simulating the gradually-varied unsteady flows effectively (Figure 1).

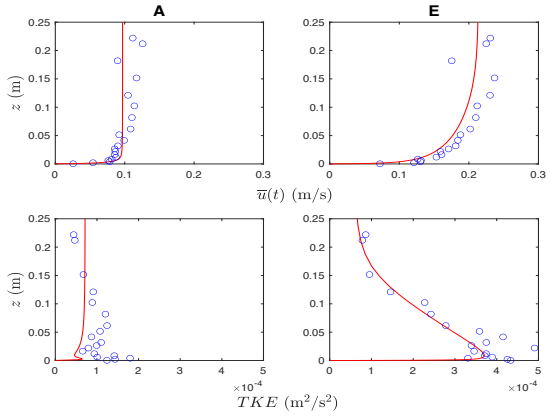

Figure 1 - Reynolds averaged velocity and turbulence kinetic energy profiles for two different points on a hydrograph. Blue circles: Kohandel sGargari et al. (2021). Red line: MatRANS results

Future studies shall be directed to improve the model performance and to obtain parametric solutions for such boundary layer problems.

REFERENCES

Fuhrman, D.R., Schløer, S. and Sterner, J. (2013): RANS-based simulation of turbulent wave boundary layer and sheet-flow sediment transport processes. Coastal Eng., 73, pp.151-166.
Kohandel Gargari, M., Kirca, V.O. and Yagci, O. (2021): Experimental investigation of gradually-varied unsteady flow passed a circular pile. Coastal Eng., 168, 103926.
Larsen, B. E., Arbøll, L. K., Kristoffersen, S. F., Carstensen, S., & Fuhrman, D. R. (2018). Experimental study of tsunami-induced scour around a monopile foundation. Coastal Eng., 138, 9-21.
Liu, P. L. F., Park, Y. S., & Cowen, E. A. (2007). Boundary layer flow and bed shear stress under a solitary wave. J. of Fluid Mech., 574, 449-463.
Sumer, B. M., Jensen, P. M., Sørensen, L. B., Fredsøe, J., Liu, P. L. F., & Carstensen, S. (2010). Coherent structures in wave boundary layers. Part 2. Solitary motion. J. of Fluid Mech., 646, 207-231.
Sumer, B. M., & Fuhrman, D. R. (2020). Turbulence in coastal and civil engineering. World Scientific.
Williams, I. A., & Fuhrman, D. R. (2016). Numerical simulation of tsunami-scale wave boundary layers. Coastal Eng., 110, 17-31.

IMPACT OF SHIPPING EMISSIONS ON RIA DE AVEIRO WATER QUALITY

Ana Picado, Centre for Environmental and Marine Studies, Physics Department, Aveiro University, Portugal, ana.picado@ua.pt
Nuno Vaz, Centre for Environmental and Marine Studies, Physics Department, Aveiro University, Portugal, nuno.vaz@ua.pt
Michael A. Russo, Centre for Environmental and Marine Studies, Department of Environment and Planning, University of Aveiro, Aveiro, Portugal, michaelarusso@ua.pt
Alexandra Monteiro, Centre for Environmental and Marine Studies, Department of Environment and Planning, University of Aveiro, Aveiro, Portugal, alexandra.monteiro@ua.pt
João Miguel Dias, Centre for Environmental and Marine Studies, Physics Department, Aveiro University, Portugal, joao.dias@ua.pt

INTRODUCTION

Shipping contributes significantly to the degradation of air quality, with emissions of CO_2, nitrogen and sulphur oxides and particulate matter. The International Maritime Organization (IMO) has set new global limits for these pollutants. To comply with these limitations, the strategy of the shipping sector has been the use of exhaust gas cleaning systems (scrubbers), where emitted compounds are trapped and directly discharged into surface water. Direct discharges to the sea of polluted waters will therefore cause substantial deterioration of marine water quality, such as acidification or eutrophication, as well as high levels of metals and polycyclic aromatic hydrocarbons (PAHs). In this context, the main aim of this work is to investigate the potential impacts of shipping emissions to water by open-loop scrubbers on a coastal lagoon (Ria de Aveiro) water quality - one of the case studies of EMERGE European project.

METHODOLOGY

A previously developed implementation of Delft3D model in Ria de Aveiro, with the hydrodynamic and water quality modules (FLOW and WAQ), was validated. The model was set up with a curvilinear orthogonal grid, and a single vertical layer since the lagoon is vertically homogeneous. The model was used to simulate tidal propagation, heat and salt transport, and water quality indicators, such as nutrients, dissolved oxygen, pH, chlorophyll, metals and PAHs. Boundary conditions for most variables were obtained from reliable databases (*in situ*, models, or reanalysis), whereas for shipping emissions from open-loop scrubbers (metals and PAHs) concentrations computed by the Chemical Drift model for the study region (Aghito et al., 2023) were considered. To evaluate the impact of shipping emissions on the water quality of Ria de Aveiro, the mean annual (MA) and maximum concentrations (MC) of metals and PAHs were computed for all the domain and compared with the current water quality standards in Portugal.

RESULTS

Model results suggest that the main source of metals and PAHs in Ria de Aveiro is the shipping emissions, however, they are much lower than MA and MC established by the water quality standards. For nickel, the MA concentration in the main channel is 0.35×10^{-8} mg/L and the MC is 1.3×10^{-8} mg/L (Figure 1), while the water quality standards allow mean values up to 8.6×10^{-3} mg/L and maximum values up to 34×10^{-3} mg/L. Regarding other metals and PAHs the results are similar.

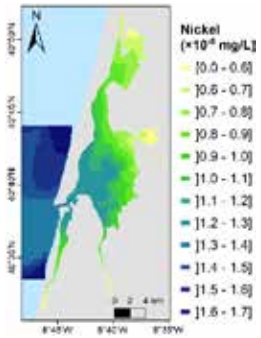

Figure 1 - Nickel annual MC (mg/L) considering shipping emissions from open-loop scrubbers.

CONCLUSIONS

Model results indicate that shipping emissions to water represent the primary source of metals and PAHs in the Ria de Aveiro. However, these emissions do not appear to compromise the water quality in the region. Several factors could contribute to this outcome. Firstly, the effective mixing and dispersion processes in the marine environment may lead to lower concentrations of pollutants, mitigating their impact on water quality. Additionally, not all ships operating in the area are equipped with scrubbers, resulting in the release of pollutants into the air. Consequently, future research should focus on examining the deposition of atmospheric metals and PAHs emitted by ships as a relevant aspect to consider.

ACKNOWLEDGEMENTS

Thanks are due to FCT/MCTES for the financial support to CESAM (UIDP/50017/2020 + UIDB/50017/2020 + LA/P/0094/2020). This project received funding from the European Union's Horizon 2020 research and innovation program under grant agreement No 874990 (EMERGE project). This work reflects only the author's view and the Innovation and Networks Executive Agency is not responsible for any use that may be made of the information it contains.

REFERENCES

Aghito (2023): ChemicalDrift 1.0: an open-source Lagrangian chemical-fate and transport model for organic aquatic pollutants, Geoscientific Model Development, vol. 16, pp. 2477-2494.

Relating grass cover strength to vegetation and soil parameters using a grass pullout test

Rens van der Meijden, University of Twente, r.vandermeijden@utwente.nl
Gosse Jan Steendam, Infram Hydren, gosse.jan.steendam@infram-hydren.nl
Jord Warmink, University of Twente, j.j.warmink@utwente.nl
Denie Augustijn, University of Twente, d.m.augustijn@utwente.nl

INTRODUCTION

Earthen dikes in the Netherlands often comprise an erosion-resistant, but species-poor grass cover. Alternatively, species-rich (i.e. containing a large number of grass and herb species) grass covers, due to their deeper and more diverse root networks, are hypothesized to be stronger than conventional covers. To pave the way for the nation-wide application of species-rich covers, the Future Dikes project investigates whether existing species-rich dikes are sufficiently erosion resistant. Strength assessments are done using the wave overtopping simulator (WOS) (Van der Meer et al., 2007) at 3 locations and a grass sod pulling method (SPM) at 20 locations (Bijlard et al., 2017). Both tests derive a critical velocity (U_c) to characterize the strength of species-rich covers in the design and assessment protocols. However, in the past, relating the results of the SPM to the WOS and environmental (root, soil) parameters was sometimes difficult, hence questioning the consistency of the device. To assess the consistency of the SPM, this study will unravel the relations between measured grass cover strength and various vegetation and soil characteristics. In doing so, insight may be obtained into the contribution of species-richness to grass cover strength as well.

DATA AND METHODS

The SPM consists of a tripod and a pull frame, which is mounted to a grass sod. Driven by an electric motor, the sod is pulled from the cover vertically, whilst recording the applied force and displacement. The peak force (i.e. at the moment when the sod fails) is translated to a critical normal stress (N/cm^2) by division over the surface area of the sod. Per dike section, 30 pullout tests are performed within an area of 8 m x 5 m. The data used in this study were acquired during two projects: Gras op Zand (GOZ, conventional grass on sand) and Future Dikes (FD, species-rich grass on silt). Both data sets include, besides sod pulling tests, extensive field research into above-ground vegetation coverage, root weight, soil granular and fertility characteristics. The mean and coefficient of variation (CV) of the 30 critical normal stresses per dike section are related to the recorded vegetation and soil characteristics. First, an exploratory Principal Component Analysis (PCA) reveals the large-scale variability and strongest relations in the datasets, after which a Redundancy Analysis (RDA) assesses whether the strength data can be explained by the environmental data in a statistically significant manner.

PRELIMINARY RESULTS

Figure 1 shows a biplot of the PCA scores and loadings based on the combined data of FD and GOZ. Besides species-richness ($N_{species}$) and coverage of herbs (%), the sites in FD and GOZ are distinctly different in terms of above-ground vegetation coverage (%), lutum and sand fractions (%), microbial activity (MicrAct) and pH. Results have shown that the critical normal stresses of FD are highest. Detailed analysis should reveal the contribution of species-richness.

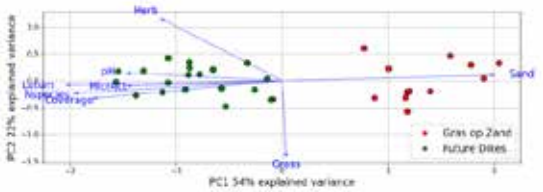

Figure 1 PCA biplot of the combined FD and GOZ data.

Figure 2 shows an RDA biplot of the GOZ data, wherein the variance of the mean and CV of the critical normal stress (CNS) is for 85% explained using 8 vegetation and soil parameters. This indicates that the magnitude and variability of the measured strength using the SPM are largely in line with what would be expected from the present vegetation and soil characteristics. In Figure 2, species-richness and increased herb coverage seem not to contribute significantly to the cover strength. However, they may affect the dry weight of (fine) roots, which will be further analyzed in the paper.

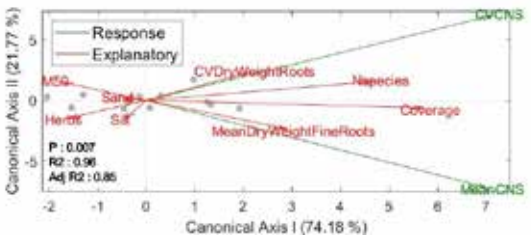

Figure 2 RDA biplot of the GOZ data.

ACKNOWLEDGEMENTS

Future Dikes is funded by the Dutch Flood Protection Program, on whose behalf Waterboard Rivierenland fulfils the role of client. The project is carried out by a consortium consisting of Radboud University Nijmegen, Wageningen Environmental Research, University of Twente, Infram Hydren, Eureco Advies, Deltares and Lumbricus Environmental Research and Consultancy.

REFERENCES

Bijlard, R., Steendam, G. Verhagen, H., & Van der Meer, J. (2017). Determining the critical velocity of grass sods for wave overtopping by a grass pulling device. *Coastal Engineering Proceedings*, *1*(35). https://doi.org/10.9753/icce.v35.structures.20

Van der Meer, J. W., Bernardini, P., Snijders, W., & Regeling, E. (2007). The wave overtopping simulator. *Coastal Engineering 2006*, 4654-4666. https://doi.org/10.1142/9789812709554_0390

COMPARATIVE DISCUSSION ON THE INTERDISCIPLINARITY OF ICZM REGULATIONS OF TURKEY AND COLOMBIA

Gulizar Ozyurt Tarakcioglu, Middle East Technical University, gulizar@metu.edu.tr
Aysen Ergin, Middle East Technical University, ergin@metu.edu.tr
Camilo M. Botero, Universidad Sergio Arboleda, camilo.botero@usa.edu.co
Gokhan Guler. Middle East Technical University, goguler@metu.edu.tr
Akdeniz Ince, Middle East Technical University, akdeniz.ince@metu.edu.tr
Carolina Santofimio, Escuela Naval Almirante Padilla, salamatura@gmail.com
Daniella García, Universidad Sergio Arboleda, daniella.garcia@usa.edu.co
Andrea C. Aguirre, Universidad Sergio Arboleda, andrea.aguirre01@correo.usa.edu.co

INTRODUCTION

Coasts are the most dynamic and valued geomorphological features on Earth. All over the world, coastal areas are under threat due to conflicting requirements that rely on natural resources such as habitats, recreation, and industry, in addition to the impacts of climate change. One of the premises of coastal zone management is interdisciplinarity. A clear and effective regulatory framework that facilitates decision-making at the national and local levels is an essential requirement. Appropriate governance mechanisms are needed to enable consultation with a wide range of stakeholders to build consensus and implement management measures, as well as communication or information pathways between stakeholders, scientists, and decision-makers (Soomai et al., 2018). Although the principles of coastal zone management are universal, the effectiveness of implementing these principles depends on the local resources and the regulatory frameworks. Additionally, there are few references to the application of interdisciplinarity, which integrates technical sciences with the legal infrastructure.

PROJECT

The joint project "Coastal scenery as core element to calculate vulnerability and support normative regulation of the coastal zones of Colombia and Turkey" funded by scientific and technological research bodies of Turkey (TUBITAK) and Colombia (MINCIENCIAS), is the first example of a collaborative project of Department of Civil Engineering, METU, Turkey and School of Law, Universidad Sergio Arboleda, Santa Marta, Colombia that aims to present the comparison of ICZM frameworks and how the country-specific regulatory frameworks affect the implementation and effectiveness of decision making considered in such plans. The use of technical tools such as multicriteria decision-making methods, vulnerability assessments, and scenery evaluation as regulatory tools are also analyzed for both countries. Consequently, this joint work is an opportunity for scientific development, both from conceptual and methodological aspects, in linking coastal engineering and legal administrative frameworks around a common goal of protecting coastal areas.

ICZM FRAMEWORK OF TURKEY AND COLOMBIA

Turkey and Colombia are both countries located in geostrategic positions. The former is the bridge between Europe and Asia, having coastal zones in the Mediterranean and the Black Sea. The latter is in the northwest corner of South America and is the only country in this subcontinent with access to the Caribbean Sea and the Pacific Ocean. Therefore, this collaboration between the partners covers four seas and more than 10.000 km of coastlines, contributing to the diversity of coastal geomorphologies, problems, and governance systems.

Some of the initial findings of the ongoing project highlight the reflections of this diversity on the legislation. The Turkish Coastal Law (No: 3621, 2018) and the corresponding Regulation of the Implementation of the Coastal Law define the physical boundaries of the coastal areas in detail, focusing on the definition of the shoreline and distances to the shoreline. The Colombian approach is to determine environmental coastal units that reflect similar coastal areas in the same spatial zone for decision-making purposes (Botero et al., 2014). The Turkish legislative system introduced the concept of regional coastal area plans as part of the regulatory framework within the spatial planning legislation in 2014 (without enforcement power). In contrast, Colombia does not have a national coastal zone management plan. On the other hand, both countries experience the disadvantages of highly fragmented regulatory systems of the coastal area governance where the decisions require input from different governmental bodies, whereas local representation can be limited. Significant discussions will be presented focusing on both countries' limitations, bottlenecks, and best practices considering coastal zone management and integration of scientific and technical tools.

REFERENCES

Botero, Milanés, Cabrera and Granados. (2014): Integrated Coastal Management in Cuba and Colombia: A Comparative Analysis. Ocean Yearbook Online. 28. 672-697. 10.1163/22116001-02801023.
Coast Law, No: 3621 (2018) T.C. Resmi Gazete, 20495, 17 Nisan 1990. In Turkish. https://www.mevzuat.gov.tr/MevzuatMetin/1.5.3621.pdf.
Soomai, Santo, Wells, and MacDonald (2018). Science, Information, and Policy Interface for Effective Coastal and Ocean Management (1st ed.). CRC Press. pp.512

EFFECTIVENESS OF SAND TRAPS IN PROMOTING SEDIMENT GAIN IN FOREDUNES OF A SEMI-NATURAL BEACH (COSTA BRAVA, SPAIN)

Carla Garcia-Lozano, University of Girona, carla.garcia@udg.edu
Carolina Martí-Llambrich, University of Girona, carolina.marti@udg.edu

INTRODUCTION:
Foredunes are natural barriers that protect coastal areas from erosion and flooding. However, they are under threat worldwide due to climate change, rising sea levels, and human activities. In Catalonia, the degradation of the dune landscape is estimated to be 90%, mainly due to urbanization and its impact on beach-dune systems (Garcia-Lozano et al., 2018). Human impacts are the primary cause of dune degradation on the low-lying coast of Costa Brava, being the implementation of nature-based solutions a successful tool to restore dune morphologies. The This study evaluates the effectiveness of sand traps in promoting sediment gain in the foredunes of a semi-natural beach in Costa Brava, two years after their implementation.

METHODOLOGY:
Digital elevation models were retrieved from UAV data collected over two years, before and after the implementation of sand traps on el Riuet Beach. The data was processed using PIX4Dmapper software to obtain digital elevation models with resolutions of 15 cm. The study area is a 4 ha semi-natural beach surrounded by croplands and included in a Natural Park. The MAVIC DJI was used for flight, and the two flights compared were from the summer of 2019 and winter of 2023 (before the storm period).

RESULTS AND DISCUSSION:
The implementation of sand traps led to a significant increase in sediment gain in the foredune area, with an average height increase of one meter, or 46%, from 2.8 to 3.8 meters above sea level. The sand traps effectively trapped sand and prevented it from being carried away by winter storms, allowing the beach-dune profile slope to recover. The zone surrounding the sand traps has been located at a maximum height of 4 m since its implementation in the winter of 2020-2021. Cordoned dunes have also considerably reduced human trampling, although cruising practices still occur. Sexual human niches are now the main cause of foredune treatment in the study area, being the main cause of dune deflation and reactivation of blowouts by means of unmanaged pathways.
The increasing demand for sustainable beach management has sparked a growing scientific and engineering interest in exploring how natural processes can provide solutions to address the degradation and vulnerability of beaches and dunes (Slinger et al., 2021). However, cruising is known to be a significant cause of dune degradation and human frequency, even when nature-base solution are implemented (García-Romero et al., 2022). While cordoned dunes may deter users with sand beach tourism, it may not be sufficient for cruising tourism. Additional measures, such as surveillance and fines, are necessary to prevent cordoned-off dunes from being crossed.

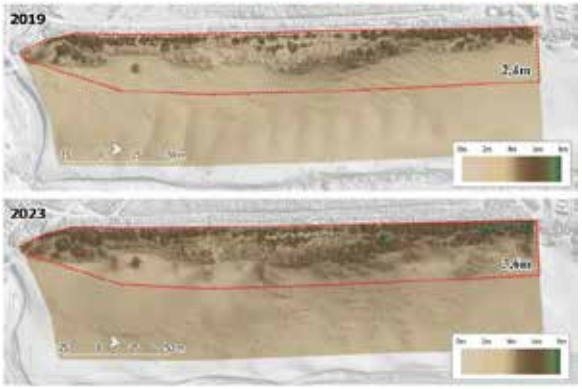

Figure 1 - Foredune evolution of Riuet Beach before (2019) and after (2023) nature-based solutions were implemented to restore dune systems.

ACKNOWLEDGMENT
This research has been carried out within the framework of the IMPETUS project (ref. 101037084) funded by the European Commission granted under the call of the Horizon 2020.

REFERENCES
Garcia-Lozano et al. (2018). Changes in coastal dune systems on the Catalan shoreline (Spain, NW Mediterranean Sea). Comparing dune landscapes between 1890 and 1960 with their current status. *Estuar. Coast. Shelf Sci.* 208, 235-247.
Slinger, J., Stive, M., Luijendijk, A. (2021). Nature-based solutions for coastal engineering and management. *Water*, 13, 3-7.
García-Romero et al. (2022). TEMPORARY REMOVAL: Sand, Sun, Sea and Sex with Strangers, the “five S's”. Characterizing “cruising” activity and its environmental impacts on a protected coastal dunefield. Jour. Env. M, vol. 301. 113931.

LOW-COST COASTAL MONITORING: REMOTE SENSING AND CROWDSOURCING

Yasser Assaf, Department of Civil, Environmental, Land, Building and Chemical Engineering, Politecnico Di Bari, yasser.assaf@poliba.it
Leonardo Damiani, Department of Civil, Environmental, Land, Building and Chemical Engineering, Politecnico Di Bari, leonardo.damiani@poliba.it
Alessandra Saponieri, Department of Innovation Engineering, Università del Salento, alessandra.saponieri@unisalento.it

The project explores cost-effective monitoring techniques for sandy beaches, utilizing tools such as Coastsnap, video monitoring, and drones. Coastsnap, developed by the University of New South Wales (UNSW) in Australia Harley et al. (2019), combines citizen science and community engagement to provide valuable insights into shoreline changes. Automated video monitoring, as described by Valentini et al. (2017), complements Coastsnap by enabling extensive data collection during daylight hours.

The study aims to analyze shoreline changes, sediment accumulation patterns, and key beach parameters like width and both foreshore and swash zone slopes. It promotes innovative and standardized methodologies for studying shallow water hydrodynamics and morphodynamics (e.g., Run-up and shoreline temporal evolution), integrating expert drone survey data with crowdsourced knowledge to investigate risk factors and design monitoring systems.

Understanding beach morphology evolution is crucial due to the increasing coastal crises and human pressures. Leveraging remote sensing techniques minimizes manpower and reduces costs, ensuring an accurate and efficient monitoring.

Figure 1 - The pilot site at the beach 'Pane e Pomodoro', Bari, Italy.

The project has two main objectives. Firstly, conducting drone-based bathymetric surveys provides valuable insights, enhancing the understanding of coastal dynamics and informing management strategies. Secondly, the project aims to establish a cost-effective monitoring network along the Apulian coastline, starting with the pilot site 'Pane e Pomodoro' beach situated on the southern coast of Italy's Adriatic Sea (Fig.1). The involvement of local communities in data collection and analysis is an integral part of this effort. This participatory approach promotes community engagement and ownership, fostering coastal conservation efforts. By integrating these methodologies and collaborative approaches, the project offers a comprehensive framework for coastal monitoring and management, contributing to evidence-based practices and a deeper understanding of shoreline dynamics.

The article explores cost-effective monitoring techniques for sandy beaches, including coastsnap, video monitoring, and drones. It seeks to examine the changes in shoreline using CCD (Color Channel Divergence) algorithm developed by Turner et al. (2001) and SDM (Shoreline Detection Model) algorithm introduced by Valentini et al. (2017). The main objectives include improving understanding of coastal dynamics through drone-based surveys and establishing an affordable monitoring network along the Apulian coastline. The study emphasizes the significance of remote sensing, participatory methods, and evidence-based practices in achieving efficient coastal management.

Keywords: Coastal monitoring, Video system, Coastsnap, Cost-effective strategies, Coastal morphodynamics, Citizen science.

REFERENCES

Harley, Kinsela, Sánchez-García, & Vos (2019): Shoreline change mapping using crowd-sourced smartphone images, Coastal Engineering, vol. 150, pp. 175-189.

Turner, Leyden, Symonds, Mcgrath, Jackson, Jancar, Aarninkhof, & Elshoff (2001): Predicted and observed coastline changes at the Gold Coast artificial reef, Coastal Engineering 2000, pp. 1836-1847.

Valentini, Saponieri, Molfetta, & Damiani (2017): New algorithms for shoreline monitoring from coastal video systems, Earth Science Informatics, vol.10, pp. 495-506.

INTEGRATION OF ECO-FRIENDLY HABITATS INTO COASTAL STRUCTURES

Dogac Sayar, University of Ottawa, ssaya056@uottawa.ca
Scott Baker, National Research Council Canada, scott.baker@nrc-cnrc.gc.ca
Ioan Nistor, University of Ottawa, inistor@uottawa.ca

Artificial coastal defense systems frequently host less varied aquatic populations than natural environments, with higher concentrations of invasive species, and can have detrimental effects on the ecosystem (Firth et al., 2016). Thus, coastal structures need to be designed with the intention of achieving sustainable objectives through the use of ecoengineering in coastal protection and habitat enhancement. To lessen the detrimental environmental effects of coastal structures, there is growing interest in ecological engineering, combining ecosystems with engineering concepts to create coastal structures that serve both people and nature. Therefore, it is necessary to develop new eco-friendly breakwater design principles which would also profit from the interdisciplinary input of marine biologists and ecologists. Since the eco-friendly breakwater concept is an emerging research area, several breakwater prototypes are proposed to be tested to observe both their structural and ecological performance. Therefore, this study is essential to encourage increased integration of ecological habitats in the design of new coastal structures and also retrofitting ecological elements into existing structures.

This research aims to provide information about the hydraulic performance, durability, and resilience of rubble mound breakwaters designed with environmentally friendly armor units and mattress combinations under challenging Canadian climatic conditions. Physical and numerical experiments will be performed within the scope of this study as a research collaboration between the University of Ottawa and the Canada National Research Council (NRC). The numerical modelling part of the project will be conducted to simulate the eco-friendly breakwater under various conditions after the physical modelling campaign is completed. The open-source numerical model is expected to become an optimization tool for the design of eco-friendly breakwaters.

The physical experiments are planned and designed to be conducted in the Large Wave and Current Flume of NRC - Ocean, Coastal, and River Engineering Research Center between March 2023 and August 2023. Various two-dimensional rubble mound breakwater cross-sections will be tested with several configurations of CoastaLock (developed by ECOncrete®) armor units at a large model scale. The test program aims to reduce scale effects caused by improper surface tension and viscous force scaling and accurately model wave-breaking processes, air entrainment, turbulence, viscous forces, and wave-structure interactions. The hydraulic performance and failure modes of the designed eco-friendly breakwater sections will be investigated against extreme wave conditions. The effect of several Coastalock armor unit placements, spacing, and configurations on structural stability will be tested to determine the most efficient and safe design parameters and breakwater properties. The outcomes of the experimental test series will provide crucial information for the growing literature on the design of environmentally friendly coastal structures.

Figure 1 - NRC-OCRE Large Wave and Current Flume in Ottawa, Canada.

The research is funded by a grant in support of a Collaborative R&D investment under the National Research Council of Canada's (NRC) Collaborative Science, Technology, and Innovation Program (CSTIP).

REFERENCES

Firth, White, Schofield, Hanley, Burrows, Thompson, Skov, Evans, Moore, Hawkins, (2016b). Facing the future: The importance of substratum features for ecological engineering of artificial habitats in the rocky intertidal. Marine and Freshwater Research, 67(1), 131-143.

NEW FORMULA FOR WAVE REFLECTION ON MOUND BREAKWATERS USING NEURAL NETWORK MODELLING

Pilar Díaz-Carrasco, Polytechnic University of Valencia, pdiacar@upv.es
Jorge Molines, Polytechnic University of Valencia, jormollo@upv.es
Esther Gómez-Martín, Polytechnic University of Valencia, mgomar00@upv.es
Josep R. Medina, Polytechnic of Valencia, jrmedina@tra.upv.es

INTRODUCTION

Wave reflection from breakwaters may influence beaches and the entrance of harbors due to dangerous wave conditions and may compromise the structure stability due to the induced scour at the structure toe. These problems will have a greater impact in the future due to climate change, sea level rise and stronger wave storms (Camus et al., 2019). The challenges of protecting coasts and harbors from the effects of global warming and the correct estimation of reflected energy from coastal structures demand more precise and easy-to-apply design formulas for mound breakwaters.

Several empirical formulas found in the literature for predicting wave reflection, K_R, are based on the Iribarren number, ξ_0, or other dimensionless parameters with calibrated coefficients and dimensionless variables selected on empirical grounds (Zanuttigh and Van der Meer, 2008; Díaz-Carrasco et al., 2021). These works considered an extensive experimental database tested with wave conditions, measurement devices and techniques specific in each laboratory. In some cases, K_R were measured in research tasks focused on the hydraulic stability, wave overtopping or wave transmission. The consequence of this variety of methods was a high uncertainty on the results and thus imprecise wave reflection estimations and empirical formulas valid only for very limited ranges.

The main objective of this study is to find a simple and more precise empirical formula to estimate wave reflection on conventional mound breakwaters under non-overtopping and non-breaking conditions.

METHODOLOGY

A Neural Network (NN) model was used to rank the influence of 11 candidate explanatory variables and to estimate the relationships between the explanatory variables and the squared wave reflection coefficient, K_R^2. The methodology comprises two main phases:

(1) Formula development by applying the NN model to experimental data performed at University of Granada (UGR) with regular and irregular waves. The experimental database of UGR included tests from a conventional mound breakwater with double-layers of cubes armor and rock homogeneous breakwaters with two seaward slopes angles.

(2) Formula validation with experimental data performed at Aalborg University (AAU) with irregular waves. The experimental database of AAU included tests from conventional mound breakwater with double-layers of cubes and rocks armors, three seaward slope angles and different composition of the porous core.

Figure 1 represents the estimations obtained with the NN model using as input variable the relationship between the relative water depth, *h/L*, and the seaward slope angle, α, that is: (h/L)/tan α. Figure 1 shows an exponential relationship between K_R^2 and the (h/L)/tan α for both slope angles tested at UGR.

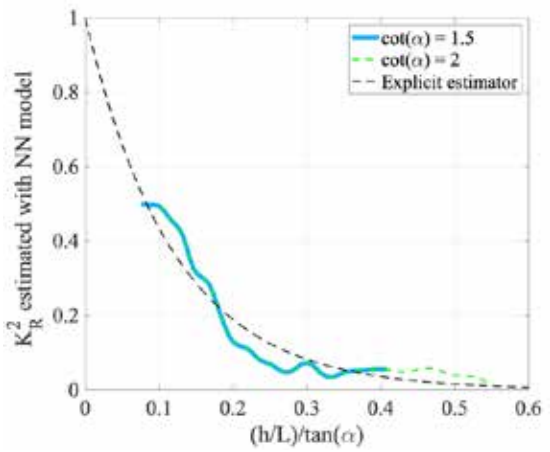

Figure 1 - Square wave reflection coefficient, K_R^2, given by the NN model with input variable (h/L)/tan α. The dash line represents the exponential relationship between explanatory variables and K_R^2.

RESULTS AND CONCLUSIONS

Using NN modelling, it was found that the main explanatory variable for wave reflection is (h/L)/ tan α. An exponential relationship between K_R^2 and (h/L)/ tan α with one fitting parameter was fitted. The explicit exponential formula showed a good agreement (R^2 = 0.88) between K_R^2 estimated and K_R^2 measured from UGR tests. At the Conference, results of validation as well as a detailed explanation of the use of NN for estimating the wave reflection formula will be shown.

REFERENCES

Camus, P., Tomás, A., Díaz-Hernández, G., Rodríguez, B., Izaguirre, C., Losada, I.J., (2019): Probabilistic assessment of port operation downtimes under climate change. Coastal Engineering 147, 12-24.

Díaz-Carrasco, P., Eldrup, M.R., Andersen, T.L., (2021): Advance in wave reflection estimation for rubble mound breakwaters: The importance of the relative water depth. Coastal Engineering 168.

Zanuttigh, B., Van der Meer, J., (2008): Wave reflection from coastal structures in design conditions. Coastal Engineering. 55, 771-779.

STABILITY OF STONE GABION ARMOR UNITS FOR COMPOSITE BREAKWATER MOUNDS

Yuri Shimizu, Chuo University, a19.8m3g@g.chuo-u.ac.jp
Toru Aota, Fudo Tetra Corporation, toru.aota@fudotetra.co.jp
Shigeru Sakamoto, Koiwa Kanaami Corporation, sg.sakamoto@koiwa.co.jp
Takeharu Konami, Okasan Livic Co., LTD, konami@okasanlivic.co.jp
Hideto Okido, Okasan Livic Co., LTD, okido@okasanlivic.co.jp
Taro Arikawa, Chuo University, taro.arikawa.38d@g.chuo-u.ac.jp

1. PURPOSE OF THE STUDY

Composite breakwater mounds must be reinforced to prevent breakage in wave-resistant designs. Internal harbor mounds are covered with armor stones, concrete armor blocks, and stone gabions that have a positive environmental impact. Here we evaluate stone gabion stability for external rubble mounds of composite breakwaters.

2. EXPERIMENTAL METHOD

Hydraulic irregular wave experiments at a scale of 1/40 were conducted on the cross-section channel, as shown in Figure 1; Table 1 lists the experimental conditions. Irregular waves with a significant wave period of $T_{1/3}$, and significant wave height of $H_{1/3}$ were artificially generated.

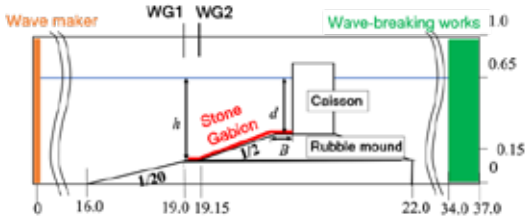

Figure 1 - The experimental cross-section channel [m]

Table 1 - The experimental conditions

case	d/h	B	$T_{1/3}$	$H_{1/3}$
case1	0.6	0.11 m	1.34 s	1 cm
case2		0.23 m		2 cm
case3	0.4	0.11 m	1.82 s	3 cm
case4		0.23 m	2.29 s	4 cm
				5 cm

3. EXPERIMENTAL RESULT

Stone gabions mainly exhibited sliding on the mound slope. The sliding amounts were divided into 0, 0–1/4, 1/4–1/2, 1/2–3/4, and 3/4–1 times the model length of the direction of the slope, and the number of sliding stone gabions was counted. D', the average sliding amounts of the direction of the slope each model, was calculated using Equation (1), where K is the sliding range upper limit, n is the number of slides of models in the corresponding sliding range, and s is the number of models on the slope.

$$D' = \frac{\sum Kn}{s} \quad (1)$$

$H_{1/3}$ of the incident wave at the embankment, $H_{I\,1/3}$, and D' are correlated using the cumulative lognormal distribution function for fitting. Considering that D' scatteres, $H_{I\,1/3}$ in Equation (2) (Hudson equation) should

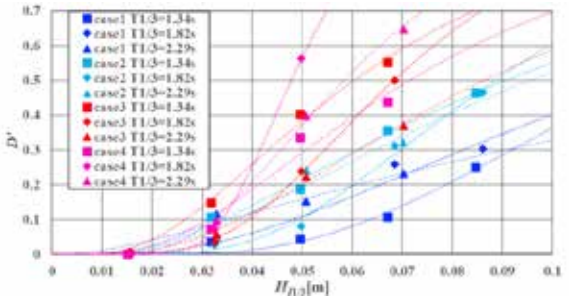

Figure 2 - The relationship between D' and $H_{I\,1/3}$

be approximately 0.04 m and 0.032 m for d/h = 0.6 and 0.4, respectively, assuming that D' is stable below 0.15. Subsequently, the stability number, Ns, is obtained by substituting $H_{I\,1/3}$ at D' = 0.15 into Equation (2) for each case in Figure 2; $B/L_{1/3}$ is obtained by nondimensionalizing the mound shoulder width, B, by the incident wave wavelength, $L_{1/3}$, at the embankment installation depth, h. Figure 3 shows the correlation between Ns and $B/L_{1/3}$.

$$M = \frac{\rho_r {H_{I1/3}}^3}{{N_s}^3 (S_r - 1)^3}, \quad (2)$$

where M, ρ_r, and S_r are the weight, density, and specific gravity of the model, respectively. For d/h = 0.6, Ns is occasionally larger than that reported by Shimosako et al. (2004) However, under d/h = 0.4, it is mostly similar.

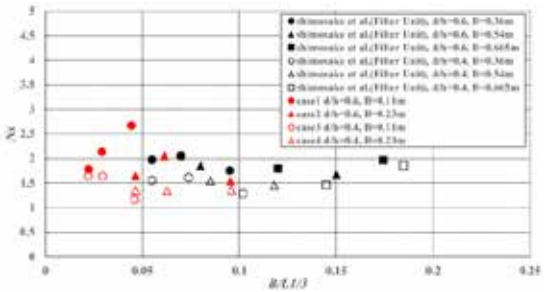

Figure 3 - The relationship between Ns and $B/L_{1/3}$

REFERENCES

Ken-ichiro Shimosako, Shin-ichi Kubota, Akira Matsumoto, Minoru Hanzawa, Yukihiro Shinomura, Nobuyoshi Oike, Tsuyoshi Ikeya, Shingo Akiyama (2004): Stability and durability of filter unit covering rubble mound of composite breakwater, Report of the port and airport research institute, Ministry of Transport, vol. 43 no. 1, pp. 49-83.

A STUDY ON FAILURE CHARCTERISTICS OF DOCK DUE TO ABNORMAL WIND WAVES

Kyu-Tae Shim, Catholic Kwandong University, aiqshim@gmail.com
Kyu-Han Kim, Catholic Kwandong University, khkim@cku.ac.kr
Hyun-Dong Kim, University of Florida, kim.h@ufl.edu
Woo-Seok Jang, Catholic Kwandong University, gim1828@gmail.com

INTRODUCTION

In a coastal area where the water depth changes rapidly, waves developed in the offshore propagate to the coast, with a massive energy without any dissipation. Particular attention should be paid to the occurrence of damage in an island, where the land is open towards the ocean, in the event of abnormal wind wave, and design of structures in such region requires thorough examination.

FIELD INVESTIGATION

The southern and northern coasts of Hongdo Island located in the western coast of South Korea face the ocean side, and are directly affected when a typhoon or a high wave occurs. Therefore, structural damage due to wave generation frequently occurred in the coasts, and repair and reinforcement work were carried out several times. In particular, the high wind wave generated in August 2016 caused large-scale damage to the dock located in the north side of the island (Fig.1).

Figure 1 - Scene of Wave Action (L) and Damage Occurrence (R) at Hong-Do Island, Korea

HISTORY OF REINFORCEMENT WORK

The dock constructed in 1995 has the block-type structure. Several repair works were carried out to repair damage by high waves and typhoon attacks. In particular, large-scale reinforcement work was carried out due to the damage caused by the typhoon that occurred in 2015. However, additional damage occurred due to the high wind wave generation within less than 6 months after the reinforcement work.

HYDRAULIC CHARACTERISTIC INVESTIGATION

Various methods were attempted in order to investigate the mechanism of structure destruction due to wind wave attack. At first, in order to estimate the wave at the time of the damage, the wave in the past was hindcasted through the wave observation data obtained from wave buoy and through a correlation analysis. The wave field and damage status in the shallow water were reproduced through the hydraulic model test. In the 2D model test, the wave pressure and structural stability under the condition at the time of the damage were examined. The damage characteristics were also investigated with the topography, wave direction, and structure installation condition as parameters, through the 3D model test (Fig.2).

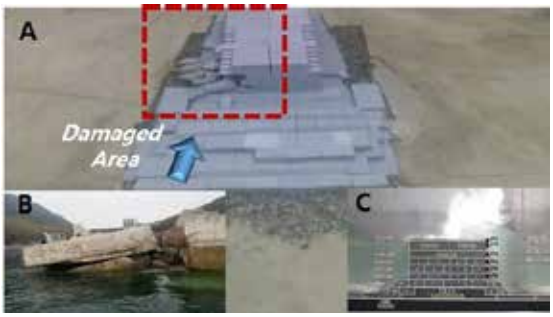

Figure 2 - Analysis of Damage Causes (A: Stability test in the 3D- wave basin, B: Damage section in the real site C: Wave pressure test in the 2D-wave flume)

FAILURE MECHANISM ANALYSIS

The failure mechanism of the dock structure was confirmed by 2D and 3D hydraulic model tests. The exfoliation and reduction of frictional force due to reinforcement work repeated over the years were also found to affect block displacement.

REFERENCES

Altomare, C.,Suzuki, T., Chen, X., Verwaest,T. and Kortenhaus,A.(2016): Wave Overtopping of Sea Dikes with Very Shallow Foreshores, Coastal Engineering, 116(2016), 236-257

Akkerman, G.J., P. Bernardini, J.W. van der Meer, H. Verheij and A. van Hoven, (2007-1). Field tests on sea defences subject to wave overtopping. Proc. of Coastal Structures Conference. Venice.

Pullen, T., Alisop, W., Bruce, T. and Pearson, J. (2009): Field and Laboratory Measurement for Mean Overtopping Discharges and Spatial Distributions at Vertical Seawalls, Coastal Engineering, 56(2), 121-140

TAW, 2002. Technical Report. Wave Runup and Wave Overtopping at Dikes. Technical Advisory Committee on Flood Defense, Delft.

NUMERICAL INVESTIGATION OF WAVE FORCES ON COASTAL BRIDGE DECKS

Masahiro Ohkubo, Chuo University, a18.dct4@g.chuo-u.ac.jp
Hiroshi Ookubo, Nippon Steel Engineering CO., LTD., kasahara.hirotsugu.rf9@eng.nipponsteel.com
Hirotsugu Kasahara, Nippon Steel Engineering CO., LTD., ookubo.hiroshi.8rb@eng.nipponsteel.com
Naoyuki Nakamura, Nippon Steel Engineering CO., LTD., nakamura.naoyuki.yt5@eng.nipponsteel.com
Taro Arikawa, Chuo University, taro.arikawa.38d@g.chuo-u.ac.jp

1. AIMS

Because coastal bridges are often damaged by the high waves generated by typhoons, an appropriate evaluation of wave forces is required at the design stage. Numerous experimental studies on wave forces at horizontal decks have been conducted, and equations for the design of coastal bridges have been proposed. However, in recent years, the application of numerical investigations, that have various advantages over experiments, to the design of coastal facilities has been emphasized. However, no previous studies have compared the numerical investigations of wave forces on coastal bridges with experimental methods. Therefore, this study aims to demonstrate the applicability of numerical investigations to wave forces acting on coastal bridge decks.

2. METHODS

Using CADMAS-SURF/3D-2F (CS2F) (2009), our numerical investigation reproduced previous experiments. The calculated cross-section is shown in Figure 1. A wave-making boundary was set at the left end of the calculated cross section, and an energy decay band and a radiation boundary were set at the right end. A structural cell simulating a coastal bridge was placed around the center of the calculated cross-section, and the pressure was measured at five locations in its lower surface cell. The y-direction is 0.1 m, where H is the wave height, h is the water depth, and s is the clearance. The numerical investigation was performed under the same wave-making conditions (Table 1) as those in Tanimoto's experiment (1978).

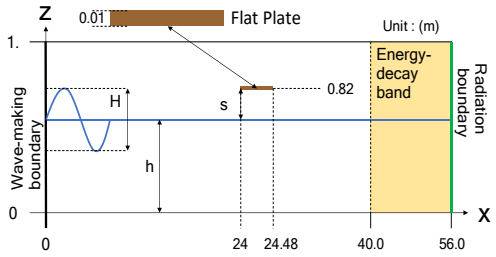

Figure 1 - Calculated cross section

Table 1 - Wave-making conditions

Wave height (cm)	Water depth (cm)	Clearance (cm)	Wave period (sec)
10, 16, 20, 24	74, 78, 82, 86	8, 4 0, -4	1.56, 2.12, 2.98

3. RESULTS

Figure 2 shows the results of the comparison between the numerical investigation and Tanimoto's experiment under the conditions of Case 1 (water depth of 78 cm, clearance of 4 cm, and wave period of 2.12 s).

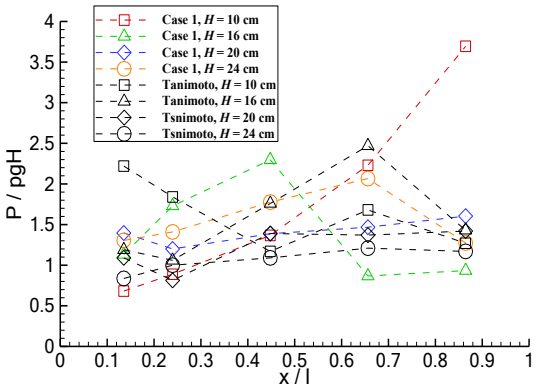

Figure 2 - Comparison of experiments and CADMAS-SURF/3D-2F

P is the pressure, ρ is the density, g is the acceleration due to gravity, x is the measured position, and l is the total length of the bridge. Under clearance conditions of 8 and 4 cm, single-peak wave forces were likely to occur owing to the presence of wavefronts under the coastal bridge. The CS2F can reproduce single-peak wave forces with the same accuracy as the experimental values. In addition, the single-peak wave forces on coastal bridge decks tend to depend on the number of wave height divisions; the longer the wave period, the more wave height divisions should be set. Under clearance conditions of 0 and -4 cm, the air is more likely to be entrained between the wave surface and coastal bridge deck. The CS2F can reproduce the air entrainment phenomenon, and the wave forces can be investigated with the same accuracy as in the experiment. However, for cases with large discrepancies from the experimental values, the vibration wave forces associated with the entrained air might not be reproduced. Using CS2F, calculations should be performed to consider the compressibility of air, and the results should be compared and verified.

REFERENCES

Arikawa, T., Yamano, T., 2009. Application of treatment for spike-noise in numerical wave tank computing impulsive wave pressure, Technical Note of the Port And Airport Research Institute, No.1175.
Tanimoto, K., Takahashi, S., Izumida, Y., 1978. A calculation Method of Uplift Forces on a Horizontal Platform, Report of the Port and Harbour Research Institute, 17(2), pp.3-47.

WAVE TRANSMISSION ON LOW CRESTED CUBE BREAKWATERS

Serhat Gümüş, serhatg2172@gmail.com
Duygu İşsever, duygu.5411@gmail.com
Esin Çevik, Yıldız Technical University, cevik@yildiz.edu.tr
Yalçın Yüksel, Yıldız Technical University, yuksel@yildiz.edu.tr

ABSTRACT
Wave climate change and resulting global sea level rise may cause structures become low crested and/or submerged. Low crested structures in touristic areas are preferred since their visual impact is minimum. In the present study, wave transmission behind the low crested conventional cross-section structure with cube breakwater is studied experimentally. The aim of the study is to determine wave transmission coefficient of low crested conventional breakwater with varying crest width and different placement and packing densities of cubes.

INTRODUCTION
The amount of transmitted wave energy depends on the incident wave characteristics, the structure geometry (slope, crest height and width), and the type of structure (rubble mound or smooth-faced; permeable or impermeable). The transmitted wave energy either pass over by overtopping and/or through the structure. Predicting the amount of energy transmitted behind the low-crested structure is highly important design parameter. The transmission coefficient, K_t, is defined as the ratio of transmitted ($H_{s,t}$) to the incident wave heights ($H_{s,toe}$). The prediction of transmission is important for different design purposes. Various researches in the past has led to various design formulae for wave transmission. D'Angremond et al. (1996) formula for the wave transmission of rubble mound structures for relatively small crest width (B/Hi<8):

$$K_t = -0.4\frac{R_c}{H_i} + 0.64\left(\frac{B}{H_i}\right)^{-0.31}\left(1 - e^{-0.5\xi}\right) \quad (1)$$

For large to very large widths (B/Hi>12) by refitting the data, Eq.(2) was obtained

$$K_t = -0.35\frac{R_c}{H_i} + 0.51\left(\frac{B}{H_i}\right)^{-0.65}\left(1 - e^{-0.41\xi}\right) \quad (2)$$

For smooth low crested structures, Van der Meer (2005) gave a prediction formula where the transmission coefficient linearly decreases with relative crest freeboard (R_c/H_{moi});

$$K_t = -0.30\frac{R_c}{H_i} + 0.75\left[1 - \exp(-0.5\xi_{0p})\right] \quad (3)$$

where R_c is the crest freeboard, B is the crest width, H_i is the incident wave height at toe of the structure, ξ is the surf parameter. Tomasicchio et al. (2011) discussed the existing formulae for the transmission coefficient and they offered a new formulation after re-calibration showed a good agreement between measured and predicted K_t.

EXPERIMENTAL SETUP AND PROCUDERES
An experimental study was carried out in the wave flume of the Coastal and Harbor Engineering laboratory at Yıldız Technical University. The flume has 26 m in length, 1 m in width and 1 m in depth. The channel is equipped with a piston type wave generator that has an active reflection compensation system.
Low crested cube armored breakwater trunk section model was tested for the determination of wave transmission for varying crest widths and different placement methods (Figure 1). The breakwater model was placed on a horizontal foreshore. The nominal diameter of the concrete cubes at the 1.5H : 1V seaside and leeside slopes and at the crest was 40 mm. The underlayer consisted of stones with a nominal diameter of 19 mm.
Three different placements; i) randomly placed in a double layer with the packing density of 57 %, ii) regularly placed in a single layer with the packing density of 57 % and iii) regularly placed in a single layer with the packing density of 68 %. The crest widths were varying as $4D_n$, $7D_n$, $10D_n$. The water depth was kept constant as 0.60 m for all tests. A total of 20 irregular wave conditions with a JONSWAP spectrum were selected for the tests. Wave conditions were measured at six different locations. One wave probe placed close to the wave board, four were in constant water depth in front of the toe of the structure with known spacing's to determine reflections from the breakwater and hence the incoming wave, one wave probe was placed behind the structure to measure transmitted wave. The wave parameters were obtained by spectral analysis. Each test lasted for about 1000 waves. The transmission tests were ended when the damage occurred at the structure.

Figure 1 - Randomly placed in double layer, ii) regularly placed in a single layer

CONCLUSION
The transmission data obtained from 2D laboratory tests of low crested cube breakwater were analyzed and adopted with the formula of D'Angremond's (1996) formula.

ACKNOWLEDGMENTS
This research is supported by the Research Fund of the Yildiz Technical University, project number: FBG-2022-4935.

REFERENCES
d'Angremond, Van der Meer, and de Jong, (1996). Wave transmission at low-crested breakwaters. Proceedings of the 25th Int. Conference of Coastal Engineering, Orlando, Florida, ASCE, 2418-2426
Van der Meer, Briganti, Zanuttigh, Wang (2005) Wave Transmission and reflection at low-crested structures: Design formula, oblique wave attack and spectral change, Coastal Engineering, 52, pp 915-929.

Tomasicchio,G. R., D'Alessandro F and Tundo G, (2011), "Further Developments In A New Formulation Of Wave Transmission", Coastal Structures, ASCE,World Scientific.

DETERMINATION OF VELOCITY PROFILES ON A RIGID BED UNDER THE EFFECT OF A PROPELLER JET

Yağızhan Bilmez, Yıldız Technical University, yagizhanbilmez@hotmail.com
Hayri Ateş, Yıldız Technical University, hayriates71@gmail.com
H. Anıl Arı Güner, Yıldız Technical University, anilariguner@gmail.com
Yeşim Çelikoğlu, Yıldız Technical University, celikogluyesim@gmail.com
Yalçın Yüksel, Yıldız Technical University, yalcinyksl@gmail.com

INTRODUCTION

Developing trade volume in the world has increased the importance of ports in particular. Along with the developing world conditions, there is continuous development in the ports in order to meet the changing demands of the international market for maritime transport. Ports are very expensive structures that contribute greatly to the country's economy. Damages that occur in ports are those that are very expensive to repair and in some cases even impossible to repair and require rebuilding. In recent years, the primary goal in the transportation sector has been to increase the carrying capacity. To that end, the ships were designed in larger sizes and reached high load capacities. With the increase in ship size, the water jets coming out of the ship's propellers cause serious damage by causing scour on the seabed, on the navigation channels, and around the quay walls and pier piles. For this reason, the interaction of the propeller jet with the flow area around the berth structures during the berthing and unberthing operations of the ships has become an important problem for the designers. There are not enough studies in the literature to determine velocity distributions in the flow field using the PIV technique (Hsieh et al. (2013) and Wei and Chiew (2018), Wei et al. (2018), Wei et al. (2019)).
Therefore, in this study, the flow field due to water jets coming out of the ship's propellers on the rigid bed was investigated. For this purpose, velocity profiles were determined on the rigid bed. Velocity measurements were performed utilizing Particle Image Velocimetry (PIV).

EXPERIMENTAL STUDY

The experiments were conducted in a rectangular flume, in which all the sides were made of glass with a total length of 6.02 m, width of 1.42 m, and height of 1.1 m, at the Hydraulic and Coastal Engineering Laboratory of the Civil Engineering Department at Yıldız Technical University (Figure 1).

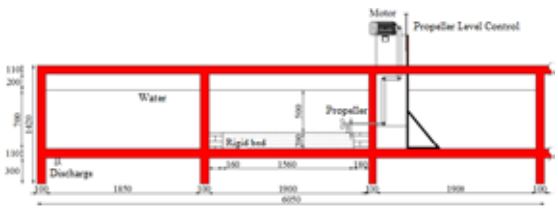

Figure 1 - Experimental set-up, Longitudinal cross-section (in mm).

There is a system to create the propeller jet inside the channel. The experiments were carried out in the case of a rigid bed. A water depth of 50 cm was created on the bed. The diameter of the propeller was D_p=100 mm. The propeller is located 10 cm above the bed. Three different propeller rotation speeds were used in the experiments (590, 670, 745 rpm). Velocity measurements were performed along the propeller axis in several sections at the downstream of the propeller (X=0.5-6D_p). Figure 2 shows the distribution of the axial velocity component in the flow field induced by the propeller jet flow for the X=D_p position at 590 rpm. As seen in the figure, for the axial velocity, the data clearly shows that a double-peak velocity distribution occurs near the propeller (X=D_p). A similar trend was observed at other propeller speeds. The results were in agreement with the studies in the literature.

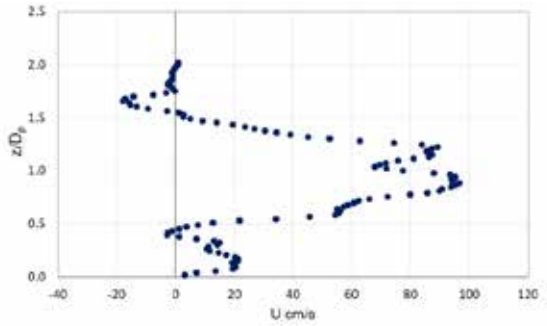

Figure 2 - Axial mean velocity profile acquired by PIV (X= Dp, 590 rpm)

ACKNOWLEDGMENTS

This study was supported by the Research Fund of the Yildiz Technical University, Turkey project number: FCD-2022-4734.

REFERENCES

Hsieh, S.C., Chiew, Y.M., Hong, J.H.; Cheng, N.S. (2013): 3-D Flow Measurements of a Swirling Jet Induced by a Propeller by Using PIV. In Proc. of the 35th IAHR World Cong., Chengdu, China, 8-13 September 2013; pp. 5141-5150.
Wei, M., Chiew, Y.M., Guan, D.W. (2018): Turbulent Flow Field of Propeller Jet around an Open-Type Quay, Journal of Coastal Research 85(sp1), 956-960,
Wei, M., Chiew, Y.M. (2018): Characteristics of propeller jet flow within developing scour holes around an open quay. J. Hydraul. Eng. 2018, 144(7), 04018040.
Wei, M., Cheng, N. S., Chiew, Y. M., Yang, F., (2019): Vortex Evolution within Propeller Induced Scour Hole around a Vertical Quay Wall, Water 2019, 11(8), 1538.

Roughness Factor of XblocPlus compared with single and double layer armour units

Tim Ruwiel[1], Pieter Bakker[1], Markus Muttray[1],
[1] Delta Marine Consultants, Gouda, The Netherlands

INTRODUCTION

Dimensions of coastal defence structures are frequently determined by overtopping requirements. Structures with a smooth armour layer may need e.g. a higher crest, a wider crest or a higher crown wall to prevent excessive overtopping. In order to enable designers of coastal structures to compare different types of armour units with regard to the expected overtopping, many different armour units were tested in a comparable test set-up during the European CLASH program in 2002-2004. Based on the CLASH tests, a roughness coefficient was concluded for the different armour units (Bruce et al., 2009).

In 2018 DMC introduced the XblocPlus armour unit. XblocPlus is a regularly placed armour unit with a very smooth appearance and a large porosity inside the armour layer. In order to obtain a comparable roughness coefficient, overtopping tests were performed in 2018 in the same test set-up as the CLASH tests. This resulted in a roughness coefficient of 0.45 (Reedijk et al., 2018).

In this paper further research into the overtopping behaviour of XblocPlus is presented. This is based on physical model tests where a comparison was made between XblocPlus, Xbloc -both in single layer- and Antifer cubes in double layer. The paper will describe the test set-up and the tests performed. It will compare the results for XblocPlus, Xbloc and Antifer cubes and it will relate this to the original CLASH test results for Xbloc and Antifer cubes. Furthermore, the new dataset will be compared with the 2018 dataset and both will be related to the CLASH test results for rock armour, Xbloc and Antifer cubes.

MOTIVATION FOR MODEL TESTS

The motivation for the recent overtopping tests were a seawall project in Africa for which the original design was made with 2m^3 Antifer cubes and where the contractor proposed to replace this by either 2m^3 Xbloc or 2m^3 XblocPlus. In order to demonstrate to the end client that the change to Xbloc or XblocPlus wouldn't lead to increased overtopping volumes, DMC performed these tests. The tests were performed with a CLASH test set-up in order to make it comparable to tests with other armour types. It is important to realise that the 2m^3 armour blocks chosen for a design wave height of the project of H_s = 3m only have a stability number of $H_s/\Delta D_n$ = 1.8.

MODEL SETUP

Physical model tests were performed in DMC's Wave Laboratory in Gouda (NL) in a wave flume (25 m long, 0.6 m wide, 1.0 m deep). The 2m^3 armour blocks were scaled geometrically in a 1:30 scale which resulted in a design wave height H_0 of 10cm. The CLASH cross-section (Figure 1) was applied where it is important to realise the following differences:

- a 1:100 foreshore slope was used whereas CLASH was based on a horizontal foreshore.
- In relation to the block sizes, the design wave height H_0 is smaller due to the fact that the size of the model blocks is chosen such that the stability number is close to the stability number $H_s/\Delta D_n$ =

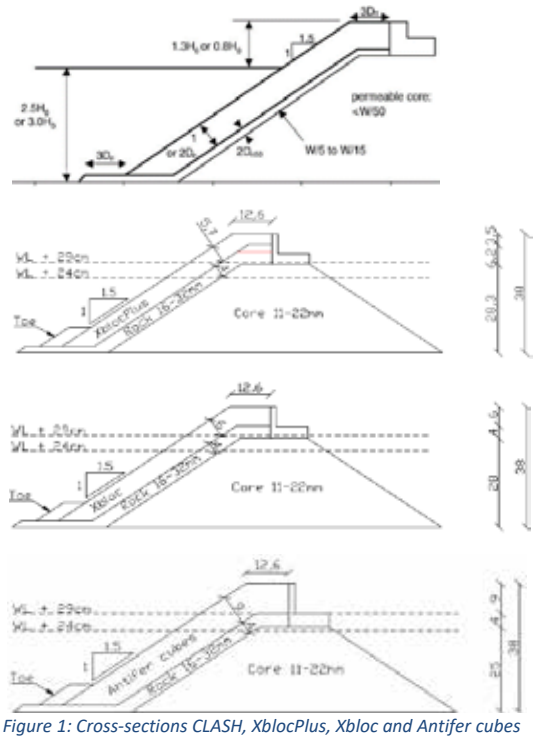

Figure 1: Cross-sections CLASH, XblocPlus, Xbloc and Antifer cubes

1.8 of the project. As a result of the relatively small stability values, the armour layer is thicker in relation to the waves than during the CLASH tests. Lower overtopping measurements were therefore expected prior to the tests.

The following conditions were tested:

- JONSWAP spectra with wave steepness $s_{0,p}$ = 0.02 and 0.04.
- Wave height H_s = 8.0 (0.8 H_0), 10.0 (1.0 H_0) and 12.0 cm (1.2 H_0)
- Test duration 1024s
- Water depth 24cm and 29cm – Freeboard 14cm and 9cm.

RESULTS 2020 OVERTOPPING TESTS

The measured overtopping rates for Antifer cube, Xbloc and XblocPlus are shown in Figure 2. Roughness coefficients were deduced from these results and are summarised in Table 1.

The following was found:

- Roughness coefficients for Xbloc and Antifer cube are slightly lower than earlier CLASH results (92% and 93% of the CLASH results).
- Based on the ratio between the 2020 tests and 1) the CLASH tests for Xbloc and Antifer cubes on the one hand, and 2) the roughness coefficient concluded from the 2020 tests for XblocPlus on the other hand, the 2018 roughness coefficient of 0.45 is confirmed.

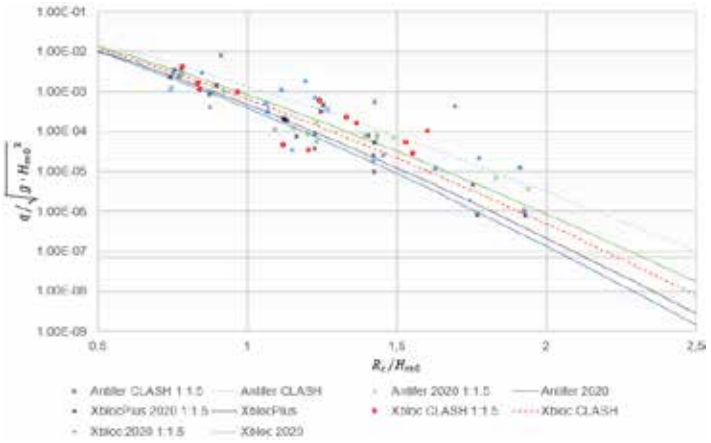

Figure 2: Wave overtopping Antifer cubes, Xbloc and XblocPlus

The lower overtopping rates are expected to be caused by the relation between the thickness of the armour layer and H_0, which was different in comparison to the CLASH tests. During the 2020 overtopping tests, the armour units were large in relation to the design wave height as this followed from the project specific block size and design wave.

	CLASH	Tests 2018	Tests 2020
Antifer cube	0.50		0.46
Xbloc	0.44		0.41
XblocPlus		0.45	0.42

Table 1: Overview roughness coefficients

CONCLUSIONS

The overtopping tests performed confirm the roughness factor for XblocPlus of 0.45 based on previous model tests in 2018.

In spite of the larger armour layer thickness, Antifer cubes lead to larger overtopping discharges.

REFERENCES

Bruce, T., Van der Meer, J. W., Franco, L., & Pearson, J. M. (2009). Overtopping performance of different armour units for rubble mound breakwaters. *Coastal Engineering*, *56*(2), 166-179.

Reedijk, B., Eggeling, T., Bakker, P., Jacobs, R., & Muttray, M. (2018). HYDRAULIC STABILITY AND OVERTOPPING PERFORMANCE OF A NEW TYPE OF REGULAR PLACED ARMOR UNIT. *Coastal Engineering Proceedings*, (36), 111-111.

ASSESSMENT OF 3D RECONSTRUCTION TECHNIQUES IN PHYSICAL MODELS

Rui Capitão, LNEC - National Laboratory for Civil Engineering, rcapitao@lnec.pt
Rute Lemos, LNEC - National Laboratory for Civil Engineering, rlemos@lnec.pt
Conceição J.E.M. Fortes, LNEC - National Laboratory for Civil Engineering, jfortes@lnec.pt
Ricardo Jónatas, FCT PhD Student, rjonatas@lnec.pt

ABSTRACT
The evaluation of damage progression caused by wave action on physical models of rubble-mound breakwaters can be accomplished through two types of methods: quantifying the movements and falls of the resistant armor elements (traditional methods) or determining the eroded volumes and depths between consecutive surveys of armor layers (more recent methods).

The latter approach involves non-intrusive surveys, utilizing photogrammetric techniques with RGB sensors, depth sensors based on the Time of Flight (ToF) methodology, and LiDAR (Light Detection And Ranging) laser scanning sensors. Depending on the survey conditions and the post-processing methodology of the acquired point clouds, these techniques enable the generation of three-dimensional surface models with varying degrees of accuracy. This research will employ the following sensors and 3D reconstruction techniques within this context:

a) Microsoft Kinect 2.0 depth, Infra-Red (IR) and RGB sensors, developed for the Microsoft Xbox game console, are handled to survey the 3D model at a constant distance of 2.0 m. The Microsoft Kinect Fusion software is utilized for the process, and post-processing is carried out using the Cloud Compare software.
b) The Microsoft Azure Kinect, an upgraded version of the previous, also incorporates depth, IR and RGB sensors but of a more refined, more accurate kind. Utilizing the Azure Kinect SDK development kit, surveys with this low-cost equipment involve swift scanning as the user moves across the designated area. Post-processing is carried out by employing a newly developed set of scripts being developed on the Github platform (Miranda *et al.*, 2022).
c) The iPhone 14 Pro smartphone that incorporates an RGB sensor. The survey involves capturing oblique photos from various angles and positions with significant overlap (+80%) around the physical model. The user moves across the model's area in both plan and altitude. The photogrammetric techniques are applied using the commercial (paid) software Metashape.
d) The same smartphone also features a low-cost LiDAR sensor that allows users to capture data while moving across the designated area covered by the model. This process is facilitated by the real-time instructions and control of the free version iOS 3dScanner application, which also handles post-processing. This is by far the least expensive and quicker alternative.

Among the various techniques available, point clouds can be generated and utilized in surface modeling, profile extraction, and eroded volume calculations (see Figure 1). However, the accuracy of the results and the convenience of implementation in a laboratory environment vary depending on the specific technique employed.

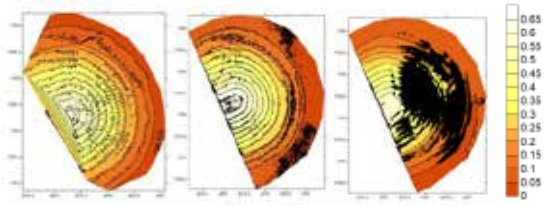

Figure 1 - Contour depths of a 3D model of a breakwater's head using Kinect+Fusion (left), iPhone+Metashape (center), and iPhone LiDAR+3dScanner (right) techniques.

These factors are strongly influenced by the equipment used, as well as the environmental conditions and survey techniques employed. Consequently, conducting a series of preliminary tests to determine the optimal parameters and environmental conditions for each technique is highly beneficial.

This paper aims to compare the effectiveness of traditional methods and more recent methods in evaluating damage caused by wave action on 3D models of rubble-mound breakwaters. Also, by comparing the results obtained from LiDAR scanning with those remaining, obtained using photogrammetric techniques will provide insight into the accuracy and efficiency of each method, as well as the potential advantages and disadvantages of using LiDAR technology in this context. Factors such as cost, ease of use, and suitability for different types of physical models could also be considered in this comparison. All these diverse techniques are applied to the physical model of the Lajes das Flores breakwater, located on the island of Flores, Azores, which is presently undergoing testing at LNEC. The performance, suitability, and usability of these techniques in assessing damage progression are comparatively evaluated. Furthermore, the advantages and disadvantages of each technique are identified, and a sensitivity analysis is presented for each one.

REFERENCES
Miranda, J.C. *et al.* (2022): AKFruitData: A dual software application for Azure Kinect cameras to acquire and extract informative data in yield tests performed in fruit orchard environments, Elsevier ScienceDirect SoftwareX 20 (2022) 101231. https://doi.org/10.1016/j.softx.2022.101231.

WAVE RUNUP AND OVERTOPPING ASSESSMENT BY USING VIDEO METHODOLOGIES IN PHYSICAL MODELS

Rute Lemos, LNEC - National Laboratory for Civil Engineering, rlemos@lnec.pt
Conceição J.E.M. Fortes, LNEC - National Laboratory for Civil Engineering, jfortes@lnec.pt
Ana Mendonça, LNEC - National Laboratory for Civil Engineering, amendonca@lnec.pt
Umberto Andriolo, University of Coimbra, uandriolo@mat.uc.p

ABSTRACT

One aspect of the design or the verification of the safety of ruble-mound breakwaters is related to the evaluation of wave runup and overtopping. In fact, those phenomena can put in danger the operations and activities that occur in the sheltered area protected by the breakwater or the breakwater itself. Moreover, due to climate change this issue is even more important since the predictable increase of frequency and magnitude of waves on those structures will contribute to the increase of runup, overtopping and flooding over them.

Physical modelling is one of the tools to help characterize wave runup and overtopping in maritime structures. Usually, the determination of wave runup is made by using resistive wave gauges along the breakwater slope while the evaluation of overtopping volumes (individual or total) is made by weighing the water overtopped with a scale that is collected in a reservoir installed on this scale.

Nowadays, non-intrusive methodologies for the assessment of those parameters are being used, due to their simplicity and low cost. Video cameras, Figure 1, constitute a good alternative to old methods; however, their performance depends essentially on the post-processing methodologies used.

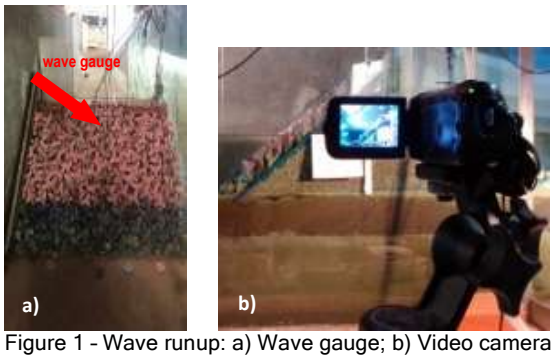

Figure 1 – Wave runup: a) Wave gauge; b) Video camera

At LNEC, promising results of wave runup parameters were obtained on 2D physical models by using a common video camera and following the methodology Timestack proposed by Andriolo (2022), Lemos et al. (2022). This methodology consists of the use of MATLAB algorithms that permit the extraction of frames from the video to be analyzed and from them the extraction of all pixels that are in a pre-defined path (transect). The definition of the transect on the slope of the breakwater allows estimating the wave runup along the slope.

In 3D models, the first steps are done to apply the same methodology, but some problems arise since the waves that reach the slope are not uniform and vary significantly over it due to wave direction.

Another development is the application of the Timestack methodology for the evaluation of overtopping, a phenomenon that results from the wave runup, when the water layer exceeds the crest of the structure. Indeed, using the same methodology, it is also possible to estimate the volume overtopped and the average overtopping flow rate, since the definition of a transect at the crest level allows estimating the thickness of the water layers resulting from the overtopping.

The present paper presents the application of the Timestack methodology done so far, in the evaluation of: wave runup in 2D and 3D physical tests of Ericeira and Leixões breakwaters and in the determination of overtopping volumes in 2D models for Peniche breakwater. In the first case, the video-derived statistical parameters of wave runup (Rumax, Rumin, Rumed e Ru2%) are compared with the corresponded ones obtained with resistive wave gauges, while in the second case, the total water volume and the average overtopping flow rate from video data is compared with the one collected by a reservoir. Those cases will illustrate the advantages and drawbacks associated with Timestack methodology.

ACKNOWLEDGEMENTS
This work was carried out within the scope of the projects: LIFE-GARACHICO (Project LIFE20 CCA/ES/001641) and C2IMPRESS (Horizon Europa, grant agreement N.º 101074004).

REFERENCES

Andriolo (2022), MATLAB programs for the video analysis of wave run-up measurements on a breakwater in a laboratory flume, Bsafe4sea project report.

Lemos, R., Fonte, R., Fortes, C.J.E.M., Andríolo, U., Rito, J. (2022). Wave runup determinaDeterminação do espraiamento em quebra-mares de talude através da metodologia timestack e através de sonda resistiva. uma análise comparativa. XXV ENMC, XIII ECTM, 9º MCSul e IX SEMENGO, 19-21 october, Online.

THE LABORATORY APPLICATION OF THE DIGITAL PHOTOGRAMMETRY FOR MEASURING ROCK SLOPE DAMAGE ON RUBBLE MOUND BREAKWATER

Stefano Marino, Dept. of Civil, Environmental, Building Engineering and Chemistry, Polytechnic University of Bari (Bari, Italy), stefano.marino@poliba.it
Rosella Alessia Galantucci, Dept. of Civil, Environmental, Building Engineering and Chemistry, Polytechnic University of Bari (Bari, Italy), rosella.galantucci@poliba.it
Leonardo Damiani, Dept. of Civil, Environmental, Building Engineering and Chemistry, Polytechnic University of Bari (Bari, Italy), leonardo.damiani@poliba.it
Alessandra Saponieri, Dept. of Engineering for Innovation, University of Salento, (Lecce, Italy) alessandra.saponieri@unisalento.it

INTRODUCTION

Rubble mound breakwaters are counted among the most widespread and explored coastal defence structures. Through the years, many research activities focused on the investigation of the interactions of waves with such structures by carrying out experimental campaigns in laboratory facilities.

As far as the hydraulic stability and the related damage level of a breakwater is concerned, different laboratory techniques can be used, among which, the most consolidated one exploits the laser profiling system, with costly and time-consuming procedures.

Hereafter an innovative method, based on photogrammetry, for the measurement of the damage of rock slope structures (i.e. depth and extension of the damaged area) is presented. The methodology has been tested and validated during an experimental campaign, carried out on a 2D-physical scaled model of a rubble mound breakwater at the EUMER Laboratory (University of Salento, Lecce, Italy).The experimental activities aimed at evaluating the hydraulic stability of the breakwater under different water conditions (ranging from intermediate to shallow, Marino (2022)). The retrieved Photogrammetric outputs have been compared with the laser derived profiles, under different structures layouts and hydrodynamic conditions. Results have proven to be accurate with a relative error lower than 5%, and above all with time and cost-effective equipment and simple acquisition and processing procedures

PHOTOGRAMMETRIC MEASUREMENT SYSTEM

The digital acquisitions have been executed to collect reality-based 3D data (point clouds) of the physical model, before and after each wave attack. Images of the physical model are gathered from specific camera locations. Each scan is of 21-23 photos to acquire the entire structure in both $x-$ and $y-$ directions. The equipment entails a simple, easy-to-use and cost effective instrumentation, including mainly a bridge digital camera, Canon PowerShot SX410 IS, with CCD 1/2,3 sensor with a resolution of 5152 px X 2896 px and a zoom lens (24 mm-960 mm), installed on a tripod support and six coded targets of 3D known coordinate placed in specific locations, to assemble landmarks for photogrammetric model scaling as well as orientation.

RESULTS

The digital acquisitions yielded reality-based data of the physical model in the form of point clouds, before and after the execution of each test, enabling the reconstruction and analysis of 2D/3D outputs, corresponding to transversal profiles of the structure, from which the temporal evolution of the structure armour layer under wave action have been evaluated and the damage extension affecting the rock slope have been quantified. Among various existing methods to evaluate 3D changing features the deviation between aligned 3D data has been computed by means of Cloud-to-cloud (C2C), which has proven to be the 'simplest and fastest direct 3D comparison method of point clouds' Girardeau-Montaut (2005). The results can be evaluated either as absolute distances or *xyz* displacements, visualized through 3D deviation maps as the one depicted in Figure1.

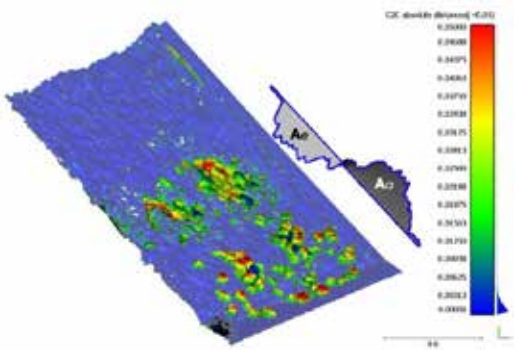

Figure 1 - Deviation map reporting both absolute and distances between pre and post corresponding points.

In conclusion, the effectiveness of the proposed method has been verified, for the quantification of both 2D and 3D eroded and accreted areas. This approach supplies reliable data, in terms of quality, accuracy and repeatability of measurements, with readily available, easy-to-use and cost-effective instrumentation.

REFERENCES

Lague D., Brodu N., Leroux J., Accurate 3D comparison of complex topography with terrestrial laser scanner: Application to the Rangitikei canyon (NZ), ISPRS J. Photogramm. Remote Sens. 82 (2013) 10-26.

Marino S., Scaravaglione G., Francone A., Valentini N., Saponieri A., Damiani L., Van Gent M.R., Tomasicchio G.R., Laboratory investigation on armour stability for extremely shallow water conditions, in: Proceedings of the 39th IAHR World Congress, 2022.

UNCERTAINTIES IN ROCK-ARMORED BREAKWATERS STABILITY LABORATORY DATA

Giulio Scaravaglione, Polytechnic of Bari, giulio.scaravaglione@poliba.it
Jeffrey A. Melby, U.S. Army Engineer Research and Development Center, jeffrey.a.melby@usace.army.mil
Giuseppe R. Tomasicchio, University of Salento, giuseppe.tomasicchio@unisalento.it
Leonardo Damiani, Polytechnic of Bari, leonardo.damiani@poliba.it

INTRODUCTION

Coastal rubble mound armor stability has historically been based on empirical equations relating armor stone movement resistance to wave-induced forces. These empirical equations are developed primarily from small-scale laboratory studies and show considerable uncertainty. While new relations have been introduced to expand ranges of application, little progress has been made in several decades to decrease equations uncertainty. Stability uncertainty is primarily due to intrinsic aleatory uncertainty related to the stochastic nature of waves, stone geometry, and inter-stone contacts/interlocking as well as epistemic uncertainty related to knowledge limitations. Here, we refer to aleatory uncertainty as irreducible while epistemic is reducible. Effects of aleatory uncertainty in hydraulic stability have often been assumed dominant over epistemic uncertainty. Nevertheless, the magnitude of both contributions has yet to be explicitly quantified to assess the validity of this assumption. Modern probabilistic design and simulation provides strong motivation for an improved understanding of uncertainty. A clear understanding of the relative magnitudes of epistemic and aleatory uncertainty could better focus studies to improve physics research. As a first step, the present study investigates the influence of hydrodynamic uncertainty from laboratory wave and water level measurements on the predictive models using a 1-D Boussinesq numerical model.

MAIN SOURCES OF UNCERTAINTY

Wave height is the dominant parameter in armor stability and damage formulae so related uncertainties are critically important. These uncertainties enter from observations and from limited parametric characterizations. Uncertainty inherent in the wave observations can be attributed to wave generation, measurements, reflection quantification methods, how and where the incident waves are observed, wave analysis procedures, and other phenomena. Wave uncertainty is typically more pronounced in shallow water conditions with wide surf zones (Hughes (1993)) because of linear wave theory methods used to resolve incident and reflected waves. Laboratory methods are relatively more influential under these conditions. Mansard and Funke (1987) conducted the same experiment at 9 laboratories with the scope to evaluate the difference in test results caused by the different experimental conditions. They found high variability in the bulk wave parameters, significantly affecting the wave-structure parameter relationships in the stability design formulae.

METHODOLOGY

A 1-D fully nonlinear Boussinesq numerical model (COULWAVE (Lynett et al. (2004)) has been set up to accurately reproduce the incident and reflected wave conditions at the toe of the breakwater which were run to obtain the stone stability dataset. An initial phase of convergence and calibration of the numerical wave tank has been conducted. Wave parameters have been matched near the wave generator and near the structure toe. Various methodologies for wave analysis used across laboratories have been analyzed including testing with and without structure in place, frequency vs time domain, variations in reflected wave analysis, and single gauge frequency analysis. In addition, contributions spanning the entire spectrum were assessed including infragravity frequencies.

RESULTS AND CONCLUSION

Initial results show considerable systematic differences when comparing studies form different laboratories and different time periods. Typical incident-reflected wave analysis using linear wave theory produces significant bias in shallow water and this bias increases with decreasing depth with a significant proportion of incident wave energy being attributed to reflection (Figure1). Variations from one incident-reflected analysis method to another are relatively less influential. Studies that utilize wave measurements without the structure in place but that utilize incident and reflected wave analysis will have relatively less bias than those with structure in place.

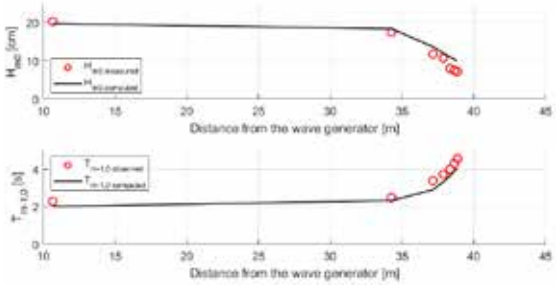

Figure 1 - Lab measured and numerical computed cross-shore variations of H_{m0} and $T_{m-1,0}$ along the wave flume.

REFERENCES

Hughes (1993): Physical models and laboratory techniques, Coastal engineering, World Scientific, vol. 7.
Lynett, Liu, Sitanggang, Kim (2008): Modeling Wave Generation, Evolution, and Interaction with Depth-Integrated, Dispersive Wave equations COULWAVE Code Manual Cornell University Long and Intermediate Wave Modelling Package v. 2.0.
Mansard, Funke (1987): Experimental and analytical techniques in wave dynamics, a comparative study. In IAHR Seminar on Wave Analysis and Generation in Laboratory Basins, pp. 91-116.

DAMAGE PROGRESSION OF A RUBBLE MOUND BREAKWATER WITH ACCROPODES II AND ACCROBERM I ARMOUR UNITS USING IMAGE-BASED APPROACHES

Elisa Leone, University of Salento, elisa.leone@unisalento.it
Alberica Brancasi, University of Salento, alberica.brancasi@unisalento.it
Antonio Francone, University of Salento, antonio.francone@unisalento.it
Agostino Lauria, University of Salento, agostino.lauria@unisalento.it
Felice D'Alessandro, University of Milan, felice.dalessandro@unimi.it
Giuseppe R. Tomasicchio, University of Salento, giuseppe.tomasicchio@unisalento.it

INTRODUCTION

Rubble mound breakwaters are crucial coastal structures designed to dissipate the energy of incoming waves and protect ports and coastal zones from wave-induced erosion. The unique shape of the Accropode II units allows them to fit tightly together, creating a robust and interconnected structure, preventing the shifting and the dislodgment of individual units by wave action, reducing the risk of damage or failure. Studying the behavior of a rubble mound breakwater with Accropode II units can help in determining its ability to withstand different wave conditions and ensure its long-term functionality. In fact, over time, wave forces and other environmental factors can cause damage to the breakwater, such as displacement or cracking of Accropode II units, erosion or scouring around the structure; understanding the behavior under extreme wave attacks and damage progression of the armour layer is crucial for maintenance and repair purposes. By conducting studies on damage progression and failure modes, engineers and researchers can gain insights into the vulnerabilities and limitations of this kind of structures and identify the specific conditions or mechanisms that contribute to breakwater failures.

LABORATORY INVESTIGATION

The present study focuses on an experimental investigation conducted in the 3D wave basin located at the EUMER lab of the University of Salento. A down-scaled physical model of a breakwater with armour layer and toe composed of Accropodes II and Accroberms I has been constructed in the wave basin, replicating realistic conditions, thus simulating a range of potential extreme scenarios. The research aims first to assess the stability of the down-scaled rubble mound under different water levels and wave conditions and identify the primary mechanisms of armour units instability and damage development when the breakwater armor layer is exposed to depth limited breaking waves. Figure 1 shows the physical model in the wave basin.

Figure 1 - Physical model of the breakwater

CONTENT OF THE FULL PAPER

In the full paper, the experimental investigation is described in detail and the progression of the damage of rocks and armour units over time is evaluated using remote technique (Marino et al., 2023), based on the use of Unmanned Aerial Vehicle (UAV) equipped with a high-resolution camera. Advanced image processing techniques are employed to extract erosion and accumulation patterns. By comparing the point clouds gained by the UAV images analysis at the beginning and after each test, the temporal evolution of the damage is quantified by means of the damage parameter, $S = A_e/D_{n50}^2$ where A_e is the eroded area and D_{n50} in the nominal diameter of the armour units and rocks (Van del Meer, 1987), as well as the eroded and accumulated volume, V, in both 2D and 3D. Figure 2 shows an example of the erosion-accretion map of the breakwater, where red and blue indicate the eroded and accumulated volumes, respectively. Results are also compared with empirical formulae available in literature (e.g., Melby and Kobayashi, 1998).

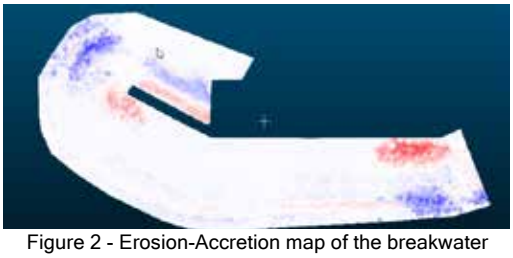

Figure 2 - Erosion-Accretion map of the breakwater

The analysis reveals significant insights into the damage progression, allowing the identification of areas most strained and vulnerable to unit dislodgement and sections prone to scouring. These findings contribute to a better understanding of the breakwater resistance and provide valuable input for optimizing the design and maintenance of similar coastal protection structures. Moreover, the experimental investigation demonstrates the potential of using UAV photo images as a valuable laboratory tool for monitoring and analyzing the damage progression of rubble mound breakwaters in non-intrusive and cost-effective way.

REFERENCES

Marino, Galantucci, Saponieri (2023). Measuring rock slope damage on rubble mound breakwater through digital photogrammetry. Measurement, 211, 112656.
Van der Meer (1987): Stability of breakwater armour layers - design formulae, Coast. Eng. 11 (3) (1987) 219-239.
Melby, Kobayashi (1998): Progression and variability of damage on rubble mound breakwaters, J. of Waterway, Port, Coastal, and Ocean Eng., 124(6), 286-294.

LABORATORY OBSERVATIONS OF TSUNAMI WAVE PROPAGATION IN A MEANDERING CHANNEL

H. Anıl Arı Güner, Yıldız Technical University, aari@yildiz.edu.tr
Yalçın Yüksel, Yıldız Technical University, yuksel@yildiz.edu.tr
Mehmet Öztürk, Yıldız Technical University, meozturk@yildiz.edu.tr
Cihan Şahin, Yıldız Technical University, cisahin@yildiz.edu.tr
G. Güney Doğan, Middle East Technical University, gguneydogan@gmail.com
Cem Yılmazer, Yıldız Technical University, cemyilmazer92@gmail.com
Barış Aydın, Yıldız Technical University, aydin.baris178@gmail.com
Onur Altıntaş, Yıldız Technical University, onuraltintas2323@gmail.com
Merve Ayaz, Yıldız Technical University, ayazmerve1@hotmail.com
Şükrü Ersoy, Yıldız Technical University, sersoy@yildiz.edu.tr
Ahmet Cevdet Yalçıner, Middle East Technical University, yalciner@metu.edu.tr

INTRODUCTION

When tsunami waves reach the coastal areas, they cause strong currents and wave amplification in the shallow water and also cause damage and inundation at the low-elevation nearshore residential and agricultural areas. In addition to these effects, tsunamis entering from the mouth of the rivers that discharge into the sea can propagate in the opposite direction towards the upstream of the rivers causing inundation and damage in the surrounding areas at the river banks. Field observations of tsunamis show that tsunami waves travel faster and further along coastal rivers than inland mainly due to low-elevation and water existence (in wet condition), reduced obstructions, meanders and converging boundaries. The interaction between the tsunami propagation and the countercurrent along the meandering stream and varying cross-sectional area and geometries along the stream generates a complex problem. To that end, this study investigates the problem by using physical modelling approaches to solve the tsunami wave motion along a meandering stream.

EXPERIMENTAL SETUP

The propagation of a tsunami wave in a meandering channel is studied in the Hydraulic and Coastal Engineering Laboratory at the Yildiz Technical University to stimulate the tsunami behavior along such channels. The waves are generated by a tsunami wave generator located downstream of the channel (Fig.1). The experiments were carried out in a meandering channel, 32.88 m in length, 0.90 m in depth, and 0.60 m in width, with an aluminum bottom and plexiglass sidewalls. It is composed of three sections: a straight part followed by two different curved channels (Fig. 1). The major problem with the physical modelling of tsunami waves is the generation of the full length of the wave and N-waves which are formed by a depression wave followed or preceded by an elevation wave. Conventional flap or piston paddle generators simply do not have sufficient stroke to reproduce the entire wavelength and depression wave (Rosetto et al., 2011). In this study, a pneumatic type tsunami generator was developed which is capable of generating N-wave within a physical model.

METHODOLOGY

The transformation of tsunami waves along the channel is investigated under different hydraulic conditions which represent the dry and wet conditions. Resistance-type wave gauges were used to measure surface elevation (at 100 Hz) at 5 sections along the channel. Flow velocities were measured at the same locations, using an Acoustic Doppler Velocimeter (ADV), at 200 Hz. To produce steady flow, the channel is equipped with a water supply mechanism (maximum discharge of 0.05 m^3/s) at the upstream end. Various discharges and water depths were tested. The experiments were performed under the still-water condition for comparison with the results of wave height under conditions with the flow.

Figure 1 - Top view (drawing) of the meandering channel and picture of the tsunami generator

ACKNOWLEDGEMENT

This research was supported by TUBITAK (the Scientific and Technological Research Council of Turkey) as part of a research project (128M858).

REFERENCES

Tiziana Rossetto, William Allsop, Ingrid Charvet, David I. Robinson (2011): Physical modelling of tsunami using a new pneumatic wave generator, Coastal Engineering, vol. 58, Issue 6, pp. 517-527,

SENARIO-BASED COASTAL FLOOD RISK ASSESSMENT CONSIDERING THE FAILURE OF SHORE PROTECTION FACILITY

Kanta Okamoto, Coastal, Marine and Disaster Prevention Department, National Institute for Land and Infrastructure Management, okamoto-k92y2@mlit.go.jp
Kazuhiko Honda, Coastal, Marine and Disaster Prevention Department, National Institute for Land and Infrastructure Management, honda-k852a@mlit.go.jp

INTRODUCTION

Japan has a high density of population and property along the coastal area. Therefore, assessing flood risk due to storm surges and high waves is important. Although the assessment is an area of active research (Tsujita et al., 2016; Hisamatsu et al., 2018), more work needs to be done on it with considering the failure of shore protection facilities (e.g., Wadey et al., 2012). The failure of shore protection facilities can severely damage coastal areas. Typhoon Faxai in 2019 caused storm surge and wave disasters on the coast of Tokyo Bays (Suzuki et al., 2020). In this event, a shore protection facility failed due to wave load exceeding its design condition, which enhanced the damage to the areas behind it. In this study, we assessed the flood risk due to storm surges and high waves induced by typhoons on some coastal areas around Tokyo Bay as a case study for assessing the flood risk with considering the failure of shore protection facilities.

FLOOD RISK ASSESSMENT

The assessment of the flood risk consists of hazard assessment and estimating the amount of damage for the flood. Floods due to typhoons for 1,000 years are estimated for hazard assessment. Typhoons for 1,000 years are generated by a stochastic typhoon model (Umeda et al., 2019). The wave overtopping and overflow over a shore protection facility are calculated with waves and storm surges by wave and storm surge forecasting for typhoons. At the same time, the wave load acting on the facility is calculated with them. When the wave load exceeds a design condition of the facility, the facility fails, and then it is reflected in the wave overtopping and overflow calculations. The inundation areas and depth are estimated by the level fill method with the total amount of the wave overtopping and wave overflow during a typhoon. Loss on assets in the hinterland is estimated with the loss function, which represents loss and the total amount of wave overtopping and wave overflow.

Fig. 1 Coastal areas for the flood risk assessment.

CASE STUDY

In this study, we assessed the flood risk in coastal areas behind a seawall in the Yokohama Port on the western side of Tokyo Bay (Fig. 1). Direct loss in the areas was predicted. The flood risk was assessed using an event curve representing loss and annual exceedance probability. Fig. 2 shows the event curves of flood in the areas due to typhoons with and without considering the facility's failure. As shown in Fig. 2, the flood risk was different depending on the consideration of the facility's failure. This result indicates that considering the facility's failure is essential to assess the flood risk appropriately.

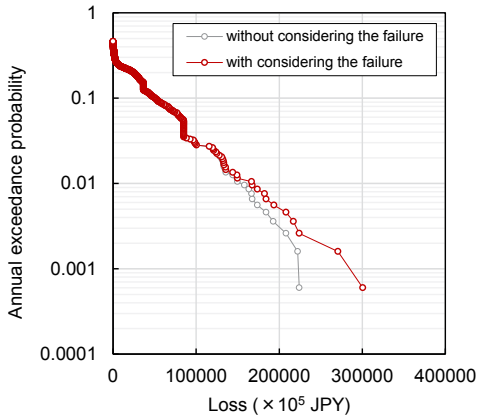

Fig. 2 Event curve of floods due to typhoons.

REFERENCES

Hisamatsu, R, KIM, S, and Tabeta, S (2018). "Estimation of storm surge loss along the Tokyo Bay coast by stochastic approach." *Ser.B1, Hydraulic Eng.*, JSCE, 74, 5, 1393-1398. (In Japanese)
Suzuki, T and 11 co-authors (2020). "Post-event survey of locally concentrated disaster due to 2019 Typhoon Faxai along the western shore of Tokyo Bay, Japan," *Coastal Eng J*, 62, 2, 146-158.
Tsujita, D, Yasuda, T, Shinohara, M, Mori, N, and Mase, H (2016). "Evaluation of aggregate loss by storm surge considering simultaneous damage occurrence in multiple areas," *Ser.B2, Coastal Eng.*, JSCE, 72, 2, 1639-1644. (In Japanese)
Umeda, J, Nakajo, S, and Mori, N (2019). "Development of global stochastic tropical cyclone model by using large ensemble GCM simulation data (d4PDF)," *Ser.B2, Coastal Eng.*, JSCE, 75, 2, 1195-1200. (In Japanese)
Wadey, M.P, Nicholls, R.J, Hutton, C (2012). "Coastal flooding in the Solent: An integrated analysis of defences and inundation," *Water*, 4, 430-459.

A TOP-DOWN APPROACH FOR THE ASSESSMENT OF COASTAL INUNDATION RISK IN THE SAN ANDRÉS ISLAND (CARIBBEAN SEA)

Francesco De Leo, University of Genoa, francesco.deleo@unige.it
Alejandro Cáceres-Euse, University of Toulon, alejandro.caceres-euse@univ-tln.fr
Pau Luque, Instituto Mediterraneo de Estudios Avanzados, pau.luque@uib.es
Marta Marcos, Instituto Mediterraneo de Estudios Avanzados, marta.marcos@uib.es
Alejandro Orfila, Instituto Mediterraneo de Estudios Avanzados, a.orfila@uib.es
Ismael Hernández-Carrasco, Balearic Islands Coastal Observing and Forecasting System, ismaelhe@gmail.com

STUDY OVERVIEW

We present a novel methodology to assess the risk of coastal inundation in the San Andrés Island (Colombia; Caribbean Sea), which is experiencing episodic storm waves that threaten benthic communities on coral reefs, beach morphology and sediment transport processes (Geister & Diaz, 2007). The workflow is organized as follows: first, wind and wave conditions derived from on 60 years long met-ocean reanalysis (Orejarena-Rondón et al., 2021) in the area are aggregated on a monthly base. Starting from these data, a reduced number of significant states is extracted through the Self-Organizing-Map (SOM) algorithm, an unsupervised learning neural network particularly suited to select patterns from large dataset. SOM are used on H_s snapshot with the maximum aggregation value per month as to characterize extreme wave events. To highlight the influence of seasonal and inter-annual variability on wave dynamics, the continuous wavelet transforms, and the cross-wavelet transform are employed. The resulting SOM patterns depict the maps that best represent the input data, determining regions with similar H_s variability and the seasonal frequency of occurrence of each pattern (Figure 1). The selected maps are next used to downscale waves to the investigated site through SWAN, leveraging an unstructured computational grid that allows to refine the resolution at the shallow reef flat surrounding the island. Resulting wave data are extracted along the 100 m depth isoline (Figure 2). Based on such forcing, the X-Beach model is finally employed to assess the potential flooding area along the San Andrés Island, yielding the first time-dependent flood risk analysis for the area.

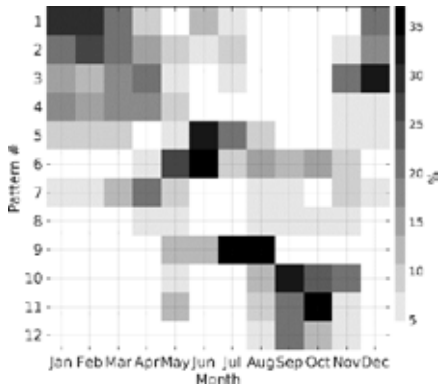

Figure 1. Seasonal frequency of the SOM maps extracted.

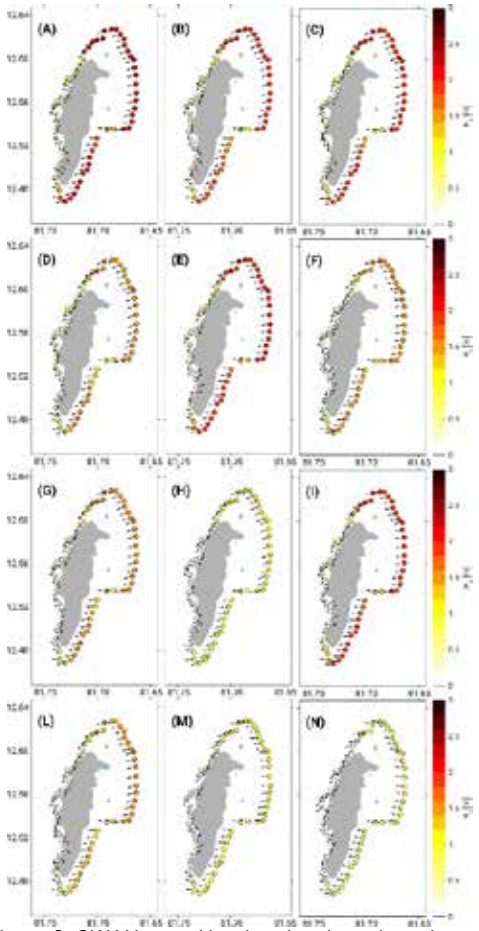

Figure 2. SWAN runs: H_s related to the selected maps around San Andrés at ≈100 m water depth.

REFERENCES

Geister, Diaz (2007). Reef environments and geology of an Oceanic Archipelago: San Andrés, Old Providence and Santa Catalina (Caribbean Sea, Colombia) with Field Guide. Boletın geológico.

Orejarena-Rondón, Orfila, Restrepo, Ramos, Hernandez-Carrasco (2021). A 60 year wave hindcast dataset in the Caribbean Sea. Data in Brief, 37, 107153.

ON THE PROBABILITY OF OCCURRENCE OF COMPOUND STORM WAVES AND HEAVY RAINFALL EVENTS IN THE NW MEDITERRANEAN

Maria Aguilera Vidal, Marc Sanuy, Maria Isabel Ortego, José A Jiménez
Universidad Politénica de Catalunya, Barcelona, maria.aguilera.vidal@upc.edu, marc.sanuy@upc.edu, ma.isabel.ortego@upc.edu, jose.jimenez@upc.edu

One of the intrinsic characteristics of floods in coastal areas is that they can be induced by different climatic drivers of different origin that often act interconnected. Under these conditions, although risk assessments usually consider the impact of marine and climate hazards individually, they must be considered as the result of compounding events. In this context, the W Mediterranean has been identified as one of the hotspots along the European coasts in terms of compound coastal flooding (Bevacqua et al. 2019). Despite this, detailed analysis of the structure of these events throughout this area is relatively scarce, with most of the existing studies being part of large-scale analysis that do not necessarily reflect well the local risk characteristics or the implications for risk management.

The Catalan coast (Spanish NW Mediterranean) is one of these hotspots where it is relatively frequent the occurrence of compound extreme events composed by heavy rainfall episodes together coastal storms (Sanuy et al. 2021). In this work, we complete their analysis in the area by characterizing the probability of occurrence of extreme events composed of heavy rainfall and wave storms. This is done from the perspective of risk management and for that, we consider two types of compound events according to the classification of Zscheischler et al. (2020): (i) *multivariate events* in which both components act simultaneously in the same location, increasing/potentiating the impact locally in the places where both hazards concur; and (ii) *spatially compound* in which they act simultaneously but in different locations, distributing the impact throughout the territory due to the simultaneous occurrence in remote places. Thus, for risk management services, both types of events are of interest because they have to manage response and emergency services differently, and also because the consequences of their impact will be different due to the existing spatial variation in exposure and vulnerability throughout the territory. In this sense, although these events occur in the same territory and under the same climatic forcing, their probability of occurrence will be different.

To this end, we have identified the two types of compound heavy-rainfall and coastal storm events in the Catalan coast during the last decades years by analyzing a set of more than 50 automatic weather stations distributed along the coastal basins and a set of wave node points located in front of each drainage basin along the coast. Extreme events were identified individually in terms of daily precipitation (P24) and Hs and wave power for rain and wave storms respectively. The presence of each type of compound event was done locally for each basin to identify multivariate, and increasing the area to consider simultaneous but at remote location events. Fig 1 shows an example of the evolution of the number of both type of compound events identified in the north half of the Catalan coast (about 200 km long).

The probability analysis to be presented includes: (i) the marginal distributions of rainstorms and wave storms; and most importantly, (ii) the joint distribution of both type of compound events (multivariate and spatially-compound) by using copulas. To this end, different classes of copulas are tested to identify the best type characterizing the analyzed compound events.

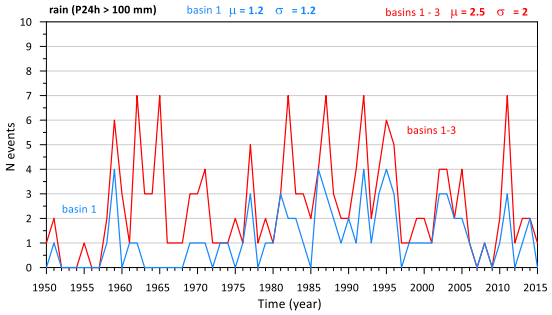

Fig. 1 - Variation of the occurrence of compound events when considering multivariate (basin 1) or multivariate and spatially compound (basins 1-3).

ACKNOWLEDGEMENTS
This work was done within the *C3RiskMed* project (PID2020-113638RB-C21, AEI/10.13039/501100011033).

REFERENCES

Bevacqua et al. (2019): Higher probability of compound flooding from precipitation and storm surge in Europe under anthropogenic climate change. *Science advances*, 5(9), eaaw5531.
Sanuy, Rigo, Jiménez, Llasat (2021): Classifying compound coastal storm and heavy rainfall events in the north-western Spanish Mediterranean, *Hydrol. Earth Syst. Sci.*, 25, 3759-3781.
Zscheischler et al. (2020): A typology of compound weather and climate events, *Nat. Rev. Earth Environ.*, 1, 333-347.

CHARACTERIZATION OF COASTAL EROSION ASSOCIATED TO TROPICAL STORMS AND HURRICANES IN MARTINIQUE, LESSER ANTILLES

Nico Valentini, BRGM-University of Montpellier, n.valentini@brgm.fr
Clement Bouvier, BRGM Martinique, c.bouvier@brgm.fr

INTRODUCTION

Small islands in Lesser Antilles are particularly vulnerable to coastal erosion and flooding due to its exposure to tropical storms and hurricanes (Chenoweth and Divine, 2008). Such events generate energetics waves and high water levels that can drive brutal changes on shoreline and are therefore an important component of the long-term coastline evolution (Harley et al., 2022).
In Martinique, the links between extreme events and coastal erosion are still poorly documented while shoreline retreat projections fundamentally rely on a robust quantitative understanding of sediment balance, including short-term sediment contributions associated to extreme events. Therefore, a better understanding of coastal erosion caused by tropical storms and hurricanes is essential for Martinique and could be a first step towards a larger-scale evaluation of coastal storm hazards in the Caribbean.

METHOD

Based on historical observations collected after storms, a new database referencing the hydrodynamic conditions and the associated impacts in terms of coastal erosion has been set up at the scale of Martinique.
To better understand and anticipate the impacts of extreme events on shoreline, we build an offline-coupling Xbeach model (Roelvink et al., 2010) at five different beaches in Martinique (Figure 1). For each location, the morphological model was forced by a 100-years return period event that have been estimated through a probability analysis from a 685-synthetic cyclones database (Wada et al., 2022; Rohmer et al., 2023). Waves have been propagated offshore to the boundary of the morphological grid using the SWAN wave model (Booij, 1999) on an unstructured mesh with a resolution ranging from 1000 m offshore, to 25 m nearshore.

RESULTS

An efficient use of scripts to transfer simulated extreme waves and water levels conditions to morphological models has been implemented at the five locations (Figure 1). The successful application of this approach was demonstrated through the hindcasting of hurricanes Maria and Fiona where the resulting storm-driven morphological evolutions were found to be satisfactory comparing with historical observations.
Simulations of the morphological evolution at the five high-stakes sectors for a 100-year return period event will be presented at the conference providing a better understanding of the impact of extreme events on shoreline evolution.

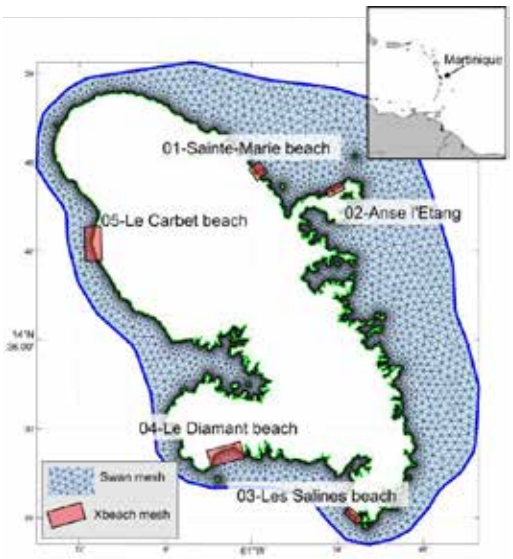

Figure 1 : Large-scale SWAN unstructured mesh with five coastal sectors which were further used for the Xbeach computation.

REFERENCES

Chenoweth, M., & Divine, D. (2008). A document-based 318-year record of tropical cyclones in the Lesser Antilles, 1690-2007. Geochemistry, Geophysics, Geosystems, 9(8).
Harley, M. D., et al. (2022). Single extreme storm sequence can offset decades of shoreline retreat projected to result from sea-level rise. Communications Earth & Environment, 3(1), 112.
Roelvink, et al. (2010). XBeach model description and manual. Unesco-IHE Institute for Water Education, Deltares and Delft University of Tecnhology. Report June, 21, 2010.
Wada, R., et al (2022). Statistical estimation of spatial wave extremes for tropical cyclones from small data samples: validation of the STM-E approach using long-term synthetic cyclone data for the Caribbean Sea. Natural Hazards and Earth System Sciences, 22(2), 431-444.
Rohmer J., Flippini A. and Pedreros R. (2023) "Combining machine learning predictions and numerical simulation results for the extreme value analysis of cyclone-induced wave heights - Application in Guadeloupe", submitted to Ocean Modelling.
Booij, N.; Ris, R.C.; Holthuijsen, L.H. A third-generation wave model for coastal regions: 1. Model 546 description and validation. J. Geophys. Res. Ocean. 1999, 104, 7649-7666.

EXPERIMENTAL AND NUMERICAL INVESTIGATION OF A FLOATING OFFSHORE WIND TURBINE PLATFORM

Umutcan Inal, umutcan.inal@yildiz.edu.tr, M.Utku Ogur, utku.ogur@std.yildiz.edu.tr
Yalcin Yuksel, yalcinyksl@gmail.com, Ferdi Cakici, fcakici@yildiz.edu.tr, Cihan Sahin, cihansahin81@gmail.com
Yildiz Technical University
Serdar Beji, sbeji@itu.edu.tr
İstanbul Technical University

INTRODUCTION

Wind energy is becoming an appreciable contribution to the solution of world's climate change and energy crisis. Offshore areas, with their abundant wind resources, are ideal locations for turbine installations. Although the usage and development of renewable energy production devices such as floating offshore wind turbines (FOWT) are gaining impetus, sufficient experimental and prototype data on the characteristics and reliability of FOWTs are lacking. The present study, as an attempt to contribute to this problem, focuses on the experimental and numerical simulation of a newly designed floating wind turbine platform.

MATERIALS AND METHODS

A 1:50-scale model platform was tested to observe its motion characteristics in waves in the wave basin at the hydrodynamic research laboratory of Yildiz Technical University. The platform consists of three cone-shaped legs, each placed on a circular heave plate. A main shaft in the middle of the platform is installed as the carrier tower of a turbine. The main shaft, buoyancy legs, and heave plates are all connected by cross braces (Figure 1). The first set of experiments was conducted for determining the stability parameters and natural periods at still water for pitch motion and three different drafts: 165 mm, 275 mm, and 435 mm. The results of these free motion tests established the natural periods of motion, damping, and mooring tension forces of the floating platform. Free decay motion CFD simulations of the platform were also performed for the above-mentioned drafts and validated against the corresponding experimental measurements. The second set of experiments was conducted in incident regular waves for the platform. The wave basin is equipped with a forty-eight-pedal piston-type wave generator, which can generate regular or irregular, unidirectional or multidirectional waves. An active device damps the reflected wave energy. Rotation modes (yaw, pitch, and roll) of the floating model were measured by using an IMU (inertial measurement unit) device while displacements (surge, sway, and heave) were measured via a camera system. CFD simulation of the floating platform in regular waves is also performed for these forced motions.

For CFD simulations, OpenFOAM which uses a finite volume approach to discretize the Unsteady Reynolds-Averaged Navier-Stokes (URANS) equations was utilized. Overset meshing tool was used for creating a fitted mesh around the floating platform that moves with the platform inside the 3-D mesh of the entire simulation domain. To capture free surface motions accurately and improve the interpolation between the fitted mesh and complete mesh, the free surface area and a region containing the fitted mesh inside were done with higher resolution (Figure 2). The numerical wave tank was created and also validated against the computational results of Wang, et al. (2022) and the experimental result of Robertson, et al. (2022) for a benchmark floating offshore model called OC6. The validation for the numerical solver was made for free and forced motions.

RESULTS AND DISCUSSION

The natural pitch periods of the model obtained from the experimental free-decaying pitching tests are 5.21 s ,7.11 s, and 8.91 s for 165mm, 275 mm, and 435 mm of drafts, respectively. The computational fluid dynamics (CFD) simulations of the semisubmersible for these motions are verified and validated. The CFD predictions of certain factors, such as the damping ratios and natural frequencies of the platform's pitch and heave motions, were compared to the actual experimental measurements. Under regular wave forcing, the motions of the platform predicted by CFD are compared with the corresponding measurements. The overall results show that CFD predictions are quite consistent with the experimental measurements.

Figure 1 - Regular Wave Experiment of Model

Figure 2 - Section View of the Computational Domain

REFERENCES

Wang, et al. (2022). OC6 Phase Ia: CFD Simulations of the Free-Decay Motion of the DeepCwind Energies,15(1), 389.

Robertson, et al. (2022). OC6 Phase Ia Definition Document: Validation of Nonlinear Hydrodynamic Loading on the DeepCwind Semisubmersible, National Renewable Energy Lab. (NREL).

Acknowledgments

This research is supported by the Research Fund of the Yildiz Technical University, project number: FCD-2021-4200.

PIPELINE ONSET OF SCOURING IN WAVES AND CURRENT: INFLUENCE OF THE SHIELDS PARAMETER

Marini Francesco, Università Politecnica delle Marche, f.marini@staff.univpm.it
Postacchini Matteo, Università Politecnica delle Marche, m.postacchini@staff.univpm.it
Corvaro Sara, Università Politecnica delle Marche, s.corvaro@staff.univpm.it
Brocchini Maurizio, Università Politecnica delle Marche, m.brocchini@staff.univpm.it

INTRODUCTION

The combined action of waves and currents can lead to the generation of free-spans that have a significant influence on pipeline on-bottom stability and structural integrity. To characterize the onset of scouring under pipelines, most of the literature link the relative embedment of the pipeline with respect to its diameter (e/D) to a dimensionless squared critical velocity. Sumer et al. (2001) provided an equation obtained for current only conditions:

$$\frac{U_c^2}{gD(1-n)(s-1)} = 0.025 \exp\left(9\left(\frac{e_{cr}}{D}\right)^{0.5}\right) \quad (1)$$

For wave conditions, the influence of the *KC* parameter ($KC = \frac{u_w T}{D}$ with u_w the wave velocity at the bottom and T the wave period) is such that the critical embedment is a function of the critical velocity, which in turn depends on *KC*. Sumer et al. (2001) also state that the results for waves should recall the only-current results for large values of *KC*. However, no explicit equation for the onset of scour under wave conditions was given.

AIMS

The main aim of the present work is to provide a method that can be valid for both waves and currents based on a re-analysis of the data of Sumer et al. (2001). The starting point of such analysis is the evaluation of the performance of Eq. 1 for currents (coefficient of determination R^2=0.89) and of the graph from Sumer et al. (2001) for waves (R^2=0.61). In Figure 1, the dimensionless value on the left-hand side of Eq. 1 is plotted as a function of the dimensionless embedment and, for the wave cases, colored as a function of the Shields parameter (θ) calculated with the friction coefficient f_w (Fredsøe & Deigaard, 1992).
In addition to the dependence of *KC*, Figure 1 shows an increase of the critical velocity with θ to the steady current condition, for a given embedment. This suggests the inclusion of the Shields parameter in the analysis.

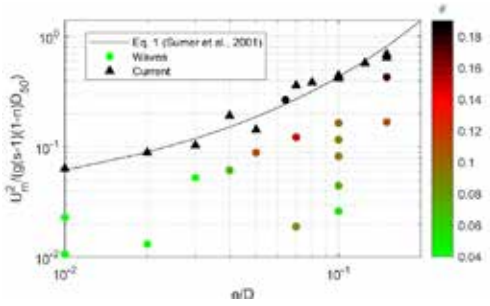

Figure 1 - Effect of the Shields parameter in the onset of scouring process under a pipeline in waves and currents.

METHOD AND RESULTS

To obtain a uniform approach for waves and currents, the dependence of both θ and *KC* is introduced in Eq. 1 which is modified as follow:

$$\frac{U_c^2}{gD(1-n)(s-1)} = a(KC,\theta)\exp\left(9\left(\frac{e_{cr}}{D}\right)^{b(KC,\theta)}\right) \quad (2)$$

Here, the new parameters *a* and *b* are introduced to account for the reduction of the critical velocity for the onset of scour in case of waves.
After a fitting procedure on the experimental data of Sumer et al. (2001), a dependence on $KC^{0.25}\theta^{0.7}$ is obtained. The parameters *a* and *b* can be described by means of exponential equations in the form of:

$$a(KC,\theta) = 0.025[1 - exp(-14KC^{0.25}\theta^{0.7})]$$
$$b(KC,\theta) = 0.5 + exp(-2.9KC^{0.25}\theta^{0.7}) \quad (3)$$

Such equations tend asymptotically to Eq. 1 values (*a* = 0.025 and *b* = 0.5) and when $KC^{0.25}\theta^{0.7} \to 0$: *a* = 0 and *b* = 1.5. The application of Eq. 2 and Eq. 3 to the Sumer et al. (2001)'s data gives the results shown in Figure 2, where the wave tests are colored according to their own θ value.

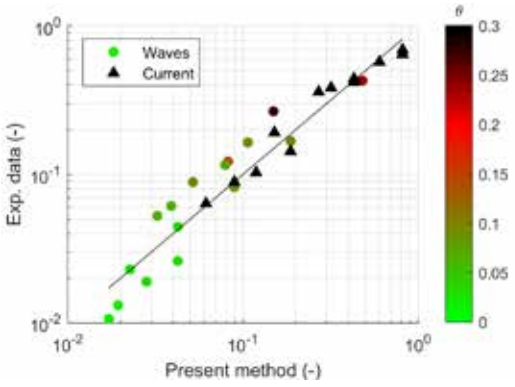

Figure 2 - Application of Eq.2 and Eq.3 coefficients to the data of Sumer et al. (2001) for waves and current.

The present method hence provides a suitable estimate (R^2=0.92) of the onset of scouring under waves by the application of an equation also valid in the case of currents by imposing an infinite value of *KC*.

REFERENCES

Fredsoe, Deigaard (1992): Mechanics of coastal sediment transport (Vol. 3), World scientific publishing company.

Sumer, Truelsen, Sichmann, Fredsøe (2001): Onset of scour below pipelines and self-burial, Coastal Engineering, vol. 42, pp. 313-335

FIELD MEASUREMENTS ON PROPELLER JET INDUCED LOADS ON QUAY WALLS DURING BERTHING AND UNBERTHING MANOEUVRES

Toni Llull, Technische Universität Braunschweig, antoni.llull-marroig@tu-braunschweig.de
Jesús Macías-Lezcano, Technische Universität Braunschweig, j.macias-lezcano@tu-braunschweig.de
Jochen Aberle, Technische Universität Braunschweig, jochen.aberle@tu-braunschweig.de

Ships manoeuvring in low bed clearance conditions induce sediment scour due to the high-speed jet generated by a rotating propeller. The impinging jet characteristics are the driving conditions on which the amount of scour depends, in terms of both eroded depth and volume. The characteristics of the jet are, in turn, dependent on several boundary conditions such as the propeller type, its speed of rotation and the clearance distance to the bed. In some cases, the propeller jet might be also confined by hydraulic structures such as berthing quay walls. In those cases, sediment scour is known to cause instability to quay structures. For this reason, the quay walls are protected when scour is expected in its vicinity. However, a comprehensive understanding of the scour phenomena is still lacking and the design of suitable countermeasures are based on estimated values of induced flow velocities and scour depths that may be far from the reality, leading to either inefficient or oversized protections.

Considerable efforts have been made to study the phenomena from different approaches. Nonetheless, scale model studies have been the preferred method due to the difficulties to measure in real conditions. Field measurements, in fact, have been traditionally lacking in literature due to the challenging conditions in which the data must be obtained such as the need of a free berthing quay, availability of vessel´s data (including ship and propellers behaviour), suitability of the instrumentation to measure within a highly turbulent jet and lack of control of the boundary conditions, making systematic studies almost impossible. This is the reason why field data on this topic is highly valuable and efforts to perform measurements in real conditions are needed. To address this topic, field measurements of flow velocities and pressure loads on a quay wall have been performed and are presented here.

The results included in this work are obtained from three different types of sensors, all of them used in parallel during the berthing and unberthing manoeuvres of several sister RoRo ships and near the bow thrusters. During the measurements, the horizontal pressure load induced by the bow thrusters and the flow velocities within the jet deflected by the quay wall are recorded, together with the water level above these instruments. To do this, 24 pressure sensors were distributed into 2 vertical frames (12 sensors per frame), being the major source of data. An Acoustic Doppler Velocimeter (ADV) was located below the pressure sensors (one at each frame) to record the flow velocities directed to the bottom of the quay wall. An ultrasonic sensor was located at the top of each frame, monitoring the variation in the water level from above. Moreover, data obtained from the vessel during the measurements are used to trigger the obtained results of flow velocity and induced pressure to the ship behaviour. Particularly, data from the Automatic Identification System (AIS) of the ship (including ship position, heading, speed over ground and course over ground) and the Engines Control Unit (including delivered power to bow thrusters, speed of rotation and propeller pitch) have been provided by the ship owner.

The results of this work deal with mean and maximum pressure loads in front of bow thrusters of RoRo ships, together with the analysis of the flow velocities near the bed. The results are presented together with the analysis of the vessel´s and propeller behaviour, which is necessary to understand the obtained data and the variation in between the different days of the campaign.

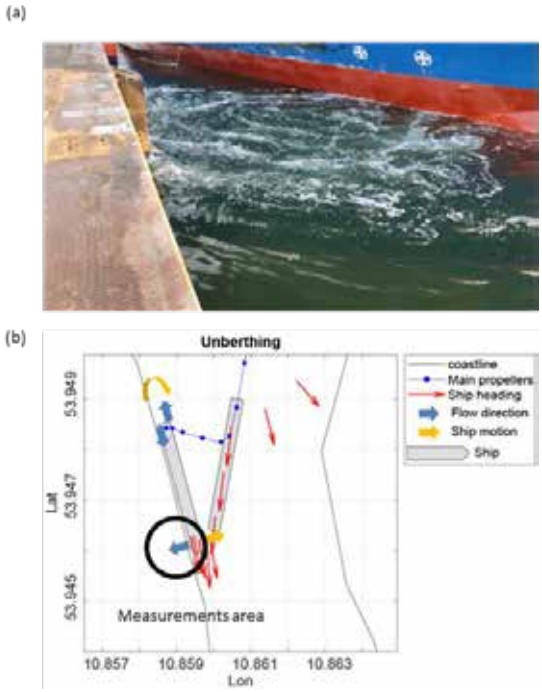

Figure 1 - (a) Flow field from the twin bow-thrusters near the quay wall in the measurement area; (b) Schematic view on the ship trajectory (red arrows and blue dots) of the departure manoeuvre of the study ship, including the flow direction due to the use of each propeller and the ship motion.

COMPARING BEHAVIOURS OF ACTUATOR DISC AND POROUS PLATE IN SIMULATING FAR-FIELD HYDRODYNAMICS IN THE STRAIT OF LARANTUKA: A CASE STUDY

Kadir Orhan, University of Kiel, korhan@corelab.uni-kiel.de
Roberto Mayerle, University of Kiel, rmayerle@corelab.uni-kiel.de
Stephan Deschner, University of Kiel, deschner@corelab.uni-kiel.de
Furkan Altas, Yıldız Technical University, frknlts@gmail.com

INTRODUCTION

In recent years, the Strait of Larantuka, located between Flores and Adunara islands in Indonesia, has attracted the attention of researchers from across the globe as well as tidal developers (Firdaus et al., 2019; Orhan and Mayerle, 2020). The suitability of the strait for tidal energy extraction through horizontal axis tidal turbines has been evaluated via field measurements and 2D/3D numerical hydrodynamic models. The strait has highly energetic tidal currents mainly forced by the barotropic energy flux from the Indian Ocean, with current speeds exceeding 3m/s during the spring tide. The channel has a ca. 3km^2 suitable area where the tidal turbines can be deployed and reach their rated potential, with average hydrokinetic power densities reaching around 9kW/m^2.

The potential hydrodynamic impacts of turbine arrays deployed with varying configurations in the Strait of Larantuka have so far been modelled through Linear Momentum Actuator Disc Theory (LMADT) incorporated into a 2D ocean circulation model (Firdaus et al., 2019) and through porous plates involved in a 3D FLOW model with high horizontal (ca. 15m) and vertical (ca. 3m) resolution to dissipate the momentum through turbine cross sections (Orhan and Mayerle, 2020). Recently, a new tool Actuator Disc tool to simulate turbine operations has been incorporated into the Delft3D-FLOW modelling system, overcoming the limitations of aforementioned studies and showing excellent results against laboratory data (Ramos et al., 2019).

In this paper, research concerning the potential impacts and performances of the tidal turbines in the Strait of Larantuka will be revisited. The behaviour of the actuator disc and the porous plates in simulating the far-field effects of the turbines will be compared for the bounded open-channel flow conditions. To configure tidal turbine arrays optimally, a postprocessing tool is planned. The tool is intended to provide information on mostly stable regions with laminar flow conditions, where turbines operate most efficiently.

METHODOLOGY

The FLOW model presented by Orhan and Mayerle (2020) has been further calibrated and validated against tidal water level and current speed measurements, and utilized to simulate the flow field in the Strait of Larantuka for the current study. The model includes the turbulent kinetic energy dissipation through the k-ε turbulence closure model and simulates horizontal large eddies within the flow field. The design turbine has been described based on the properties of commercially available tidal turbines. A tidal turbine, which can harness a bi-directional flow with a rotor diameter of ca.16m and with a rated power of 1MW has been taken into account for simulations. Considering the efficiencies of the various turbine components, the power coefficient of the device (C_p) was assumed as 0.41, and correspondingly, the thrust coefficient (C_t) of the porous plates was chosen as 0.8 (Orhan and Mayerle, 2020). The loss coefficients for the actuator discs (C_{loss-x}, C_{loss-y}) have been derived from the thrust coefficient. The hydrodynamic impacts of the tidal turbine arrays with varying configurations have been simulated throughout a neap-spring tidal cycle via porous plates and actuator discs, and resulting changes in the flow field, turbine wakes and turbine wake interactions have been presented in comparison. The postprocessing tool has been used to further analyze the simulated flow field, to calculate the strain-rate tensors and energy dissipation rates, and to determine the regions of laminar flow where the turbines have the highest energy conversion efficiency.

RESULTS

The results confirm that the Porous Plate and Actuator Disc approaches show considerable differences when modelling the effects on the far-field hydrodynamics associated with tidal turbine operation. When the turbines operate in their rated range, the Porous Plate approach seems to underestimate the disruptions created in the near and far wakes. Conversely, for tidal flow velocities higher than the rated speed of the turbine, the tendency is reversed. This fact highlights that the representation of the loss coefficient terms (constant for the Porous Plate vs. velocity dependent for the Actuator Disc) and the consideration of the cut-in and cut-out turbine velocities (Actuator Disc) are of greater importance than the geometric representation of the rotor's turbine. It was also found that the proposed postprocessing tool is successful in finding the optimal locations for the turbines to operate most efficiently in horizontal and vertical planes.

REFERENCES

Firdaus, Houlsby & Adcock (2019): Tidal energy resource in Larantuka Strait, Indonesia. Proceedings of the Institution of Civil Engineers-Energy, 173(2), 81-92.

Orhan & Mayerle (2020): Potential hydrodynamic impacts and performances of commercial-scale turbine arrays in the strait of Larantuka, Indonesia. Journal of Marine Science and Engineering, 8(3), 223.

Ramos, Carballo & Ringwood (2019): Application of the actuator disc theory of Delft3D-FLOW to model far-field hydrodynamic impacts of tidal turbines. Renewable energy, 139, 1320-1335.

RENEWABLE ENERGY

ABOUT THE ENERGY YIELD FROM THE TWO-LAYERED BOSPHORUS EXCHANGE FLOW BY MARINE CURRENT TURBINES

Furkan Altas, Yıldız Technical University, frknlts@gmail.com
Kadir Orhan, University of Kiel, korhan@corelab.uni-kiel.de
Stephan Deschner, University of Kiel, deschner@corelab.uni-kiel.de
Mehmet Öztürk, Yıldız Technical University, meozturk@yildiz.edu.tr
Cihan Sahin, Yıldız Technical University, cisahin@yildiz.edu.tr
Yalcin Yuksel, Yıldız Technical University, yuksel@yildiz.edu.tr
H. Anil Ari Guner, Yıldız Technical University, aari@yildiz.edu.tr
Roberto Mayerle, University of Kiel, rmayerle@corelab.uni-kiel.de

INTRODUCTION

The Bosphorus Strait, located in Istanbul in northwestern Turkey, links the Black Sea in the north with the Sea of Marmara in the south, and it is one of the busiest maritime passages in the world. The flow through the strait is a typical example of a two-layer exchange flow. Although tidal forcing is negligible, current speeds are comparable to those observed in tidal environments. Ozturk et al. (2017) analyzed the current energy potential of the Bosphorus currents using one-year-long model predictions. The results showed that the current speeds in the strait reach 2.5m/s during peak periods, corresponding to kinetic power density values of around 8kW/m² (Yuksel et al., 2008; Ozturk et al., 2017). Although the exchange dynamics in Bosphorus and the hydrokinetic power density of the undisturbed Bosphorus Flow have been studied and demonstrated in earlier studies (Yuksel et al., 2008; Ozturk et al., 2017; Sozer and Ozsoy, 2017; Ozturk and Altas, 2022), there is still a need to improve the understanding concerning the interaction between marine current turbines (MCT) and highly energetic, stratified currents in the channel. Such a flow structure imposes unique challenges concerning the selection of suitable locations to deploy the MCTs and the optimization of large-scale MCT array layouts and requires a better understanding of the interaction between the turbines and flow layers with spatiotemporally varying thicknesses. In this study, an improved site selection method to determine the suitable MCT deployment locations in stratified flow conditions will be proposed. Furthermore, recovery and interaction of turbine wakes in two-layered Bosphorus exchange flow will be studied extensively to later optimize the configurations of multi-MCT arrays.

METHODOLOGY

Ozturk and Altas (2022) provide extensive information about the properties of Bosphorus exchange flow based on the year-long measurements carried out for the design and construction of the Bosphorus Tube Crossing. In this study, an additional set of continuous water level, current speed, salinity and temperature measurements were performed to improve the current understanding of the flow dynamics and to further calibrate the Bosphorus Delft3D model within the framework of the partnership between the University of Kiel and Yildiz Technical University. The numerical model, with a horizontal resolution of ~45m and a vertical resolution ~3m, was able to capture the flow field with sufficient detail. Much attention has been given to the meteorological forcing and conditions at the open sea boundaries to simulate the density gradients and flow fields along the strait with adequate precision. The interaction between the turbines and the two-layered exchange flow has been simulated with the Actuator Disc approach, taking floating and fixed MCTs with varying array configurations into account.

RESULTS

The results show that there is a strong variation in available hydrokinetic power throughout both horizontal and vertical planes along the channel. Thus, while MCTs floating responding to the water level variations are found more suitable to harness the hydrokinetic energy flux of the upper flow layer towards the south end of Bosphorus, devices bottom-fixed can be deployed to operate within the lower layer towards the north of the strait. It was also found that the varying layer thicknesses and turbulent kinetic energy dissipation need to be considered while deciding the rotor geometry and the deployment depth of the MCTs.

ACKNOWLEDGEMENTS

This research is supported by the Scientific and Technological Research Council of Turkey (TUBITAK) with project number 222M240.

REFERENCES

Yuksel, Ayat, Ozturk, Aydogan, Guler, Cevik and Yalçıner (2008): Responses of the stratified flows to their driving conditions–A field study. Ocean Engineering, 35(13), 1304-1321.

Ozturk, Sahin and Yuksel (2017): Current power potential of a sea strait: The Bosphorus. Renewable Energy, 114, 191-203.

Sozer and Ozsoy (2017): Modeling of the Bosphorus exchange flow dynamics. Ocean Dynamics, 67, 321-343

Ozturk and Altas (2022): Seasonal variability of stratified flow properties in a Non-tidal Strait-A field study. Estuarine, Coastal and Shelf Science, 264, 107700.

NUMERICAL ANALYSIS OF AN INNOVATIVE FLOATING PLATFORM FOR OFFSHORE WIND TURBINES

Elif Girgin, Izmir Institute of Technology, elifgirgin@iyte.edu.tr
Bergüzar Özbahçeci, Izmir Institute of technology, berguzarozbahceci@iyte.edu.tr

INTRODUCTION

Offshore wind turbines offer higher power generation potential due to the availability of high wind speeds at lower altitudes over the open sea. The installation of offshore turbines has been increasing worldwide, with China surpassing the EU in capacity (WFO, 2022). In Turkey, where most coastal waters have depths exceeding 50 meters (WBG, 2019), floating platforms have emerged as a viable solution. At IZTECH, an innovative floating platform has been designed by combining the stabilizing characteristics of Spar and semisubmersible platforms to provide an alternative solution. This study is based on the calibration and validation of the hydrodynamic performance results of the innovative floating platform, which has previously undergone extensive hydraulic model tests under various wave and wind conditions using ANSYS™AQWA® package. Details of the experimental study are given in Girgin (2022).

METHODOLOGY

Free oscillation tests are frequently employed in research to calibrate simulation damping, incorporating linear and quadratic damping matrices for all six modes (Gueydon et al., 2014). The hydrodynamic linear and quadratic damping coefficients of the structure are calibrated through free decay tests (FDT). The resulting damping coefficients are determined through analysis and fitting procedures. In addition, the added mass values for the six degrees of freedom were investigated for the calibration of the platform's natural period. With this approach, the natural period, linear damping, and quadratic damping values of the numerical model were calibrated using the experimental results from the free oscillation tests of the innovative platform (Fig.1). After the calibration of the numerical model, comparison results were obtained by comparing the laboratory test results conducted under wave and wind conditions with the numerical model results.

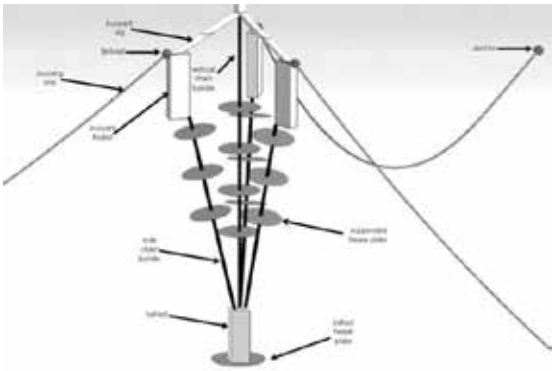

Figure 1 - Innovative floating platform design

RESULTS

The natural period values and damping behavior of the experimental and numerical models were found to be consistent after the calibration process. When comparing the maximum response values of the platform under the regular wave and windy regular wave conditions, a good agreement is observed between the experimental and numerical results in the surge, heave, and pitch directions. This agreement is also evident when examining the spectrum distributions of the irregular wave and windy irregular wave experiments. Additionally, throughout all these experiments, the tensions in the chains connecting the platform to the seabed were measured and compared. In this regard, better results were obtained for the posterior two chains, while the anterior chain exhibited poor agreement between the numerical and experimental models.

CONCLUSION

The stability of the new platform and the compliance of the responses with acceptable limits have been confirmed through extensive testing under various wave and extreme wind conditions. The hydrodynamic responses of the offshore turbine on the new floating platform have been calibrated and analyzed using a numerical model, which has shown good agreement with the experimental results. This indicates that the system's geometry can be optimized, and performance can be improved at the prototype scale using the numerical model. Strong evidence of the technology's feasibility has been provided through laboratory-based physical and numerical tests. The platform's technology readiness level (TRL) of 4 has been achieved in this study. The next step involves demonstrating the platform's performance in the relevant sea environment to elevate its TRL to 6 in future studies.

ACKNOWLEDGEMENT

This study has been funded by grants 217M451 and 121M933 by the Scientific and Technological Research Council of Turkey (TUBITAK).

REFERENCES

Girgin (2022): Hydrodynamic Investigation of an Innovative Floating Platform for Offshore Wind Turbines.
Gueydon, Tiago, and Jason M. (2014): Comparison of Second-Order Loads on a Semisubmersible Floating Wind Turbine, Proceedings of the International Conference on Offshore Mechanics, and Arctic Engineering - OMAE 9A (March).
World Bank Group (2019): Expanding Offshore Wind to Emerging Markets, World Bank Group Proceedings.
World Forum Offshore Wind (2022): Global Offshore Wind Report.

VALIDATION OF WIND-BLOWN SAND CALCULATIONS IN SAND TRANSPORT MODEL

Taiki Sekiguchi, Chuo University, a18.b6kx@g.chuo-u.ac.jp
Akiyoshi Katano, ECOH CORPORATION, katano@ecoh.co.jp
Yota Enomoto, Chuo University, a17.p7cj@g.chuo-u.ac.jp
Taro Arikawa, Chuo University, taro.arikawa.38d@g.chuo-u.ac.jp (corresponding author)

1. AIMS

The sand at beaches is distributed on land and in water through the usual sand deposition and erosion and through sand transport via waves and wind. While field surveys have been conducted on sandy beaches, and numerical studies have investigated sand drift and wind-blown sand, no studies have simultaneously calculated both the sand drift and wind-blown sand. Therefore, this study aims to examine the applicability of incorporating wind-blown sand calculations into the drifting sand calculation equation by conducting model experiments.

2. EXPERIMENTAL METHOD

The experimental cross section is shown in Figure 1. H is the height from the floor to the top. The experiment was conducted for two conditions H = 50 cm and H = 25 cm. A Suiden SJF-300RS-1 portable air blower was used to blow air into the experimental cross section by connecting a flexible duct. Sand with an average grain size of approximately 0.2 mm was used. The amount of wind-blown sand was captured by placing a box at the end of the experimental terrain, and its weight was measured after the experiment by using an electronic scale. The experiment lasted 5 min and was conducted thrice. When the sand was placed, partitions were set up in front and behind it. Immediately before starting the experiment, the partitions were removed, and the experiment was conducted with the sand in a naturally deformed state. The wind speed was measured using a hot-wire anemometer. Measurements were taken at four locations:0, 10, 20, and 30 cm from the bottom at H = 50, and at 0, 5, 10, and 15 cm from the bottom at H = 25 cm. The measurement position in the y-direction was at the center of the channel.

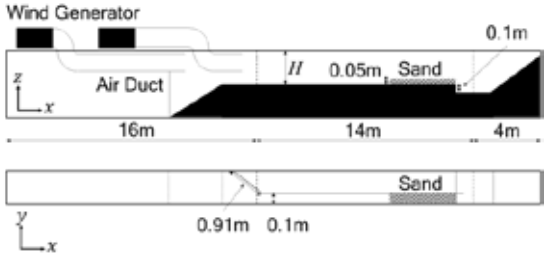

Figure 1 - Experimental cross section

3. CALCULATION METHOD

CADMAS-STR-STM was used for the numerical analysis. This model is based on the coupled numerical wave tank and structural deformation calculation method (CADMAS-STR) proposed by Arikawa et al. (2009) coupled with the sediment transport model (STM) based on the theory of Takahashi et al. (1999). The calculation conditions were the same as those for the experimental terrain, and 5 cm mesh computational grids were used.

4. RESULTS

For H = 25 cm, the average amount of wind-blown sand was 0.862 g/(cm･s). At H = 50 cm, the average wind speed at 10 cm above the bottom was 5.957 m/s, whereas the average wind speed at the same location for H = 25 cm was 8.233 m/s, approximately 1.4 times higher. Figure 2 shows the relationship between the Bagnold and Kawamura equations for friction velocity and the amount of wind-blown sand superimposed on the experimental and calculated results for H = 25 and 50 cm. The coefficients of the Bagnold and Kawamura equations are B = 2.5 and K = 1.0, 2.0, and 3.1. The calculation and experimental results showed good reproduction of the amount of wind-blown sand obtained using the formulas. Therefore, the validity of this method for calculating wind-blown sand is demonstrated.

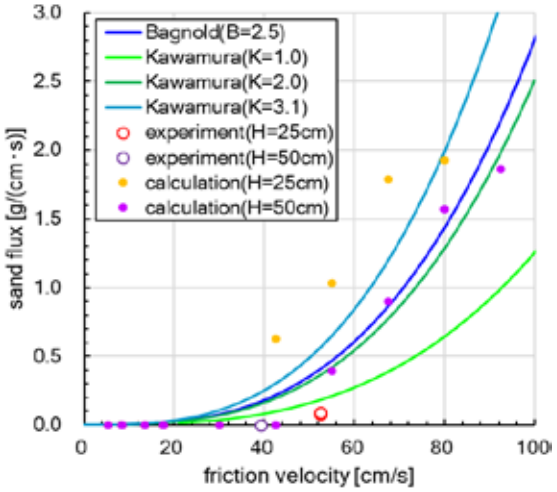

Figure 2 - Relation between the wind-blown sand volume equation and results (experiment and calculation)

REFERENCES

T. Arikawa, K. Hamaguchi, K. Kitagawa and T. Suzuki (2009): Development of Numerical Wave Tank Coupled with Structure Analysis Based on FEM, Journal of Japan Society of Civil Engineers, Ser. B2 (Coastal Engineering), vol.65(1), pp.866-870.
T. Takahashi, N. Shuto, F. Imamura and D. Asai (1999): Development of Tsunami Moving Bed Model Considering Exchange Sand Volume between Bed Sand Layer and Suspended Sand Layer, Proceedings of Coastal Engineering, JSCE, vol.46, pp.606-610.

RIVER PLUME DYNAMICS IN SMALL-SCALE MICRO-TIDAL ESTUARINE SETTINGS: THE MISA RIVER CASE STUDY

Agnese Baldoni, Dipartimento di Ingegneria Civile, Edile e Architettura (DICEA), Università Politecnica delle Marche, a.baldoni@pm.univpm.it
Maurizio Brocchini, Dipartimento di Ingegneria Civile, Edile e Architettura (DICEA), Università Politecnica delle Marche, m.brocchini@univpm.it
Eleonora Perugini, Department of Civil and Environmental Engineering (CEE), University of Strathclyde, eleonora.perugini@strath.ac.uk
Pierluigi Penna, National Research Council – Institute of Marine Biological Resources and Biotechnologies (CNR IRBIM), pierluigi.penna@cnr.it
Luca Parlagreco, Italian Institute for Environmental Protection and Research (ISPRA), luca.parlagreco@isprambiente.it

We studied the evolution of the Misa River (Senigallia, Italy) plume by integrating different sources of information. The Misa River estuary was taken as representative of those small-scale river systems characterized by torrential regimes that flow into micro-tidal environments. Although such small rivers contribute for 75% to the sediment discharged into the Adriatic Sea (Milliman, 2016), relatively little attention has been given to them.
We focused on some local mechanisms, occurring at the river mouth, that could contribute to the riverbed mobilization and sediment resuspension. In particular, the sediment resuspension triggered by sea waves within the final reach of the river has been investigated.
The plume spreading at sea is driven by some transport mechanisms, that somehow differ from those affecting sediment dispersal in large-scale river systems. In fact, small-scale plumes evolve in a short time under the strong influence of the wind forcing (Osadchiev, 2019).
Both generation and transport mechanisms have been studied through the integration of the observed data, included some video-monitoring products, and numerical simulations.

METHODOLOGY

Optical images from two video-monitoring stations and Satellite were used to observe the plume events and to track their fronts. While images from video-monitoring stations provided a higher temporal resolution, allowing to capture the dynamical evolution of the plume, Satellite images allowed us to visualize a larger area.
Plume events were correlated with the estuarine forcing, trying to give a first classification based on the generation mechanisms. However, for some events that were influenced by a combination of factors, it was difficult to distinguish the role of each forcing.
Therefore, numerical simulations were run to verify the hypotheses originally made and to clarify the plume generation and transport mechanisms.
Finally, Particle Tracking Velocimetry analyses were performed on the basis of videos collected by the SGS video-monitoring station (www.morse.univpm.it) showing some debris (woods) floating on the water surface. This allowed us to compute the plume surface velocity and its relationship with the plume extension.

RESULTS

Correlation of the information retrieved from the images with the estuarine forcing revealed the existence of a number of typical plume shapes and colours, associated with both the generation and transport mechanisms. To distinguish the role of each forcing, we run Delft3D parametric simulations, activating only one mechanism at a time: river discharge, sea waves, wind, etc.. Results showed that the river discharge generates the densest and most extended plumes, but also sea waves can stir, suspend, and drag plume sediments. Furthermore, wave-induced currents are also responsible for the transport of the plume sediments along the coast. However, the transport mechanism that mainly affects the plume alongshore expansion is the wind. Particle Tracking Velocimetry provided further results that strengthened the observed and modelled ones. These have been summarized by a power law linking the plume offshore extension with the plume velocity components (Figure 1). The findings reveal that the plume offshore extension is directly proportional to the plume alongriver velocity, mainly determined by the river speed, while it decreases because of the action of those transport mechanisms that contribute to the alongshore plume velocity.

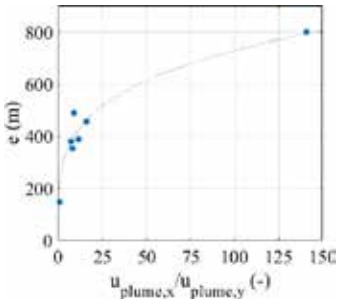

Figure 1 - Power law relating the plume offshore extension (e) and the ratio between the alongriver (x-) and alongshore (-y) components of the plume surface velocities.

REFERENCES

Milliman, Bonaldo, Carniel (2016): Flux and fate of river-discharged sediments to the Adriatic Sea, Advances in Oceanography and Limnology, vol. 7(2), pp. 106-114.
Osadchiev and Sedakov (2019): Spreading dynamics of small river plumes off the northeastern coast of the Black Sea observed by Landsat 8 and Sentinel-2, Remote Sensing of Environment, vol. 221, pp. 522-533.

SEDIMENT TRANSPORT PROCESSES

MODELLING THE BERM FORMATION ON AN ARTIFFICIAL PEBBLE BEACH DURING STORM EVENTS USING XBEACH-G

Hanna Miličević, Faculty of Civil Engineering, University of Zagreb, hanna.milicevic@grad.unizg.hr
Dalibor Carević, Faculty of Civil Engineering, University of Zagreb, dalibor.carevic@grad.unizg.hr
Suzana Ilić, Lancaster Environment Centre, Lancaster University, s.ilic@lancaster.ac.uk

The growing tourism demand for beach capacity has driven the construction of artificial mainly pocket gravel beaches along the Croatia's eastern Adriatic coast (Pikelj et al., 2018) without sufficient knowledge on the most appropriate beach parameters used for design, such as beach profile slope, grain size and shape. There is also a lack of knowledge on how the beach can withstand a range of wave forcings and the frequency of storm events. The BEACHEX project aims to address some of these gaps. The data collected on and the understanding of beach responses to a range of wave events, gained in this project, provide the opportunity to evaluate numerical models used to predict beach changes. In this paper, we investigate the feasibility of the 1D model XBeach Gravel (McCall et al., 2016) for predicting beach changes, namely the location and height of the beach berm after storm events, at the artificial gravel beach Ploče in the northwestern part of the city of Rijeka in the Kvarner Bay.The open-source numerical model XBeach Gravel was selected because it was developed to simulate storm-induced changes in gravel beaches (McCall et al., 2016) and has been used in previous studies of gravel beach changes (McCall et al., 2016). The numerical model has been calibrated for application to gravel beaches under fetch-limited conditions (Bogovac et al., 2023).

The beach Ploče is 320 m long, and it is divided by a 30 m long central groyne into two cells of approximately equal length. The beach is exposed to strong wind waves during the winter months, which cause significant sediment transport and erosion. Topographic data of beach changes were collected using SfM photogrammetry over a period of one year, in parallel with wave data measurements (Tadić et al., 2022). For this paper, 4 field surveys, i.e., two energetic events (UAV4&5, UAV15&16) were selected; the first event (Hs=1.57 m, Tp= 4.55 s) due to the shortest period between the topographical surveys (only one day) and the second event due to the largest significant wave height (Hs=1.8 m, Tp= 5.56 s). More details can be found in the paper by Tadić et al. (2022). XBeach-G is one-dimensional and does not allow simulation of longshore beach processes, only cross-shore profile changes. Changes were simulated on two beach profiles aligned with the incoming wave direction. The wave parameters and tide levels used for the simulations were obtained from the wave buoy deployed in Rijeka Bay and the "Bakar" tide gauge, respectively. The simulations were run with the maximum and averaged significant wave heights of the highest recorded values during the event. These were kept constant for the entire duration of the simulations. Simulations were run for 15000 s (cca 3000 waves). The sediment properties hydraulic conductivity (0.4 m/s) and median grain size D50 (0.032 m) were taken from (Bogovac et al., 2023). The van Rijn formula (McCall et al., 2016) was used for sediment transport and three different values for the transport coefficient (γ) were used, namely 0.5, 1 and 3. The results showed that the model can simulate the formation of beach berms and predict their location, but the simulated heights depend on the value of the chosen transport coefficient (γ). Figure 1 shows the results from the simulation of berm formation between surveys UAV15&16; after the most energetic event recorded.

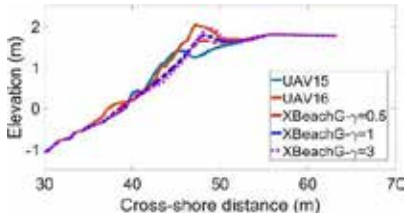

Figure 1. Position and height of berms for different g coefficient (UAV15&16)

The simulation was run with an average significant wave height (Hs) of 1.78 m, a an average peak period (Tp) of 5.27 s, and a tide level of 0.64 m.The berm location estimated by XBeach-G is the same as in the post-event survey (UAV16 and dashed lines in the graph) regardless of the transport coefficent (γ) chosen for the simulations. However, the simulations have also shown that the location of the maximum berm height and the height of the berms depend on the transport coefficent (γ), the higher the transport coefficient, the greater the height of the berm and vice versa.

In summary, the results of the simulations have shown that the XBeach-G numerical model can be used to simulate gravel beach berms in a fetch-limited environment, which has not been tested before. Future work, will include further sensitivity testing of the model for different parameter values, validation of the model on different gravel beaches (e.g. size of pocket beaches) and conditions with low longshore sediment transport.

REFERENCES

Bogovac, Carević, Bujak, Miličević (2023): Application of the XBeach-Gravel model for the case of east Adriatic Sea-wave conditions, J.Mar.Sci.Eng, vol.11

Pikelj, Ružić, Ilić, James, Kordić (2018): Implementing an efficient beach erosion monitoring system for coastal management in Croatia, Ocean and Coastal Management, ELSEVIER,vol.156, pp. 223-238.

Tadić, Ružić, Krvavica, Ilić (2022): Post-nourishment changes o fan artificial gravel pocket beach using UAV imagery, J. Mar.Sci.Eng., vol. 10

HYDRODYNAMIC FORCE COEFFICIENTS FOR SPHERICAL SHELL FRAGMENTS: DEPENDENCE ON THE ASPECT-RATIO AND FLATNESS

Ian Adams, National Research Council Research Associateship Program, ian.adams.ctr@nrlssc.navy.mil
Julian Simeonov, Ocean Sciences Division U.S. Naval Research Laboratory, julian.simeonov@nrlssc.navy.mil

MOTIVATION

Sand Shell mixtures are ubiquitous on many inner shelf areas, but the dynamics of how this mixture sorts and is transported is poorly understood. To better understand this process, we need to improve our understanding of the dynamics of shell fragments to improve modeling of shell fragment dynamics in Euler-Lagrange simulations. This requires hydrodynamic models of drag and lift forces on individual particles. Many common assumptions used in parameterization of these sediment transport models are ill suited for non-spheriod particles. Often shape, rotation, and fluid shear are ignored in parameterizing the fluid forces on sediment particulates. Currently there are no universal models that can prescribe these forces for both irregularly shaped and arbitrarily orientated particles. In this work, we create a force coefficient parameterization of the fluid force on a triangular spherical-shell fragment that accounts explicitly for the object rotation.

PROCEDURE

In this work, we present a series of OpenFOAM Reynolds-Averaged Navier-Stokes (RANS) numerical simulations of steady bottom-boundary layer flow around a series of triangular spherical-shell fragments with varying aspect-ratio and flatness qualities and varying orientation with respect to the mean flow. These simulations calculate the force coefficients of drag, lift, and side force with respect to the domain. We show that the forces in the object frame of reference can be represented by a linear combination of the velocity components in the object frame of reference. This work is an extension of previous modeling efforts which resulted in a successful predictive hydrodynamic force model for arbitrary rotations of an intact limpet shell.

For each of the considered shell shapes, we placed the shell into a bottom boundary layer shear flow in a series of 67 simulations with unique orientations to the flow, with independently varying pitch, roll, and yaw each ranging from 0 to 180 degrees. We assume a logarithmic velocity forcing profile at the inlet of our domain, with an upstream velocity of 1.7m/s at the height of the particle. This results in a particle Reynolds number of 34,000. The shell fragments used are generated as triangular selections of a spherical shell with theta and phi angles proscribed based on aspect-ratio and flatness parameters (varying between 1 to 5, and 0.02 to 0.2 respectively). The fragment base length is used as the particle length scale and is held constant at 2cm.

The numerical simulations explicitly resolve the wall viscous boundary layers using O(y+=1) grid spacing at the shell fragment surface. The SST k-omega turbulence closure model was chosen for its accuracy in simulating fully resolved wall effects (Ahmad [2011]). Forces in the domain frame of reference are calculated for each orientation, and are then rotated into the object-oriented frame of reference. Particle specific, force coefficient tensors in the object frame of reference were then calculated through linear regression methods. Both the coefficients in the domain frame of reference and the coefficient tensors calculated through the linear regressions are compared to lift and drag coefficients observed from flat plate experiments of Ortiz [2015].

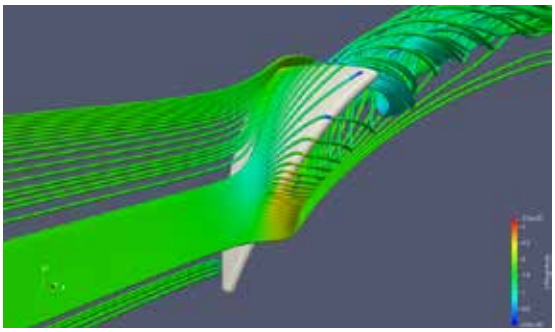

Figure 1 - Streamlines of Velocity around a shell fragment in a shear flow

RESULT

The numerical estimates for the forces from all simulations were used to develop a parameterization that explicitly accounts for the rotation using unique tensor coefficients that relate the force and the velocities in the object frame of reference. These coefficient tensors were used to create hydrodynamic force predictions in the object frame of reference which match well with simulated forces rotated into the object frame. This results in robust parameterizations of the drag and lift on an arbitrary shell fragment as a function of aspect ratio and flatness characteristics, as well as orientation of the shell fragments. Components of the coefficient tensor are examined as a function of changing particle characteristic aspect-ratio and flatness parameters.

REFERENCES

Ahmad, McEwan, Watterson, and Cole (2005): RANS turbulence models for pitching airfoil, WIT Transactions on The Built Environment, vol. 84

Ortiz, Rival, and Wood (2015): Information Processing at Forces and Moments on Flat plates of Small Aspect Ratio with Application to PV Wind Loads and Small Wind Turbine Blades, Energies, vol. 8, pp. 2438-2453.

SEDIMENT TRANSPORT PROCESSES

SEASONAL SEDIMENT DYNAMICS IN A NON-TIDAL RIVER DELTA COAST: OBSERVATIONS AND 3-D MODELING

Mehmet Ozturk, Yildiz Technical University, meozturk@yildiz.edu.tr
Cihan Sahin, Yildiz Technical University, cisahin@yildiz.edu.tr
Ahmet Altunsu, Yildiz Technical University, ahmetaltunsu53@gmail.com
H. Anil Ari Guner, Yildiz Technical University, aari@yildiz.edu.tr
Yalcin Yuksel, Yildiz Technical University, yalcinyksl@gmail.com
Kerem Guner, Yildiz Technical University, krmgnr@live.com

INTRODUCTION

River discharge and storm waves are dominant forcing mechanisms controlling sediment dynamics in river delta systems. During floods and storms, gravity-driven seaward transport is dominant, and inner shelf flood deposits are formed at the end of the storm. During the low-energy periods, the dominant processes are the winnowing of fines and the bypass of sediment without any recent deposition on the inner shelf (Lopez et al., 2017). This study investigates the sediment dynamics in a wave-dominated river delta coast during different seasons using in-situ observations and during storm events representing dry and wet seasons using numerical model results.

STUDY SITE

The study site (Karasu Beach) is in the north of the Sakarya province, Turkey, on the southwestern Black Sea coast (Figure 1) with an approximately 80 km long shoreline. River discharge and energetic wind and wave climate are the major physical processes that control the sediment transport pattern along the shoreline and cause the formation of natural beach areas with dunes behind them. Due to the decrease of sediment runoff to the coast related to the construction of large volume reservoirs along the river stream and the coastal structures along the coast, a 7.5 m/year retreat of the coastal line occurred. A series of dunes protect the floodplain forest at the western side of the river which has been designated as a Special Area of Conservation. The erosion problem threatens the coastal area as well as floodplain forests.

FIELD EXPERIMENT

Field observations were conducted in different seasons (February, July and November) covering different meteorological and hydrological conditions to observe variations of hydrodynamics and sediment dynamics under different forcing conditions. In the field studies, vertical salinity, temperature, and turbidity profile measurements were carried out along one cross-shore (A) and two long-shore transects (B and C; Figure 1). Salinity and temperature measurements were carried out with CTD sensors. Turbidity sensors were used to estimate the suspended sediment concentration. An upward-looking ADCP was deployed at the seafloor at a depth of approximately 15 m to observe currents and surface waves. River cross-section variations were determined by the water depth measurements in a section 400 m behind the river mouth during field campaigns. Bathymetry profiles perpendicular to the shore were acquired in each season to observe the seasonal sea-floor variations. In addition to observing the seasonal behavior of the delta system, in-situ data were also used to validate the numerical model.

Figure 1 - Sakarya River delta environment and the measurement locations

NUMERICAL MODELING

Mike 3 Flow Model FM and Mike 21 ST coupled model were used for modeling the hydrodynamics and sediment processes along the Karasu coastline. A higher-resolution grid that covers the nearshore region was nested in this Black Sea grid. The model is forced at its boundaries by waves simulated by the MIKE21-SW model. The atmospheric forcing was obtained from the ECMWF ERA-5 data. The initial bed sediment size distribution was provided by in situ samples. River water discharges were measured, and solid discharges were estimated from empirical relationships.

RESULTS

Field measurements indicate significant seasonal variability in hydrodynamics, sediment dynamics, and river morphology. The results on resuspension, advective transport processes, and erosion/deposition patterns during wet and dry storm events were compared to determine the inner shelf environment response under different forcing conditions.

ACKNOWLEDGEMENTS

This research is supported by the Scientific and Technological Research Council of Turkey (TUBITAK) with project number 117Y333.

REFERENCES

Lopez, Guillen, Palanques, Grifoll (2017): Seasonal sediment dynamics on the Barcelona inner shelf (NW Mediterranean): A small Mediterranean river- and wave-dominated system. Continental Shelf Research, 145, 80-94.

Poster
PRESENTATIONS

CLIMATE CHANGE IMPACTS AND RISKS OF EXTREME COASTAL WATER LEVEL EVENTS IN THE MEDITERRANEAN SEA

Filippo Giaroli, University of Genoa (Italy), filippo.giaroli@edu.unige.it
Andrea Margarita Lira Loarca, University of Genoa (Italy), andrea.lira.loarca@unige.it
Giovanni Besio, University of Genoa (Italy), giovanni.besio@unige.it

Coastal areas around the world are characterized by a high population density, by important socio-economic activities, by the presence of trading nodes both by sea and land and by important infrastructure, therefore they can be considered a crucial place for the development and the life of modern society. However, they are increasingly threatened by natural phenomena that manifest themselves with more and more strength, and due to climate change driven by global warming, extreme events have become more frequent and intense.
Locally, sea-level variations and wind waves are the most affecting components of many coastal hazards, causing, among other things, flooding phenomena in several countries of the world which fight against sea level rise to protect the cities located in the most vulnerable position and the people who reside there, as the case of Venice, one of the key-example in the Mediterranean Sea.

Future projections of storm surge in the whole Mediterranean Sea, with a coastal high spatial resolution (from 50 km in open sea up to about 300 m near the coastline) and hourly temporal resolution using the modelling software Delft 3D Flexible Mesh have been developed (Fig. 1).

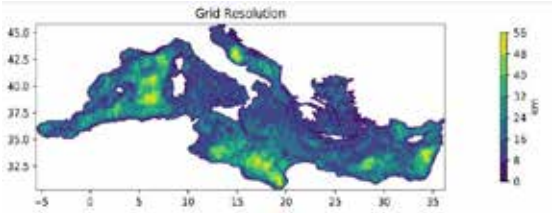

Figure 1 - Resolution of the computational grid used to evaluate the storm surge projections.

Storm surge datasets with such features have been developed up to the end of the XXI century considering different input atmospheric scenarios among those proposed by the IPCC.
Comparisons between hindcast datasets and future projections related to different scenarios are performed, to identify the trends of change driven by climate change, as well as extreme value analyses to investigate the frequency with which extreme events are expected to occur and to observe the variation in hazard for coastal locations.

The phenomenon is also jointly studied with wind waves projections obtained from the same atmospheric input through Copula models. This is of particular interest for characterization of coastal hazard because the simultaneous presence of extreme events can increase the negative effects for the coastal environment, constituting a greater hazard. The figures below show the variation in time of the joint occurrence probability and the joint return period of simultaneous extreme events (Fig. 2).

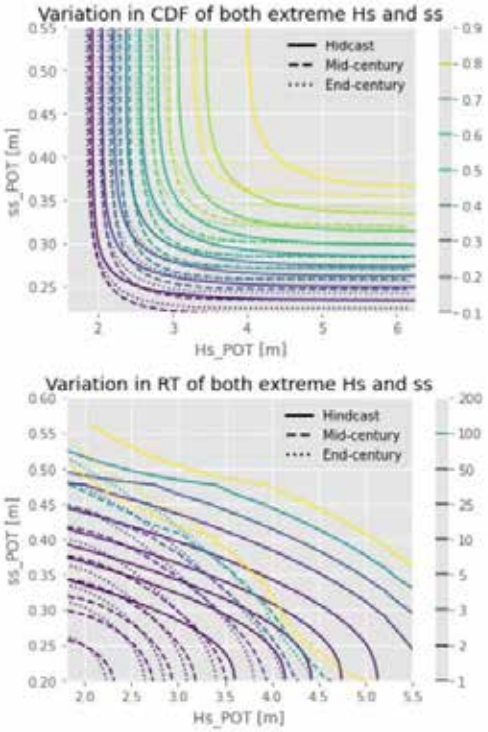

Figure 2 - Comparison among past and future CDF and return period of joint wind waves and storm surge extreme phenomena in a point located in the Ligurian Sea.

REFERENCES

Woodworth et al., 2019. Forcing factors affecting sea level changes at the coast. Surveys in Geophysics, 40(6), pp.1351-1397.

Vousdoukas et al., 2018. Global probabilistic projections of extreme sea levels show intensification of coastal flood hazard. Nature communications, 9(1), pp.1-12.

EXTREME WATER LEVEL PROJECTIONS AT THE COASTAL HERITAGE SITES OF TURKIYE

A. Cagatay Uysal, Middle East Technical University, cauysal@metu.edu.tr
Gulizar Ozyurt Tarakcioglu, Middle East Technical University, gulizar@metu.edu.tr
Iremnaz Kosem, Middle East Technical University, e216226@metu.edu.tr
Akdeniz Ince, Middle East Technical University, akdenizince@gmail.com

INTRODUCTION

Climate change has led to changes in the severity and frequency of extreme weather events, storm surges, and sea level rise, increasing the future extreme water levels (EWL) in many places worldwide. In the scope of The Scientific and Technological Research Council of Turkiye (TUBITAK) funded project "Vulnerability of Coastal Cultural Heritage Areas to Sea Level Rise and Its Impacts," a preliminary statistical and spatial analysis has been carried out to investigate the projected EWLs at the coastal cultural heritage sites of Turkiye. The objective of this study is (i) to determine those cultural and natural heritage sites having higher EWLs, (ii) to discuss using rates of change of EWLs as a classification for flooding risks due to EWL, and (iii) to compare different EWL datasets in the literature under various RCP scenarios within the context of vulnerability of the coastal areas with heritage characteristics.

METHODOLOGY

The heritage sites at the coast of Turkiye are extracted as GIS (Geographic Information System) layers from the open-source ATLAS database (www.atlas.gov.tr) of Ministry of Environment, Urbanization, and Climate Change. The EWL projections obtained from the studies of Large Scale Integrated Sea-level and Coastal Assessment Tool (LISCOAST, Vousdoukas et al., 2018) and Kirezci et al. (2020) are assigned to the coastal heritage sites in the QGIS environment. These databases provide the probabilistic EWL projections for Representative Concentration Pathways (RCPs) 4.5 and 8.5. RCPs are emission rate scenarios described by the Intergovernmental Panel on Climate Change (IPCC), where RCP4.5 is a moderate pathway, and RCP 8.5 is considered the worst case. The projected EWL for 2100 and the changes during BL-2100, BL-2050, and 2050-2100 are investigated for every data point nearest to the heritage sites around Türkiye. Table 1 shows the range of the results for both datasets of EWLs.

Table 1. The ranges of the investigated parameters of EWL at the coastal heritage sites of Turkiye

Data Base	RCP Scenario	EWL for 2100 (m)	% change BL-2100	% difference BL-2050 and 2050-2100
LISCOAST	RCP4.5	1.12-1.65	34%-70%	-0.8%-+12.7%
	RCP8.5	1.44-1.94	57.3%-118%	+7.8%-+18.6%
Kirezci et al. (2020)	RCP4.5	0.65-1.4	46.6%-200%	-29%-+1%
	RCP8.5	0.85-1.6	68%-287%	-10%-+12.9%

RESULTS

The results based on the LISCOAST dataset show that most heritage sites are projected to have EWLs higher than 1.35m for the next century. Based on the RCP 4.5 scenario, 32 % of the archeological coastal cultural heritages and 26% of the natural heritage sites will have an EWL above 1.5 m. Under RCP 8.5, 56% (archeological) and 39% (natural) of the coastal heritage sites will have an extreme water level above 1.7 m. Kyzikos Ancient City in Balikesir is expected to have the maximum EWL reaching 2 m. For the moderate RCP scenario, 32% of the archeological heritage sites and 29% of the natural heritage sites will experience at least 50% of EWL increase in 100 years. Although there are some exceptions, there is a significant acceleration trend of EWLs between 2050 and 2100 for the shorelines with heritage characteristics (90% of the sites for RCP4.5 and 100% for RCP8.5). 9% of the archeological sites and 4% of the natural heritage sites are expected to have EWL doubled under RCP8.5.

While similar trends in EWLs are determined with Kirezci et al. (2020) dataset, there are some notable differences for the Turkish coast. One such difference is that the RCP8.5 projections of Kirezci et al. (2020) dataset is already within the projected values of LISCOAST dataset for RCP4.5 scenarios indicating a significant reduction of expected impact in terms of flooding for the same regions. In contrast, the rate of change is significantly higher, almost double LISCOAST values. Furthermore, some locations indicate a deceleration in the rate of sea level rise after 2050, which is another outcome. Still, the heritage sites expected to be threatened by flooding due to EWLs are 90% similar, indicating that these coastal areas should be considered for further assessments, which is the main objective of the TUBITAK-funded project. In addition to these initial results, the possible reasons for the differences between the two datasets and the consequences on the coastal heritage sites and their prioritization based on vulnerability and adaptation will be discussed.

REFERENCES

Vousdoukas, Mentashi, Voukouvalas, Verlaan, Jevrejeva, Jackson, Feyen. (2018): Global Extreme Sea Level projections. European Commission, Joint Research Centre (JRC) [Dataset] doi: 10.2905/jrc-liscoast-10012
Kirezci, Young, Ranasinghe, Muis, Nicholls, Lincke, Hinkel. (2020). Projections of global-scale extreme sea levels and resulting episodic coastal flooding over the 21st Century. Scientific reports, 10(1), 11629.

PROJECTION OF WAVE STORM CHARACTERISTICS UNDER THE RCP8.5 SCENARIO OFF THE ISTANBUL CANAL

Recep Emre ÇAKMAK, Bursa Uludag University, remrecakmak@uludag.edu.tr
Khalid AMAROUCHE, Bursa Uludag University, khalidamarouche@uludag.edu.tr
Adem AKPINAR, Bursa Uludag University, ademakpinar@uludag.edu.tr

INTRODUCTION

Wave conditions are one of the most important fundamental oceanic characteristics that will affect activities, existing structures, design, and planning in the marine environment and coastal areas. In the field of maritime transportation, appropriate routes can be determined by knowing the wave conditions. The Istanbul Canal is being designed as an artificial waterway as an alternative to the existing Istanbul Strait between the Black Sea and the Sea of Marmara. This waterway is expected to be used by passenger vessels and heavy tonnage cargo ships, as well as by vehicles that will serve a wide range of purposes such as fishing and tourism. Considering such widespread use, the knowledge of the wave storms on the offshore side of the canal is of great importance. Besides knowing the current storm characteristics, predicting future wave storm conditions is also crucial for the design of such a long-term project. Due to climate change, sea waves are predicted to change (Hemer et al., 2013) as in other parameters. Therefore, future changes in wave storm conditions should be considered in order to ensure accurate design and operations. The present study aims to project the changes in the storm waves that may be observed in the offshore area on the Black Sea side of Canal Istanbul at the end of the 21st century.

DATA

To investigate the change of wave storms, eight EURO-CORDEX regional wind simulations of the CMIP5 experiments covering the Black Sea basin with a spatial resolution of 0.11° and a temporal resolution of 6 hours were used. The different wind fields have in common the period 1970-2005 for the historical period and 2006-2099 for the future simulations. The future wave climate is simulated based on the RCP8.5 scenario representing the most severe case of CMIP5. SWAN spectral wave model was used for wave simulations. The wave data with a spatial resolution of about 8 km and hourly temporal resolution were obtained for the Black Sea.

STORM CHARACTERISATION

A wave storm can be identified as an occurrence in the ocean where the significant wave height (SWH) surpasses a defined threshold (SWH_t) over a significant duration of time. The minimum duration is considered 12 hours for a wave storm (Anfuso et al., 2016). The SWH threshold is determined based on the long-term wave regime (Mendoza et al., 2013). The SWH threshold is calculated with the following equation,

$$SWH_t = \bar{X} + 2\sigma \quad (1)$$

where $\bar{X}$ is the long-term SWH average and σ standard deviation of SWH. If the SWH remains below the SWH_t for a consecutive duration of 48 hours, the storms are regarded as separate from each other (Ojeda et al., 2017). To evaluate the intensity of the wave storm events, total storm wave energy (TSWE) and storm power index (SPI) are computed considering changes in storm duration. Arena et al. (2015) describe TSWE as:

$$TSWE = \int_{t_0}^{t_n} P_w(t)dt \quad (2)$$

where P_w is wave power. SPI is formulated (Dolan et al., n.d.) using SWH and storm duration T_d.

$$SPI = (SWH)^2 \times T_d \quad (3)$$

In order to evaluate the change of the wave storm regime at the end of a century, the storm characteristics of the future period 2070-2099 were compared with the characteristics of the period 1970-1999. The maximum and mean TSWE, SPI, SWH, and duration of storms were characterized for thirty-year periods.

RESULTS

The majority of future wave simulations project an increase in the number of storm events in the Black Sea. The results based on six of the climate models show a probable increase in wave storm intensity.

REFERENCES

Anfuso, Rangel-Buitrago, Cortés-Useche, Iglesias Castillo, Gracia (2016). Characterization of storm events along the Gulf of Cadiz (eastern central Atlantic Ocean). *International Journal of Climatology*, *36*(11), 3690-3707. https://doi.org/10.1002/JOC.4585

Arena, Laface, Malara, Romolo (2015). Estimation of Downtime and of Missed Energy Associated with a Wave Energy Converter by the Equivalent Power Storm Model. *Energies 2015, Vol. 8, Pages 11575-11591*, *8*(10), 11575-11591. https://doi.org/10.3390/EN81011575

Dolan, Davis (1992). An intensity scale for Atlantic coast northeast storms. *JSTOR*. Retrieved May 23, 2023, from https://www.jstor.org/stable/4298040

Hemer, Fan, Mori, Semedo, Wang (2013). Projected changes in wave climate from a multi-model ensemble. *Nature Climate Change*, *3*(5), 471-476. https://doi.org/10.1038/nclimate1791

Mendoza, Trejo-Rangel, Salles, Appendini, Lopez-Gonzalez, Torres-Freyermuth (2013). Storm characterization and coastal hazards in the Yucatan Peninsula. *Https://Doi.Org/10.2112/SI65-134.1*, *65*(sp1), 790-795. https://doi.org/10.2112/SI65-134.1

Ojeda, Appendini, Mendoza (2017). Storm-wave trends in Mexican waters of the Gulf of Mexico and Caribbean Sea. *Natural Hazards and Earth System Sciences*, *17*(8), 1305-1317. https://doi.org/10.5194/NHESS-17-1305-2017

PLACING ANTIFER BLOCKS ON ATLANTIC TIDAL COASTLINE USING ECHOSCOPE® & INNOVATIVE HYDRAULIC SYSTEM AT NEW SAFI PORT

Levent Cengiz, STFA Construction Group, lcengiz41@gmail.com
Orhun Serhat Yarar, STFA Construction Group, serhatyarar@gmail.com

ABSTRACT In the New Safi Port Project, constructed in the Moroccan city of Safi on North Africa's Atlantic west coast, Antifer blocks were used as the main breakwater armour layer.
The project's location was exposed to rough sea conditions resulting from the significant Atlantic swells. Due to a very tight work schedule, the project team had to focus on an alternative placement technique for the Antifer blocks rather than the conventional divers methods. It was decided to use the Echoscope® system to overcome poor visibility and improve productivity.
The project engineering department designed a unique hydraulic lifting apparatus and frame to adapt this sonar imaging system to the cranes. The system gave a 3D view underwater in real-time and allowed the crane operator to place the blocks. Consequently, the operation continued 24 hours a day, independent of the underwater visibility and in most sea conditions. In a short while, the daily installation rate improved from a maximum of 20 blocks per crane to over 90 blocks per day.
This was the first time the Echoscope®, a hydraulic lifting apparatus, was used to place Antifer blocks in a tidal Atlantic coast port project.

Figure 1 - General view of Antifer blocks placed in the main breakwater.

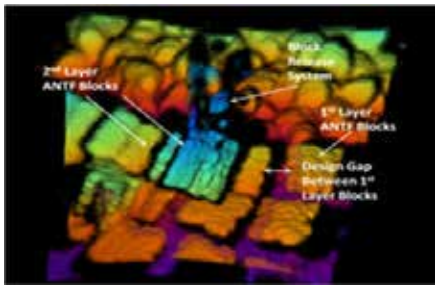

Figure 2 - Underwater views of Antifer blocks taken by Echoscope®

ACKNOWLEDGEMENTS

The author acknowledges that all parties contributed to developing the presented solution.

REFERENCES

Coda Octopus, 2023, Echoscope® 3D sonar systems product information, http://www.codaoctopus.com/products/3d/echoscope-product (accessed 10/03/2023)

Frens, AB., van Gent, MRA. & Olthof, J. et al. (2008) Placement Method For Antifer Armour Units. Proceedings of the 31st International Conference on Coastal Engineering, Hamburg (Smith JM (ed)). World Scientific Publishing, Singapore, pp. 3337-3346.

Frens AB (2007) The impact of placement method on Antifer-block stability. MSc thesis, Delft University of Technology, Delft, Netherlands.

Maquet J. (1985), Developments in Geotechnical Engineering, 37. Design and construction of mounds for breakwaters and coastal protection - Port of Antifer, France, P. Bruun (Ed.). Elsevier Science Publishers B.V., Amsterdam, Netherlands, pp. 696-703.

MLP-NN MODEL-BASED BIAS CORRECTION METHOD FOR SIGNIFICANT WAVE HEIGHT HINDCAST DATA TRAINED BASED ON SATELLITE ALTIMETRY OBSERVATIONS

Khalid Amarouche, Bursa Uludağ University, khalidamarouche@uludag.edu.tr
Adem Akpınar, Bursa Uludağ University, ademakpinar@uludag.edu.tr
Murat Kankal, Bursa Uludağ University, mkankal@uludag.edu.tr
Bahareh Kamranzad, University of Strathclyde, bahareh.kamranzad@strath.ac.uk

OVERVIEW

Knowledge of wave climate has become crucial for all marine activities, e.g. coastal and offshore structure design, naval architecture and marine renewable energy exploitation. For this application, it is necessary to dispose of accurate hindcast wave data. Accurate hindcast of significant wave height (SWH) allows us to ensure sustainable and economic development of coastal and offshore structures and to ensure an accurate projection of change and trend in SWH.
The performance of 3rd generation spectral wave models has been evaluated for the Black Sea through several studies (Amarouche et al., 2021a; Soran et al., 2022). the results revealed that the accuracy of the wave model for estimating SWH varies depending on the sea location and the wind climate of the area concerned by the simulation (Amarouche et al., 2021b). This variation may depend on the dominance of the swell compared to the wind sea in each location. Thus, the spatial variation in the model accuracy may depend on the precision of the wind input (Çakmak et al., 2019).
The calibration of wave models often allowed an improvement in the prediction of SWHs. However, varying amounts of bias can be observed depending on the geographical area and local wind conditions. The bias variation between the different locations also depends on the swell and wind sea contribution rate. There are currently several methods proposed for wave bias correction. Those evaluated by Parker and Hill (2017) are among these methods. Recently, a deep learning-based method was proposed for ocean wave correction (Sun et al., 2022). Thus ANN models are applied for Bias Correction of Operational Storm Surge Forecasts by (Tedesco et al., 2023).

STUDY OBJECTIVES

This study proposes an innovative approach for SWH correction at the spatial scale and 1D wave spectra correction at the local scale. The proposed method is based on the perceptron multilayer placement ANN model and satellite altimeter data. Nothing that the estimated SWH accuracy mainly depends on the local wind accuracy, the estimated swell partition, and other geographical factors at the spatial scale, the ANN model is trained and tested based on an estimated wind sea and swell partitions, coastal distance, and bathymetry as input, and satellite altimetry observations as output data for spectral biases correction. Figure 1 shows the used MLP-NN bias correction model structure.

PRIMARY RESULT

The ANN model developed in this study has resulted in a considerable improvement in the accuracy of SWH hindcast data in the whole Black Sea.
The methodology proposed here can be further improved by increasing the wave data measurements within the ANN model training and testing process.

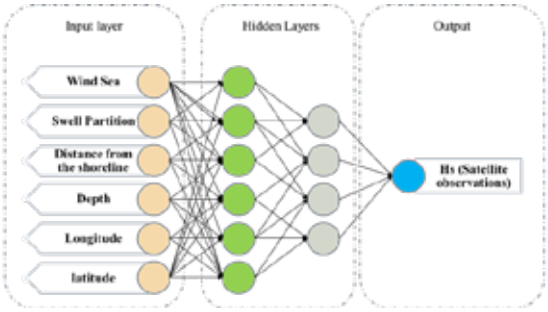

Figure 1 - MLP-NN bias correction model structure.

REFERENCES

Amarouche, Akpınar. Semedo, (2021a). Wave storm events in the Western Mediterranean Sea over four decades. Ocean Model. 170, 101933.
Amarouche, Akpınar, Soran, Myslenkov, Majidi, Kankal, Arkhipkin, (2021b). Spatial calibration of an unstructured SWAN model forced with CFSR and ERA5 winds for the Black and
Çakmak, Akpinar, Van-Vledder, (2019). Comparative Performance Analysis of Different Wind Fields in Southern and North-Western Coastal Areas of the Black Sea. Mediterr. Mar. Sci. 20, 427-452.
Parker, Hill. (2017). Evaluation of bias correction methods for wave modeling output. Ocean Model. 110, 52-65.
Soran, Amarouche, Akpınar, (2022). Spatial calibration of WAVEWATCH III model against satellite observations using different input and dissipation parameterizations in the Black Sea. Ocean Eng. 257, 111627.
Sun, Huang, Luo, Luo, Wright, Fu, Wang, (2022). A Deep Learning-Based Bias Correction Method for Predicting Ocean Surface Waves in the Northwest Pacific Ocean. Geophys. Res. Lett. 49, e2022GL100916.
Tedesco, Rabault, Sætra, Kristensen, Aarnes, Breivik, Mauritzen, Sætra, (2023). Bias Correction of Operational Storm Surge Forecasts Using Neural Networks. arXiv preprint arXiv:2301.00892.

.

DNS MODELING OF TRANSITION TO TURBULENCE IN OSCILLATORY WAVE BOUNDARY LAYERS

Selman Baysal, Çanakkale Onsekiz Mart University; and also Istanbul Technical University, selmanbaysal@comu.edu.tr
V. S. Ozgur Kirca, BM SUMER Consultancy & Research; and also Istanbul Technical University, kircave@itu.edu.tr
B. Mutlu Sumer, BM SUMER Consultancy & Research, bms@bmsumer.com

INTRODUCTION

The orbital motion of water particles under a progressive wave, in shallow waters, becomes a straight line parallel to the bottom, i.e., oscillatory motion, at the seabed. A new time-dependent boundary layer develops over the seabed for each half cycle of this motion. Turbulent oscillatory wave boundary layer is of great importance in many engineering applications, especially in coastal engineering. Even though both laminar and turbulent regimes have been considered in oscillatory boundary layers, of particular interest is the transitional regime. The laminar-to-turbulent transition first occurs in the form of tiny turbulent patches close to the wall, called turbulent spots, just before the near-bed flow reversal. These coherent structures are arrowhead-shaped isolated areas where the flow bursts with intense oscillations, in an otherwise laminar boundary-layer flow (Sumer and Fuhrman, 2020). Single or multiple spikes in the bed shear stress signal reaching up to 3 or 4 times the magnitude of the bed shear stress is a good indicator of a turbulent spot (Carstensen et al., 2010). Although much experimental and numerical research have been conducted (e.g., Carstensen et al. 2010, Jensen et al. 1989), there are still many unanswered questions regarding the transition. This study aims to address these questions using the DNS method, which has become very popular in turbulence-related problems (e.g., Mazzuoli et al. 2011, Xiong et al. 2020), by focusing on observing turbulent spots and locating their birthplace, concurrently with the bed shear stress under the spot structure. The present study are being conducted in close collaboration with Professor Liang Cheng and Drs. Chengwang Xiong and Chengjiao Ren of the University of Western Australia. The study is only in the early stages, and some early results will be presented at the meeting.

COMPUTATIONAL METHODS

The DNS model was conducted by the open-source Nektar++ framework. This section summarizes the implemented method, originally developed by Xiong et al. (2020). The governing equations for the oscillatory flow were solved using the *IncNavierStokesSolver* embedded in Nektar++. A 2-D mesh was defined and Fourier discretization was implemented in the spanwise direction to resolve the full 3-D features of the flow. An isolated roughness element was placed on the centre of the wall by using *LinearElasticSolver* to trigger the initial perturbations. This hump was removed at the very moment the primary vortex tube appeared. The length, the height and the breadth of the computational domain were chosen 500π, 100 and 32, respectively. While the no-slip condition was introduced on the lower boundaries, the slip boundary condition was applied on the upper boundaries of the computational domain. A high-order Neumann pressure condition was adapted to both the lower and upper boundaries and periodic condition was specified to the spanwise and streamwise boundaries. Also, the time-step (Δt) was carefully selected concerning the Courant-Friedrichs-Lewy (stability) criterion. The present model was validated against Xiong et al. (2020)'s results.

RESULTS AND CONCLUSIONS

The early results of the study indicate that the birth and growth of arrowhead-shaped turbulent spots, the characteristic features of transition to turbulence in the boundary layer, can be explicitly detected by the present method, whereby these structures can be traced in the numerical domain (Fig. 1). The focus in the later stages of the study shall be directed to capturing the hydrodynamic conditions (such as the instantaneous velocity and pressure values as well as their gradients) in the boundary layer that lead to the transtition to turbulence.

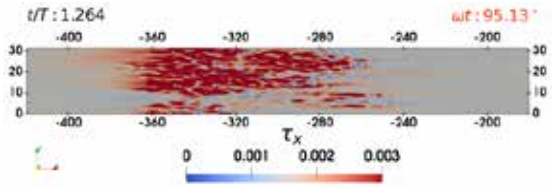

Figure 1 - The arrowhead-shaped pattern of bed shear stress. The Reynolds number is Re_δ=600.

ACKNOWLEDGEMENT

This work is funded by the Scientific and Technological Research Council of Turkiye (TUBITAK) through the project titled ''Qualitative and Quantitative Investigation of Laminar-to-Turbulent Transition in Steady and Unsteady Boundary Layers'' under Grant No. 122M024.

REFERENCES

Carstensen, Sumer, and Fredsøe (2010): Coherent structures in wave boundary layers. part 1. oscillatory motion, Journal of Fluid Mech., vol. 646, pp. 169-206.
Jensen, Sumer, and Fredsøe (1989): Turbulent oscillatory boundary layers at high Reynolds numbers, J. Fluid Mech., vol. 206, pp. 265-297.
Mazzuoli, Vittori, and Blondeaux (2011): Turbulent spots in oscillatory boundary layers, Journal of Fluid Mech., vol. 685, p.p. 365-376.
Sumer and Fuhrman (2020): Turbulence in Coastal and Civil Engineering, World Scientific.
Xiong, Qi, Gao, Xu, Ren, and Cheng (2020): The bypass transition mechanism of the stokes boundary layer in the intermittently turbulent regime, Journal of Fluid Mech., vol. 896, A4.

APPLICATION OF THREE-DIMENSIONAL POINT CLOUDS FOR MONITORING MORPHOLOGICAL CHANGES OF THE BEACH

Andrea Tadić, University of Rijeka, Faculty of Civil Engineering, andrea.tadic@uniri.hr
Suzana Ilić, Lancaster Environment Centre, Lancaster University, s.ilic@lancaster.ac.uk
Igor Ružić, University of Rijeka, Faculty of Civil Engineering, iruzic@uniri.hr

INTRODUCTION

Accurate topographic measurements with high spatial resolution are of increasing importance for the study of morphological changes and processes on beaches. In recent decades, geomorphological research has therefore turned to structure-from-motion (SfM) photogrammetry. This is a relatively inexpensive method based on the processing of three-dimensional (3D) point clouds generated from a series of photographs (James and Robson, 2012). There are few studies that address short-term changes following storms. Monitoring is more complex due to sensitivity of surveying precision in repeated high-resolution measurements. Survey quality depends on tide level, wave action, light conditions, camera position, texture and roughness of the filmed surface (Swirad et al., 2019). This paper describes the application of SfM photogrammetry to monitor morphological changes on the emerged part of Ploče beach in Rijeka, an artificial gravel beach, where waves cause significant erosion.

METHODOLOGY

The beach was surveyed 19 times between January 17, 2020 and February 26, 2021. Prior to the first survey, 12 ground control points (GCP) were marked along the fixed beach sections (concrete promenade, groynes; Figure 1).

Figure 1 - Study area

Point clouds were created in Agisoft Metashape from imagery from two unmanned aerial vehicles (UAV): Matrice 600 Pro Matrix with a Sony ILCE-7M2 camera and the Phantom 4 Pro. Positional RMSE values of the GCPs average 3.4 mm for X coordinate and 3.7 mm for Y. Vertical precision (Z) is slightly worse, with an average of 5.4mm for all surveys. Survey accuracy was verified in *CloudCompare* with the M3C2 plugin by comparing point clouds on fixed parts of the scene. A detailed procedure is described in the paper by Tadić et al. (2022). The same plugin was used to calculate the elevation changes and to display the erosion zones.

RESULTS

The accuracy and precision results show that there is no significant difference between the point clouds acquired by the two UAVs. The lower performance of the Phantom 4 is compensated by a lower flight altitude, more photos and flight time. The changes in the surface area and volume of the beach body were also analysed. Cross-shore and long-shore sediment migrations are well recorded. The analysis of the volume is associated with a calculated precision as the product of the beach area and the potential elevation error (± 5 cm). The results are shown in Figure 2D. The recorded volume changes are below the achieved accuracy for the volume, which is about ± 50 m³, but trends can be observed (e.g., increase in beach area and volume due to nourishment carried out after the 2nd and 10th survey).

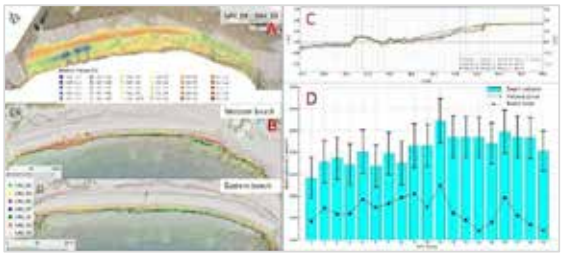

Figure 2 - Ploče beach monitoring: elevation changes (A), shoreline position (B), cross sections (C), volume and beach area (D) (source: Tadic et al., 2022)

CONCLUSIONS

The SfM photogrammetric method using drones allows the collection of a large amount of spatial data in a relatively short time, and can be used with satisfactory accuracy to monitor morphological changes of gravel beaches. It is primarily possible to monitor elevation changes between successive measurements, which are significantly higher on studied beach than the achieved accuracy of point clouds. It was found that the changes are non-uniform and occur on different parts of the beach, ranging from minor changes along the shoreline to major changes affecting the entire beach during storms.

REFERENCES

James, Robson (2012): Straightforward reconstruction of 3D surfaces and topography with a camera: Accuracy and geoscience application, Journal of Geophysical Research: Earth Surface, vol. 117, 3.
Swirad, Rosser, Brain (2019): Identifying mechanisms of shore platform erosion using Structure-from-Motion (SfM) photogrammetry, Earth Surface Processes and Landforms, vol. 44, pp. 1542-1558.
Tadić, Ružić, Krvavica, Ilić (2022): Post-Nourishment Changes of an Artificial Gravel Pocket Beach Using UAV Imagery, Journal of Marine Science and Engineering, vol. 10, 358.

3D NUMERICAL MODELLING OF SOLITARY WAVE INTERACTION OVER A CONICAL ISLAND

Firoj Shaik, Indian Institute of Technology Kharagpur, firojshaik222@gmail.com
Afzal Mohammad Saud, Indian Institute of Technology Kharagpur, saud1231@gmail.com

ABSTRACT
In this paper, three-dimensional numerical modelling of flow around a conical island is presented. The open source CFD model REEF3D is employed to investigate the solitary wave impact over a conical island. The numerical model solves the incompressible Reynolds Averaged Navier-stokes (RANS) equations using the finite difference method. The free surface is modeled with the level set method based on a two-phase flow approximation. The model is validated first with the experimental data of a solitary wave propagating over a conical island and good agreement between the experiment and simulation data is observed. The model is then applied to study the detailed 3D velocity field, vorticity evolution and impact of wave forces in both emerged and submerged condition. Maximum run-up heights were computed around the island and under certain conditions, enhanced runup and wave trapping on the lee side of the island were observed.

INTRODUCTION

Coral reef islands are accumulations of unconsolidated carbonate sand and gravel deposited on reef platforms by wave and current processes (For example Vabbinfaru island as shown in Figure 1). These reef top landforms typically have a maximum elevation less than 5 m above mean sea level and sustain populations of small island nations throughout the world's tropical seas (Beetham et al. 2014). As a consequence of their low elevation and unconsolidated sediment, reef islands and reef island communities are considered vulnerable to the threat of rising sea level. Therefore, the runup/inundation of solitary wave on a reef island is an important subject to evaluate risk of tsunami waves to coastal regions.
In this study, we numerically investigate the solitary wave interaction and associated hydrodynamic characteristics such as flow field, vorticity evolution, impact of wave forces, and runup of single-crest solitary wave on a conical island using open source numerical model REEF3D.

NUMERICAL MODEL

The open-source CFD model REEF3D solves the fluid flow problem using the incompressible Reynolds-Averaged Navier-Stokes (RANS) equations along with the continuity equation:

$$\frac{\partial u_i}{\partial x_i} = 0 \qquad (1)$$

$$\frac{\partial u_i}{\partial t} + u_j \frac{\partial u_i}{\partial x_j} = -\frac{1}{\rho}\frac{\partial p}{\partial x_i} + \frac{\partial}{\partial x_j}\left[(\nu + \nu_t)\left(\frac{\partial u_i}{\partial x_j} + \frac{\partial u_j}{\partial x_i}\right)\right] + g_i \qquad (2)$$

Where u_i is the fluid velocity, ρ is the fluid density, p is the pressure, ν is the kinematic viscosity, ν_t is the eddy viscosity and g is the acceleration due to gravity. The convective terms of the momentum and level set equations are discretized using the fifth-order Weighted Essentially Non-Oscillatory (WENO) scheme and time discretization is done using the third-order total variation diminishing (TVD) Runge-Kutta Scheme. The adaptive time-stepping technique is used to ensure the stability of the solution. The simulations are carried out in a 3D numerical wave tank, Solitary waves are generated by specifying different wave heights in both emerged and submerged condition of conical island.

Figure 1 - Google image of Vabbinfaru Island

REFERENCES

Beetham, E. P., & Kench, P. S. (2014). Wave energy gradients and shoreline change on Vabbinfaru platform, Maldives. *Geomorphology*, *209*, 98-110.

OBSERVATION OF LONG-PERIOD WAVES AND SHIP OSCILLATION IN SAKATA PORT, JAPAN

Yuhi Hayakawa, Alpha Hydraulic Engineering Consultants. Co., Ltd., hayakawa@ahec.jp
Yuya Yoshida, Alpha Hydraulic Engineering Consultants. Co., Ltd., y-yoshida@ahec.jp
Ryosuke Sudayama, formerly Tohoku Regional Development Bureau, Sakata Port Office, sudayama-r82ab@mlit.go.jp
Osamu Hayakawa, formerly Tohoku Regional Development Bureau, Sakata Port Office, hayakawa-o82ab@mlit.go.jp
Takehito Horie, Alpha Hydraulic Engineering Consultants. Co., Ltd., horie@ahec.jp
Hitoshi Tanaka, Alpha Hydraulic Engineering Consultants. Co., Ltd., h-tanaka@ahec.jp

INTRODUCTION

In winter, ship oscillation occurs at Sakata Port, Japan, affecting mooring cargo and even breaking mooring ropes. Although the origin of the oscillation may be long-period waves, it has not been identified yet. This study reports observations of waves and ship movements to identify the origin of the ship oscillation at Sakata Port.

METHODOLOGY

(1) Wave measurements : Wave observation was conducted at Takasago (St.1) and Kominato (St.2) quays from November 8th, 2020 to December 25th, 2021. Ultrasonic wave-height meters (WAVE HUNTER, I.O.Technic Co., Ltd.) were deployed at each quay. Wave characteristics were calculated by zero-up-crossing analysis and time resolutions for short-period (T<30s) and long-period (T=30-300s) waves were 20 and 60 minutes, respectively.
(2) Ship movement observation: Ship oscillation was observed by video camera during wave measurements and amplitudes of surge, sway, and heave were analyzed with image analysis.

RESULTS

(1)Wave measurements (Figure 1): The significant wave heights of short-period and long-period waves inside the port were correlated with the temporal changes in wave height outside the harbor. The wave energy of long-period waves increased as the energy of short-period waves increased. Spectral analysis revealed a peak appeared at 0.01 to 0.03 Hz, when long-period waves developed in Sakata. Although energy of short-period waves inside the port reduced, that of long-period waves decreased slightly, and equivalent energy to that outside the port propagated inside the port, as observed from the offshore spectrum estimated from water level data collected at Nowphas Akita Port.
(2)Ship oscillation: Both container and pellet ships exceeded cargo handling oscillation limits (PIANC, 1995) in terms of surge and sway. Interviews with the cargo handling operators after observation confirmed that the mooring rope had broken in the pellet ship. Spectral analysis for both motion components showed that peaks appeared in the long-period range (T=30-300 seconds). Amplification ratio of surge and sway to long-period wave component was found to be high based on wave observation results and vessel motion, calculated from the power spectrum of surge and sway which exceeded the allowable cargo handling oscillation limits (Figure 2).

DISCUSSION

Among wave components developed offshore of Sakata Port, the short-period component declined due to wave breaking and the shielding of breakwaters, though the long-period waves had less attenuation same as Sakakibara and Kubo (2008). The horizontal plane (sway, surge and yaw) is strongly correlated with the total wave energy in the system and, more importantly, with the ratio of LF (low frequency, 2.5-40 mHz) band to total energy (López and Iglesias, 2014). As evidenced by the amplification of the vessel motion spectrum in the long-period range for surge and sway, the long-period waves were the main cause of vessel motion.

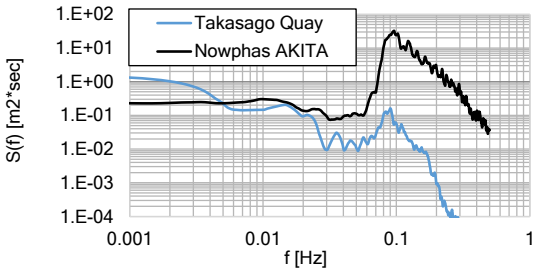

Figure 1 - Wave power spectrum when long-period wave developed (Dec 15, 2020)

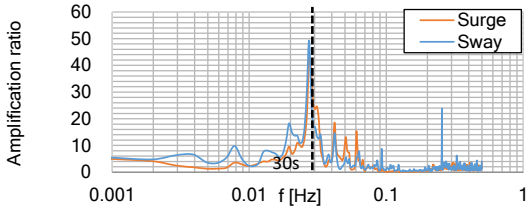

Figure 2 - Amplification ratio of surge and sway to surface wave

REFERENCES

López, Iglesias (2014): Long wave effects on a vessel at berth, Applied Ocean Research, ELSEVIER, vol. 47, pp.63-72.
PIANC (1995): Criteria for movements of moored ships in harbours -A practical guide, Report of Working Group No.24 of the Permanent Technical Committee II.
Sakakibara, kubo (2008); Characteristics of low-frequency motions of ships moored inside ports and harbors on the basis of field observations, Marine Structures, ELSEVIER, vol. 21, pp.196-223.

INVESTIGATION OF WAVE LOADS AT THE LEE-SIDE OF A RUBBLE MOUND BREAKWATER HEAD

Cem Sevindik, Middle East Technical University, cem.sevindik@metu.edu.tr
Furkan Demir, Middle East Technical University, demir.furkan@metu.edu.tr
Baris Ufuk Senturk, Middle East Technical University, ufuk@metu.edu.tr
Hasan Gokhan Guler, Middle East Technical University, goguler@metu.edu.tr
Cuneyt Baykal, Middle East Technical University, cbaykal@metu.edu.tr
Gulizar Ozyurt Tarakcioglu, Middle East Technical University, gulizar@metu.edu.tr
Isikhan Guler, Middle East Technical University, isikhan@metu.edu.tr
Ahmet Cevdet Yalciner, Middle East Technical University, yalciner@metu.edu.tr
Aysen Ergin, Middle East Technical University, ergin@metu.edu.tr

INTRODUCTION

Many experimental and numerical studies have been previously performed to understand the wave-structure interaction for the rubble mound breakwaters. In general, it is a common practice to use heavier rock or artificial armor layer units at the head section since this section is more critical than the trunk section due to "high cone-overflow velocities" enhanced by wave refraction and breaking and reduced support of neighboring units (CIRIA et al., 2007; USACE, 2011). The fact that the lee-side of the head section suffers from excessive damage compared to the other regions of head section is highlighted in several references. However, the relation between the wave loads and the damage focused there has not been investigated in detail. The objective of this study is to investigate the relation between wave parameters (individual wave height, wave period, breaking type, etc.) and wave load acting on the lee-side of the breakwater head by utilizing physical model experiments and computational fluid dynamics (CFD) modelling studies.

EXPERIMENTAL SET-UP AND DATA ANALYSIS

Experimental studies were performed in the wave flume at Middle East Technical University, Civil Engineering Department, Coastal and Ocean Engineering Laboratory having 26.9 m length, 6.0 m width, and 1.0 m depth. The tested breakwater cross-section was an existing rubble mound breakwater head, constructed using antifer armor units with a model scale of 1/60. Tests with regular waves were conducted having twelve different wave periods between 1.5 s - 2.5 s and wave heights in the range of 0.14-0.27 m at six different water depths between 0.57 m - 0.67 m in front of the wave generator. Water surface elevation and particle velocity measurements were performed respectively at three and six separate locations. Velocity measurements were conducted using an Acoustic Doppler Velocimeter. Moreover, a single pressure sensor was flush-mounted on the top surface of an antifer armor unit, and this antifer unit was placed at a location where the damage at the head is focused. The tested cross-section is shown at an instant during the experiments, indicating the locations of the pressure sensor and a wave gauge in Fig. 1.

The pressure and velocity signals were denoised applying several different signal filtering techniques including low pass filters, moving average and various wavelet transform methods. The results are assessed comparatively based on several statistical parameters to find out the best filtering method. The experimental measurements are investigated systematically using non-dimensional parameters, revealed as a result of detailed dimensional analysis.

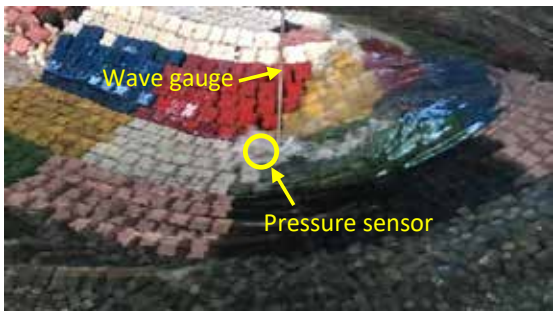

Figure 1 - Experimental set-up of the physical model

CFD MODELLING STUDIES

CFD modelling studies were also carried out to elucidate on the physical processes causing the focused damage at the lee-side of rubble mound breakwater heads. The waves2Foam (Jacobsen et al., 2012) package was used in the CFD modelling studies, capable of generating and absorbing waves, solving flow characteristics inside and outside the porous media and capturing free-surface. In the CFD simulations, the flow characteristics around breakwater head section were computed, and the experimental and numerical observations are compared.

RESULTS

The results of the present work show that the hydro-dynamic loading over a single antifer unit during the passage of a wave significantly varies based on the breaking characteristics of the wave and the location of the breaker with respect to the antifer unit.

REFERENCES

USACE (2011). Coastal Eng. Manual. (3rd Update).
CIRIA, CUR, CETMEF (2007). The Rock Manual - The use of rock in hydraulic engineering. C683. England.
Jacobsen, Fuhrman, Fredsoe (2012). A wave generation toolbox for the open-source CFD library: OpenFoam. Int. J. Numer. Meth. Fluids. 70:1073-1088.

EFFECTS OF ANTIFER PLACEMENT METHODS ON WAVE OVERTOPPING AND WAVE LOADS ON CROWN-WALLS

Furkan Demir, Middle East Technical University, demir.furkan@metu.edu.tr
Berkay Erler, Middle East Technical University, erler.berkay@metu.edu.tr
Baris Ufuk Senturk, Middle East Technical University, ufuk@metu.edu.tr
Hasan Gokhan Guler, Middle East Technical University, goguler@metu.edu.tr
Cuneyt Baykal, Middle East Technical University, cbaykal@metu.edu.tr
Gulizar Ozyurt Tarakcioglu, Middle East Technical University, gulizar@metu.edu.tr
Dogan Kisacik, İzmir Institute of Technology, dogankisacik@iyte.edu.tr
Isikhan Guler, Middle East Technical University, isikhan@metu.edu.tr
Ahmet Cevdet Yalciner, Middle East Technical University, yalciner@metu.edu.tr
Aysen Ergin, Middle East Technical University, ergin@metu.edu.tr

INTRODUCTION

The wave overtopping over the conventional rubble mound structures and the wave loads acting on the crown walls have been studied widely in the literature (see e.g. CIRIA et al. 2007; EurOtop 2018). The roughness of the armor layer depending on the unit type has been parameterized in the existing wave run-up and overtopping formulas. However, the effect of the armor unit placement methods has not yet been addressed in above formulas. On the other hand, armor unit types and placement methods have not been considered in the design of crown walls, though these have apparent effects on the loading based on run-up and overtopping observations. The aim of this study is to investigate the effect of different placement methods and packing densities of antifer units on the wave overtopping and the wave loads on the crown walls. In this context, an experimental study has been conducted on a conventional rubble mound breakwater cross-section with a crown wall, constructed with antifer units in the armor layer.

METHODOLOGY

Experimental studies were performed at Middle East Technical University, Civil Engineering Department, Coastal and Ocean Engineering Laboratory in a wave flume having 26.9 m length, 6.0 m width, and 1.0 m depth. In the physical modelling experiments, a rubble mound breakwater trunk section with a face slope of 1:2 was built in the wave flume without a foreshore slope. In this study, two closed pyramid (CP), four double pyramid (DP) and two irregular (IR) placement methods for antifer units were tested with different packing densities. In total, two bichromatic (for further numerical investigations) and five irregular wave series with the wave steepnesses ($H_{m0}/L_{m-1,0}$) ranging in between 0.025-0.038 and the relative crest heights (R_c/H_{m0}) in between 0.68-1.35 were used in the experiments. The water surface elevations were measured at ten different locations along the wave flume. The individual wave overtopping measuring system was set-up at the breakwater crest following recommendations by Koosheh et al. (2022). In addition, pressure transducers were installed flush on the front and bottom faces of the crown wall at a total of twelve locations. Water particle velocity measurements were performed at two different locations along the wave flume using an Acoustic Doppler Velocimeter (ADV). The experimental setup of the is presented in Figure 1.

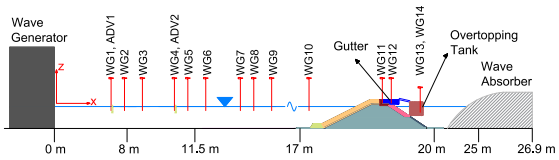

Figure 1 - Experimental set-up.

RESULTS

The results of the present work show that different antifer placement methods and the packing densities significantly change the wave overtopping and the wave loads acting on the crown wall. For the same packing density, the mean overtopping rate for DP placement method was observed 185% larger than IR placement method. Packing density increase of 5% for same placement method caused an increase in mean overtopping rate up to 30%. For similar packing densities (CP and DP), the maximum pressure values observed for CP were 60% less than the DP on the front face of the crown wall. With a 5% increase in packing density, maximum pressure values decreased by up to 50%.

ACKNOWLEDGMENT

This study is funded by the research project ''Modeling the Effects of Different Units and Placement Methods on Wave Overtopping and Forces Acting on Crown-Walls of Rubble Mound Breakwaters'' supported by the Scientific and Technological Research Council of Turkey (Grant No. 122M053).

REFERENCES

EurOtop (2018). "Manual on wave overtopping of sea defences and related structures. An overtopping manual largely based on European research, but for worldwide application". Van der Meer, Allsop, Bruce, De Rouck, Kortenhaus, Pullen, Schüttrumpf, Troch, and Zanuttigh, www.overtopping-manual.com.

CIRIA, CUR, CETMEF (2007). The Rock Manual - The use of rock in hydraulic engineering. C683. England.

Koosheh, Etemad-Shahidi, Cartwright, Tomlinson, van Gent. (2022). Distribution of individual wave overtopping volumes at rubble mound seawalls. Coast. Eng. 177, 104173.

ASSESSING STORM SURGE IMPACTS ON A GAS TO POWER PROJECT SITE: A COMPARATIVE ANALYSIS IN COLON, PANAMA

Mehrdad Salehi, Sargent & Lundy, Mehrdad.Salehi@sargentlundy.com

This conference abstract presents a comprehensive study that focuses on assessing storm surge impacts specifically on a Gas to Power project site in Colon, Panama. The analysis incorporates regional wind and water level data from reputable sources such as the National Oceanographic and Atmospheric Administration (NOAA), the National Aeronautics and Space Administration (NASA) National Hurricane Center (NHC), and the Joint Typhoon Warning Center (JTWC).

The study begins by reviewing the regional wind data and comparing it to hurricane and tropical storm tracks, satellite images, and the Saffir-Simpson category ranges. The proximity of storms to regional wind stations and the Gas to Power project site in Colon is evaluated, providing crucial insights into storm behavior and intensity within the specific context.

Furthermore, available local water level data is examined to calculate extreme total water levels (See Figure 1), which combine both tide and storm surge. The suitability of these water level records for estimating return periods and correlating specific water level events with storm tracks is also assessed, ensuring the accuracy and relevance of the findings within the Colon region. Figure 2 indicates that some tropical cyclones generated in the Southern Caribbean off the coast of Panama track north, away from the coast of Panama.

The analysis proceeds by ranking historic storm surges by magnitude and identifying surges that exceed a predetermined threshold above the highest astronomic tide. These surges are then linked to the named hurricanes occurring on the same dates, establishing a direct association between storm events and their corresponding surges specifically in the Colon area.

Additionally, a one-dimensional storm surge analysis is conducted, leveraging estimates of extreme winds and local bathymetric data to model and predict the potential impacts of storm surges on the Gas to Power project site in Colon.

By comparing the water level, wind data, and storm tracking information, this study aims to assess the risk of storm surge impacts on the Gas to Power project site in Colon, Panama. The findings will provide valuable insights into the vulnerability of the site to storm events, enabling improved preparedness and mitigation strategies for the Gas to Power project.

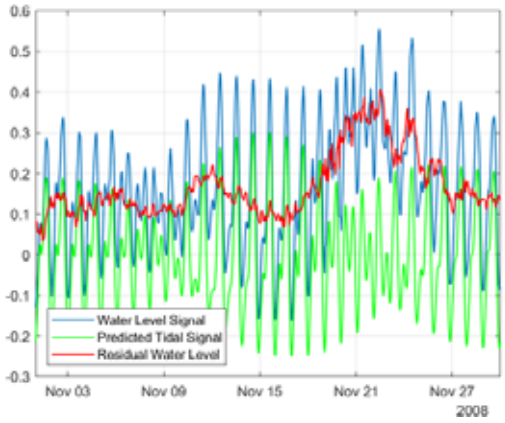

Figure 1 - Example sub-series showing decomposition of station water level record into predicted tidal signal and residual water level.

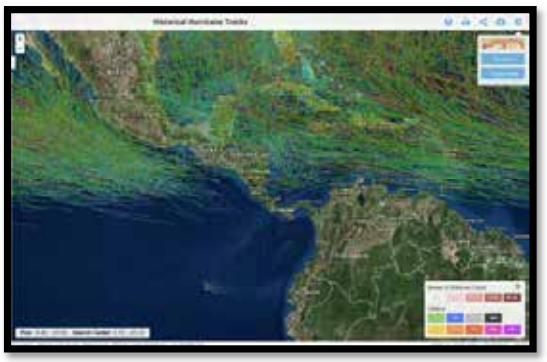

Figure 2 - Historical cyclone tracks in the vicinity of Panama from 1862 to present. (Source: NHC, 2018)

Keywords: storm surge impacts, regional wind data, water level analysis, Gas to Power project, Colon, Panama.

REFERENCES

National Hurricane Center, (2018). Historical Hurricane Tracks Tool. Version 4.0. https://www.coast.noaa.gov/hurricanes/

National Oceanic and Atmospheric Administration (NOAA) (2018) National Hurricane Center: Saffir-Simpson Hurricane Scale. Accessed 2018-08-08 at https://www.nhc.noaa.gov/aboutsshws.php

COASTAL VULNERABILITY ASSESSMENT OF THE FRENCH MEDITERRANEAN COASTS TO STORMS FLOODING AND EROSION PHENOMENA, MORPHODYNAMIC MODELING UNDER CLIMATE CHANGE PROJECTIONS

Nico Valentini, BRGM - University of Montpellier, n.valentini@brgm.fr
Yann Balouin, BRGM - University of Montpellier, y.balouin@brgm.fr

INTRODUCTION

Storm events on sandy coastal environments already weakened by a sediment deficit can generate a strong erosion of the beach-dune system, accentuating the phenomena of marine flooding and damage to infrastructures. In order to assess this risk of coastal flooding under stormy conditions and taking into account climate change and the new IPCC projection (IPCC, 2021), modeling approaches nowadays provide a robust tool. In this study, a modeling chain is used to simulate present-day and future coastal hazards on the Mediterranean French coastline, taking into account the complex interaction of hydrodynamic and morpho dynamic phenomena.

METHOD

In order to build a regional strategy for the evaluation of the coastal hazards under storm events, a methodology is proposed to evaluate the reality of a potential increase of coastal flooding following dune/beach erosion and to identify the concerned coastal regions for prioritizing regional coastal zone management actions.
First, a coastal-dune vulnerability index is built at a regional scale and a clustering analysis used to identify the most vulnerable sites. Then, two representative sites are used for being modelled for coastal flooding assessment, under climate change scenarios.
The vulnerability index is based on an adaptation of the protocol proposed by García-Mora et al. (2000, 2001), Idier et al. (2013) and applied in Ciccarelli et al. (2017). Four groups of variables have been studied: geomorphological conditions of the dune system, marine influence, vegetation condition and the anthropic effects. In this study, 81 coastal sectors, based on geomorphic features are chosen and 17 variables, including both the quantitative and the qualitative parameters, are considered in the coastal dune vulnerability classification. A hierarchical clustering to create homogeneous sector groups from the similarity matrix of sector variables is applied. The sites of Canet-en-Roussillon and Frontignan are chosen from the two main clusters for a numerical approach to analyze the effects of storm erosion on the magnitude of flooding, based on the coupling of SWAN and the XBEACH morpho dynamic model, in its surf beat mode. This implementation allowed a calibration phase using historical data available under storms events, a large sensitivity test to adjust physical and numerical parameters is performed. This approach allowed identifying the main processes leading to flooding. In a second step, the modeling chain is used to simulate extreme events scenarios with a 10 and 50-year return period (on wave heights), by including the sea level rise contributions, in order to assess the coastal risks associated.

RESULTS

Beyond this strong disparity between the different groups obtained in the clustering analysis, it appears that the overall vulnerability index is high (value greater than 0.5)

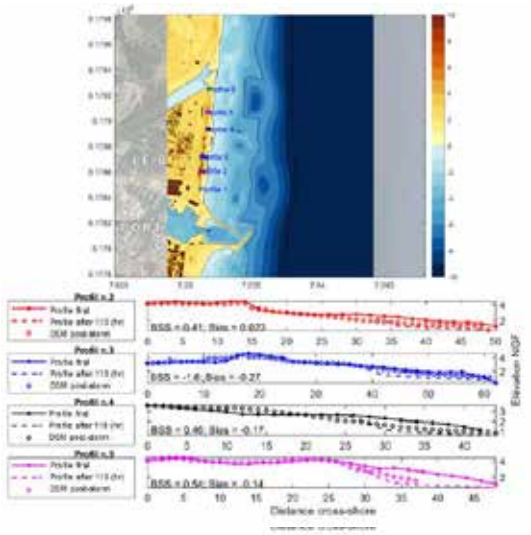

for a significant length of the regional coastline. This represents about 35% of the coastline that would present an increased vulnerability to marine submersion due to their sensitivity to coastal erosion events. The amplitude of the XBEACH-modelled erosion and flooding at both sites are in line with observations made during and after storms. Figure 1 shows the profile-based XBEACH performance at Canet-en-Roussillon. The results of the modeling chain with the IPCC projections scenarios depicts the great influence of sea-level-rise contribution in linearly increasing the submerged volumes.

REFERENCES

Ciccarelli, D., Pinna, et al. (2017). Development of a coastal dune vulnerability index for Mediterranean ecosystems: A useful tool for coastal managers? Estuarine, Coastal and Shelf Science, 187, 84-95.
García-Mora, M.R., Gallego-Fernandez, J.B., Williams, *A.T., García-Novo, F., (2001).* A coastal dune vulnerability classification. A case study of the SW Iberian Peninsula. J. Coast. Res. 17, 802-811.
Idier, D., Castelle, B., et al. (2013). Vulnerability of sand coasts to climate variability. Climate Research 57, 19-44.
IPCC, 2021: Summary for Policymakers. In: Climate Change 2021: The Physical Science Basis. Contribution of Working Group I to the Sixth Assessment Report of the Intergovernmental Panel on Climate, etc.

HIDRALERTA SYSTEM - AVEIRO HARBOUR

Conceição J.E.M. Fortes, LNEC - National Laboratory for Civil Engineering, jfortes@lnec.pt
Liliana Pinheiro, LNEC - National Laboratory for Civil Engineering, lpinheiro@lnec.pt
Ana Catarina Zózimo, LNEC - National Laboratory for Civil Engineering, aczozimo@lnec.pt
Michelle Kleinjan < >, LNEC - National Laboratory for Civil Engineering / Saxion University of Applied Sciences, 495465@student.saxion.nl

ABSTRACT

The C2IMPRESS project, Co-creative improved understanding and awareness of multi-hazard risks for disaster-resilient society, is funded by the European Union through the Horizon Europe programme. The project consortium is made up of sixteen partners from different countries. C2IMPRESS aims to develop an innovative set of products (e.g., models, methods, tools, and technologies) that contribute to a more resilient society in the face of isolated risks and multiple risks due to extreme weather events under different climate change scenarios. More specifically, it intends to provide quantitative and qualitative data with high spatial and temporal resolution, solutions adapted to each location, and forecasts with less uncertainty. The project's social and technical innovations will allow for a better understanding and awareness of citizens in the face of risks associated with multiple hazards (e.g., river and coastal floods, fires, heat waves, earthquakes), the multidimensional impacts associated with these risks, as well as to vulnerabilities and resilience to extreme events in four case study areas (CSA) in Europe. The four CSAs are: Egaleo (Greece), Ordu (Turkey), Mallorca (Balearic Islands, Spain), and the Central Region (Portugal). The CSAs present different characteristics and challenges, allowing to broaden the representativeness of the results foreseen in the project.

The CSA case of Portugal is subdivided in five different sub-cases, being one of those sub-cases the Aveiro harbour and adjacent beach areas, where coastal flooding, wave overtopping, forces on moorings, and ship maneuvering will be studied. Aveiro is a city in the center of Portugal about seventy kilometers south of Porto, with an extensive sandy coastal line. Aveiro has a large port (Figure 1) inserted in a river's mouth, with several sectors of industry accommodated within the port.

Figure 1 - Aveiro harbour, Portugal

Extreme wave events occur in Aveiro harbour and adjacent beach areas, such as coastal flooding, wave-induced overtopping, and risks for moored and maneuvering ships. To reduce the impact of these multi-hazards risks, one of the tasks of C2IMPRESS is to develop a forecast and early warning system for Aveiro's harbour region, based upon HIDRALERTA (Poseiro, 2019). This system can be very cost-effective and provides solutions for disaster preparation thus helping the responsible authorities to respond correctly and promptly to emergency situations.

HIDRALERTA system is a wave overtopping/moored ships forecast system with early warning and risk assessment capabilities. As a forecast and early warning tool, HIDRALERTA enables the identification of emergency situations in advance, prompting the responsible entities to adopt measures to avoid loss of lives and minimize damage. The system provides forecasts, 72 hours in advance and with a 3-hour interval of wave climate characteristics, associated consequences, and associated risk levels. As a long-term planning tool, the system uses datasets of several years of sea-wave/water level characteristics and/or pre-defined scenarios, to evaluate wave overtopping and flooding risks of the protected areas, allowing the construction of risk maps. HIDRALERTA uses a combination of numerical models to simulate wave propagation, estimate mean overtopping discharge over port infrastructures and costal defense structures and determine motions and mooring forces of ships.

This paper presents the prototype of HIDRALERTA for the port of Aveiro, showing the potential of the system, both as a tool for forecasting and warning of emergency situations and as a tool for planning and managing the risk in climate change scenarios. The prototype for Aveiro harbour showcases a new feature of HIDRALERTA system, which is the early warning system for maneuvering ships along the entrance channel, following the work of the BlueSafePort project.

ACKNOWLEDGEMENTS
C2IMPRESS (Horizon Europe, grant agreement N.º 101074004), BlueSafePort Project FA_04_2017_016 and the National Infrastructure for Distributed Computing (INCD)

REFERENCES

Poseiro, P. (2019). *Forecast and Early Warning System for Wave Overtopping and Flooding in Coastal and Harbour Areas: Development of a Model and Risk Assessment*. PhD Thesis, IST-UL.

NEW DEVELOPMENTS IN THE PRAIA DA VITÓRIA BAY AND HARBOUR EARLY WARNING SYSTEM

Liliana V. Pinheiro, National Laboratory for Civil Engineering, Lisbon, lpinheiro@lnec.pt
Ana Catarina Zózimo, LNEC - National Laboratory for Civil Engineering, aczozimo@lnec.pt
Conceição J.E.M. Fortes, National Laboratory for Civil Engineering, Lisbon, jfortes@lnec.pt

ABSTRACT
Praia da Vitória bay and harbour Early Warning System (EWS), Pinheiro et al. (2020), is running daily to provide emergency situations alerts related to wave overtopping and ship navigation in ports, as well as operational constraints. Port terminals downtime leads to large economic losses and largely affects the port's overall competitiveness. So, the goal of such EWS is to reduce the port's vulnerability by increasing its planning capacity and efficient response to emergency situations.
The system uses available forecasts of regional wind and sea-wave characteristics offshore, together with astronomical tidal data as inputs to a set of numerical models. These numerical models provide estimates of wave and wind characteristics in all domains, from regional scales simulated with several nested grids with SWAN model (Booij et al., 1996), to local scale, using a non-linear boussinesq-type model or a linear mild-slope model (Figure 1). Finally, the ship's response to those wave and wind forcings is computed using a hydrodynamic 3D panel method model (Korsemeyer et al. 1988) and a motion equation solver (Figure 2).
Forecasted hourly movements and mooring forces are compared with pre-set thresholds. Probability assessment of exceedance of those values results in a risk level assessment. Finally, based on the forecasted risk level, emergency situations as well as port operations' safety can be foreseen in advance (72h) and the adequate warning alerts can be issued.
All information provided by this EWS is available in a dedicated website and mobile application. Additionally, an alert bulletin is sent by email to interest parties. Thus, port stakeholders benefit from a decision- support tool to timely implement mitigation measures and prevent accidents and economic losses.
Within the LIFE Garachico project this system is being extended to include methodologies for creating an effective flexible adaptation strategic framework for coastal area of Praia da Vitória. This strategic framework is based on the definition of acceptable risk levels and specific interventions at the local level, allowing to increase the resilience of coastal urban areas against extreme coastal events (both present and future) consequences of climate change.
One upgrade is the implementation of adaptation measures for flood risk prevention in the regions and the creation of a manual of technical recommendations.
Another upgrade to the system is the use of neural network tools for calibrating the wave propagation models. As any EWS, its usefulness depends greatly on its reliability and accuracy. To achieve more accurate predictions a new method was developed to optimize forecasts produced by the system. Using available database from buoys, pressure sensors and meteorological stations, neural networks were trained to optimize numerical models results. The trained networks proved to provide more accurate estimates for certain variables, thus improving the reliability of the EWS.

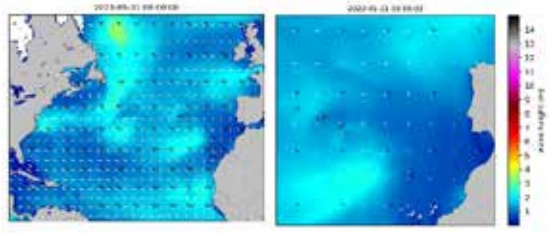

Figure 1 - Wave and wind forecasts. ECMWF-WAM & CMEMS Copernicus Marine Service Forecasts.

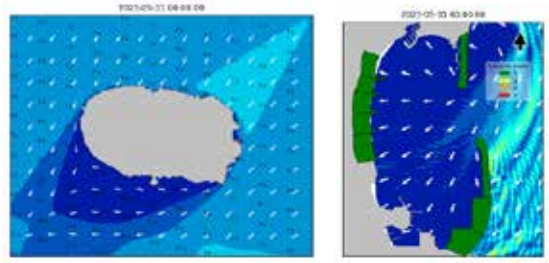

Figure 2 - Wave forecasts and Alerts. SWAN and DREAMS numerical models.

ACKNOWLEDGMENTS
The authors thank the financial support of LIFE garachico Project (LIFE20 CCA / ES / 001641), "Fundo Azul" project BlueSafePort (Ref: FA_04_2017_016) - Safety System for Maneuvering and Moored Ships in Ports and the FCT project To-SeAlert: (Ref. PTDC/EAM-OCE/31207/2017).

REFERENCES

Booij, Holthuijsen, Ris, (1996): The SWAN wave model for shallow water. ICCE 96 Orlando, pp. 668-676.
Korsemeyer, Lee, Newman, Sclavounos (1988): The analysis of wave effects on tension-leg platforms, 7th International Conference on Offshore Mechanics and Arctic Engineering, Houston, Texas, pp. 1-14.
Pinheiro, Fortes, Reis, Santos, Guedes-Soares (2020): Risk Forecast System for Moored Ships. Coastal Engineering Proceedings, (36v), management.37. https://doi.org/10.9753/icce.v36v.management.37
Pinheiro, Fortes, Reis, Santos, Guedes-Soares (2022): Neural Networks For Optimization Of An Early Warning System For Moored Ships In Harbours. Coastal Engineering Proceedings, (36v), management.37. https://doi.org/10.9753/icce.v36v.management.37

INVESTIGATION OF THE DAMAGE ON THE FLOATING DOCKS DUE TO TSUNAMI-INDUCED FORCES CALCULATED BY TWO DIFFERENT MODELS

Berguzar Oztunali Ozbahceci , İzmir Institute of Technology, berguzarozbahceci@iyte.edu.tr
Hilal Celik, İzmir Institute of Technology, hilalcelik@iyte.edu.tr
Gozde Guney Dogan, Middle East Technical University, gguneydogan@gmail.com
Yagiz Arda Cicek, KU Leuven, yagizarda.cicek@kuleuven.be
Isikhan Guler, Middle East Technical University, isikhanguler@gmail.com
Ahmet Cevdet Yalciner, Middle East Technical University, yalciner@metu.edu.tr

INTRODUCTION

A strong earthquake (Mw=6.6) occurred on October 30, 2020, between offshore Seferihisar (Izmir, Turkey) and Samos Island (Greece) generating a tsunami that affected a region in the Aegean Coast of Turkey. The tsunami caused strong currents, water level fluctuations coastal inundation, and severe damage to coastal structures (Dogan et al. 2021). Especially, floating docks in Teos Marina, Seferihisar were highly damaged due to tsunami hydrodynamic forces. It was observed that the mooring chains and fairleads were broken, and the pontoons were dragged offshore. Moreover, the aluminum frames of docks and the moored ships were damaged.

METHODOLOGY AND RESULTS

In this study, the effect of tsunami-induced sea-level changes and currents on the floating docks of Teos Marina is investigated by numerical hydrodynamic modeling. Firstly, tsunami-induced currents and sea-level changes at Teos Marina are calculated using two different numerical models. One is a high-resolution tsunami model, NAMI DANCE. NAMI DANCE solves the nonlinear form of shallow water equations using the water surface disturbances as the inputs and simulates propagation and coastal amplification of long waves. (Lynett et al., 2017)). The second model is XBeach Non-hydrostatic v1.23.5526 which considers the dispersive behavior of long waves by solving the non-linear shallow water equations with non-hydrostatic pressure correction. Tsunami-induced currents and water level change results of both models are used in an effort to calculate the hydrodynamic response of floating docks and forces on the mooring lines and connectors between the docks in six degrees of freedom. A hydrodynamic numerical model, ANSYS-AQWA based on potential theory is used in the study. It can model the coupled motions of all six degrees of freedom of floating pontoons with connections under the influence of gravitational, hydrostatic, hydrodynamic, wind, mooring, and current loads either in the frequency-domain for rapid evaluation or in the more rigorous time-domain analysis (ANSYS Inc., 2013). Floating docks of the first pier close to the marina entrance were modeled as seen in Fig.1.
Tsunami-induced water level changes and current outputs of the two models are given in the points shown in Fig.1. While the water level results of both models are in very good agreement, the current values are comparable at point 23 but different, especially at points 19, 20, and 21.

Fig.1. Teos Marina lay-out and numerical gauge points

While water level changes are introduced as spectral densities in frequency base, the currents are transferred to forces in time series in the hydrodynamic model. Floating docks with connections and the mooring chains modeled in AQWA are shown in Fig.2.

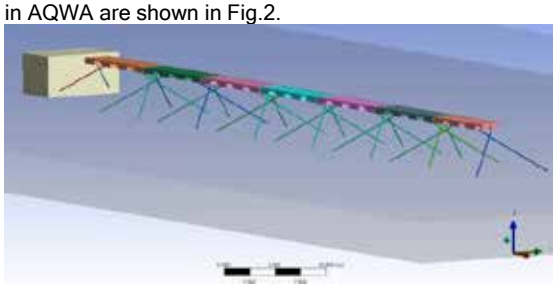
Fig.2. Floating docks modeled in AQWA

CONCLUSION

Calculated tensions greater than the breakage load in the chains and high responses in surge and sway directions show that the damage observed in the floating pontoons can be numerically simulated by the considered hydrodynamic model, given the uncertainties in the earthquake source model

REFERENCES

Dogan, G. G., Yalciner, A. C., Yuksel, Y., Ulutaş, E., Polat, O., Güler, I., ... & Kânoğlu, U. (2021). The 30 October 2020 Aegean Sea tsunami: post-event field survey along Turkish coast. Pure and applied geophysics, 178, 785-812. https://doi.10.18118/G6H088
Inc, ANSYS, (2013). Aqwa Theory Manual, 174
Lynett,.Gately,…Yalciner, Yamazaki, Zaytsev and Zhang (2017). Inter-model analysis of tsunami-induced coastal currents. Ocean Modelling, 114, 14-32.

TSUNAMI RISK MAPPING ALONG THE CALABRIAN COASTS

Giuseppe Barbaro, Mediterranea University of Reggio Calabria, DICEAM Department, giuseppe.barbaro@unirc.it
Giandomenico Foti, Mediterranea University of Reggio Calabria, DICEAM Department, giandomenico.foti@unirc.it
Francesca Minniti, Mediterranea University of Reggio Calabria, DICEAM Department, francesca.minniti@unirc.it
Luigi Mollica, Calabria Region, Civil Protection Department, lu.mollica@regione.calabria.it
Michele Folino Gallo, Calabria Region, Civil Protection Department, m.folinogallo@regione.calabria.it

INTRODUCTION

Tsunami is a natural phenomenon consisting of a series of sea waves produced by the rapid movement of a large mass of water. In the open sea, tsunami waves propagate very quickly, covering great distances with almost imperceptible heights (even less than a meter) but with wavelengths that can even reach tens of kilometers. Approaching the coast, wave celerity decreases due to the shallow waters, so wave height rapidly increases, reaching the order of tens of meters. Consequently, it spread even for many kilometers inland and a subsequent rapid retreat action with potentially devastating effects. Therefore, the extension of tsunami risk areas depends on the morphological characteristics of the emerged and submerged coast. Tsunamis are triggered mainly by earthquakes, volcanoes, and landslides. The latter include both underwater landslides and landslides along slopes close to the coast. However, in state-of-art knowledge, tsunamis cannot be predicted. In closed seas such as the Mediterranean Sea, wave arrival times are very short, and this reduces alert times. Within the Mediterranean Sea, the areas between Calabria and North-Eastern Sicily in the Southern Italy and North-Western Greece are particularly exposed to tsunami risk (Schambach et al., 2020; Minniti et al., 2022).
This paper analyzes the current Italian legislation on tsunami risk mapping and describes a more accurate procedure, applied along the Calabrian coasts.

ITALIAN LEGISLATION

In Italy, tsunami warning system is managed by the SiAM (National Warning System for Tsunamis Generated by Earthquakes) which involves different institutions and concerns only tsunamis generated by earthquakes. The system is based on the estimated severity of tsunami and has two alert levels which coincide with the analogous alert levels adopted within UNESCO/IOC for the tsunami alert system in the Northeast Atlantic, Mediterranean and connected seas region (ICG/ NEAMMTWS): orange (Advisory), red (Watch).
Therefore, mapping method of tsunami risk areas includes two bands: orange (Advisory), covers the coast to the topographic level 1.5 m a.s.l.; red (Watch) covers the area between the level 1.5 to level 10 m a.s.l.
The mapping method is not very accurate since did not consider the real bathymetry and the anthropic obstacles such as buildings, roads, infrastructures, which are fundamental in the calculation of the wave run-up.

CALABRIAN PECULIARITIES

Calabria is a region of southern Italy which is an interesting case study due to its geomorphological, climatic, and anthropogenic peculiarities.

Regarding geomorphological analysis, Calabria is in the center of the Mediterranean Sea, and it is surrounded by two seas, the Tyrrhenian and the Ionian, by the Strait of Messina and by the Gulf of Taranto. Both are characterized by different climatic conditions and different fetch extensions. Concerning climatic analyis, mountain areas are characterized by their typically climate, frequent snowfalls during winter season. Instead, coastal areas are characterized by a Mediterranean climate, with significant differences in rainfall and temperatures between the two coasts, and intense atmospheric perturbations, which sometimes are like hurricanes, the so-called Medicane (Mediterranean Hurricane) or Tropical Like Cyclones (TLC). Ultimately, from the anthropogenic point of view, after the end of the Second World War, a considerable migration from inland to coastal areas was observed in most of the coastal territories. The considerable anthropogenic pressure led in many towns to a disorganized and unplanned urban growth which affected both coastal and river areas.

NEW MAPPING PROCEDURE

The new procedure will be divided into two phases. In the first one, a perimeter will be carried out with greater precision, taking into consideration the levels of alert and mapping above mentioned, by using detailed data. In the second phase, the two levels of alert and mapping are expected to be updated by means of numerical modeling and neural networks that consider triggering mechanism of tsunami (earthquake, landslide, multi-source approaches etc.), the propagation mechanism of tsunami wave, coastal morphology and presence of erosive processes.
The first phase will be developed by using the open-source software QGIS based on the following detailed data:
- bathymetry off the coast of Calabria (source: EMODNET portal https://emodnet.ec.europa.eu/en/bathymetry).
- detailed bathymetries available at the various institutions or from surveys.
- DTM and DSM Last and First with 1x1 m and 2x2 m resolution (source National Geoportal http://www.pcn.minambiente.it/mattm/).
- design drawings of buildings, roads, infrastructures available at the institutions above mentioned or from surveys.

REFERENCES

Minniti, Barbaro, Foti (2022): Modeling of the 1783 Tsunami Event in Scilla Generated by Landslide. Land, vol. 11(1), 69.
Schambach, Grilli, Tappin, Gangemi, Barbaro (2020): New simulations and understanding of the 1908 Messina tsunami for a dual seismic and deep submarine mass failure source. Marine Geology, vol. 421, 106093.

NUMERICAL SIMULATION OF A FLEXIBLE FLAT NET IN CURRENTS BASED ON THE APPLICATION OF SMOOTHED PARTICLE HYDRODINAMICS

Raúl González-Ávalos, Corrado Altomare, Xavi Gironella, Maritime Engineering Laboratory LIM/UPC Universitat Politècnica de Catalunya - Barcelona, Spain. raul.alexis.gonzalez@upc.edu; corrado.altomare@upc.edu; xavi.gironella@upc.edu

Alejandro J.C. Crespo, Iván Martínez-Estévez, José M. Domínguez, Environmental Physics Laboratory, CIM-UVIGO University of Vigo, Spain, alexbexe@uvigo.es; ivan.martinez.estevez@uvigo.es; jmdominguez@uvigo.es

The aim of this study is to evaluate the applicability and suitability of the Smoothed Particle Hydrodynamics (SPH) method for modeling a flexible flat net subjected to a constant current flow. The SPH-based model DualSPHysics coupled whit mooring solver MoorDyn+ (Domínguez et al., 2019) is used for the purpose. Currents are generated by means of open boundary conditions (Inlet) in DualSPHysics. An algorithm developed with MATLAB generates the net configuration that preserves its hydrodynamic and structural properties. First, the method is validated by determining the drag coefficient of a single sphere in a viscous fluid for different Reynolds numbers. Subsequently, an analysis is performed on a set of fixed spheres, determining the drag forces on the set of spheres and their interaction with the fluid. Finally, a flexible flat net of 0.3 x 0.3 m in a fixed frame is simulated in a current of 0.226 m/s, applying the proposed methodology. The analysis provides information in the drag forces of the net, as well as on the velocity field of the fluid around it. The obtained results are compared with drag force results calculated based on analytical solutions.

The methodology used for the discretization and simulation of the net is based on dividing the net into macroelements while preserving their hydrodynamic and structural properties. Within the SPH framework, the geometry of the net is discretized as a sum of spherical nodes (N), which together maintain the solidity of the net (Sn) and interact with fluid particles falling within their support region, thus establishing the fluid-structure interaction. These nodes are in turn connected with dynamic mooring (l) generated with MoorDyn+. The methodology is based on the following equations:

a) Conservation of solidity: The projected area of the physical net is equivalent to the projected area of the nodes that make up the net in the numerical model:

$$Sn_{Net} \cong Sn_{NM} \tag{1}$$

b) Equivalent rigidity: The rigidity of the net is equivalent to the rigidity of the connections in the numerical model, where η_{Net} is the number of threads in the net, A_{Net} is the area of the cross-section of the thread in the net, and E_{Net} is the Young's modulus of the thread in the net. Similarly, η_{NM} is the number of connections in the numerical model, A_{NM} is the area of the cross-section of the connection in the numerical model, and E_{NM} is the Young's modulus of the connection in the numerical model:

$$\eta_{Net} \cdot A_{Net} \cdot E_{Net} \cong \eta_{NM} \cdot A_{NM} \cdot E_{NM} \tag{2}$$

c) Equivalent Drag Forces: The drag force in the numerical model must be equivalent to the drag forces in the physical net (Eq. (3)). The drag force in the numerical model is the sum of the drag forces on the set of nodes (F_N) and their connections (F_l).

$$F_{Net} \cong F_N + F_l \tag{3}$$

d) Equivalent Weight: The submerged weight of the numerical model should be equivalent to the submerged weight of the physical net (W_{net}). The submerged weight in the numerical model is defined as the sum of the submerged weight of each node (W_N) and the sum of the submerged weight of each connection (W_l) that makes up the system.

$$W_{net} \cong \sum W_N + \sum W_l \tag{4}$$

The proposed methodology contrasts with state of the art of the traditional methods, where the interaction between fluid and the net is not directly resolved. The proposed approach based on SPH allows solving this problem by applying one of the most interesting capabilities of DualSPHysics, it accuracy simulate fluid-driven structures. In this way, it is possible to derive the motion of the net and its interaction with the fluid as shown in Fig 1.

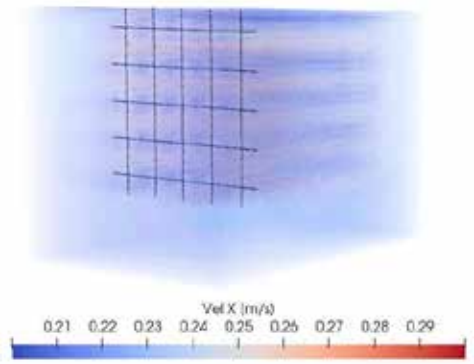

Figure 1. Numerical simulation of a 0.3 m x 0.3 m flat flexible net and fluid velocity field around it.

REFERENCES

[1] J. M. Domínguez, A. J.C. Crespo, M. Hall, C. Altomare, M. Wu, V. Stratigaki, P. Troch, L. Cappietti and M. Gómez-Gesteira, 2019. "SPH simulation of floating structures with moorings," Costal Engineering. vol. 153.

DESIGNING HARBOUR LAYOUT WITH STRONG REFRACTION IN THE GULF OF RIGA, EASTERN BALTIC SEA

Rain Männikus, Tallinn University of Technology, rain.mannikus@taltech.ee
Widar Weizhi Wang, Norwegian University of Science and Technology, widar.weizhi.wang@outlook.com
Fatemeh Najafzadeh, Tallinn University of Technology, fatemeh.najafzadeh@taltech.ee

INTRODUCTION

Wave refraction may convert seemingly well-sheltered coastal areas into hot spots of wave energy. Although a harbour on a small island of Ruhnu in the Gulf of Riga, eastern Baltic Sea, is sheltered from strong SW and NNW winds, its interior often suffers from inconveniently high waves and sudden changes in the water level (Männikus et al., 2022). Undesirable wave conditions often occur even during westerly winds against which the harbour seems perfectly protected. In order to improve the layout of the harbour, we have measured and modelled waves with status quo and possible new configurations.

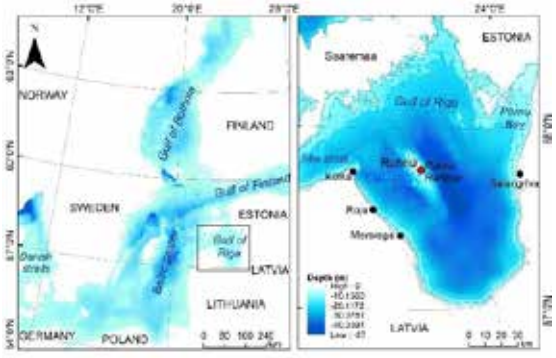

Figure 1 - The location of Ruhnu harbour.

DATA

Waves were measured at 15-20 minute intervals with 2 wave buoys and with 2 pressure sensors in 2021 and 2022. The total measurement period was 12 months. Water levels were observed visually at Ruhnu in 1945-1988 and from 2012 (a gap of 24 years). Hence, we employed a more complete and frequent time series of water levels from neighbouring Latvian stations to construct a new time series for Ruhnu. Water levels at Ruhnu and wind data from Ruhnu were provided by Estonian Weather Service. Water levels from Latvian stations (Salacgriva, Mersrags, Roja and Kolka) were taken from Latvian Environment, Geology and Meteorology Centre.

METHODS

We used wave measurements to calibrate and validate SWAN (Booji et al., 1999) wave model for Ruhnu. This model with a four-level nested scheme of rectangular grids was forced with non-stationary and unidirectionally steady wind and water level measurements. We compared three different wind data sets in the wave model, in order to select the most reliable source.
For the design of the harbour layout and structures, we constructed wind-water level scattered plots for different directions (30° step). By drawing contours, representing different return periods, we were able to select winds and water levels which were used as design conditions to force the validated SWAN model in stationary mode. Together with harbour authority we changed the layout and types of structures at Ruhnu wave model and compared the resulting wave patterns visually and quantitively at various locations. The resulting wave parameters were used for harbour and breakwater design. We also employed phase-resolving wave models SWASH and REEF3D::FNPF (Wang et al., 2022) for harbour basin analysis and performance comparisons.

RESULTS AND CONCLUSION

Besides wave climate, we had to consider the accessibility and possible costs. Currently, ferries connecting to the mainland of Estonia approach to harbour from southeast. Hence, we did not change the entrance radically. Fig 2 shows a new proposed layout with extensions of breakwaters and removed structures. The study showed that employing homogenous one-point winds yields acceptable results for harbour design.

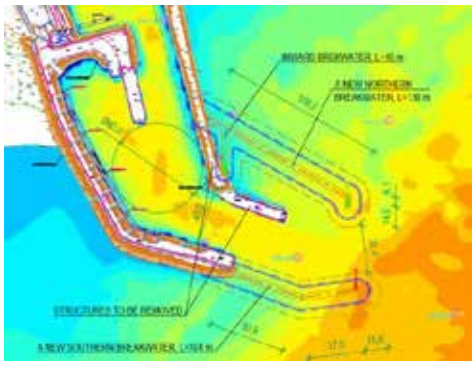

Figure 2 - New layout on the background of water depths.

REFERENCES

Booij, Ris, Holthuijsen, (1999): A third-generation wave model for coastal regions: 1. model description and validation. Journal of Geophysical Research-Oceans, vol. 104, pp. 7649-7666.
Männikus, Soomere, Najafzadeh (2022): Refraction may direct waves from multiple directions into a harbour: a case study in the Gulf of Riga, eastern Baltic Sea. Estonian Journal of Earth Sciences, vol. 71, pp. 80-88.
Wang, W., Pákozdi, C., Kamath, A., Fouques, S. and Bihs, H. (2022). A flexible fully nonlinear potential flow model for wave propagation over the complex topography of the Norwegian coast. Applied Ocean Research, 122, 103103.

AN EXAMPLE OF AN OVERTOPPING DEVICE-TYPE WAVE ENERGY CONVERTER LOCATED ON A VERTICAL SEAWALL

Semih Can, İzmir Institute of Technology, semihcan@iyte.edu.tr
Dogan Kisacik, İzmir Institute of Technology, dogankisacik@iyte.edu.tr
Lorenzo Cappietti, University of Florence (UNIFI), lorenzo.cappietti@unifi.it

Climate change is the largest challenge, recently. Traditional sources of energy such as oil, gas and coal are not renewable and cause pollution by releasing carbon dioxide and other pollutants into the atmosphere. Evidence shows that pollution harms the environment in many ways, from global warming to sea level rising. The Kyoto Protocol regarding the reduction of greenhouse gases and pollutant emissions is strictly linked to the development of Renewable Energy Sources (Vicinanza, 2008).

Wave energy is the renewable energy source having the highest energy density and a global wave energy potential of 32,000 TWh/year is estimated to reach the world coastlines, a value close to the yearly mean world energy consumption (Mork, 2010). Wave energy is convertible into electricity with wave energy converters (WECs). There are many types of WECs. Despite the potential benefits of WECs, such as low greenhouse gas emissions and high energy density, many technical and economic challenges must be overcome before they become widely deployed.

This research aims to ensure that a coastal protection structure where the promenade works as a Stilling Wave Basin (SWB), generates energy while it protects the coastline against flood. Wave-overtopping is a significant consideration for the safety of coastlines. There are several methods to decrease the amount of overtopping. One of the standard methods is increasing the crest height of the coastal protection structure, such as dikes, and seawalls. However, it is not always possible to implement this method approach due to recreational concerns. The crest top of a coastal protection structure, generally used as a promenade, works as an SWB within this concept. According to the study, SWB can be considered the reservoir of an Overtopping Device (OD) Wave Energy Converter (WEC). The amount of overtopped wave, collected in SWB, is discharged to the sea with the help of a drainage orifice. A hydraulic turbine is located inside this orifice, generating electrical energy from the potential energy of the collected overtopped water.

OD WECs are investigated by small-scale physical model tests. The experiments are performed in the Wave-Current flume of the Maritime Engineering Laboratory (LABIMA) at Florence University (abbreviated as 'LABIMA-WCF') in Italy. The model is tested under irregular wave conditions for two different water depths. In total, one hundred twenty-six tests are performed for different geometric configurations of the SWB. Accumulated water in the basin is measured for each combination. The amount of energy generated by the hydraulic turbine has a relation with the volume of water in the basin. It is necessary to supply water to the turbines as continuously as possible for efficiency. Therefore, the number and the capacity of turbines are optimized according to the experimental and numerical data.

Figure 1 - Sketch of the Overtopping Device WEC Concept Located on a vertical sea wall

REFERENCES

Vicinanza, Frigaard (2008): Wave pressure acting on a sea-wave slot-cone generator, Coastal Engineering, ELSEVIER, vol. 55, pp. 553-568.

Mork, Barstow, Kabut, Pontes (2010); Assessing the Global Wave Energy Potential, Offshore and Arctic Engineering (OMAE), Proceedings of the 29th International Conference on Ocean

ESTIMATION OF SCOUR DEPTH AROUND A CYLINDER BY FLOW

Yota Enomoto, Chuo University, a17.p7cj@g.chuo-u.ac.jp
Taro Arikawa, Chuo University, taro.arikawa.38d@g.chuo-u.ac.jp

1. PURPOSE OF THE STUDY

Estimating the maximum scour depth around a cylinder due to flow is based on the Shen et al. (1969) equation. However, in this equation, the diameter of the cylinder is the only variable; the flow velocity and ground conditions are not considered. Therefore, this study proposes a maximum scour depth estimation formula that considers these conditions.

2. EXPERIMENTAL METHOD

Through experiments, this study examined scour depth trends based on various combinations of ground conditions and flow velocities. The experiments were conducted at model scales:1/65 and 1/130, and two different sand grain sizes were used for the ground. In this study, the scour depth was defined as the amount of change from the ground level at the beginning of the experiment to zero, with erosion as negative and sedimentation as positive. The scour depth was determined by measuring the sandy soil profile before and after the experiment using a Leica BLK360 3D scanner and calculating the difference in soil elevation. Figure 1 shows the experimental model, and Table 1 lists some experimental conditions.

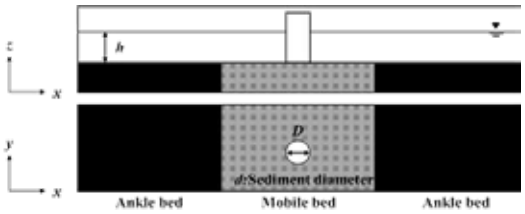

Figure 1 - Experiment mode

Case No.	Velocity	Sediment diameter
Case1(a,b)	0.04 m/s	0.075 / 0.106 mm
Case2(a,b)	0.08 m/s	0.075 / 0.106 mm
Case3(a,b)	0.12 m/s	0.075 / 0.106 mm
Case4(a,b)	0.16 m/s	0.075 / 0.106 mm

Table 1 - Experiment condition

3. SIMIRARITY LAW

We followed the method described by Yamano et al. (2013) for raw similarity and adopted a similarity rule that matched the number of seals.

$$\frac{v_m}{w_{sm}} = \frac{v_p}{w_{sp}} \quad (1)$$

Here, v is the flow velocity and w is the settling velocity of the soil particles. The subscript m represents the prototype, and p represents the model.

4. EXPERIMENT RESULTS

Scouring by flow is considered to be dominated by the number of seals, and the number of seals is a parameter that considers the particle size and flow velocity. The Prandtl-Karman logarithmic distribution law was used to determine friction velocity u^* from the velocity distribution. Here, κ is the Karman constant (κ =0.4), k_s is the equivalent roughness (k_s=d_{50}), and A_r is an experimental constant. Shields number τ^* was calculated using the friction velocity u^*.

$$\frac{u}{u_*} = A_r + \frac{1}{\kappa} ln \frac{z}{k_s} \quad (2)$$

$$\tau_* = \frac{u_*}{sgd_{50}} \quad (3)$$

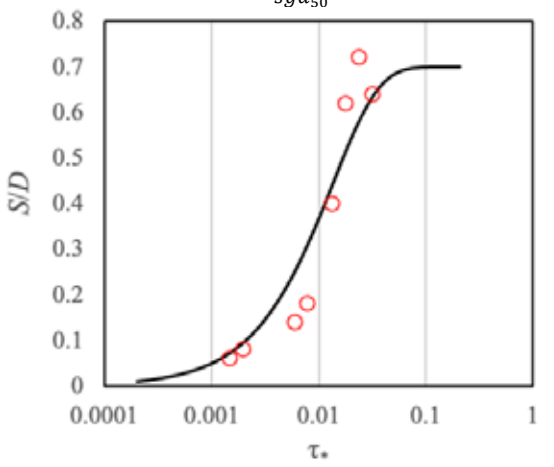

Figure 2 - Relationship between Shields number and maximum scouring depth (S is maximum scouring depth, D is cylinder diameter)

The relationship between the number of seals obtained and the maximum scour depth measured using a 3D scanner is shown in Figure 2.
As the number of seals increases, the maximum scour depth becomes about 0.7 times the diameter of the cylinder. In sections with a large number of seals, the maximum scour depth is considered to be constant and is considered to be about 0.7 times the diameter of the cylinder. From these results, the maximum scour depth around the cylinder due to flow, which also considers the sea and ground conditions, can be evaluated using the Shields number.

REFERENCES

Shen, Schneider, and Karaki (1969): Local Scour around Bridge Piers, Proc. ASCE, Journal of the Hydraulics Division, vol. 95, pp.1919-1940.
Yamano, Fujiwara, Nomura, Shiraki (2013): The Horizontal Characteristics to Local Scour around the Pile-supported Wave Absorbing Breakwater and the Effect of Countermeasure against Local Scour, Coastal Engineering, Journal of JSCE, vol. 69, pp. I_591-I_595.

SENSITIVITY OF A NORTH SEA MODEL TO BEDFORM RELATED BOTTOM ROUGHNESS

Julietta Weber, Federal Waterways Engineering and Research Institute, julietta.weber@baw.de
Robert Hagen, Federal Waterways Engineering and Research Institute, robert.hagen@baw.de
Frank Kösters, Federal Waterways Engineering and Research Institute, frank.koesters@baw.de

INTRODUCTION

We currently develop a 3D hydro-numerical model of the North Sea to set up a comprehensive database of hydrodynamics, bathymetry and sedimentology for the UNESCO World Heritage site of the Wadden Sea (see https://trilawatt.eu). Hydrodynamic data are obtained from a numerical model which we see as a spatial and temporal interpolator. Our aim is to hindcast the years 2005, 2010 and 2015 to 2020 in a consistent way considering changes in bathymetry and sedimentology over this time. Here we present the calibration process based on the van Rijn (2007) roughness predictor.

A HIGH-RESOLUTION 3D NORTH SEA MODEL

The model extends over the entire North Sea and focuses on the Wadden Sea (see Fig. 1), which is the largest coherent channel-shoal environment worldwide.

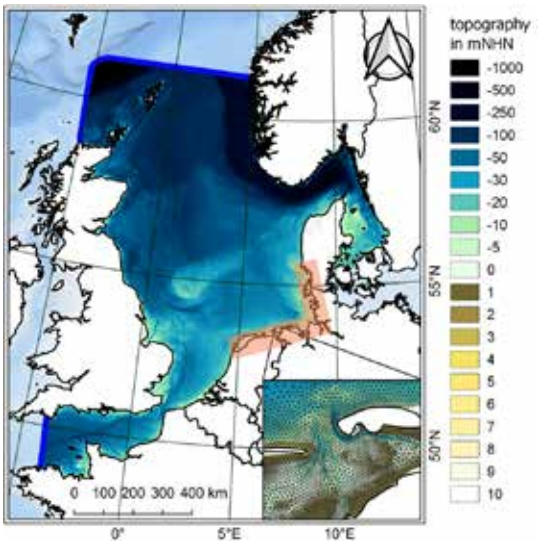

Figure 1 - Domain of the North Sea model with the Wadden Sea highlighted in orange (modified from Hagen et al. 2021)

We conduct numerical modeling using the 3D hydrodynamic UnTRIM2 framework with the well-established subgrid approach (Casulli and Walters 2000; Casulli 2009). Our model considers

- tides, surge, waves,
- salinity,
- temperature, and
- sediments (bedload, suspended load).

The model grid is based on annual bathymetries with 10 m resolution and annual surface sediments (approximated with spatial and temporal interpolation from over 45,000 sediment samples).

THE SENSITIVITY OF THE VAN RIJN BED ROUGHNESS PREDICTOR

Van Rijn (2007) established a roughness predictor that predicts bed forms from physical input parameters: sediment distribution, water depths and current velocity. He distinguishes between ripples, mega-ripples and dunes. We used the predictor to tune the model roughness and could achieve a high model skill based on a consistent physical approach. Even though we have a high-quality bathymetry and sedimentology database available additional roughness must be applied locally.

Since the model is highly sensitive to bottom roughness, our calibration was based on more than 150 tide gauges. Our results show water level signals with the region-typical tidal wave characteristics dominated by semidiurnal components. The calibration allowed us to fit amplitude and phase of the tidal wave very close to observations (RMSE water level generally < 5 cm, phase < 10 min). Especially the tidal wave amplitude is highly sensitive to bed roughness. In the calibration we found an optimal relative distribution of ripples, mega-ripples and dunes of 0.90, 0.18 and 0.01, where each of the values can vary between 0 and 1.

SUMMARY

A high-quality database of bathymetry and sedimentology is the door opener for near-to-nature modelling. This comprehensive data base allows a physical consistent model calibration using the van Rijn bed roughness predictor.

REFERENCES

Casulli, Walters (2000): An Unstructured Grid, Three-Dimensional Model Based on the Shallow Water Equations. Int. J. Numer. Meth. Fluids, vol. 32, pp. 331-348.
Casulli (2009): A high-resolution wetting and drying algorithm for free-surface hydrodynamics, Int. J. Numer. Meth. Fluids, vol. 60, pp. 391-408.
Hagen et al. (2021): An integrated marine data collection for the German Bight – Part 2: Tides, salinity, and waves (1996-2015), Earth Syst. Sci. Data, vol. 13, pp. 2573-2594.
van Rijn (2007): Unified view of sediment transport by currents and waves. I: Initiation of motion, bed roughness, and bed-load transport. J. Hydraul. Eng., vol. 133, pp. 649-667.

SEDIMENT TRANSPORT PROCESSES

SOFT MEASURES AGAINST TO COASTAL FLOODING AS A RESULT OF EXPECTED SEA LEVEL RISE IN IZMIR BAY

Onur Deniz Türkseven, İzmir Institute of Technology, onurturkseven@iyte.edu.tr
Dogan Kisacik, İzmir Institute of Technology, dogankisacik@iyte.edu.tr
Cuneyt Baykal, Middle East Technical University, cbaykal@metu.edu.tr
Isikhan Guler, Middle East Technical University, isikhan@metu.edu.tr

Sea level rise is expected as a result of climate change. Consequently, there will be an increase in the number and magnitude of coastal flooding, increasing the coastal cities' vulnerability. The Izmir Bay offers a significant expanse of the residential area. Coastal flooding from rising sea levels can pose vital problems for people living close to structures in these habitats. The municipality of coastal cities like İzmir should consider increased risk levels. Mainly two different measure types exist: hard and soft measures. Preventing coastal flooding with soft solutions is an environmentally friendly approach since it is not using artificial structures.

The natural shoreline will soon adapt to new sea-level conditions to minimize incident wave energy. Under the new circumstance, the flood level behind the shoreline should be determined to check whether it is above or below the threshold values. In the case of any risk, beach nourishment can be considered a solution. Beach nourishment is considered a soft solution that restores the beach and provides a protective zone that absorbs the energy of the incident waves and sea level rise conditions. Many natural shores exist along Izmir Bay (Figure 1). Soft solutions will be developed based on the specific characteristics of the selected coastal regions.

Figure 1. Areas Suitable for Soft Solution in Izmir Bay

The seabed changes under new hydrodynamic conditions due to sea level rise will be examined by numerical models. XBeach is an effective and powerful tool developed at Delft University for the simulation of morphological changes under extreme conditions. It has the capability to simulate dispersive and non-dispersive wave conditions. Hydrodynamic condition, seabed sediment characteristics, and model bathymetry were determined from selected site specifications.

XBeach model is calibrated with the results of physical model tests conducted in the wave flume of Middle East Technical University (METU) (Işık, 2019). The dimensions of the wave flume are 29.0 meters in length, 6.0 meters in width, and 1.0 meters in depth (Figure 2.) The physical model simulates shoreline and seabed changes under different wave conditions. Tests start with an initial condition of an artificial uniform coastline created with uniform sand. After each test, bathymetry is measured to obtain the newly formed seabed geometry. Physical test results showed that beach erosion is influenced by an increase in significant wave height and wave steepness. Then XBeach model results are validated with the different physical tests set up, which are not considered in calibration processes. Finally, the calibrated model will run for the conditions of the natural coastline of İzmir Bay under the changing sea level and extreme wave conditions to evaluate the soft solution option as a measure against coastal flooding.

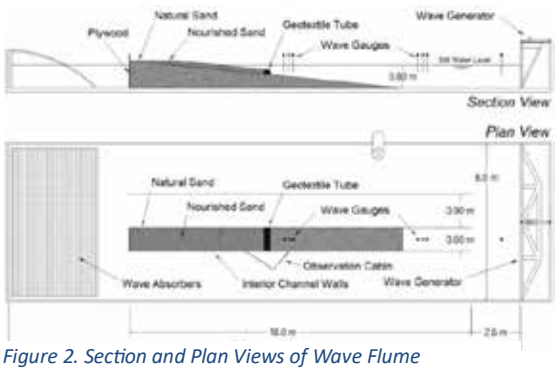

Figure 2. Section and Plan Views of Wave Flume

REFERENCES

Işık, E. (2019). An experimental study on the performance of geotextile tubes in beach nourishment applications (Master's thesis). Middle East Technical University, Civil Engineering Department.

NUMERICAL INVESTIGATION OF A BEACH RESTORATION PROJECT IN MERSIN USING XBEACH AND ONELINE NUMERICAL MODELS

Cüneyt Baykal, Middle East Technical University, cbaykal@metu.edu.tr
Cem Sevindik, Dolfen Engineering and Consultancy Company, cemsevindik@dolfen.com
Mert Yaman, Dolfen Engineering and Consultancy Company, mertyaman@dolfen.com
Can Özsoy, Dolfen Engineering and Consultancy Company, canozsoy@dolfen.com
Işıkhan Güler, Middle East Technical University, isikhan@metu.edu.tr

INTRODUCTION

In this study, the beach restoration project to create an artificial beach for the use of citizens in Afetevler distinct in Mersin upon request of Mersin Metropolitan Municipality is presented. The coastal defense system designed in the project is described and the numerical investigations on the performance of the defense system are presented. The numerical investigations were performed using XBeach (Roelvink et al., 2009) and a one-line numerical model (Ergin et al., 2006) models.

METHODOLOGY

As the first step of this study, wind and wave climate of the project area were studied to determine the deep water and nearshore wave characteristics of the project region. For this purpose, four different wind and wave databases were considered: CFSR, ECMWF, CMEMS-Copernicus databases and 'Türkiye Kıyıları Rüzgar ve Derin Deniz Dalga Atlası' (Özhan, Abdalla, 1999). Long-term and extreme wave statistics were carried out for the data gathered to determine the design wave characteristics. SWAN numerical model was used to obtain the nearshore wave characteristics of the design waves, which were inputted to the numerical models XBeach and CSIM. The bathymetric data to be used in the numerical models was gathered from GEBCO, Navionics, and the measured bathymetry data. The sediment parameters to be used in the beach nourishment, were determined based on the results of the conducted sediment sampling and sieve analyses.

Studies in the scope of this project were separated into two parts as West and East sides of Mersin Marina. Several alternative defense systems were studied to find the optimal solutions for these regions. In the study, four different scenarios were studied for 1 year, 5 years and 10 years projections. In the first step, using CSIM, the shoreline change for the following years was studied for the present situation of the beach that no soft or hard measures are applied. After this step, alternative defense system solutions that include only soft measures (nourishment), only hard measures (coastal structures), and both soft and hard measures were simulated using XBeach and CSIM numerical models. CSIM numerical model was used to observe the longshore sediment transport variations and corresponding shoreline changes for the proposed solutions by using CERC (1984) and Kamphuis (1991) methods. XBeach was used to perform one-dimensional cross-shore profile modeling to observe the morphological change perpendicular to the shoreline. The proposed solutions were also studied in XBeach two-dimensionally to observe both longshore and cross-shore sediment transport effects of the proposed solutions.

Figure 1 - Layout of the proposed defense system including artificial nourishment and coastal structures.

CONCLUDING REMARKS

Upon request of Mersin Metropolitan Municipality, a beach restoration project was prepared to create an artificial beach in Afetevler distinct, Mersin. In the scope of this project, several alternative defense systems were proposed and future shoreline projections of these solutions were carried out by using XBeach and CSIM numerical models to determine their effectiveness. The success of the proposals will be tested with field observations and measurements to be made after the implementation of the project.

REFERENCES

Özhan, E., & Abdalla, S. (2002). Türkiye kıyıları rüzgar ve derin deniz dalga atlası, MEDCOAST, ODTÜ.

Ergin, Güler, Yalciner, Baykal, Artagan, Şafak. (2006). A One-Line Numerical Model for Wind Wave Induced Shoreline Changes, 7th Int. Congress on Advances in Civil Engineering, Yildiz Technical University, Istanbul, Turkey

Roelvink, Reniers, van Dongeren, de Vries, McCall, Lescinski (2009). Modelling storm impacts on beaches, dunes and barrier islands, Coastal Engineering. 56:1133-1152.

Keynote

ABSTRACTS

PORT DEVELOPMENT IN A CHANGING WORLD

Han Ligteringen, Delft University of Technology, h.ligteringen@tudelft.nl

SUMMARY

Since the 1950-ties the global trade volume has steadily increased. As more than 80% of this trade is carried by ship, the growth of maritime transport and port facilities followed this increase at the same pace. Ships were getting bigger, containerisation caused a small revolution, both in terms of productivity, transport costs and labour.

But overall the changes were gradual, reasonably predictable and manageable.

This is in contrast with the major changes that the world is facing today: Climate Change, Energy Transition, Sustainability Goals and IT-applications all have their impact on international trade, sea-transport and ports. In this Key-Note lecture I have tried to depict the consequences of these changes, starting with the results of research on some long-term trends, up till the year 2100. It goes without saying that each of these trends has a large amount of uncertainty, which will influence the time path available for adaptation of the current practices in maritime transport and port operations.

Consequences are related to, amongst other, different types of measures to reduce CO2 emissions from shipping and port operations, downsizing of certain trades and emergence of other ones, innovations in port infrastructure and further automation. Often measures are interconnected. And because port operations are not governed by an international body – like IMO, that can issue legislation for shipping- measures often need to be voluntary, driven by incentives.

But they are taking place already, as will be outlined in the presentation at the hand of some examples.

NUMERICAL MODELING OF COASTAL SEDIMENT TRANSPORT TO PREDICT BLUFF EROSION AND SAND AND STONE INTERACTIONS

Nobuhisa Kobayashi, University of Delaware, nk@udel.edu

INTRODUCTION

The cross-shore numerical model CSHORE was developed to predict coastal sediment transport for engineering applications (Kobayashi 2016). CSHORE has been extended to predict erosion by wave action of consolidated cohesive sediment containing cohesionless sediment (Kobayashi and Zhu 2020). This version of CSHORE has been applied to predict bluff erosion (Zhu and Kobayashi; 2021a). CSHORE has also been expanded to predict sand transport inside and over a rubble mound structure (Kobayashi and Kim 2017). This CSHORE option for sand and stone interactions has been applied to predict the effectiveness of a rubble mound in reducing wave overwash and crest lowering of a sand barrier (Zhu and Kobayashi 2021b) as well as to predict the recovery of an eroded beach after the closure of a breached channel by a rubble mound (Zhu and Kobayashi 2023).

BLUFF EROSION

CSHORE for cohesive and cohesionless sediments was used to investigate bluff erosion processes. Available wave basin data were used to calibrate and verify the cohesive sediment model. The measured bluff recession rates under oblique breaking waves for bluffs built of wet sand and a sand/clay mixture was reproduced by accounting for sand loss associated with the alongshore gradient of longshore sand transport. For cohesive sediment with weak resistance against wave action, the bluff recession rate was limited by the sand removal by longshore and cross-shore sand transport. The recession rate decreased when the resistance of the bluff material exceeded a critical value related to the sand removal capacity.

SAND AND STONE INTERACTIONS

Irregular wave overwash and landward migration of a narrow sand barrier were investigated in a laboratory experiment for three different barriers with no structure, a rock mound, and a rock cover. The rock mound consisting of three layers of stable stones reduced the landward migration and crest lowering of the sand barrier. The rock cover consisting of a single layer of stable stones was not effective in reducing the barrier deformation because of the stone settlement and spreading and the exposure of underlying sand to direct wave action. CSHORE was calibrated to reproduce the measured barrier deformation in the three tests but the stone spreading in the single layer test could not be predicted.

BREACHED BEACH RECOVERY

The option of sand and stone interactions in CSHORE was applied to field data. A rubble mound structure was constructed in 2011 across the 2 km wide channel breached by Hurricane Katrina in 2005. This breached channel is called Katrina Cut in Dauphin Island, Alabama. The recovery of the eroded beach seaward of the closed Katrina Cut during 2015-2020 was reproduced using CSHORE. The dry beach width increased more than 80 m seaward of the Katrina Cut structure and decreased up to 37 m on the neighboring beach. The recovering beach reduced the depth-limited breaking wave height and wave action on the rubble mound structure during Hurricane Nate in 2017.

REFERENCES

Kobayashi (2016): Coastal sediment transport modeling for engineering applications. J. Waterway, Port, Coastal, Ocean Eng. (JWPCOE), 142(6).
Kobayashi and Kim (2017): Rock seawall in the swash zone to reduce wave overtopping and overwash of a sand beach, JWPCOE, 143 (6).
Kobayashi and Zhu (2020): Erosion by wave action of consolidated cohesive bottom containing cohesionless sediment, JWPCOE, 146(2).
Zhu and Kobayashi (2021a): Modeling of soft cliff erosion by oblique breaking waves during a storm, JWPCOE, 147(4).
Zhu and Kobayashi (2021a): Rock mound to reduce wave overwash and crest lowering of a sand barrier, Coastal Eng. J., 63(4).
Zhu and Kobayashi (2023): Recovery of eroded beach seaward of closed Katrina Cut in Dauphin Island, Alabama, J. Coastal Offshore Science Eng., 2(1).

COASTAL HAZARDS AND RISKS IN THE MEDITERRANEAN SEA CAUSED BY ANTHROPOGENIC CLIMATE CHANGE

Piero Lionello, University of Salento, piero.lionello@unisalento.it

INTRODUCTION

The Mediterranean is a microtidal sea with densely populated coastlines. The population of the region is more than 500million people, it is expected to further grow in the southern Mediterranean countries and presents a high concentration of urban settlements and industrial infrastructure close to sea level (Ali et al., 2022) that are potentially affected by marine hazards and extreme events. Coastal floods are determined by the effect of storm surges, which reach the largest level in the North Adriatic and Gulf of Gabes (Lionello et al. 2023). Several stretches of the coast are also affected by flash floods caused by extreme precipitation events (Llasat et al. 2020). Risks posed by meteorological and climate hazards (which include also decrease of water resources, warming of the marine and terrestrial environment) are further increased by other drivers of environmental change: pollution, overexploitation and biological factors such as non-indigenous species (Cherif et al., 2020).

CLIMATE CHANGE HAZARDS

Sea level rise (SLR) in the Mediterranean is expected to reach values in the range from 0.3 to 1.4m at the end of the 21st century (similar to the global mean SLR) depending on the emission scenario and with uncertainties related to poorly constrained processes that can lead to rapid ice caps melting (Ali et al., 2022). SLR will increase frequency and magnitude of coastal floods (Vousdoukas et al., 2020), eventually leading to the permanent inundation of some areas (Ali et al., 2022). In comparison the change of magnitude of meteorological extreme events (storms) will play a minor role (Lionello et al., 2017), being the frequency of cyclones and Mediterranean hurricanes expected to diminish, though with an increase of maximum intensity (Ali et al., 2022).

EXPOSURE AND RISKS

Settlements and population along the coastline are exposed to the risks of flooding and erosion (Wolff et al., 2018). Future SLR will be the main cause of coastal erosion of sandy beaches, analogously to other coastlines of the world (Vousdoukas et al., 2020). Coastal cultural heritage and UNESCO sites are vulnerable to SLR, erosion and floods (Reimann et al, 2018), Venice representing a well-known paradigmatic case (Lionello et al., 2021). Climate change together with overexploitation of aquifers causes salt intrusion affecting the water suitability for irrigating crops (Mastrocicco and Colombani, 2021), with potential negative impacts in agriculture (Ali et al., 2022). Risks are present also for port operations, tourism and coastal ecosystems (Ali et al., 2022). Sea levels considered by adaptation plans differ among countries and this may lead to inequal future impacts (Bednar-Friedl et al., 2022). If SLR will exceed few tens of centimeters, adaptation will be expensive and residual risks unavoidable in some cases (Ali et al., 2022).

REFERENCES

Ali, Cramer, Carnicer, Georgopoulou, Hilmi, Le Cozannet, and Lionello (2022): Cross-Chapter Paper 4: Mediterranean Region. In: Climate Change 2022: Impacts, Adaptation and Vulnerability. Contribution of Working Group II to the Sixth Assessment Report of the Intergovernmental Panel on Climate Change Cambridge University Press, pp. 2233-2272.

Bednar-Friedl, Biesbroek, Schmidt, Alexander, …and L.Whitmarsh (2022): Europe. In: Climate Change 2022: Impacts, Adaptation and Vulnerability. Contribution of Working Group II to the Sixth Assessment Report of the Intergovernmental Panel on Climate Change, Cambridge University Press, pp. 1817–1927

Cherif, Doblas-Miranda, Lionello, Borrego, Giorgi, Rilov,... and Zittis, (2020); Drivers of change. Climate and Environmental Change in the Mediterranean Basin-Current Situation and Risks for the Future. First Mediterranean Assessment Report, pp.59-180.

Llasat, Llasat-Botija, Prat, Porcu, Price, Mugnai, ... and Nicolaides (2010). High-impact floods and flash floods in Mediterranean countries: the FLASH preliminary database. Advances in Geosciences, 23, pp.47-55.

Lionello, Conte, Marzo and Scarascia (2017): The contrasting effect of increasing mean sea level and decreasing storminess on the maximum water level during storms along the coast of the Mediterranean Sea in the mid 21st century. Glob. Planet. Chang., vol.151, pp 80-91.

Lionello, Nicholls, Umgiesser and Zanchettin (2021): Venice flooding and sea level: past evolution, present issues, and future projections (introduction to the special issue). Nat. Hazards Earth Syst. Sci., vol.21, pp.2633-2641.

Lionello, Sannino and Vilibić (2023): Surface wave and sea surface dynamics in the Mediterranean. In Oceanography of the Mediterranean Sea, Elsevier, pp. 161-207.

Mastrocicco and Colombani, N. (2021). The issue of groundwater salinization in coastal areas of the mediterranean region: A review. Water, vol.13, pp.90.

Reimann, Vafeidis, Brown, Hinkel and Tol (2018): Mediterranean UNESCO World Heritage at risk from coastal flooding and erosion due to sea-level rise. Nat. commun., vol.9 , pp.4161.

Vousdoukas, Mentaschi, Voukouvalas, Verlaan and Feyen, L. (2017): Extreme sea levels on the rise along Europe's coasts. Earth's Future, vol.5, pp. 304-323.

Vousdoukas, Ranasinghe, Mentaschi, Plomaritis, Athanasiou, Luijendijk and Feyen (2020): Sandy coastlines under threat of erosion. Nat. clim. Chang., vol.10, pp.260-263.

Wolff, Vafeidis, Muis, Lincke, Satta, Lionello. ,... and Hinkel (2018): A Mediterranean coastal database for assessing the impacts of sea-level rise and associated hazards. Scientific data, vol.5, pp.1-11.

THE ROLE OF WAVE OVERTOPPING PREDICTIONS IN THE DESIGN OF CLIMATE ADAPTIVE COASTAL STRUCTURES

Marcel R.A. van Gent, Delft University of Technology & Deltares, marcel.vangent@deltares.nl

ABSTRACT
In the design of coastal structures future sea level rise (SLR) needs to be accounted for. Projections of sea level rise (SLR) vary in time and go together with large uncertainties, see for instance the development of IPCC projections of SLR over time. Not only the projections of SLR vary in time, also the estimated uncertainties in SLR vary in time. Besides uncertainties around a climate scenario resulting in estimates of SLR, IPCC (2021) defines various climate scenarios, each with their own uncertainty (see Figure 1). However, IPCC does not provide estimates of the likelihood of each of the defined climate scenarios. This makes the assessment of the optimal adaptation measures of coastal structures to account for SLR somewhat complicated.

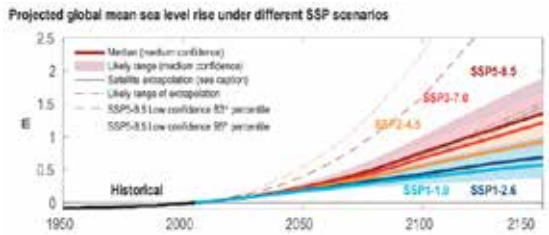

Figure 1 - Projections of SLR for different climate scenarios (IPCC, 2021).

Changes in SLR can also cause significant changes in the hydraulic loading on coastal structures, especially for structures for which the waves at the toe of the structures are depth limited. Since important changes can occur within the lifetime of coastal structures it is wise to anticipate for potential future adaptations, rather than ignoring potential future threats or constructing coastal structures for the worst-case scenario which causes unnecessary costs if SLR appears to be less than expected.

Analyses based on adaptation pathways for coastal structures were focused on adaptation measures like (1) adding a low-crested structure in front of the breakwater, (2) adding a shallow foreshore in front of the structure (nourishment), (3) adding a berm to the seaward slope, (4) adding a crest wall, and (5) raising the crest of the armour layer. Van Gent (2019), Hogeveen (2021) and Teng (2023) showed that for adaptation of coastal structures often more than one adaptation measure is required.

To determine the optimal adaptation measure or optimal combination of adaptation measures accurate predictions of wave overtopping are required. Current design guidelines are often based on data based on a single adaptation measure (*e.g.* for a berm in the seaward slope, but not in combination with a shallow foreshore), rather than on a combination of measures. However, for instance in Van Gent *et al* (2022) the combination of adding a berm and adding a crest wall has been investigated. Nevertheless, the accuracy of existing guidelines for wave overtopping is unknown for several other combinations of adaptation measures. Validation and potential improvements of design methods, especially for the combination of adaptation measures, can lead to a different sequence or different moment in time to implement the adaptation measures of coastal structures under a changing climate. Recent developments with respect to prediction of wave overtopping will be discussed.


Figure 2 - Wave overtopping event at a coastal structure, see also Van Gent *et al*, 2023).

REFERENCES

Hogeveen (2021): Climate adaption of rubble mound breakwaters; A study to the accuracy of overtopping formulas for combination of solutions, M.Sc. thesis, Delft University of Technology. Delft.

IPCC (2021): Ocean, Cryosphere and Sea Level Change. In Climate Change 2021: The Physical Science Basis, by Fox-Kemper *et al*.

Teng (2023): Sea level rise adaptation of rubble mound breakwaters, M.Sc. thesis, Delft University of Technology.

Van Gent (2019): Climate adaptation of coastal structures, Keynote lecture at Applied Coastal Research (SCACR 2019), Bari, Italy.

Van Gent, Wolters and Capel (2022): Wave overtopping discharges at rubble mound breakwaters including effects of a crest wall and a berm, Coastal Engineering, 176.

Van Gent, Van der Bijl, Wolters and Wüthrich (2023): The maximum influence of wind on wave overtopping at seawalls with crest elements, ICE, Proc. Breakwaters 2023, Portsmouth.

THE UE RRF IN ITALY FOR RENEWABLE ENERGIES IN SEA ENVIRONMENT: WAVES VS. WIND

Giuseppe Roberto Tomasicchio, Professor at the University of Salento,
giuseppe.tomasicchio@unisalento.it

The role of the renewables for replacing the fossil fuels is a central theme in the political discussion, and scientific and industrial research field. Also considering the energy crisis across various countries, the opportunities offered by an economy based on renewable energy sources are growing, which allows a more independent energy governance.

Offshore wind and wave energy are expected to play an increasing role in the energy sector. Although several design, cost and performance challenges still remain, many governments funding, developers and researchers are turning to offshore wind and wave energy.

The UE Recovery and Resilience Facility strongly supports the green transition path of Country members, also by financing the development of wave and wind offshore plants.

The lecture informs about the state of wind and wave energy research and development, makes a comparison of the typologies, and illustrates the dedicated chapter of the UE Recovery and Resilience Facility.

THREATS OF COASTAL WATER QUALITY: LESSONS from the ARABIAN GULF ECOSYSTEMS

Waleed Hamza, Biology Department, College of Science, United Arab Emirates University. 15551 Al Ain, UAE,
whamza@uaeu.ac.ae

ABSTRACT

Coastal areas are the most stressed environments worldwide, not only because of their highly inhabited by human populations, but mainly because of the intensive impacts resulted from anthropogenic activities on its water quality. It is well known that coastal waters occupy only 10% of the global marine environment, while it is inhabited by almost 90% of the total marine biota. A fact that makes any degradation of coastal water quality negatively affect the living marine resources as well as the economic values of such areas. The Arabian Gulf is a very specific water body, due to its semi closed basin, and its subtropical location with harsh atmospheric conditions, that resulted in its high-water temperature and its elevated water salinity compared to the other water bodies. Indeed, the high oil production and exportation by the surrounding countries have added a major stressor to its ecosystems.

Moreover, the Arabian Gulf whole basin is considered a coastal water environment, especially with its shallow water which has an average depth of only 35 meters. Additionally, the seaward expansions of the western countries territorial waters are considered the boundaries of the eastern countries coastal water. These features have made its marine environment vulnerable to any natural and/or anthropogenic impact, which not only affects its water quality but consequently its resources. Different threats to the water quality have been recorded for the marine environment of the Arabian Gulf, starting from Oil pollution resulted from oil extraction and its transportation to brine discharge resulted from water desalination plants. That is in addition to increasing of water temperature both naturally during summer months and in winter due to powerplants and industrial discharge of hot water from machinery cooling systems.

Recently, nuclear power plants have been added to the region, which needs specific protection measures and legislation. In order to face such major threats to the water quality, the Gulf countries have issued different legislatives and announced different standards to limit the degradation of the Gulf water quality.

Moreover, some countries have taken remarkable steps to reduce oil pollution in the Gulf; such as building treatment receptors for ballast water of oil tankers before discharging to the marine environment. One country has dislocated its oil exporting port to the Sea of Oman to be out of the Arabian Gulf. There are many other actions and lessons that can be benefited from the actions taken by Gulf countries' governments toward the conservation and protection of its coastal waters and its living resources, which will be communicated in this lecture.

SPONSORS

Thanks to our Sponsors

YILDIZ TECHNICAL UNIVERSITY 1911

YTU MARINE research center

ANADOLUPORT

ARAS marine YATIRIM HOLDING

arti proje

BİAS MÜHENDİSLİK

DANTEC DYNAMICS

emay EMAY ULUSLARARASI MÜHENDİSLİK ve MÜŞAVİRLİK A.Ş www.emay.com

eren ENERJİ

FİBROBETON

GİSAŞ GEMİ İNŞA SANAYİ A.Ş.

GİSBİR

hrwallingford

kalyon

KUZEY STAR SHIPYARD

NORTEK

Poliport

Sentez GEOPIER FOUNDATIONS

YDU

SCACR 2023

Short Course/Conference on Applied Coastal Research

4 - 6 SEPTEMBER 2023 • ISTANBUL / TURKEY

www.scacr2023.org